TIMOTHY T. DUIGNAN

MODELLING SPECIFIC ION EFFECTS WITH THE CONTINUUM SOLVENT APPROACH

MODELLING SPECIFIC ION EFFECTS WITH THE CONTINUUM SOLVENT APPROACH

TIMOTHY T. DUIGNAN

A thesis submitted for the degree of Doctor of Philosophy in Physics

Applied Mathematics Department

Australian National University

January, 2015

Timothy T. Duignan: *Modelling Specific Ion Effects with the Continuum Solvent Approach,* A thesis submitted for the degree of Doctor of Philosophy in Physics, © January, 2015

SUPERVISORS:

Barry W. Ninham

Drew F. Parsons

DECLARATION

This thesis is an account of research undertaken between February 2011 and February 2015 at The Applied Mathematics Department, School of Physics and Engineering, The Australian National University, Canberra, Australia.

Except where acknowledged in the customary manner, the material presented in this thesis is, to the best of my knowledge, original and has not been submitted in whole or part for a degree in any university.

January, 2015

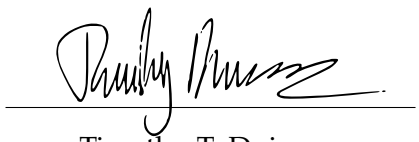

Timothy T. Duignan

ACKNOWLEDGMENTS

I would like to thank my supervisors Drew Parsons and Barry Ninham for providing me with all of the time, advice and support I could need. They have made the experience extremely rewarding and enjoyable. Thanks to all my friends in Canberra, my fellow students and everyone else in the Applied Mathematics Department for providing such a friendly and supportive environment. Thank you to everyone who has provided input and feedback to help improve my work. In particular, Prof. Thomas Beck and Prof. Vincent Craig. Thank you to my family without whom I could not have done this. And finally, thank you to Lisa for helping make the last four years so wonderful.

ABSTRACT

Electrolyte solutions play a central role in many processes from industry to biology. Understanding and building predictive models of their properties has therefore been a fundamental goal of physical chemistry from its beginnings. The challenge remains.

In this thesis I outline a continuum solvent model of univalent monatomic ions in water. This model calculates the free energy of: 1) a single ion in bulk, 2) of an ion approaching the air–water interface and 3) of two ions approaching each other. Its central advancements are to include quantitatively accurate ionic dispersion interaction energies, missing from classical theories, including the higher order multipole moment contributions to these interactions. It also includes the contribution from the cavity formation energy consistently, including the effect of changes in the cavity's shape. Lastly, it uses a quantum mechanical treatment of the ions and provides satisfactory values for their size parameters. Because one consistent framework is used with the same assumptions to calculate the free energies in these three different situations the number of parameters can be minimised and the model can be properly tested.

These three calculations can be used to reproduce experimental solvation free energies, solvation entropies, partial molar volumes, surface tensions and activity/osmotic coefficients of the alkali-halide electrolyte solutions. A minimum of parameters are used and crucially no salt–specific fitting parameters are necessary. The model is quantitative and predictive and is therefore a satisfactory model of electrolyte solutions.

It provides an explanation of several key qualitative puzzles regarding these properties. Namely that ions of the same size can have different solvation energies, that large ions can adsorb to the air–water interface and that ions in solution that have similar solvation energies are more strongly at-

tracted to each other than ions that have dissimilar solvation energies. The continuum solvent model and separate *ab initio* calculations show that dispersion interactions play a key role in controlling these effects. In particular, dispersion energies explain the attraction of large ions for each other in water and the difference in solvation energy of ions of the same size. The success of the model implies that it is possible to understand the key properties of electrolyte solutions using a continuum solvent model. This is an important conclusion considering the massive computational demands of explicit solvent treatments.

PUBLICATIONS

Much of this thesis is reproduced with minor changes from the following publications. All of the work and writing used in this thesis is my own, with the usual advice and comments from my supervisors.

- B. W. Ninham, T. T. Duignan, and D. F. Parsons. Approaches to Hydration, Old and New: Insights through Hofmeister Effects. Curr. Opin. Colloid Interface Sci., 16:612–617, Dec. 2011. (Ref. 191)

- T. T. Duignan, D. F. Parsons, and B. W. Ninham. A Continuum Solvent Model of the Multipolar Dispersion Solvation Energy. J. Phys. Chem. B, 117:9412–9420, 2013. (Ref. 66)

- T. T. Duignan, D. F. Parsons, and B. W. Ninham. A Continuum Model of Solvation Energies Including Electrostatic, Dispersion, and Cavity Contributions. J. Phys. Chem. B, 117:9421–9429, 2013. (Ref. 67)

- T. T. Duignan, D. F. Parsons, and B. W. Ninham. A Continuum Solvent Model of the Partial Molar Volumes and Entropies of Ionic Solvation. J. Phys. Chem. B, 118:3122–3132, 2014. (Ref. 68)

- T. T. Duignan, D. F. Parsons, and B. W. Ninham. Collins's Rule, Hofmeister Effects and Ionic Dispersion Interactions. Chem. Phys. Lett., 608:55–59, 2014. (Ref. 69)

- T. T. Duignan, D. F. Parsons, and B. W. Ninham. Ion Interactions with the Air–Water Interface Using a Continuum Solvent Model. J. Phys. Chem. B, 118:8700–8710, 2014. (Ref. 70)

- T. T. Duignan, D. F. Parsons, and B. W. Ninham. A Continuum Solvent Model of Ion–Ion Interactions in Water. Phys. Chem. Chem. Phys., 16:22014-22027, 2014. (Ref. 71)

- T. T. Duignan, B. W. Ninham, D. F. Parsons. Modelling Water as a Continuum Solvent to Understand Ion–Specific Effects, Aqua Incognita 443–455 Conner Court Publishing: Ballarat, 2014. (Not peer reviewed) (Ref. 72)

CONTENTS

I MAIN 1

1 INTRODUCTION 1

1.1 Water 1

1.2 Specific Ion Effects 2

1.2.1 Description 2

1.3 Models 4

1.3.1 Criteria for a Satisfactory Model 5

1.3.2 Specific Phenomena 6

1.3.3 Free Energies 8

1.3.4 Model Approaches 8

1.3.5 Statistical Mechanics Methods 11

1.4 Specific Models 12

1.4.1 Primitive Models 12

1.4.2 Explanations 13

1.4.3 Explicit Solvent Approach 15

1.4.4 Continuum Solvent Models 17

1.5 New Model 18

1.6 Overview 20

2 THE MULTIPOLAR DISPERSION SOLVATION ENERGY 23

2.1 Introduction 23

2.1.1 Dispersion Interactions 23

2.1.2 Explicit Solvent Approach 24

2.1.3 Continuum Solvent Approach 25

2.1.4 Goal 27

2.2 Theory 28

2.2.1 Dispersion Contribution 28

2.2.2 Electronic Properties 35

2.2.3 Size Parameters 36
2.3 Results and Discussion 43
2.4 Conclusion 47
3 TOTAL IONIC SOLVATION ENERGIES 49
3.1 Introduction 49
3.1.1 Background 49
3.1.2 Significance 50
3.1.3 Modelling Approaches 50
3.1.4 Goal 56
3.2 Theory 57
3.2.1 Electrostatic Contribution 57
3.2.2 Dispersion Contribution 57
3.2.3 Cavity Contribution 58
3.2.4 Input Data 59
3.3 Results and Discussion 61
3.3.1 Uncertainty 64
3.3.2 Implications 66
3.3.3 Further Applications 68
3.4 Conclusion 69
4 PARTIAL MOLAR VOLUMES AND ENTROPIES 71
4.1 Introduction 71
4.2 Theory 72
4.2.1 Entropies 72
4.2.2 Partial Molar Volumes 76
4.2.3 Parameters 78
4.2.4 Experimental Values 81
4.3 Results 82
4.3.1 Entropies 82
4.3.2 Partial Molar Volumes 87
4.4 Discussion and Conclusion 90
4.4.1 Criteria Comparison 91
4.4.2 Implicit Solvent Models 92

5 *ab initio* DISPERSION INTERACTIONS 95

5.1 Introduction 95

5.2 Methods 96

5.3 Computational Details 97

5.4 Results and Discussion 98

5.4.1 Ion-Water Interactions 98

5.4.2 Ion-Ion Interactions 101

5.5 Conclusions 106

6 ION INTERACTIONS WITH THE AIR-WATER INTERFACE 107

6.1 Introduction 107

6.2 Theory 110

6.2.1 Electrostatics (COSMO) 111

6.2.2 Image Charge 114

6.2.3 Cavity Energy Contribution 115

6.2.4 Dispersion Contribution 116

6.2.5 Surface Potential 117

6.2.6 Additional Contributions 118

6.2.7 Calculation Details 118

6.2.8 Comparisons 120

6.3 Results 122

6.3.1 Surface Tensions 126

6.4 Discussion 130

6.4.1 Dispersion Contribution 130

6.4.2 Mechanism of Iodide Adsorption 131

6.4.3 Surface Potential 133

6.4.4 Specific Ion Effects 134

6.4.5 Entropic Contribution 135

6.4.6 Implications 136

6.5 Conclusion 137

7 ION-ION INTERACTIONS 139

7.1 Introduction 139

7.2 Theory 143

7.2.1 Direct Electrostatic Contributions 144
7.2.2 Cavity Energy 146
7.2.3 Dispersion 147
7.2.4 Experimental Values 150
7.2.5 Calculation Details 153
7.3 Results and Discussion 154
7.3.1 Interactions 154
7.3.2 Experimental Comparison 156
7.3.3 Possible Causes of Over–Attraction 159
7.3.4 Mechanism of Collins's law 161
7.4 Conclusion 164
8 CONCLUSIONS 167
8.1 Summary 167
8.2 Implications 169
8.2.1 Continuum Solvent Modelling 169
8.2.2 Dispersion and Cavity Interactions 170
8.2.3 Combining Contributions 171
8.3 Future Work 171

II APPENDIX 175

A APPENDIX A 177
A.1 Scattering Green's Function for a Spherical Cavity 177
A.2 Polarisability 180
A.3 Energies 184
A.3.1 Dipole 184
A.3.2 Quadrupole 185
A.3.3 Octupole 187
A.4 Anisotropic Molecules 188
B APPENDIX B 189
C APPENDIX C 193

BIBLIOGRAPHY 197

LIST OF FIGURES

Figure 1.1 Specific phenomena 7

Figure 1.2 Model hierarchy 21

Figure 2.1 Noble gas Born-Mayer b parameters 37

Figure 2.2 Diagram of ion cavity and water 42

Figure 2.3 Diagram of two interacting water interfaces 42

Figure 2.4 Ionic dispersion solvation energies 44

Figure 2.5 Noble gas dispersion solvation energies 44

Figure 3.1 Born model solvation energies 52

Figure 3.2 Experimental comparison of ionic solvation energies 62

Figure 3.3 Contributions to noble gas solvation energies 63

Figure 3.4 Contributions to ionic solvation energies 64

Figure 4.1 Experimental comparison of solvation entropies 84

Figure 4.2 Error in solvation entropy calculation 85

Figure 4.3 Experimental comparison of corrected solvation entropies 86

Figure 4.4 Experimental comparison of partial molar volumes 89

Figure 4.5 Experimental comparison of corrected partial molar volumes 90

Figure 6.1 Cavity shape change 111

Figure 6.2 Ion-surface interactions 123

Figure 6.3 Ion-surface interaction contributions 125

Figure 6.4 Born vs. induced dipole contributions 127

Figure 6.5 Experimental comparison of surface tensions 128

Figure 7.1 Osmotic coefficients of alkali halides 142

Figure 7.2 Depiction of ion–ion interaction calculation 145

Figure 7.3 Ion–ion interaction potentials 156

Figure 7.4 Experimental comparison of B coefficients 158

Figure 7.5 Theoretical and experimental B coefficients 159
Figure 7.6 Ion–ion interaction contributions 161
Figure 7.7 B coefficients with Hartree–Fock and COSMO only 164

LIST OF TABLES

Table 2.1 Ionic size parameters 38

Table 2.2 Experimental comparison of R_S values 39

Table 2.3 Dispersion solvation energies 43

Table 3.1 Experimental comparison of solvation energies 62

Table 4.1 Ionic entropy contributions 83

Table 4.2 Experimental comparison of solvation entropies 83

Table 4.3 Experimental comparison of noble gas entropies 87

Table 4.4 Ionic partial molar volume contributions 88

Table 4.5 Experimental comparison of partial molar volumes 89

Table 5.1 Dispersion energy comparison 99

Table 6.1 Cavity size values 120

Table 6.2 Energies at contact minimum 126

Table 6.3 Experimental comparison of surface tensions 129

Part I

MAIN

1

INTRODUCTION

Substantial sections of this chapter are reproduced from Ref. 72:
T. T. Duignan, B. W. Ninham, D. F. Parsons. Modelling Water as a Continuum Solvent to Understand Ion–Specific Effects, Aqua Incognita 443–455 Conner Court Publishing: Ballarat, 2014. (Not peer reviewed)

1.1 WATER

Water is obviously one of the most important materials in existence. Most of the earth's surface is covered in water and its behaviour is a dominant driver of the earth's climate system. The biochemical processes that make life possible almost all occur in water. The provision of clean water for drinking, irrigation and cleaning is of vital importance both to humanity and to many of the earth's ecosystems. Water is also used in a vast number of industrial applications, primarily as a medium for carrying out chemical processes.

One of the reasons it is so important is that it is an excellent solvent. It can dissolve a huge range of molecules and the interactions of these molecules are dramatically altered by the surrounding water in surprising, complex and poorly understood ways. The properties of water itself are also strongly affected by these solutes. Understanding what these changes are, and what causes them is a central problem of physical chemistry. Due to the ubiquity and importance of water, such an understanding necessarily leads to a huge number of potential applications. They include explanations of the mechanics of life, improved medical knowledge and treatments, an improved understanding of the effects of carbon emissions, improvements in water treatment and materials design as well as a host of other industrial applications.[79]

1.2 SPECIFIC ION EFFECTS

1.2.1 *Description*

Ions form a particularly important class of solutes in water. These are atoms or molecules which have a net negative or positive charge due to either more electrons than protons (anions) or more protons than electrons (cations). Without water, ions form crystals (salts) where the anion and cation are bound together due to their electrostatic and other intermolecular forces. These salts dissolve in water and the ions become separated, forming aqueous electrolytes. This is due to the strong interaction of the ions with the water molecules, as well as the entropic gain from mixing. Strong electrolytes, which concern us, are those that disassociate in water completely.

This class of solutes are very important for two reasons. The first is their ubiquity. They are almost always present in water. The ocean has a high concentration of salt. (3.5% or 0.6 M) This is mainly in the form of sodium chloride, although there are smaller concentrations of many other salts. Blood and cells have high and carefully regulated concentration of many different types of salts. The water used in a huge number of industrial applications such as electrolysis depends on specific and significant concentrations of ions in the water. The second reason for the importance of these solutes is because they can have a dramatic effect on the measurable properties of the water they reside in. Some examples of this are:

- The thermodynamic properties of the water such as its freezing point, osmotic pressure, density and surface tension all change upon addition of salt.[79]
- The pH has a complex and poorly understood relationship with the background salt concentration.[32]
- The forces between two surfaces are strongly affected by the salt concentration of the water in between them.[113]

- The ability of other material to be dissolved in water is also affected. For instance, the stability of colloidal particles in solution as well as the solubility of proteins is strongly affected by the ions in the water.[187]
- Many other properties such as the coalescence of air bubbles[54] are significantly affected.

As a result, ions in water must be modelled accurately if we wish to understand a huge range of naturally occurring aqueous systems such as the blood and the ocean. In addition, it is desirable to harness the properties of these aqueous electrolytes for industrial applications. This also requires accurate models of their properties. Without these models unnecessary redundancy has to be built in to industrial systems and much laborious trial and error experimental work is required to determine the best conditions for various applications. An additional problem is that potentially important novel applications may never even be conceived of.

Some specific examples of applications where salt water is important are:

- Physiological processes such as muscle contraction and nerve signals.[91]
- The interpretation of pH measurements.[32]
- The stabilisation vs. coagulation of colloidal and protein systems, which is important for many fields from mineral ore extraction to medicine.[236]
- Medical drugs and/or supplements, such as lithium salts in the treatment of bi-polar disorder.[255]
- The assembly of nanoparticles in solution.[159]

The effect of ions on water depends sensitively on the salt concentration and temperature as well as the specific pairs of ions which make up the salt. No adequate theories have been developed that can fully explain all of the properties of electrolyte solutions. In particular, the dramatic dependence on the type of ion is poorly understood. This area of research, known as 'Specific Ion Effects', has been with us since the beginnings of physical chemistry, notably in the unexplained 'Hofmeister Effects.' The term refers

to the inadequacy of classical theories of electrolytes. This area has received significant scientific attention over the past two decades. It involves the experimental measurement and investigation of the behaviour and properties of electrolyte solutions, as well as improved theoretical modelling of them, in order to provide explanations of their behaviours. These Specific Ion Effects are often ignored by the wider scientific community and electrolyte solutions are often treated with primitive models that are inadequate for reproducing these effects.

Some key publications summarising this area of research are the books 'Molecular Forces and Self Assembly'[187] and 'Specific Ion Effects',[137] and a number of review papers.[136,140,153,292,293] The range of challenges that we still face in understanding water more generally are outlined in the book: Aqua Incognita, Why Ice Floats on Water and Galileo 400 years on,[188] which summarises the proceedings of a recent conference in Florence.

1.3 MODELS

In order to understand these phenomena both qualitatively and quantitatively, it is necessary to build models. As already mentioned models developed thus far have had limited success in explaining and predicting the properties of electrolyte solutions. I will first discuss modelling more generally, and then review the models of Specific Ion Effects presented in the literature up to this point.

There are two key tasks which modelling is important for.

- The first is giving quantitatively accurate and predictive calculations of the properties of these solutions.
- The second is to provide justified qualitative explanations of the properties of these solutions.

The first purpose means the outcome of experiments can be predicted. This allows modelling to determine behaviour for applications rather than

having to use experimental trial and error. It can also demonstrate that in principle the causes of an effect are known.

The second purpose is important because it is not sufficient in science simply to be able to predict the outcome of an experiment. It is also desirable to have a coherent explanation in terms of simpler and well understood concepts that explains the outcome of an experiment. A qualitative explanation of this form is intellectually satisfying and useful as it allows the phenomena to be thought about intuitively. This is necessary for the formation of hypotheses which allow new and interesting experiments to be designed as well as new tools and materials to be created. Qualitative explanations should be consistent with quantitative modelling but can also help guide improvements to to it.

1.3.1 *Criteria for a Satisfactory Model*

We need to outline a set of criteria the model must meet in order to be considered satisfactory. Some parameters will inevitably be necessary in the modelling of aqueous salt solutions. These criteria must include restrictions on these parameters to ensure that the model is not just an exercise in curve fitting but that it actually represents the physics accurately. I propose the following criteria:

- The model calculates properties of several different experiments without varying the parameters from one situation to another.
- The contributions and parameters should be justifiable, physically interpretable and conceptually and numerically sensible.
- Parameters should be predictable by *ab initio* or straightforward empirical means. Ideally, they should not be derived from any experiments the model is designed to reproduce.

Hünenberger and Reif's text book, 'Single–Ion Solvation',[110] argues that there is currently no 'satisfactory' continuum model of ionic solvation using essentially a more specific version of these criteria. (See Section 3.1.4)

Although not strictly necessary for a model to be satisfactory, it is also desirable for it to be simple, easy to use and as transparent as possible.

1.3.2 *Specific Phenomena*

The logical place to start modelling is with the simplest properties of aqueous electrolyte solutions. This is firstly because these properties will have the least number of variables, and so their explanation should be the most straightforward. Secondly, with a firm foundation laid, models that explain these properties can be generalised to explain more complex systems with confidence. Thirdly, for these simple systems we can apply different levels of theoretical modelling and see what level of detail is necessary to reproduce experimental properties.

A reasonable choice for the simplest properties of electrolyte solutions are: ionic solvation energies, surface tensions and activity/osmotic coefficients. A depiction of these properties is given in Figure 1.1.

The solvation energies consist of the free energy change on transferring an ion from vacuum to water. The surface tensions give the free energy cost per unit area of creating new air–solution interface. The activity coefficients give a correction to the chemical potential of an ion in solution to account for the non–ideality of the solution. More precisely, if $\gamma(\rho)$ is the activity coefficient of an ion, then the chemical potential is:

$$\mu(\rho) = \mu^{o} + \ln \gamma(\rho)\rho \tag{1.1}$$

The activity coefficient can be related to the osmotic coefficients, which are the correction to the osmotic pressure of the solution due to non-ideality. The osmotic pressure is the pressure exerted by the solution on a membrane that is permeable only to the solvent. If $\phi(\rho)$ is the osmotic coefficient of an ion, then the osmotic pressure of the solution is given by:

$$\Pi = k_B T \phi(\rho)\rho \tag{1.2}$$

Currently our understanding of all of these properties is inadequate. We have some qualitative explanations, but quantitative agreement with experiment has been elusive. Parameters like assumed ionic radii for each ion or salt pair must be adjusted to reproduce experiment. Worse still, the parameters for a given salt change with experiment. There is still even a degree of disagreement about the underlying physical mechanisms responsible for some observed behaviours. The result is that all predictability is lost.

There are several qualitative observations related to these three properties that are somewhat counterintuitive and not well understood. Explaining these observations with a model that has a minimal number of physically based parameters would be strong evidence for its power and usefulness.

Much research[109,18,120,186,75,157] has focused on three important examples of these observations. They are:

- The difference in the solvation energies of cations and anions of the same sizes.
- The affinity of large ions for the air-water interface.
- The observation that oppositely charged ions with similar solvation energies are more strongly attracted to each other in water than ions of dissimilar solvation energy.

All three of these phenomena have been experimentally verified and much speculation in the literature exists about their origin. No fully satisfactory model has been able to give a coherent explanation of them.

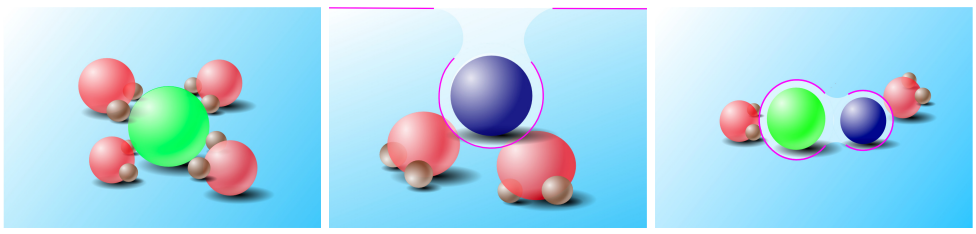

(a) (b) (c)

Figure 1.1: Depiction of the specific phenomena I aim to explain in this thesis. Namely: (a) Single ions in bulk water (solvation energies), (b) ions near the air–water interface (surface tensions), and (c) ion pairs (activity/osmotic coefficients).

1.3.3 *Free Energies*

The central difficulty in calculating these properties is the calculation of free energies. For example, the theoretical free energy of transferring an ion into water can be compared directly with experimentally measurable solvation energies. The free energy change as an ion approaches another ion and the free energy change as an ion approaches the air–water interface can be used to determine the activity/osmotic coefficients and the surface tension of electrolyte solutions. These free energies are equivalent to potentials of mean force (pmfs) or effective interactions. In addition, the entropy of solvation and the partial molar volumes can be calculated from the temperature and pressure derivatives of the free energy respectively.

The free energy change as an ion approaches the air–water interface is essentially the change in the solvation free energy of the ion as it approaches the interface. Similarly, the interaction free energy of two ions in water is simply the change in solvation energy of the pair of ions as a function of separation plus their direct interaction energy. The calculation of solvation energies of molecules is a very large research area with many approaches undergoing continuous development and improvement.[259,260,55] It is important to note that even though ions are a specific class of solutes in water, the methods used to model them are informed by the more general literature of modelling solutes in water. Advances in the modelling of ions in water may have implications for the modelling of nonionic solutes in water. A model of aqueous electrolytes can thereby help improve our understanding of the physical chemistry of aqueous solutions more generally.

1.3.4 *Model Approaches*

In what follows, I outline three approaches to the modelling of electrolyte solutions, or more specifically the calculation of the relevant free energies. The

current literature on modelling Specific Ion Effects will then be discussed with reference to these approaches.

1.3.4.1 *Fundamental Quantitative Approach*

The most basic approach to modelling these systems is to start from the basic physical laws and calculate the properties of the system making as few assumptions as possible. The appeal of this approach is that it accurately reproduces the underlying physical mechanisms of the system. This approach basically involves solving the Schrödinger equation with physically justified assumptions such as the Born-Oppenheimer approximation. This approach in essence is *Ab initio* molecular dynamics.[172] Researchers have begun to apply this approach to Specific Ion Effects only in the last few years.[146,14,217]

1.3.4.2 *Parametrised Quantitative Approach*

The second method is to make approximations which parametrise the theory, i.e., to approximate some aspect of the system with a physically justified mathematical expression that contains some parameters. These parameters can then be determined through empirical comparison or possibly determined *ab initio*. One example is to assume that the interatomic electrostatic forces can be represented with point charges interacting via Coulomb's law, where the position and magnitude of the charges are adjusted to reproduce experiment or quantum mechanical calculations. Almost all attempts to model Specific Ion Effects are of this type, due to the large number of molecules which make fundamental calculations very computationally demanding.

Models of this type can be classed into two general categories. The first are 'bottom up' approaches. These begin from the fundamental quantitative approach but approximate some aspects of the system using functions with fitted parameters. The best example of this are classical molecular dynamic simulations, where the interaction potentials are modelled using point charges and a Lennard–Jones type potential, and the parameters are fitted to reproduce experimental solvation energies of the ions. These models include

the behaviour of all of the water molecules and are hence referred to as explicit solvent models. For many properties these calculations are necessary. For example, treating the dynamics of water molecules in the solvation shell obviously requires that some of the water molecules be treated explicitly.

The second class are 'top down' approaches which start from a more macroscopic model where parameters from experiment are used to take into account the complex molecular behaviour by averaging or smoothing it out. The classic example of this approach is the use of an experimentally determined dielectric constant in order to calculate the damping of the electrostatic interaction in water. These approaches are normally referred to as continuum solvent models but can also be referred to as implicit solvent models to contrast them with explicit solvent simulation techniques. These models can be applied when it is only the distribution of solute particles in the water that needs to be determined. This approach is much less computationally demanding than the explicit solvent approach. It is also normally more physically transparent, that is, the origin of any observed behaviours can be straightforwardly determined. However, there is debate regarding the degree of accuracy possible with this approach.

1.3.4.3 *Qualitative Approaches*

Finally, a qualitative understanding of the system can also be gained through other methods. These involve attempting to identify universal trends or patterns. These can be used to qualitatively predict behaviours in other contexts. Quantitative predictions can be made through finding numerical correlations between certain properties. Normally this approach includes some qualitative justification of the observed trends in terms of an underlying physical argument, which is not necessarily modelled quantitatively. The model is instead supported based on its plausibility as well as its explanatory and predictive power. The most widely known example of this approach in the context of Specific Ion Effects research is Collins's Law of Matching Water Affinity. This law observes a correlation between the affinity of ions

for each other and the difference in their solvation energy.[52] This law is discussed in more detail in Chapters 5 and 7.

1.3.5 *Statistical Mechanics Methods*

Also important are the statistical mechanical methods, which use interaction energies to determine the experimental properties mentioned in Section 1.3.2. This is because most of the important physical properties of electrolyte solutions can be accessed through ionic distribution functions or concentration profiles. These give the probability of finding an ion at a given distance from an interface or from another ion. The following methods can be used to calculate these distribution profiles.

1.3.5.1 *Poisson–Boltzmann Equation*

In this method the Poisson equation is used to calculate the electrostatic potential for a given distribution of ions, and the ion distribution is determined by a Boltzman factor incorporating the electrostatic potential. The equation is non–linear and can be solved self-consistently. This method is extensively used, well developed and tested, particularly as a tool to calculate the ion–surface distribution functions. See chapter 11 of Ref. 137.

1.3.5.2 *Ornstein-Zernike Equation (HNC Closure)*

This method solves self consistently the formally exact integral equations originally formulated by Ornstein and Zernike. Their solution depends on an assumed, approximate closure relation. These equations describe how to calculate the correlation between pairs of molecules given some interaction potentials. This is useful in calculating ion–ion distributions and hence osmotic coefficients. For electrolytes the HNC closure is normally used with an implicit solvent approach. Its advantage over a Poisson–Boltzmann approach for instance is that it can include direct ion–ion correlations. See chapter 10 of Ref. 137.

1.3.5.3 *Molecular Dynamic Simulation*

Here an ensemble of molecules is allowed to evolve with time to an equilibrium state, the molecules behave according to Newton's laws. The forces are given by intermolecular interaction potentials determined empirically or theoretically. This approach is the most common explicit solvent approach. See chapter 9 of Ref. 137.

1.3.5.4 *Monte Carlo*

This method is a less commonly used alternative to molecular dynamics. It uses a random sampling of the molecular positions rather than calculating the molecules behaviour deterministically. Its usefulness arises from the ability to use probability to solve the very high dimensional integrals common in statistical mechanics.[262] This can be used for implicit and explicit solvent approaches.

These different methods have been well tested and shown to agree with each other for some important properties.[199] In principle all of these methods are applicable in either implicit of explicit solvent models, although some are better suited for one or the other. A wide variety of methods can be used to calculate properties from ionic distributions such as the Kirkwood Buff theory[133] and the Gibbs adsorption isotherm.[65] It is also possible to hybridise these methods, for instance combining molecular dynamics simulation with Poisson–Boltzmann[106] or HNC calculations.[268]

1.4 SPECIFIC MODELS

1.4.1 *Primitive Models*

The classical or primitive model of electrolyte solutions is the name given to the original attempt to model these solutions, and it is an example of the 'top down' parametrised quantitative approach. It normally treats the ions as point charges, although it is often extended to include finite size, where

the size parameters are adjusted to reproduce experimental properties such as solvation energies or activity/osmotic coefficients. In the case of solvation energies this 'primitive' approach corresponds to the Born model.[28] It gives a reasonable estimate of the solvation energies including the right qualitative 1/r dependence. However, the size parameters have to be adjusted unphysically to fit the experimental values precisely. For example, cation and anion crystal sizes have to be adjusted by different constants.[229]

This primitive model gives the Onsager-Samaris and Debye-Hückel theories for the surface tensions of the air–water interface[195] and the activity/osmotic coefficients of bulk electrolyte solutions.[60] These models are adequate at very low concentrations where the ions are indistinguishable from one another. However, to achieve agreement at higher concentrations where there is significant ion–specificity the size parameters have to be adjusted to unphysical values to bring the theory into agreement with experiment. For instance, iodide must be smaller than fluoride to reproduce the low surface tension of iodide electrolyte solutions, and the size parameters are non-additive for the osmotic coefficients.[233]

Further extensions have been made to the primitive model to incorporate the structure near ions induced by the ion–water interactions. These normally invoke additional terms with fitted parameters and have been referred to as 'civilised' models. A term introduced by Stokes in his classic work with Robinson.[233] The primitive model and its extensions are examples of continuum solvent models.

1.4.2 *Explanations*

The question of why Specific Ion Effects exist at higher concentrations has been a long standing one, going back over one hundred years to the work of Franz Hofmeister. In a series of pioneering experiments[139] he showed that the concentration at which salts cause a solution of dissolved proteins to coagulate depended sensitively on the type of salt added.

Probably the earliest explanation of these Specific Ion Effects is the idea that the ions alter the structure of the surrounding water, i.e., some ions break the structure of water (chaotropes) and some increase the structure of water (kosmotropes). It is argued that kosmotropes, via their structuring effect, somehow deprive proteins of hydration water, hence enhancing their precipitation. Ball and Hallsworth[16] provide an interesting account of the history of this concept. This idea has fallen out of favour recently[292,293,16] due to evidence that the water structure is not significantly affected beyond the first or second hydration layer,[194] as well as the difficulty in modelling this effect. This hypothesis does however highlight one of the reasons for the failure of the primitive model: it does not account for changes in the water surrounding an ion.

A more recent explanation of this specificity is that the ions undergo non–electrostatic, i.e., dispersion interactions.[187,191] These quantum mechanical forces are missing from classical theories. They depend on a balance of ion size and polarisability[206] and are hence ion-specific. So far they have mainly been applied to ion interactions with surfaces, where it has been established that they clearly make a substantial contribution to ionic distribution profiles near interfaces and hence to measurable macroscopic properties.[30,33,204] It is unlikely however that the extension of primitive models with these potentials is sufficient to build a quantitatively accurate and predictive model.

This is because of the aforementioned failure of the primitive models to account for the role of the water adequately. A third missing component in the modelling of Specific Ion Effects, derives from the fact that although the water structure is only altered in the first one or two water layers surrounding an ion, this water interacts with the ion in a unique way, depending on the ion's size, or more specifically, surface charge density[136] as well as other specific properties of the ion such as the sign of its charge and its polarisability (via the dispersion interaction.) For ions to interact with other molecules in solution these short range water molecules must be removed or rearranged, resulting in a highly ion–specific short range interaction. This ion specificity in the interaction of ions with water is clear from the solvation energy of

ions, which varies dramatically between different ions. This mechanism of ion–specificity is often referred to as a hydration effect. The effect is used to justify including additional fitted parameters in many models that would otherwise not agree with experiment. This is due to the difficulty so far of modelling this effect explicitly. For example, this effect is used to justify adjusting the size parameters of ions to fit experiment, and so called 'civilised models' are an attempt to include its effect in other ways.[233] More specifically Friedman's model of activity/osmotic coefficients is a good example of this.[227] It adds Gurney potentials to the standard electrostatic ion–ion interaction. The Gurney potentials are proportional to the overlap of the ion's hydration shells, and they are scaled by a parameter fitted to reproduce experiment. Their purpose is to include the energy change of moving the water from the ion's hydration shell to bulk.

1.4.3 *Explicit Solvent Approach*

The importance of hydration effects, our third hypothesised mechanism for ion-specificity, has led to the belief that it is necessary to use explicit solvent models. This belief has led to research focussing on developing classical molecular dynamic simulation of ions in water.

Additionally, the possibility of 'chemical interactions' between an ion with water molecules in the first solvation layer has spurred attempts at *ab initio* treatments of ions in water. Either through full DFT molecular dynamic simulation,[14] hybrid QM/MM approaches[261] or energy calculations of geometry optimized clusters combined with continuum models.[291]

Classical molecular dynamics is currently the most widely used technique that attempts to model Specific Ion Effects. As computational power has increased it has become more feasible. The most important success has been the prediction of an affinity of large ions for the air–water surface.[120] Progress toward accurately calculating bulk properties such as the osmotic coefficients has also been made, where this approach has been hybridised with

HNC calculations,[268] and there has been qualitative success reproducing Collins's law of matching water affinity.[75]

It would be very unfortunate if it was true that electrolyte solutions cannot be described without models that explicitly track the position and orientation of every individual water molecule. This is because these models make dramatic computational demands. Pure quantum mechanical approaches are impractical for anything but simple systems and properties. With significant simplifying approximations computational demands can be decreased and the range of applicability widened. Even so, scaling these models up to the large systems relevant for biology or using them to test large classes of molecules for particular properties becomes prohibitively expensive.

There are also significant questions regarding the potential accuracy with these more approximate methods. For instance, some of the assumptions used, such as pair–wise additivity, Lennard–Jones potentials and small box sizes, are problematic. These approximate models also involve many fitted parameters. As a result it is far from certain that they will work outside the range of experiment they have been adjusted to reproduce. For instance, it appears that models adjusted to reproduce bulk properties of water, such as SPC/E, may not do a good job reproducing the properties of water at an interface such as surface potentials.[231] Similarly, polarisable models seem to overstabilise ions at the interface,[235] and salt specific fitting parameters are required to reproduce ion–ion interactions quantitatively.[83] It also means that when building a model there are many decisions to be made with regards to parameter choice and functional form, which may lead to substantially different predictions and conclusions. For example, the solvation energies of individual ions is still a matter of debate due to a substantial variation in theoretical values that depend on the model used.[110] In addition to this, the interaction potentials of anions with the air–water interface are known to be highly model dependent.[257]

Thirdly, even if agreement with unrelated experiment is observed, the models do not necessarily provide a conclusive qualitative explanation or guidance as to the physical cause. For instance, the surface excess of large

anions has been observed in agreement with experiment, but the physical cause of this excess is still the matter of theoretical debate.[186]

1.4.4 *Continuum Solvent Models*

In some ways the ideal model of ions in solution is a continuum solvent model. These models are dramatically less computationally demanding, this allows them to be scaled up to situations of biological interest and to test large sets of molecules. They also generally provide direct and unambiguous physical insight due to their derivation. Indeed these models are still widely used in applications for these very reasons, and there is significant research effort focussed on improving them.[259,187,137,113] Primitive models are also still used due to their physical insight. For example, Debye-Hückel and Born models are very useful pedagogically and for informing intuition. Continuum models are also useful in the simulation of biologically important systems.[47,85] This is despite the fact that so far they have not proven totally satisfactory[110] at properly reproducing the simplest properties of electrolyte solutions described above.

The clear and obvious problem with these models is that they are only rigorously true in the macroscopic limit, where the solutes become substantially larger then the water molecules, probably on the order of several nanometres. This is clear from the mathematical derivation of the approach which requires the fields be averaged over volumes that contain many molecules.[114]

However, it is possible that these models remain somewhat accurate outside the range where they are strictly applicable. This would be hugely advantageous, for the reasons discussed above. And it would be more then unfortunate if these models were to go undiscovered because enough effort was not focussed on finding them. There are a large number of improvements that can still be made to continuum solvent models that may bring them into agreement with experiment while meeting the criteria laid out above. These must be attempted before any conclusions about the range of applicability of these models are justified.

1.5 NEW MODEL

We should then proceed by assuming that the continuum solvent approach is valid and build the best models that we can. By comparing the models predictions with experiment we should be able to determine the degree of accuracy possible with the continuum solvent model. Indeed, in this thesis I show that it is possible to achieve an impressive degree of experimental agreement with the continuum solvent approximation, although for some properties we can begin to see the limitations of this approximation. (See Chapter 4 and Chapter 7.)

As mentioned above many continuum solvent models are focussed on describing complex properties that are difficult to address with explicit solvent models.[47] This is reasonable as it may seem that there is little point in modelling properties with these simple and approximate models when they can be, or soon will be, described by sophisticated and comprehensive explicit solvent simulations.

I believe that there are three reasons to do this. Firstly, any model of electrolyte solutions should reproduce the simplest properties first for the reasons outlined in section 1.3.2. Secondly, simple models are often more useful and satisfying than complex models even if they are less accurate. Newton put it best: 'Truth is ever to be found in the simplicity, and not in the multiplicity and confusion of things'[162]Thirdly, it is very useful to be able to compare implicit and explicit solvent models in order to test that they are physically realistic, i.e., the partitioning of energies should be similar in both approaches.

As mentioned above explicit solvent models can suffer significant problems due to the large number of fitted parameters. However, many continuum solvent models have been built that rely on parameters adjusted to reproduce experiment and hence suffer all the same problems. As Feynman pointed out 'The first principle is that you must not fool yourself, and you are the easiest person to fool.'[77] This is why we need to apply the strict

criteria outlined above to any model, which can help prevent any such self–deception.

To build models which meet these criteria we need to account for both of the key mechanisms that cause ion specificity outlined above. Firstly, this means we must include dispersion interactions of the ions with water and other molecules in water. It turns out that the continuum model is particularly suited to this type of calculation due to the development of Lifshitz theory [187,160] and its many simplifications and generalisations. Secondly, we must include the direct interaction of the ion with the water in the first solvation shell, this must include the energy of cavity formation or of breaking the water–water bonds in water. Once this is accurately modelled it also needs to be included in the interaction energy of ions in water. For instance, as lithium approaches a surface or another ion there will be a large cost of removing the strongly bound water from its first solvation layer.

Satisfactory models of these properties need to be applicable to various experiments without adjusting parameters as mentioned in the model criteria above. This approach is exemplified by Kunz et al. in Ref. 138, where a consistent model with one set of fitted parameters is developed in an attempt to reproduce the osmotic coefficients and surface tensions simultaneously. The approach had limited success but serves as a framework for future work. We can improve upon Ref. 138 by basing the calculation on a solid foundation, namely a satisfactory solvation model.

There are many potential improvements to the modelling of these two effects within a continuum solvent approach. New quantum chemical and physical insights have come to light in recent years which can be utilised to improve agreement. Many of these improvements have been made possible by the dramatic improvement in computational power and tools over the last several decades. These improvements will be outlined in the following chapters in more detail but the four key ones are:

- Higher order multipole dispersion interactions.
- Consistent inclusion of cavity formation energy.

- Realistic quantum treatment of solutes.
- Realistic cavity shapes.

In Figure 1.2 I graphically outline a hierarchy of models of electrolyte solutions. At one extreme of the hierarchy are *ab initio* explicit solvent models that are in principle sufficiently accurate for any practical purposes, but which are extremely computationally demanding and do not provide direct physical insight. At the other end is the primitive model which is only accurate for a limited set of properties at very low concentrations. On the other hand the primitive model does provide clear physical insight with effectively no computational demands.

In between these two end points the degree of accuracy possible is unknown and the subject of debate. For a given level of desired accuracy I believe that the best models are as far to the right of the hierarchy as possible in order to minimise computational demands and maximize physical insight. Despite this, currently research seems to be focussed on polarisable and non-polarisable molecular dynamics simulation, which are located at the left end of the spectrum. This thesis outlines the development of a model located at the red dot. This location is characterized by models that are as sophisticated as possible while preserving a continuum treatment of the solvent. I believe this is relatively unexplored territory, and models of this type have the potential to achieve a balance between achieving a practically useful degree of accuracy for some applications while still preserving as much computational simplicity and physical insight as possible.

1.6 OVERVIEW

In this thesis I describe a continuum solvent model of the free energy of: 1) a single ion in bulk, 2) of an ion approaching the air–water interface and 3) of two ions approaching each other. The model meets the criteria for a satisfactory model. I establish that the model is quantitative and predictive

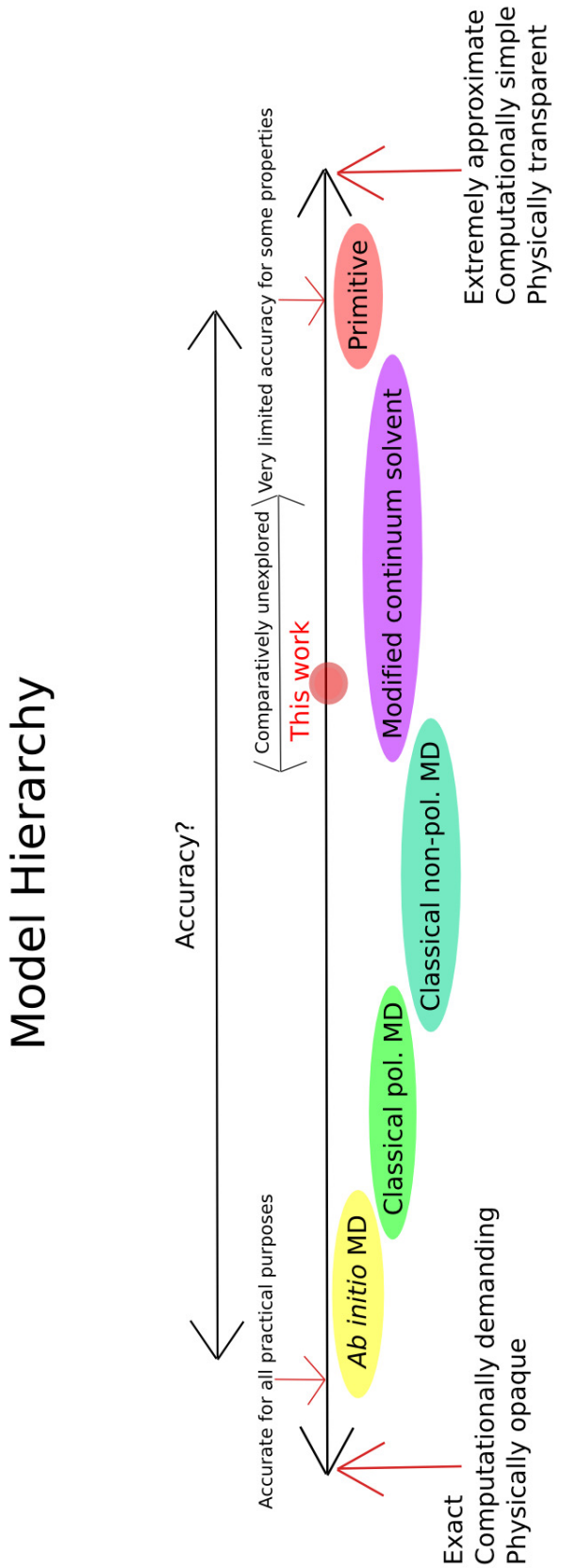

Figure 1.2: A hierarchy ranking the various approaches to modelling the properties of electrolyte solution.

and also provides direct and intuitive explanations of the driving forces that explain experimental results.

In Chapter 2 I outline an improved calculation of the dispersion contribution to the solvation energy of monatomic solutes on the basis of a Lifshitz style model. Crucially, I include higher order multipole contributions to this energy. I also outline a consistent method for determining the ionic size parameters. In Chapter 3 I combine this contribution with an estimate of the electrostatic and cavity formation energy in order to show that they provide a reasonable account of the solvation energy of univalent and monatomic ions and noble gas atoms. In Chapter 4 I take the temperature and pressure derivatives of these solvation energy contributions in order to show that the model gives a reasonable account of solvation entropies and partial molar volumes, although a semi-empirical correction has to be introduced to account for the values of the smaller ions. In Chapter 5 I use Symmetry Adapted Perturbation Theory to confirm the dispersion contributions calculated in Chapter 2 and also to demonstrate that ion–ion dispersion interactions play an important role in determining activity and osmotic coefficients. In Chapter 6 I generalise the solvation model to an ion near an air-water interface to calculate its interaction free energy with that interface and show the adsorption of iodide and that the surface tension increments are well reproduced. In Chapter 7 I apply the solvation model to the calculation of the free energy of a pair of ions as a function of ion–ion separation and show that the like–prefers–like affinity can be reproduced as well as experimental activity/osmotic coefficients, although a large over–attraction has to be corrected for, likely associated with the neglect of explicit water structure. Finally, in Chapter 8, I summarise the entire work, emphasize the important conclusions and outline future directions of research.

2

THE MULTIPOLAR DISPERSION SOLVATION ENERGY

This chapter is reproduced with minor changes and with permission from Ref. 66: T. T. Duignan, D. F. Parsons, and B. W. Ninham. A Continuum Solvent Model of the Multipolar Dispersion Solvation Energy. J. Phys. Chem. B, 117:9412–9420, 2013. Copyright 2013 American Chemical Society.

2.1 INTRODUCTION

2.1.1 *Dispersion Interactions*

Dispersion or Van der Waals interaction are the (usually) attractive quantum mechanical fluctuation forces that act between all molecules and that arise from correlations in the motions of the molecule's electrons. They were originally derived from quantum mechanical perturbation theory by Wang in 1927 and by Eisenschitz and London in 1930. Further developments by Casimir and Lifshitz revealed the subtlety of these interactions, demonstrating how fluctuations of different frequency contributed differently and how to calculate these interactions for macroscopic materials.[160] There is a large and still developing literature dedicated to understanding these interactions.[160,200,239,276,62,61]

This fascinating and important phenomenon plays a significant role in the properties of many materials. For instance, the short range of this interaction potential between molecules means that it is central to any theory of liquids, where the molecules are in close proximity but not chemically bound to each other.

The accurate calculation of these energies will therefore be an essential ingredient in the explanation and prediction of the properties of solutions. A

particularly important example and illustration of this is the solvation energy of molecules and ions. These are the free energy changes that occur in transferring a solute particle from vacuum into solution. A large literature[110,258] is focused on calculating these energies for molecules of all ranges of sizes and types. This is a vital step in understanding chemistry in the condensed phase.

The dispersion interaction of the solute particle with the surrounding solvent makes up a significant proportion of the solvation energy.[29,6] It is often neglected or subsumed into 'effective potentials,' which depend on fitted parameters so that predictability is lost. The highly specific dispersion forces of ions have hardly been included in theories of electrolytes until quite recently, and then only in very crude approximation.[187]

2.1.2 *Explicit Solvent Approach*

In explicit solvent simulations it is particularly difficult to incorporate dispersion interactions. In classical Molecular Dynamic (MD) simulations the dispersion interaction is included by an empirically parametrized Lennard-Jones potential. The values for these parameters reported in the literature for the same model system vary over a significant range.[110] They depend on the method of parametrization and the experimental properties they are parametrized against.[107] The mathematical form of the Lennard–Jones potential used in these simulations is also highly questionable. We know that at close range the $1/r^6$ term is only one of several contributions to the dispersion interaction, higher order multipole moment contributions and wavefunction damping terms are also important. These factors mean that the real contribution of dispersion forces is hidden. It also means that for mixed electrolytes predictability is lost.

Accurate inclusion of the dispersion interaction in explicit solvent *ab initio* calculations requires sophisticated correlated quantum mechanical methods with large basis sets. The computational demands of these methods mean that the dispersion energy is often included through a separate approxi-

mate calculation which is added to a simpler Density Functional Theory (DFT) level calculation.[93] These methods are referred to as DFT-D and are being rapidly improved. There are many complications involved in calculating these energies separately: higher order multipole contributions, many body contributions, damping and repulsion contributions from wave function overlap. These complications are difficult to incorporate, but are particularly important in condensed phase, where the large separation limit can not be used.

2.1.3 *Continuum Solvent Approach*

Because of the computational demands and the complexity of using explicit solvent water models a large amount of research has focused on calculating solvation energies using continuum solvent models. These calculations often include a significant number of fitted parameters. Nonetheless they have been surprisingly successful at reproducing experimental solvation energies. The classic illustration of this is the Born model,[28] which reproduces the solvation energy of the alkali halide ions with surprising accuracy using two temperature dependent fitted parameters. One parameter is added to the cation's crystal radius to give the value for the radius used in the Born equation. A second, smaller parameter is added to the anion's crystal radius.[142] This can be seen in Chapter 3 (Figure 3.1) where electrostatic solvation energies are discussed in more detail. Generalizations of the Born model, that include a distributed molecular charge, can be applied to a wider class of molecules such as neutral inorganic atoms, large and possibly polar organic molecules and polyatomic ions. Normally these models require a number of parameters fitted to reproduce a given set of solvation energies, the models are then tested against a larger set of solvation energies in order to determine their accuracy.[152,56]

Some of these models[258,56] use accurate quantum mechanical treatments of the solute particle in calculating the electrostatic contribution to the solvation energy. The wave function of the solute is calculated self consistently

and the electric field created by the polarisation of the dielectric medium is included. For spherical ions this approach is very similar to the original Born model calculation. Many of these continuum models account for the dispersion interaction by coarse approximation. It is often assumed to be proportional to the surface area of the solute so that it can be modelled with a surface tension model. This introduces further unknown parameters and is undesirable. These interactions are complex and depend sensitively on the properties of the solute and solvent. The calculation of the dispersion energy should be amenable to calculation at the same level of approximation as the electrostatic energy.

Because these interactions are normally treated so crudely, the development of simple and accurate models of the dispersion energy that can be easily and generally applied is an important task. In this chapter I will develop such a model. My model uses uses a multipole polarisability and a cavity in the solvent.

2.1.3.1 *Continuum Dispersion Models*

There are examples in the literature of calculations of the dispersion energy using a continuum solvent model. The Born model requires the molecular charge and dielectric constant. Similarly, these continuum models[55] require accurate knowledge of quantum mechanical properties of the solute as well as the accurate dielectric susceptibility function of water at imaginary frequencies. $\left(\epsilon\left(i\omega\right)\right)$ This function captures the polarisation response of the dielectric material to oscillating electric fields. There are several approximations to this function in the literature.[59,200] But for these purposes the differences between them are immaterial.

Ref. 55 gives a review of the approaches to the modelling of dispersion energies with a continuum solvent model. Here I discuss two of the most useful methods. They are both similar to the model presented here.

The closest model in the literature to the one presented here is that of Amovilli and Mennucci.[6,8] This treats the solute particle on a quantum mechanical level, it finds a self consistent solution for the wave function of a

solute particle in a cavity surrounded by a polarisable continuum. This approach is significantly more sophisticated than almost all of the dispersion energy calculations used in the literature. However some problems with this approach are in the neglect of solute-solvent wave function overlap. It does not rest on firm theoretical grounds and requires quantum mechanical calculations including the presence of the solvent, which are more difficult than straightforward calculations in vacuum.

Amovilli's model is mainly applied to large neutral solutes. An alternative model, also similar to the one presented here, was developed and applied to ionic solutes by Mahanty, Boström, and Ninham.[160,29,203] This model is relatively simple and easy to apply. Its accuracy can be improved significantly by removing unphysical aspects of the calculation such as the assumption of a gaussian dipole distribution, the neglect of the cavity created by the solute and the neglect of higher order multipole moment contributions.

A broader review of previous attempts to model these dispersion solvation energies within a continuum solvent model is provided in Ref. 259 and Ref. 260. Since publishing the work presented in this chapter Amovilli and Floris[7] have published a new model of dispersion solvation energies using a quantum Monte Carlo method and Pomogaeva and Chipman[220] have published a model that adapts a gas phase treatment of intermolecular forces to calculate dispersion solvation energies.

2.1.4 *Goal*

The aim of this chapter is to find an improved approach to calculate dispersion solvation energies. It builds on, corrects and quantifies the background literature outlined above. The approach is to be accurate, and it will draw on and balance the advantages of both the approaches mentioned above. It does so by making the following improvements:

One is to include the effect of the overlap of the wave functions of the solute and solvent molecules. This is achieved by use of Tang-Toennies overlap damping functions.[252]

The second improvement is to insert the solute into a cavity inside the dielectric medium. This puts the dispersion energy on the same level of theory as the Born model. It allows, for the first time, the use of a single consistent cavity size in the calculation of both electrostatic and dispersion contributions. This calculation is placed on a firm theoretical foundation by using Macroscopic Quantum Electrodynamic methods.[239]

A third development is the inclusion of multipole moments up to the octupole term. This gives a better account of the finite size of the solute particles. This is because the induced multipole moments are proportional to the derivatives of the electric field at the centre of the solute, so by including them you include the variation of the electric field over the finite size of the solute.

Finally, I have endeavored to facilitate ease of use and generalizations of the theory by writing equations in terms of simple fundamental properties that are either already available in the literature or that can be determined with standard quantum chemistry calculations of the solute particle in vacuum. This last improvement removes the need to perform quantum chemistry calculations in the solvated environment, which can be difficult.

2.2 THEORY

2.2.1 *Dispersion Contribution*

Scheel and Buhmann have presented an approach to calculating dispersion forces between individual quantum mechanically treated atoms and macroscopic bodies modelled with a dielectric response.[40,239] Some of their results are consistent with earlier work.[160] However they provide a very convenient framework for calculating energies in more complex situations.

Here I apply their method to calculate the dispersion interaction of a molecule with bulk solvation water. The solvent is modelled as a continuous macroscopic object with a frequency–dependent polarisation response. It is assumed that the continuum of water contains a spherical cavity occu-

pied by a solute particle. The solute is modelled with a multipole expansion at the centre of the cavity, where each multipole moment has a calculated polarisability. This is the same level of approximation used by the Born model. The result is that the two contributions, electrostatic and dispersion, are consistent with each other.

2.2.1.1 *Expressions*

I first review the most general equations derived in the theory from which the specific expressions for the solvation energies can be derived. Their dispersion energy of a solute particle is referred to as a Casimir-Polder interaction energy. The dipole dispersion energy is:[239]

$$U_D(\mathbf{r}_A) = \frac{4\pi k_B T}{c^2} \sum_{n=0}^{\infty} \left(1 - \frac{1}{2}\delta_{n0}\right) \xi_n^2 \boldsymbol{\alpha}^{(2)}(i\xi_n) \bullet \mathbf{G}^{(1)}(\mathbf{r}_A, \mathbf{r}_A, i\xi_n) \quad (2.1)$$

Here the $\boldsymbol{\alpha}^{(2)}(i\xi_n)$ is the dipole polarisability tensor of rank two, it includes a factor of $1/4\pi\epsilon_0$ and so has units of m^{-3}. The summation is evaluated at the Matsubara frequencies: $\xi_n = 2\pi k_B T n/\hbar$. $\mathbf{G}^{(1)}(\mathbf{r}, \mathbf{r}', i\xi_n)$ is the scattering part of the dyadic Green's function for the Helmholtz equation with the boundary conditions determined by the shape of the dielectric material.[239] The $\bullet$ denotes the Frobenius inner product, and $\otimes$ represents the tensor product. These operators are defined in Section A.3.

The next step is the inclusion of the quadrupole energy, given in Eq. (15) of Ref. 57. I drop the second term in that equation because it is a thermalized ground state atom[39] giving:

$$\begin{aligned} U_Q(\mathbf{r}_A) = \Bigg| \frac{4\pi k_B T}{c^2} \sum_{n=0}^{\infty} \left(1 - \frac{1}{2}\delta_{n0}\right) \xi_n^2 \boldsymbol{\alpha}^{(4)}(i\xi_n) \bullet \\ \left[\overrightarrow{\nabla} \otimes \mathbf{G}^{(1)}(\mathbf{r}, \mathbf{r}', i\xi_n) \otimes \overleftarrow{\nabla}'\right] \Bigg|_{\mathbf{r},\mathbf{r}' \to \mathbf{r}_A} \end{aligned} \quad (2.2)$$

from Ref. 58 the octupole contribution is:

$$\begin{aligned} U_O(\mathbf{r}_A) = \Bigg| \frac{4\pi k_B T}{c^2} \sum_{n=0}^{\infty} \left(1 - \frac{1}{2}\delta_{n0}\right) \xi_n^2 \boldsymbol{\alpha}^{(6)}(i\xi_n) \bullet \\ \left[\overrightarrow{\nabla} \otimes \overrightarrow{\nabla} \otimes \mathbf{G}^{(1)}(\mathbf{r}, \mathbf{r}', i\xi_n) \otimes \overleftarrow{\nabla}' \otimes \overleftarrow{\nabla}'\right] \Bigg|_{\mathbf{r},\mathbf{r}' \to \mathbf{r}_A} \end{aligned} \quad (2.3)$$

$\boldsymbol{\alpha}^{(4)}(i\xi_n)$ is the quadrupole polarisability tensor of rank 4, it has units of units of m^{-5}. $\boldsymbol{\alpha}^{(6)}(i\xi_n)$ is the octupole polarisability tensor of rank 6, it has units of units of m^{-7}. Definitions of these quantities are given in Ref. 58 and in Appendix A.

$\mathbf{G}^{(1)}(\mathbf{r}, \mathbf{r}', i\xi_n)$ is the scattering part of the dyadic Green's function[239] with the boundary conditions of a spherical cavity in a dielectric medium. This is known.[149] The Green's function can be simplified by taking the non-retarded limit, i.e., by calculating $\lim_{\xi/c\to\infty} (\xi/c)^2\, \mathbf{G}^{(1)}(\mathbf{r}, \mathbf{r}, i\xi)$.[237] I have compared the dipole dispersion energy for the retarded and non-retarded cases, establishing that the contribution due to retardation is negligible, i.e., less than 1%.

I am dealing with isotropic solute particles, it is therefore useful to rewrite the polarisability tensors in terms of the standard scalar isotropic polarisabilities, which are:

$$\alpha_l(i\omega) = \frac{1}{4\pi\epsilon_0}\frac{2e^2}{\hbar}\sum_{n=1}\frac{\omega_{n0}\left|\langle n|Q_l^0|0\rangle\right|^2}{\omega_{n0}^2+\omega^2} \tag{2.4}$$

For $l = 1$ this expression gives the dipole polarisability, for $l = 2$ it gives the quadrupolar polarisability and for $l = 3$ it gives the octupolar polarisability. Q_l^0 is the relevant multipole moment, defined in Section A.2. After some algebra (see Appendix A), we can relate $\boldsymbol{\alpha}^{(2)}(i\xi_n)$, $\boldsymbol{\alpha}^{(4)}(i\xi_n)$ and $\boldsymbol{\alpha}^{(8)}(i\xi_n)$ to a general isotropic tensor of the same rank multiplied by $\alpha_1(i\xi_n)$, $\alpha_2(i\xi_n)$ and $\alpha_3(i\xi_n)$ respectively.

Making these substitutions and simplifying we arrive at the following expressions for the dispersion contribution to the solvation energy.

$$G_D = -\frac{6k_BT}{R_{cav}^3}\sum_{n=0}^{\infty}\left(1-\frac{1}{2}\delta_{n0}\right)\alpha_1(i\xi_n)\frac{\epsilon(i\xi_n)-1}{2\epsilon(i\xi_n)+1} \tag{2.5}$$

$$G_Q = -\frac{15k_BT}{2R_{cav}^5}\sum_{n=0}^{\infty}\left(1-\frac{1}{2}\delta_{n0}\right)\alpha_2(i\xi_n)\frac{\epsilon(i\xi_n)-1}{\frac{3}{2}\epsilon(i\xi_n)+1} \tag{2.6}$$

$$G_O = -\frac{28 k_B T}{3 R_{cav}^7} \sum_{n=0}^{\infty} \left(1 - \frac{1}{2}\delta_{n0}\right) \alpha_3(i\xi_n) \frac{\epsilon(i\xi_n) - 1}{\frac{4}{3}\epsilon(i\xi_n) + 1} \tag{2.7}$$

A full retarded expression for the dipole term (Eq. 2.5) has been given before in an equivalent formulation. (Eq. 49 of Ref. 237) At small separations between solvent and solute molecules, i.e., small R_{cav}, the higher order multipole moments will be of significant magnitude. As far as I am aware the higher order multipolar dispersion energies have not been derived before.

I equate these expressions with free energy changes rather than internal energies. This is based on the same justification for why the Born model gives free energies rather than internal energies. Both calculations account for the energy change of the total system including the energy cost of polarising the dielectric material. They depend on temperature through the temperature dependence of the dielectric susceptibility and the cavity radius, this gives an entropic component.

These equations are consistent with a pure Lifshitz calculation of the dispersion interaction of a dielectric sphere with a surrounding medium. In order to show this we need the nth order polarisability of a dielectric sphere. This can be determined by calculating the electrostatic multipole moment induced on a dielectric sphere in a dielectric medium. Where the sphere has been placed in an externally applied static electric field equal to the the nth order term in the expansion of the potential in terms of Legendre polynomials.[114] The polarisability of a dielectric sphere of radius R_S and dielectric constant ϵ_S in vacuum, is:

$$\alpha_n^S(i\xi) = R_S^{2n+1} \frac{\epsilon_S(i\xi_n) - 1}{\epsilon_S(i\xi_n) + \frac{n+1}{n}} \tag{2.8}$$

Substituting this expression into Eq. 2.5, Eq. 2.6, and Eq. 2.7 above reproduces Eq. (33) of Ref. 201 to first order.

2.2.1.2 *Wave Function Overlap*

A problem arises with the expressions above for ions, for which the water molecules are very close to the solute; The multipole expansion does not converge. Instead of decreasing, the higher order moment contributions to the solvation energy increase in magnitude as the order increases. This problem can be attributed to the fact that the multipole expansion used is only valid at large separation, i.e., large cavity sizes, where there is negligible overlap of the electronic shells of the interacting atoms. (p. 103 of Ref. 124) At such small separations the wave-function of the ions overlap with those of the water molecules, which leads to the rapidly diverging multipole expansion. Usually, to account for this effect in the theory of intermolecular interactions, semi-empirical damping functions have to be introduced. These reduce the size of the dispersion interaction. Higher orders are damped more and the damping becomes increasingly large the smaller the separation.[252,124] This effect is put forward as a reason the polarisability of water molecules needs to be reduced in polarisable water simulations.[141]

One of the best methods of correcting for this effect in the context of calculating pair wise interactions are the Tang-Toennies damping functions:[252]

$$f_m(r) = \left(1 - \sum_{k=0}^{m} \frac{(br)^k}{k!} \exp^{-br}\right) \tag{2.9}$$

The b parameters are Born-Mayer parameters, which are related to the spatial spread of the wave function. They are used in the Born-Mayer repulsive potential.[253] The r value gives the distance between the centres of the two interacting molecules. The multipole expansion of the dispersion interaction between two atoms including these functions up to the octupole moment becomes

$$\sum_{n=3}^{5} f_{2n}(r) C_{2n} / r^{2n} \tag{2.10}$$

I can apply these functions to the dispersion solvation energy problem with some minor adjustments. I assume that the damping of the dispersion interaction of the solute with the bulk solvent is the same as the damping of the vacuum pairwise dispersion interaction between the solute and the closest water molecule. This assumption can be justified. The damping is due to the wave-function overlap with the nearby water molecules which restricts the degree of polarisation of the solute. This means the solute will have a smaller dispersion interaction with all of the solvent molecules. So we simply multiply each of Eq. 2.5, Eq. 2.6, and Eq. 2.7 by a damping function of the form of Eq. 2.9.

This combination of a macroscopic/continuum treatment of the dispersion interaction with a microscopic/wavefunction based estimate of the damping of that dispersion energy is somewhat unusual. But it is essentially a symptom of the observation (pointed out in Section 1.4.4) that the continuum solvent approximation is not strictly valid in the microscopic regime. And so to apply it successfully it is necessary to separately include some microscopic detail in the model. The addition of these damping functions is a clear example of this.

The value of m is determined by the distance behaviour of the interaction type. To determine the correct distance behaviour we need to be able to compare Eq. 2.5, Eq. 2.6, and Eq. 2.7 with the point-wise interactions which the Tang-Toennies damping functions were developed for.

I can do this by using the expression for the multipole polarisability of a spherical cavity in water:

$$\alpha_n^{cav}(i\xi) = R_{cav}^{2n+1}\,\epsilon(i\xi_n)\,\frac{1-\epsilon(i\xi_n)}{1+\frac{n+1}{n}\epsilon(i\xi_n)} \tag{2.11}$$

This expression is calculated in the same way as Eq. 2.8. R_{cav} is the size of the cavity and ϵ is the dielectric constant of the medium.

Substituting this into Eq. 2.6 I arrive at:

$$G_Q = \frac{15k_BT}{2R_{cav}^{10}\epsilon(i\xi_n)}\sum_{n=0}^{\infty}\left(1-\frac{1}{2}\delta_{n0}\right)\alpha_2(i\xi_n)\alpha_2^{cav}(i\xi_n) \tag{2.12}$$

Apart from a constant factor, this has the same form as the quadrupole–quadrupole contribution to the pairwise interaction energy. (Eq. (3.50) of Ref. 124) This indicates that Eq. 2.6 is analogous to a quadrupole-quadrupole pairwise interaction with a $1/r^{10}$ dependence. Hence, the damping function of the quadrupole dispersion solvation energy term should take $m = 10$. By similar reasoning, $m = 6$ and $m = 14$ are used for the dipole and octupole terms respectively.

The other two parameters in the Tang-Toennies equations are the b values and the r separation parameter, which I will refer to as R_S. The b parameters used in the Tang-Toennies functions need to be an average of the two molecules. I use a well tested[244] combining rule for the determination of this parameter for two unlike atoms coming into contact,

$$b_{12} = 2b_1 b_2/(b_1 + b_2) \tag{2.13}$$

where b_1 and b_2 are the Born-Mayer parameters for the solute-solute and water-water interactions. The determination of these parameters will be discussed below.

The final expressions, including the damping functions, for the dipolar, quadrupolar and octupolar dispersion contribution to the solvation energy are:

$$\begin{aligned} G_D = &-\left(1 - \sum_{k=0}^{6} \frac{(bR_S)^k}{k!} \exp^{-bR_S}\right) \frac{6k_B T}{R_{cav}^3} \\ &\times \sum_{n=0}^{\infty} \left(1 - \frac{1}{2}\delta_{n0}\right) \alpha(i\xi_n) \frac{\epsilon(i\xi_n) - 1}{2\epsilon(i\xi_n) + 1} \end{aligned} \tag{2.14}$$

$$\begin{aligned} G_Q = &-\left(1 - \sum_{k=0}^{10} \frac{(bR_S)^k}{k!} \exp^{-bR_S}\right) \frac{15k_B T}{2R_{cav}^5} \\ &\times \sum_{n=0}^{\infty} \left(1 - \frac{1}{2}\delta_{n0}\right) \alpha_2(i\xi_n) \frac{\epsilon(i\xi_n) - 1}{\frac{3}{2}\epsilon(i\xi_n) + 1} \end{aligned} \tag{2.15}$$

$$G_O = -\left(1 - \sum_{k=0}^{14} \frac{(bR_S)^k}{k!} \exp^{-bR_S}\right) \frac{28 k_B T}{3 R_{cav}^7} \times \sum_{n=0}^{\infty} \left(1 - \frac{1}{2}\delta_{n0}\right) \alpha_3(i\xi_n) \frac{\epsilon(i\xi_n) - 1}{\frac{4}{3}\epsilon(i\xi_n) + 1} \tag{2.16}$$

Here $b = b_{12}$ as given in Eq. 2.13. Once the parameters are known, these expressions allow a very simple and quick calculation which gives the dispersion solvation energy.

2.2.2 *Electronic Properties*

For the calculation of the dispersion energies various properties are also needed. The dielectric function of water at imaginary frequencies ($\epsilon(i\xi_n)$) has been determined by Dagastine.[59] Accurate polarisabilities are essential in calculating these interactions. This means high level correlated quantum calculations are necessary for quantitative results.[203] I use the polarisabilities of the halide ions and the noble gas atoms up to the octupole moment calculated at the TDMP2 level of theory by Hättig and Hess.[99,100] The alkali ion polarisabilities for lithium up to rubidium were provided by Jim Mitroy based on a semi-empirical calculation.[178] The polarisabilities of all of these atoms and ions were also calculated using the Amsterdam Density Functional (ADF) software package (v2010.01)[254,94,242] using the response program[263,197] with the Model LB94 functional[264] and ZORA/QZ4P[265] or ET/ET-QZ3P-3DIFFUSE[49] basis sets, which gave reasonable agreement with the calculations of Hättig and Hess for the dipole and quadrupole polarisabilities. For instance, the dispersion solvation energy of argon calculated using these ADF polarisabilities is within 1.5% of the dispersion solvation energy calculated from the polarisabilities given in Ref. 99, where aug-cc-pV5Z basis sets with additional diffuse functions are used. However, there was a significant difference in the octupole polarisability. The ADF calculation underestimates the polarisability by over 50%, compared to the more sophisticated approaches. The imaginary frequency polarisabilities of cesium,

copper(I) and silver(I) were calculated using this software. These properties were used to calculate the dispersion solvation energy for these ions. So far as I am aware these properties have not been published elsewhere. The inaccuracy of the octupole polarisability does lead to similar uncertainty in the octupole contribution to the solvation energy for these ions.

These polarisabilities are for molecules in the gas phase. There is significant evidence[51,50,224,116,180,121] that anions in condensed phase have polarisabilities that are significantly reduced from the gas phase values. This effect arises from constriction of the anion's wave function in solvent. This effect is much weaker for cations. For that reason I follow Lamoureux and Roux[141,287] in reducing the polarisability of all of the anions by a factor of 0.724 from their gas phase values and I leave the cation and noble gas polarisabilities the same as in gas phase. The single factor of 0.724 was chosen for simplicity although there is evidence this effect may be stronger for smaller anions and larger cations.[180]

2.2.3 *Size Parameters*

2.2.3.1 *Born-Mayer Parameters*

A definition of the radii of the noble gas atoms with coordination number 6 is given by Zhang and Xu.[294] These radii were chosen to be consistent with ionic radii of coordination number 6 that were given by Shannon[243] and Marcus.[167] I will refer to these two sets of radii as R_I. The b parameters are known for the noble gases.[253] As shown in Figure 2.1 these values are approximately linearly related to the R_I values for the noble gas atoms. I therefore use a simple interpolation of this relationship to determine the b parameters for the ions. Similarly the b parameter for water can be determined by using the value of 1.38 Å for R_I. This water molecule radius is determined with the same method used to determine the noble gas radii.[294]

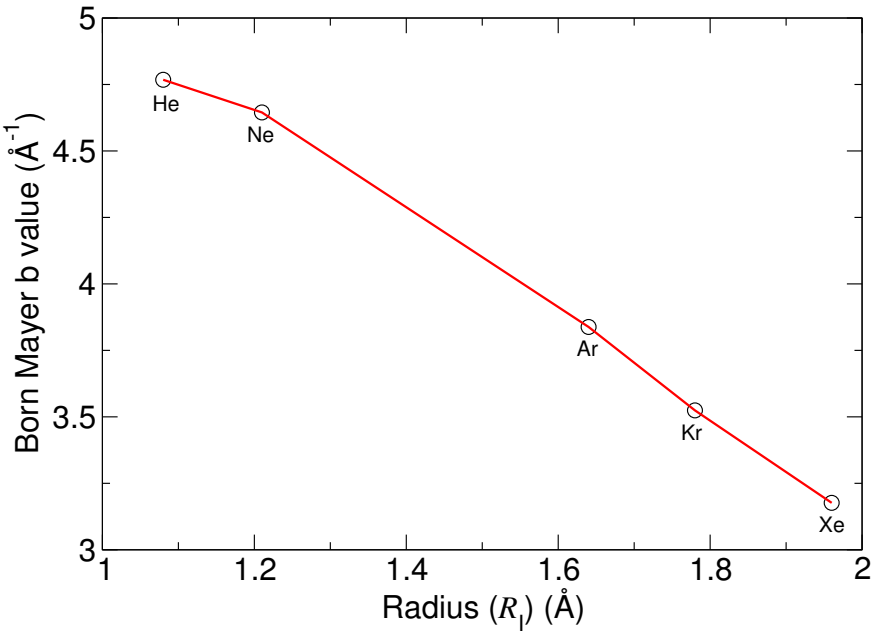

Figure 2.1: The monotonic relationship between the Born-Mayer b parameters[253] and the inherent radius for noble gas molecules is shown.

2.2.3.2 R_S *Parameters*

I now need the R_S parameter, which gives the distance between the centre of the two molecules. A reasonable choice for this parameter can be determined from solute-oxygen radial distribution functions. These functions give the probability distribution of finding a water molecule (oxygen atom) as a function of distance from the solute centre. These functions normally have a strong initial peak at some small separation which corresponds with the first water layer around the solute. The distance to this peak therefore serves as a good choice for the solute-water separation parameter, (R_S). Ref. 193,168,82 compile a large number of experimental measurements of the R_S parameter, determined from diffraction and X-ray absorption fine structure (EXAFS) experiments for many of the important ions. I use the average of these values to get a good estimate of the R_S parameter. The values determined in this way are presented in Table 2.1.

Following the example of Ref. 202 it would be useful to have additional justification of this choice of ion size parameters from quantum mechanical

Atom/Ion	R_I(Å)	R_S(Å)	b(Å^{-1})	R_{cav}(Å)[g]
Li^+	0.76[a]	2.06 ± 0.02[c]	5.49[e]	1.22
Na^+	1.02[a]	2.35 ± 0.02[c]	5.00[e]	1.51
K^+	1.38[a]	2.79 ± 0.03[c]	4.33[e]	1.95
Rb^+	1.52[a]	2.92[c]	4.06[e]	2.08
Cs^+	1.67[a]	3.11 ± 0.04[c]	3.77[e]	2.27
Cu^+	0.77[a]	2.25[h]	5.47[e]	1.41
Ag^+	1.15[a]	2.41 ± 0.01[c]	4.76[e]	1.57
F^-	1.33[a]	2.68 ± 0.06[c]	4.42[e]	1.84
Cl^-	1.81[a]	3.20 ± 0.01[c]	3.47[e]	2.36
Br^-	1.96[a]	3.35 ± 0.03[c]	3.18[e]	2.51
I^-	2.20[a]	3.64 ± 0.01[c]	2.71[e]	2.80
He	1.08[b]	3.08[i]	4.89[f]	2.24
Ne	1.21[b]	3.21 ± 0.01[d]	4.64[f]	2.37
Ar	1.64[b]	3.55 ± 0.01[d]	3.84[f]	2.71
Kr	1.78[b]	3.73 ± 0.03[d]	3.52[f]	2.89
H_2O	1.38[b]	–	4.33[e]	–

[a] Ref. 243 [b] Ref. 294 [c] Average of values from Ref. 193,168,82 [d] Ref. 111,78 [e] Interpolation of b versus. R_I for noble gas particles [f] Ref. 253 [g] $R_S - 0.84$Å [h] *ab initio* calculation [i] Extrapolated by linear relationship between R_I and R_S

Table 2.1: The solute crystal size of coordination number 6 (R_I), solute-oxygen distance (R_S), Born-Mayer parameter (b), and cavity size (R_{cav}).

Table 2.2: A comparison between theoretical and experimental estimates of the ion-oxygen distance in water

Atom/Ion	R_S(Å)(Experiment)	R_S(Å)(Theory)
Li^+	2.06 ± 0.02	2.10
Na^+	2.35 ± 0.02	2.35
K^+	2.79 ± 0.03	2.73
Rb^+	2.92	2.93
Cs^+	3.11 ± 0.04	3.12
Ag^+	2.41 ± 0.01	2.46
F^-	2.68 ± 0.06	2.75
Cl^-	3.20 ± 0.01	3.23
Br^-	3.35 ± 0.03	3.32
I^-	3.64 ± 0.01	3.54

calculations. I performed structure optimizations of ion-water clusters at the MP2 level, with six water molecules placed with D_{2h} symmetry around a central ion. The TURBOMOLE package (v6.4)[1,5] was used with the jobex program.[97,272,273] The aug-cc-pVQZ[128,284,285,274] basis sets were used for the anions up to bromide and water, aug-cc-pVQZ-PP were used for iodide,[212,101] copper and silver.[211] The def2-QZVPP[271,102] basis sets were used for the alkali cations. This allowed a value for the ion-oxygen distance to be determined theoretically. These values are given in Table 2.2 along with the experimentally determined values for R_S, showing they are largely consistent with each other.

Usefully, this method allows a determination of the size of the copper (I) ion in water, which can not be determined experimentally due to its poor solubility.

The R_S parameters for the noble gas atoms are taken from averaging values from MD calculations and EXAFS measurements of the radial distribution functions.[111,78] The exception is helium, which I determine from the linear extrapolation of R_I and R_S for the other noble gas atoms.

These values for the ion size in water are largely consistent with the very intuitive expression:

$$R_S = R_I + R_{wat} \tag{2.17}$$

originally observed by Marcus,[163] who took R_{wat} = 1.38 Å. The only exceptions to this are silver (I) and copper (I), which have R_S values roughly 0.1 Å smaller than this rule predicts.

2.2.3.3 *Cavity Size Parameter*

The cavity size parameter is the last one that needs to be determined. The solvation energies are quite sensitive to the value of this parameter through the $1/R_{cav}^n$ terms. The cavity size defines the spherical region where the relative dielectric function has the value of unity as it is for a vacuum. Outside this spherical cavity the bulk water dielectric function is used. This change occurs at the position where the polarisation of the water becomes significant. This will occur in the first hydration layer around the solute. In principle the dielectric function will increase continuously from 1 to the bulk water value in the region between R_I and R_S from the solute centre. For simplicity however, I model it as a discontinuous boundary, somewhere within this region. So I define R_{cav} as the distance from the centre of the solute particle at which the dielectric changes discontinuously from vacuum to that of the solvent. I assume that it can be written as

$$R_{cav} = R_S - R_{adj} \tag{2.18}$$

Where R_{adj} is fixed for all solutes and $0 < R_{adj} < R_{wat}$ (where R_{wat} = 1.38 Å is the radius of a water molecule.)

To recapitulate, the principle behind the calculations presented here was to use a model that calculates the dispersion contribution to the solvation energy at the same level at which the Born model calculates the electrostatic energy. Indeed, as this discussion does not depend on whether this is the frequency or static dielectric function it is reasonable to conclude that the cavity size for the electrostatic (Born) contribution should be the same as for the dispersion contribution.

An expression for the electrostatic cavity size parameter has been determined from a more sophisticated derivation of the Born equation using an MSA model. The expression is[73]

$$R_{cav} = R_I + 0.54 \text{ Å} \tag{2.19}$$

I can combine Eq. 2.17, Eq. 2.18 and Eq. 2.19 to arrive at

$$R_{adj} = 0.84 \text{ Å} \tag{2.20}$$

Using this value for the cavity size to calculate the electrostatic (Born) energy of solvation for the lithium ion gives a value within 5% of the experimental solvation energy. For this ion the electrostatic component should dominate as its small size and polarisability mean that its cavity formation and dispersion solvation energies will be minimal.

This indicates that this choice of cavity size parameter is appropriate. Because of the consistency of the dispersion and electrostatic contribution I therefore use this value for the cavity size in determining the dispersion contribution to the solvation energy for all of the molecules studied in this thesis. Figure 2.2 provides a visualization of the choices for the size parameters.

Further validation for the choice of $R_{adj} = 0.84$ Å can be found from models of surface tension. Israelachvili (p. 277 of Ref. 113) has shown that the surface tension of a wide range of weakly polar liquids can be estimated using a Lifshitz calculation. The separation between the two dielectric surfaces is taken to be $l = \sigma/2.5$. Where σ is the atomic spacing of the liquid. This expression is derived by comparison with a molecular level calculation assuming pairwise additivity. From Figure 2.3 it is clear that R_{adj} can be written in terms of l as

$$R_{adj} = \frac{\sigma - l}{2} = \frac{3\sigma}{10} \tag{2.21}$$

For water a reasonable choice for σ is 2×1.38 Å $= 2.76$ Å which gives $R_{adj} = 0.83$ Å. Very similar to the estimate based on the MSA model.

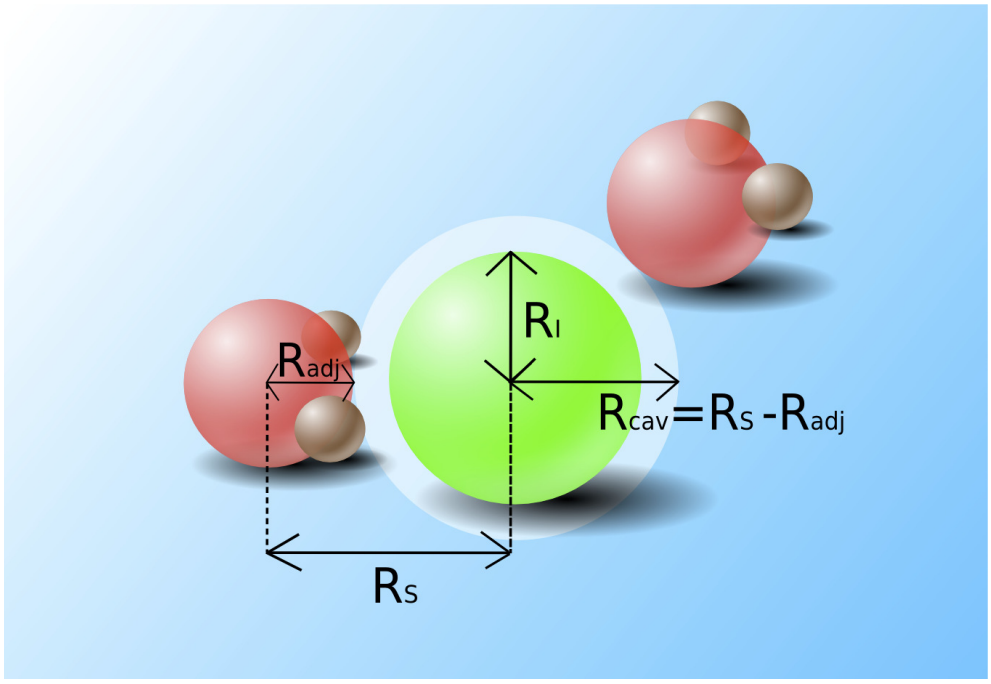

Figure 2.2: Diagram of an ion in a cavity visualising the size parameters.

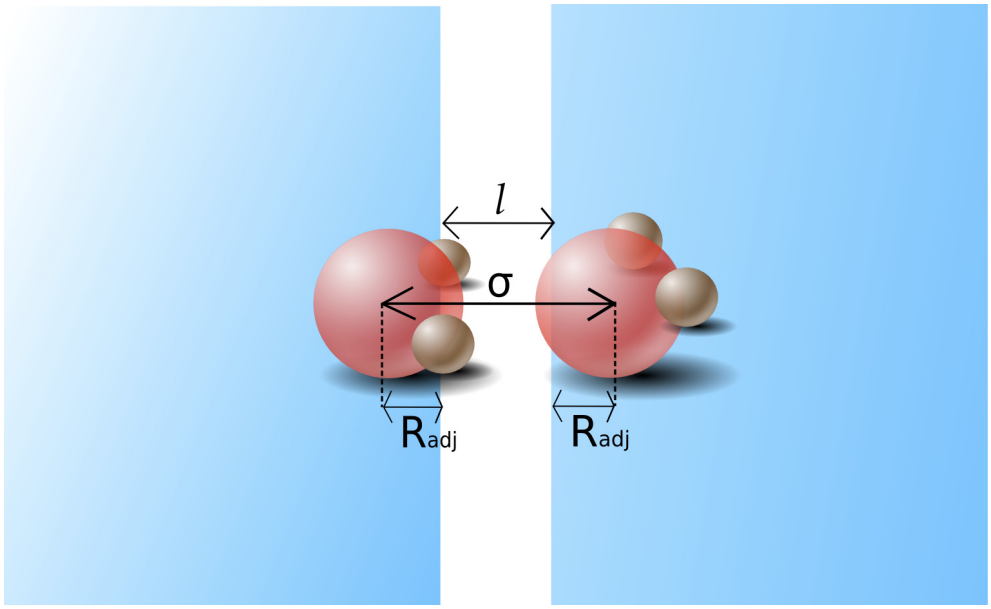

Figure 2.3: Diagram of two interacting water interfaces.

Atom/Ion	G_{Disp}	G_{Dipole}	$G_{Quadrupole}$	$G_{Octupole}$
Li^+	−7.1	−6.5 (91%)	−0.6 (8%)	−0.0 (1%)
Na^+	−21.5	−17.9 (83%)	−3.0 (14%)	−0.6 (3%)
K^+	−46.2	−35.1 (76%)	−8.9 (19%)	−2.1 (5%)
Rb^+	−61.6	−44.7 (73%)	−13.2 (21%)	−3.7 (6%)
Cs^+	−74.9	−52.4 (70%)	−19.3 (26%)	−3.2 (4%)
Cu^+	−112.5	−75.4 (67%)	−21.1 (19%)	−16.0 (14%)
Ag^+	−119.8	−90.9 (76%)	−22.1 (18%)	−6.8 (6%)
F^-	−100.5	−47.3 (47%)	−31.0 (31%)	−22.2 (22%)
Cl^-	−90.3	−46.8 (52%)	−27.0 (30%)	−16.5 (18%)
Br^-	−93.3	−49.0 (53%)	−28.0 (30%)	−16.3 (17%)
I^-	−85.4	−47.1 (55%)	−25.1 (29%)	−13.2 (15%)
He	−6.5	−5.6 (86%)	−0.8 (12%)	−0.1 (2%)
Ne	−12.0	−9.8 (82%)	−1.8 (15%)	−0.4 (3%)
Ar	−28.2	−21.1 (75%)	−5.5 (19%)	−1.6 (6%)
Kr	−33.4	−24.5 (74%)	−6.8 (20%)	−2.1 (6%)

The percentages of the total dispersion energy are in brackets.
The free energies are given in units of $kJmol^{-1}$

Table 2.3: The contributions to the dispersion solvation energies of some simple ions and noble gas atoms.

2.3 RESULTS AND DISCUSSION

Dispersion contributions to the solvation energy have been calculated using the methods outlined here. The results for the noble gas atoms and some monatomic and monovalent ions are presented in Table 2.3. They are also plotted as a function of size in Figure 2.4 (ions) and Figure 2.5 (noble gas atoms)

These values cannot be directly compared with experiment as there are important contributions from the cavity formation and electrostatic energies which contribute to the solvation energies. These need to be taken into account before comparison with experimental solvation energies can be made. This work is outlined in Chapter 3.

2.3.0.4 *Magnitude*

These dispersion energies are of significant size when compared with the experimental solvation energies.[127,26] For example, iodide's dispersion energy

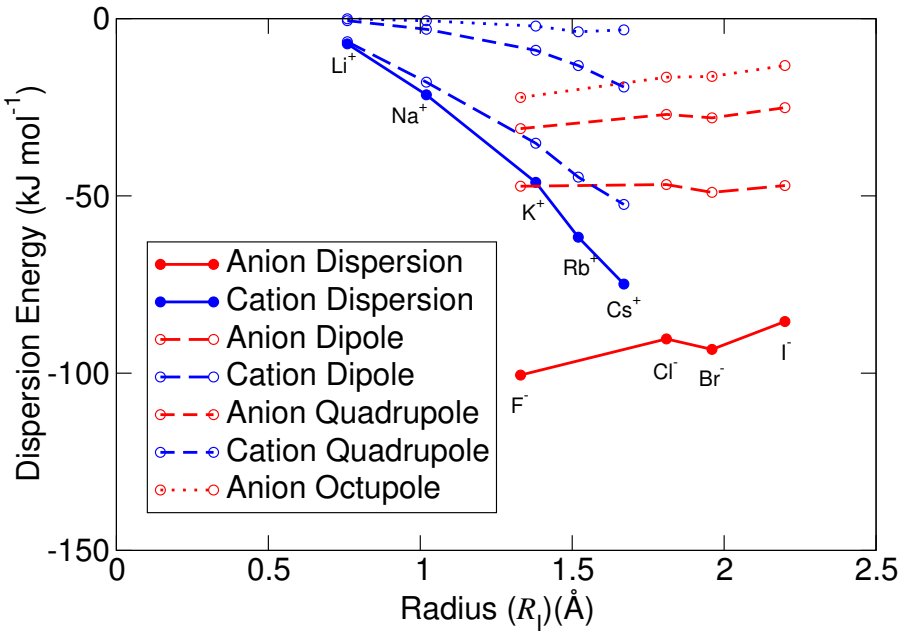

Figure 2.4: The dispersion contribution to the solvation energy of the alkali halide ions as a function of their inherent radius.

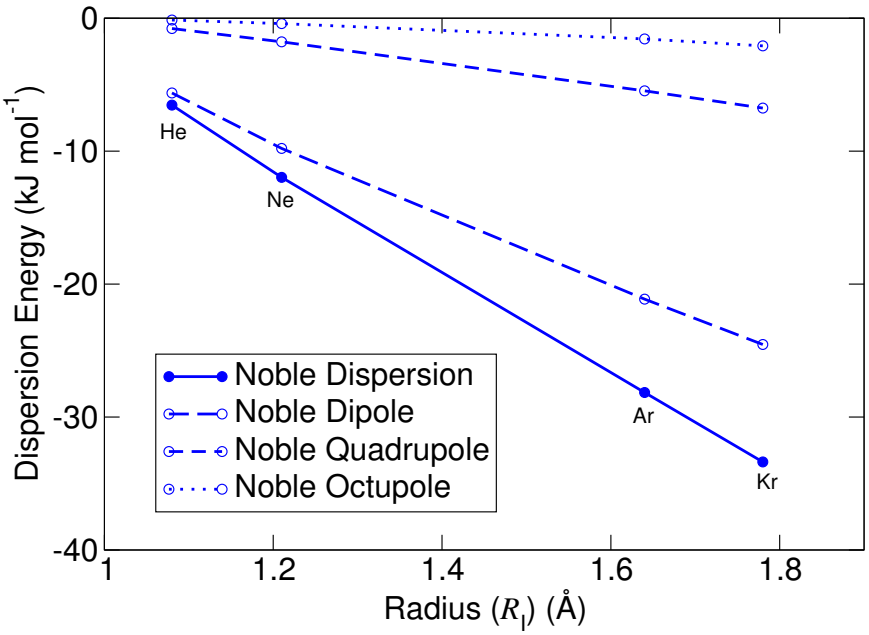

Figure 2.5: The dispersion contribution to the solvation energy of the noble gas atoms as a function of their inherent radius.

is 34% of its solvation energy. The conclusion is inescapable. The dispersion energy makes an important contribution. Even more so for anions. The particular importance of the dispersion interaction for the anions has been noted before.[30,205] This helps explain why anions play a more important role in many Specific Ion Effects.[30,136] Their large size and polarisability means the electrostatic interaction is comparatively weak and so the dispersion interaction may play an increasingly important role. Since publishing this model Amovilli and Floris[7] have published a new separate model, which uses quantum Monte Carlo methods to calculate the dispersion solvation energy of solutes. They adjusted the size parameters for the noble gas atoms and for the fluoride anion to reproduce the solvation energies calculated in this chapter. The resulting size parameters were very similar to the cavity sizes calculated here: 1.82 Å for F^-, 2.17 Å for He and 2.26 Å for Ne. This provides independent confirmation that the dispersion solvation energies calculated with this model are accurate.

There are two reasons for the importance of the dispersion energy in the solvation of anions. The first is that their excess electron makes them highly polarisable, resulting in a larger dispersion interaction. Although the electron does make the ions larger, this effect is not significant enough to compensate for the increased polarisability. Secondly, due to the charge on an ionic solute, the water dipoles are pulled significantly closer to the ions than they are to the neutral noble gas solutes. This is clear from the R_S parameters. The value of R_S for argon is larger than for any of the ions including iodide. The short range nature of the dispersion interaction means that this pulling in of the water molecules significantly increases the magnitude of the dispersion energy. This reduction in the R_S parameter occurs for both cations and anions. But the lower polarisability of cations, due to the missing electron, mitigates this effect for the smaller alkali ions resulting in a dispersion energy similar to the noble gas atom's dispersion energy, and hence relatively small compared with the electrostatic contribution. This is not true however, for copper (I) and silver (I), which are comparatively small, such that this pulling in of water molecules is particularly pronounced. For instance, silver

(I) has the same dipole polarisability as rubidium, but it has an R_S value only slightly larger than that of sodium. This results in a relatively large dispersion energy for these ions as well.

2.3.0.5 *Size Dependence*

An interesting observation clear from Figure 2.4 is that the magnitude of the dispersion contribution to the solvation energy actually decreases with ion size for the halides. This means that the fluoride ion actually has a slightly larger dispersion solvation energy than iodide. This is a surprising and counterintuitive result. However, it can be understood if we consider the increase in polarisability compared to their isoelectronic noble gas atoms. Fluoride has 6 times the dipole polarisability of neon, whereas bromide has less than three times the polarisability of Krypton. So as the atoms become larger the relative effect of one less proton becomes less pronounced. The dispersion interaction is therefore less enhanced. This is also consistent with certain calculations of the Lennard-Jones dispersion potentials, fitted by comparison to experiment, which assign to fluoride the largest dispersion interaction.[251] I also verify this effect using *ab initio* calculations in Chapter 5.

There is significant disjunction between anions, cations and noble gas solutes in the relationship between their size and their dispersion energy contribution. This is shown in Figure 2.4 and Figure 2.5. These results clearly indicate that the relationship between dispersion energy and size is far from trivial and depends sensitively on the electronic properties of the solute. It can not be assumed that solutes of the same size will have the same dispersion energy. This fact means there will be be significant error in models which assume the dispersion energy of all solutes scales with their size.[3,164]

2.3.0.6 *Multipoles*

Figure 2.5 shows that the dipole contribution gives a reasonable estimate of the dispersion energy for the smaller noble gas atoms. But as these atoms get larger the higher orders, particularly quadrupole, start to provide a significant correction. This is also true for the alkali cations as shown in Figure

2.4. Table 2.3 shows that copper(I) and silver(I) have surprisingly significant higher order contributions given their size. This is due to the pulling in of the water molecules. For the anions, Figure 2.4 shows that the higher order multipole moments are very important. This is particularly true for small anions such as fluoride, where the higher order multipole moment contributions comprise over half of the total dispersion energy. This is understandable as these terms account for the variation of the electric field over the region that the molecule occupies. In other words they account for the finite size of the ion. The electron cloud around an anion is quite disperse and so this finite size contribution is significant.

2.4 CONCLUSION

In summary this model provides a method for calculating the dispersion contribution to the solvation energy. It is based on the continuum model and uses the same level of approximation as the Born model, it is simple to apply using properties available in the literature. Counter intuitively, the dispersion solvation energy increases with cation size, but decreases with anion size. The higher order multipole moment contributions are essential, making up over 50% of fluoride's dispersion solvation energy.

In the next chapter I combine this model with a calculation of the electrostatic and cavity contributions to the solvation energy in order to compare with experiment. This model would be advanced further by more accurate calculation of the frequency–dependent higher order polarisabilities of additional molecules. Generalizations of the equations could be made to anisotropic molecules and to cases where the multipole moment is not at the centre of the cavity. These improvements would allow the application of the model to a much wider class of molecules. In addition, the determination of the Green's function for more general situations would be very useful. For example, an ellipsoidal cavity, a cavity near a surface, or two cavities near each other. This would provide a calculation of the contribution of the dispersion energy to a wider class of experimental properties such as os-

motic coefficients and surface tensions. This problem is discussed further in Chapter 6 and Chapter 7.

3

TOTAL IONIC SOLVATION ENERGIES

This chapter is reproduced with minor changes and with permission from Ref. 67: T. T. Duignan, D. F. Parsons, and B. W. Ninham. A Continuum Model of Solvation Energies Including Electrostatic, Dispersion, and Cavity Contributions. J. Phys. Chem. B, 117:9421–9429, 2013. Copyright 2013 American Chemical Society.

3.1 INTRODUCTION

In order to understand Specific Ion Effects it is essential to begin with a quantitative theory of the solvation free energies of ions.[110] These properties are important in their own right, e.g, in ion exchange, purification and physiological applications. But they are also important in laying the foundations on which to build better models of electrolyte solutions. This in turn is important for all of the reasons outlined in the introduction.

3.1.1 *Background*

Solvation energies measure the change in free energy of a solute immersed in water compared to that of the solute in vacuum. A large and venerable literature[110,135] is dedicated to their calculation for ions (and molecules), for different sizes and shapes, using a variety of methods. The free energy change arises from three sources: The first two are the electrostatic and dispersion interaction energy of a solute molecule with water. The third is the change in the free energy of the water due to the rearrangement and displacement of the water molecules around the solute particle. This includes

the cavity formation energy, i.e., the energy of carving out the hole in water that the ion occupies.

3.1.2 *Significance*

As mentioned above, predicting free energy changes of ions in water is a crucially important goal and achieving this goal first requires an understanding of solvation free energies of ions in bulk water. This is because the change in the ion-water and water-water interactions make up a significant contribution to the total free energy change in many processes. This fact is demonstrated in Chapters 6 and 7 where I outline how this solvation model can be generalised to calculate the surface tension and activity/osmotic coefficients of electrolytes.

3.1.3 *Modelling Approaches*

A recent book[110] gives an overview of the situation. In this section I provide some context to the model presented in this chapter by discussing some specific models antecedent to it. This is followed by a general discussion of the current approaches found in the literature.

3.1.3.1 *Born Model*

The first and most important is the Born model.[28] This model gives the electrostatic contribution to the solvation energy due to polarisation of the solvent from the ion's charge. The ion is modelled as a point charge placed in a cavity inside a dielectric medium. The input parameters it requires are the static dielectric constant, the ionic valency and the cavity size.[229]

It includes both an enthalpic and entropic contribution as the dielectric constant and possibly the cavity size are temperature dependent. Its extension to include ionic correlations, at a mean–field level, gives Debye-Hückel theory.[233]

The Born equation is

$$G_{Born} = -\frac{q^2}{8\pi\epsilon_o R_{cav}}\left(1 - \frac{1}{\epsilon_r}\right) \tag{3.1}$$

Here R_{cav} is normally interpreted as the size of the cavity in water that the ion creates. Although this model is much criticized and rather simplistic, there is some justification for believing it is relatively accurate in capturing the essence of electrostatic interactions, at least for monovalent ions.[115,238,113] Given its simplicity and neglect of other contributions, this model is surprisingly successful at reproducing the experimental solvation energies.

Indeed several calculations of solvation energies based solely on this model have been put forward. They adduce various justifications for choices of the cavity radius. These are typically related to the crystal radius of the ion, referred to as R_I, by taking $R_{cav} = R_I + R_{add}$. Here R_{add} is some additional cavity increment, which may be different depending on whether it is for a cation or anion, with some physical rationalization.[229,13,73] Or alternatively, as in Chapter 2, the distance to the peak (R_S) in the ion-oxygen radial distribution function (RDF) is used instead of the crystal radius: $R_{cav} = R_S - R_{adj}$.[240]

The success of this schema can be seen in Figure 3.1 which plots the solvation energy as a function of radius, where two fitted values of R_{add} have been chosen. With $R_{add} = 0.55$ Å the Born model follows the cations almost exactly. With $R_{add} = 0.35$ Å, on the other hand, it roughly follows the anionic experimental solvation energies. The need for different values of R_{add} for cations and anions, can be clearly seen from the smaller anions, which have a significantly larger solvation energy then a cation of the same size would.

It is also possible to derive the Born equation from the apparently more sophisticated mean spherical approximation (MSA), which treats the solvent on a molecular level. This model can also be used to derive a value of $R_{add} = 0.54$ Å.[73]

There is some debate regarding what the best experimental solvation energy values to compare against are. This will be discussed below. The experimental values used here are those of Tissandier et al.[256,127]

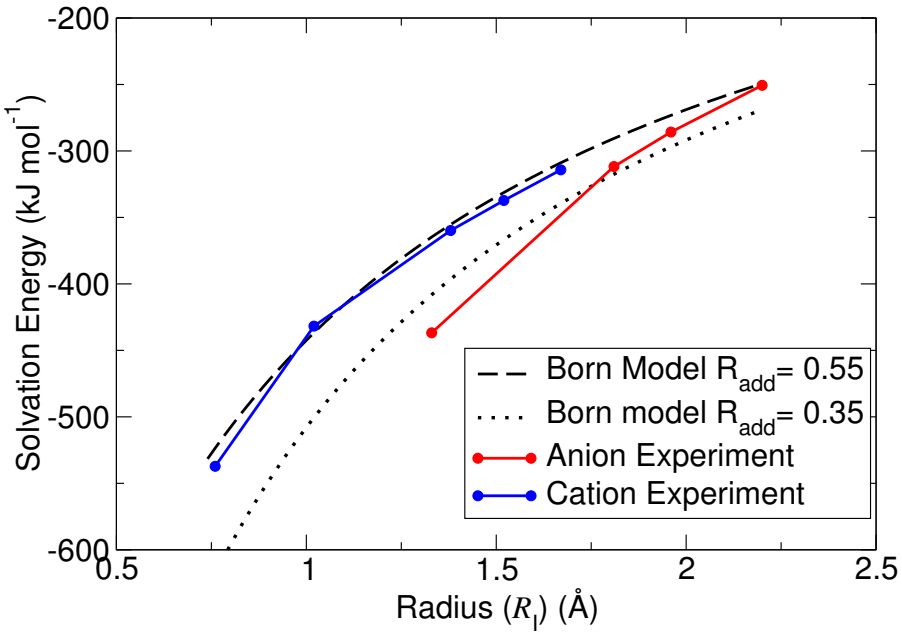

Figure 3.1: The Born model solvation energy of the alkali halide ions compared to experiment. Plotted as a function of the crystal radius of the ion R_I. The ionic cavity radius is $R_{cav} = R_I + R_{add}$.

3.1.3.2 *Cavity Size*

The cavity radius represents the distance at which the polarisation distribution of the water effectively begins. Various physically based arguments for why this R_{add} parameter is different for cations and anions have been put forward.[13,240,110,186] In brief, the argument is that the distribution of water dipoles should be considered to be further away from cations than anions due to the orientation of the water molecules in the first solvation layer.

This difference in solvation energy of similarly sized anions and cations is a problem even in more complex continuum models. For instance, Marcus's solvation energy model[164] included an arbitrary correction which shifted the solvation energy of cations and anions a constant amount in opposite directions to improve agreement with experiment. The need for this correction was again attributed to the difference in orientation of the water molecules in the first layer.

This fact is often cited as evidence of the importance of water structure on electrolyte properties. It is argued that the specific size and orientation of the water molecules play an important role. Hence it is concluded that explicit solvent models are necessary to understand the properties of electrolyte solutions.[186,110,157]

An objection to this argument can be raised based on several observations. The first is clear if we look at the sodium and fluoride ions. These ions have almost identical solvation energies.[127] However, if we look at the distance from the centre of these ions to the centre of the oxygen atoms in the nearest water molecules we see that the water molecules are substantially (0.33 A) further away from the fluoride ion. So clearly the difference in orientation is not allowing the water molecules to approach any closer. The second is that the electrostatic potential created around a water molecule, given in Ref. 192, is in fact roughly symmetric around a water molecule. This is true in the sense that at a distance of 2.75 Å from the central oxygen atom in a water molecule the maximum positive and negative potentials are equal in magnitude (± 100 kJmol^{-1}). This implies that the electrostatic interaction energy of an ion of fixed size with a water molecule should be the same irrespective of whether it is positively or negatively charged. That is R_{add} should be the same for cations and anions.

An additional problem with attributing different R_{add} parameters on the basis of different water orientation is that it does not explain the variation in this parameter that occurs with cations. Consider the solvation energy of a silver ion and of a sodium ion. Both have essentially the same size[163] but silver has a solvation energy 65 kJmol^{-1} more negative then sodium. The water molecules will have the same orientation in both cases. So the use of a different R_{add} can not be justified with this argument.

This then raises the question of how to account for the clear difference in the solvation energies of two ions of the same size. A common answer is to argue that 'chemical' interactions occur between the ions and water. In the context of a many body system of molecules with closed electron shells it is not at all clear what the distinction between chemical and physical inter-

action means. It would be unfortunate, if true. Presumably it would mean that *ab initio* explicit water simulations will be necessary in order to model even the simplest properties of ions in water. I therefore seek simpler models and explanations of these solvation energies without attributing them to unquantifiable 'chemical' interactions.

3.1.3.3 *Additional Contributions: Dispersion and Cavity Energies*

A problem with using the Born model to calculate solvation energies is that it leaves out other known contributions. These contributions can be roughly categorized as cavity formation and dispersion energy contributions. Both have been shown to be significant.[29,215] They need to be modelled separately and included along with the Born contribution. The cavity contribution has an opposite sign to the dispersion contribution, and there is reason to believe they will be of comparable magnitude too[276] and so will largely cancel. In fact this cancellation is very likely the reason for the surprising successes of the Born model. This means that both of these contributions must be taken into account to improve experimental agreement. Both contributions increase with solute size. This is consistent with the fact that the Born model is less accurate for the larger anions compared with the smaller cations.

With the above as background, I now attempt to remedy the deficiencies of continuum solvent theory. I present a model which shows that the failures of the Born model can be fixed without having to resort to arguments regarding specific orientation of water molecules. This is achieved by including an accurate calculation of the dispersion and cavity contributions. Qualitatively the argument is that the larger solvation energy of fluoride and silver compared with potassium and sodium respectively, is explained by the fact that fluoride and silver are much more polarisable than potassium and sodium. Hence they will have larger dispersion contributions to the solvation energy. Incorporating an accurate description of the dispersion interaction of ions with the surrounding water validates this argument and removes the need to vary the R_{add} parameters of the ions. This is a much more satisfactory explanation for the discrepancy. It is conceptually simple, and in principle this

approach does not necessarily require time consuming and highly nontrivial explicit water simulation. However, computer simulation methods may be useful in determining the size parameters where X-ray data is not available. Further, it does not depend on arbitrarily adjusted parameters to fix the difference in solvation energy between ions of similar size.

3.1.3.4 *Simple Models*

One approach in the literature to account for the cavity and dispersion contributions is to assume that they are functions of the size of the solute. For instance, some models[3,164] use the noble gas solvation energies. They argue that with a consistent definition of ion and gas particle size the contribution to the ionic solvation energy from these two contributions can be determined by interpolation of the solvation energy of the noble gases as a function of size. Other models include the dispersion and cavity energies in a surface tension parameter.[55] This approach is sensible for some contributions. For instance, I will argue below that a surface tension parameter is a sensible way to incorporate the energy cost of cavity formation.

However, as argued in Chapter 1, this approach is not reasonable for the dispersion energy. The dispersion energy is a function of the polarisability, the size of the solute particle, and the solute-solvent separation. This significantly complicates the situation when ions are concerned.

This means we need an independent and accurate calculation of the dispersion contribution to the solvation energy. To test that the cavity and dispersion contributions are being modelled accurately it is important that any solvation model used to account for the solvation energies of ions, can also give a sensible interpretation of the solvation energies of neutral molecules as well.

3.1.3.5 *Dispersion Model*

In Chapter 2 I outlined a method which calculates the dispersion contribution to the solvation energy of a molecule at the same level of theory as the

Born model. This means it is consistent to use the same cavity size for both Born and dispersion calculations.

3.1.4 *Goal*

Hünenberger and Reif[110], in their book 'Single Ion Solvation' published in 2011, outline a set of criteria that a continuum solvent must meet in order to be considered 'satisfactory.' I provide my own interpretation of these criteria here:

- The model cannot include ad hoc corrections nor rely on unreasonable assumptions or approximations.
- It must depend on very few, if any, fitted parameters, that are adjusted to reproduce experiment only within physically reasonable ranges.
- The contributions must be additive.
- Qualitative properties of solvation energies such as the charge hydration asymmetry (CHA),[184] must be reproduced and explained.
- It must reproduce: solvation free energies, entropies (enthalpies), and partial molar volumes.

These criteria form the basis of Hünenberger and Reif's claim that there is no quantitatively accurate continuum model of the solvation energy of ions that 'can be regarded as entirely satisfactory.'[110] These criteria are essentially a more specific version of the criteria laid out in Section 1.3.1 but applied to the problem of single ion solvation.

In this chapter and the next I present a continuum solvent model of solvation energies that is aimed at satisfying these criteria. I use the calculation of the dispersion contribution to the solvation energy outlined in Chapter 2, which includes quadrupole and octupole moment contributions. In Section 4.4.1 I provide an assessment of the model using these criteria.

The goal is to accurately reproduce and explain the solvation energy of ions and atoms, while also conserving computational time and conceptual

simplicity. By doing this I can provide physical insight into these properties and provide a stepping stone for Chapters 6 and 7, where I tackle more complex Specific Ion Effects like surface tensions and activities.

Although this is not an explicit solvent model, the methods presented and discussed here still have implications for the modelling of dispersion interactions in explicit solvent approaches. They may be useful in a hybrid approach or may provide an indication of what to expect from explicit water models.

3.2 THEORY

3.2.1 *Electrostatic Contribution*

I include the Born model in this calculation to account for the electrostatic contribution to the solvation energy.[28] The expression is Eq. 3.1. Many modifications to this model have been proposed (p. 491 of Ref. 110) to incorporate dielectric saturation,[38] electrostriction,[283] or other such higher order effects.[19] These methods often involve a spatially dependent dielectric function. However, there is no clear consensus in the literature regarding the best method for incorporating these effects or how important they are. For this reason, as well as to keep the model simple, and to minimize the number of fitted parameters, I use the unmodified Born model.

3.2.2 *Dispersion Contribution*

I use the dispersion calculation outlined in Chapter 2. More specifically, Eq. 2.14–2.16.

3.2.3 *Cavity Contribution*

Calculating the free energy cost of creating a cavity in the solvent for a solute to occupy is a much studied, but not well resolved, problem.[215,108] Evidence from molecular dynamics simulations shows that for small hard sphere solutes, of the size considered in this thesis, the effective surface tension reduces to zero roughly linearly with the radius. This means that for these small solutes the energy of cavity formation scales with the volume of the cavity.[44,225]

The hard sphere solutes used in these calculations are very similar to the noble gas solutes because the dispersion interaction does not significantly alter the structure of the surrounding water. They might then be expected to be a good model for the cavity formation energy of noble gas solutes.

Because these models use a simple hard sphere solute to model the cavity, the volume of the cavity is defined as the region where the centres of the water molecules are excluded. This means that the most appropriate choice of radius for this cavity is R_S, as this gives the average distance to the centre of the closest water molecules.

I therefore model the cavity formation energy of the noble gas elements with the following expression.

$$G_{\text{NG-Cav}} = \sigma_{\text{NG}} R_S^3 \tag{3.2}$$

Here σ_{NG} is a parameter determined from explicit water simulation.[225] I use the same value as Ref. 148, $\sigma_{\text{NG}} = 0.73$ kJmol^{-1} Å^{-3}.

However the situation for the ions is quite different. The reason the effective surface tension of a hard sphere solute cavity reduces to zero is that the water molecules around very small sized cavities can form hydrogen bonded networks.[44] This means that the cavities do not break the structure of the water, and hence there is a smaller energy cost to their formation. However, for small ions this is not the case. The electric field of the ion reorients the water molecules, breaking the hydrogen bonded structure and costing energy. This

is similar to the effect that very large solutes have on water, where the bulk surface tension parameter is accurate.[44] This means that it is more appropriate to use the bulk surface tension in determining the cavity formation energy of ions. I therefore use the expression:

$$G_{\text{Ion-Cav}} = \sigma_{\text{Ion}} 4\pi R_S^2 \tag{3.3}$$

For σ_{Ion} I use the surface tension of bulk water $\sigma_{\text{Ion}} = 0.434$ kJmol^{-1} Å^{-2}.[110]

3.2.4 *Input Data*

I compare the solvation energies calculated with this model against the experimental ionic solvation energies taken from the work of Kelly et al.,[127] and noble gas solvation energies taken from the work of Ben-Naim and Marcus.[26]

3.2.4.1 *Cavity Size*

The cavity size used for electrostatic and dispersion contributions is $R_{\text{cav}} = R_S - 0.84$ Å (determined in Section 2.2.3.3). R_S is the distance between the centres of the solute and the water molecules in the first layer, taken as the position of the peak in the solute-oxygen radial distribution function. The determination of these values using *ab initio* and experimental methods is given in Chapter 2. The values are given in Table 2.1. As established in Ref. 202, a consistent and quantum mechanical definition of ion size is crucially important for these calculations. It is important to distinguish between the R_{cav} parameter which is used in the Born and dispersion energy calculations, and the parameter used to determine the cavity formation energy which is R_S. R_{cav} represents the region where the water is not significantly polarised. R_S gives the average distance between the centres of the solute and the water molecules in the first solvation shell. It is therefore a more appropriate measure of the region from which the water molecules are excluded.

3.2.4.2 *Proton Solvation Energy*

The values for the experimental solvation energies of individual ions used here are the so called 'benchmark experimental values'[43] of Tissandier et al.[256,127] They are significantly shifted from the values of Marcus,[167] which are used most often in the Specific Ion Effects literature.

This difference is due to the difficulties associated with the splitting of the measured salt pair solvation energies into two contributions from the individual ions. Fixing the value of the solvation energy for one ion (normally the proton) allows all the other ionic solvation energies to be determined from the pair data. There are two important implications of the more recent experimental values determined by Tissandier et al.[256] One is that the gap between anions and cations of the same size is now significantly reduced. This makes it more plausible that the discrepancy is due to dispersion interactions. It also means that justifications for different choices of the Born radius need to be reconsidered as they have been chosen to agree with experimental data which may not be correct. Another important implication is that these new experimental results seem to show a qualitatively different trend from the Born model predictions as seen in Figure 3.1. There is no choice of R_{add} that gives adequate agreement with the experimental halide ion solvation energies. This indicates that there are additional contributions to the solvation energy which the Born model neglects.

3.2.4.3 *Surface Potential*

A complicating factor in comparing theoretical and experimental solvation energies is the contribution from the surface potential of water. This is the potential difference over a water interface due to a charge imbalance. There is ongoing debate in the literature as to whether Tissandier's values include some contribution from the surface potential.[11] If there is some contribution of this type to Tissandier's values, then this would need to be corrected for before the values could be compared with a continuum type model such as this one, which neglects any such contribution.

In this chapter I compare with the uncorrected estimates of Tissandier's values given in Ref. 127. I agree with the argument of Tissandier, Hünenberger and Reif (p. 451 of Ref. 110) that these values do not include any surface potential contribution. An accurate value can be obtained from clusters containing only one water molecule. The notion that there will be a significant contribution from the surface potential of bulk water at this small a cluster size seems unlikely. In addition, any surface potential contribution should change as the cluster size increases resulting in Tissandier's estimate of the proton solvation energy varying with cluster size. But the estimate is independent of cluster size up to six water molecules.[127] This implies that there is no surface potential contribution included in this estimate. Hünenberger and Reif (p. 469 of Ref. 110) also give a comprehensive review of the literature regarding the proper choice of the intrinsic solvation energy of the proton. They conclude, based on multiple lines of evidence, that the best choice is a value basically the same as the one used here.

If this contribution were important it would not be clear at all how to correct the values to account for it. The correct surface potential of bulk water is still debated.[126] In addition to this the surface potential contribution to the solvation energy will have a contribution from both the bulk air-water interface and the ion-water interface which are likely to significantly cancel.[96] This means that knowing the bulk air-water interface potential would be insufficient to go forward. Finally, even if this contribution had been accurately calculated, there is little reason to believe that it will be the same in the very small ion-water clusters used in Tissandier's experimental estimates.

3.3 RESULTS AND DISCUSSION

The solvation energy values calculated with this method are given in Table 3.1. Figure 3.2 shows that the model gives good agreement with experimental solvation energies. The mean absolute error is 12 $kJmol^{-1}$ (3%). Figure 3.3 shows the model also agrees well with the solvation energies of the noble gases, where the error is 2.6 $kJmol^{-1}$ (30%). The percentage error is quite

Table 3.1: The contributions to the solvation energies of some small ions and noble gas atoms.

Atom/Ion	G_{exp}	G_{theory}	Electrostatic	Cavity	Dispersion
Li^+	−537.2	−546.1	−562.1(105%)	23.1(−4%)	−7.1(1%)
Na^+	−431.8	−445.6	−454.2(105%)	30.1(−7%)	−21.5(5%)
K^+	−359.8	−355.4	−351.7(98%)	42.4(−12%)	−46.2(13%)
Rb^+	−337.2	−344.9	−329.7(98%)	46.5(−14%)	−61.6(18%)
Cs^+	−314.2	−324.3	−302.1(96%)	52.7(−17%)	−74.9(24%)
Cu^+	−591.2	−571.3	−486.4(82%)	27.6(−5%)	−112.5(19%)
Ag^+	−496.6	−524.9	−436.8(88%)	31.6(−6%)	−119.8(24%)
F^-	−436.8	−434.1	−372.7(85%)	39.1(−9%)	−100.5(23%)
Cl^-	−311.7	−325.1	−290.6(93%)	55.8(−18%)	−90.3(29%)
Br^-	−285.8	−305.4	−273.2(96%)	61.1(−21%)	−93.3(33%)
I^-	−250.6	−258.2	−244.9(98%)	72.2(−29%)	−85.4(34%)
He	11.5	14.8	0	21.3(185%)	−6.5(−57%)
Ne	11.2	12.2	0	24.1(216%)	−12.0(−107%)
Ar	8.4	4.5	0	32.7(390%)	−28.2(−336%)
Kr	6.9	4.5	0	37.9(547%)	−33.4(−482%)

The rounded percentage contributions to the total are given in brackets. The free energies are given in units of $kJmol^{-1}$

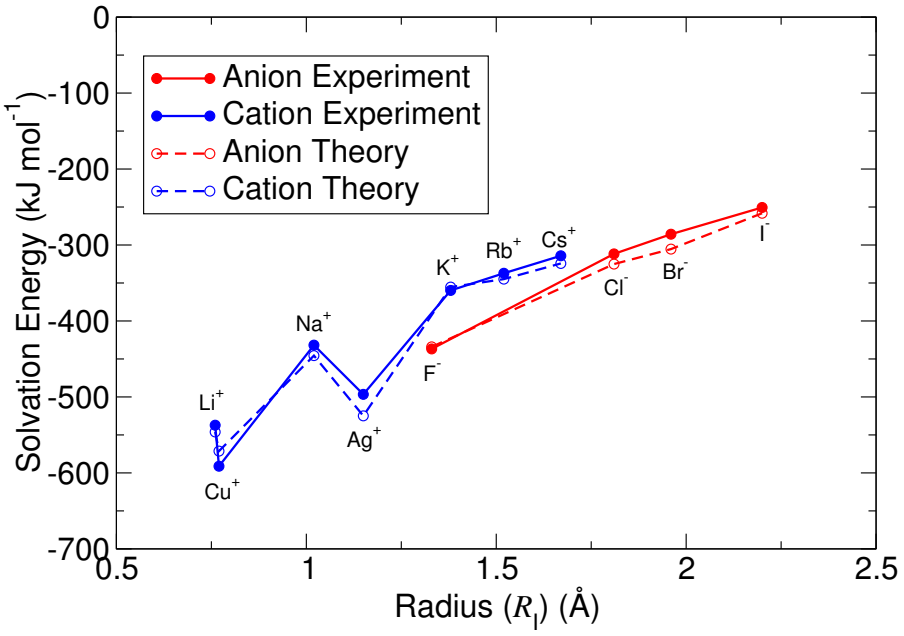

Figure 3.2: Calculated solvation energies compared with experiment for some ions.

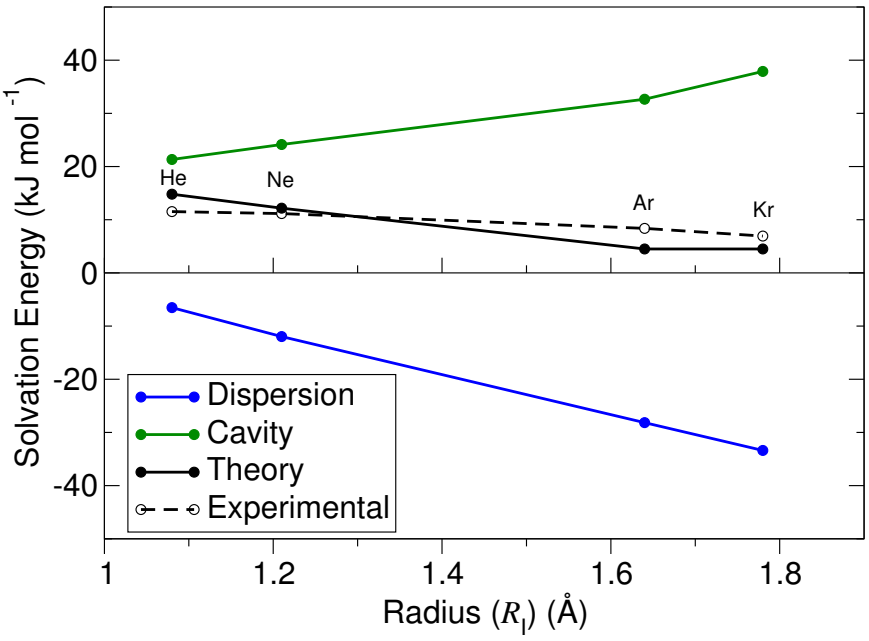

Figure 3.3: Calculated contributions to the solvation energy of the noble gases. Including comparison to the experiment values.

large due to the significant cancellation of the cavity and dispersion contributions. This cancellation can be seen in Figure 3.3 and Figure 3.4, which give the contributions to the solvation energy. In addition, Figure 3.2 and Figure 3.3 both show that the model reproduces all of the qualitative features of the solvation energies. In particular, the non monotonic jumps due to $Cu^+(R_I = 0.77)$ and $Ag^+(R_I = 1.15)$ are reproduced. The large cancellation of dispersion and cavity formation energies has also been accurately captured. Obviously the situation for divalent ions, Cu^{2+} in particular, is significantly more complicated.

The fact that only one value for the R_{adj} parameter is needed to fit the solvation energy of both cations and anions, is significant. This indicates that differences in water orientation around the two types of ions does not play a significant role. The explanation of the unusually large solvation energies of the copper and silver ions with no adjustments to the model confirms the success of the model.

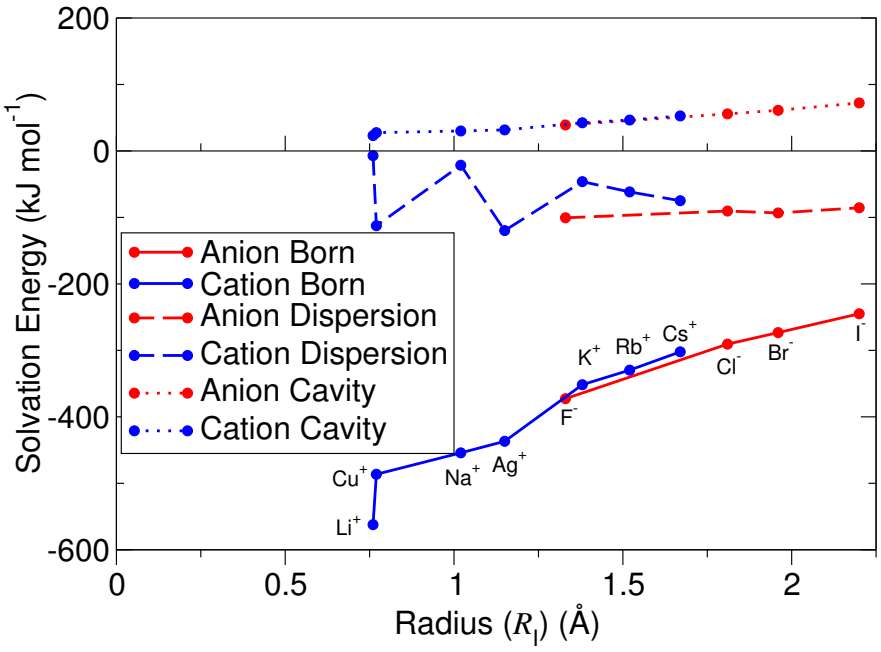

Figure 3.4: Calculated contributions to the total ionic solvation energy

Unfortunately, as with any model, there is a degree of subjectivity involved. This means it is possible that prior knowledge of the experimental data has had some influence on the choice of parameters. However, I emphasize that this model shows quantitative agreement with solvation energies for eleven ions and four noble gas atoms without the use of any parameters fitted to reproduce the data. The parameters all have good independent physical rationalizations. This addresses a common criticism of continuum solvent models, that they are simply equations with parameters fitted to the data with little physical basis or predictive power. The independent origin of the parameters used in this model nullifies such objections.

3.3.1 *Uncertainty*

The minimum value for the error in the experimental values is 2 kJmol^{-1}.[127] This is significantly smaller than the error associated with the theoretical values. One important source of error in the theoretical values is the poor convergence of the multipole expansion of the dispersion solvation energy

for the halide ions. For fluoride even the octupole dispersion energy is quite significant. This means that it may be necessary to take into account even higher order multipole moments, which is difficult, or use an entirely different approach. With a simple linear extrapolation I can infer that the next higher order contribution for fluoride may be roughly $-8\ \mathrm{kJmol^{-1}}$. This is 2% of the solvation energy and is quite significant.

In the case of the pairwise dispersion interaction between neutral atoms, one approach is to cut off the energy expansion at the octupole moment even if the energy has not fully converged. This is because this gives a good approximation to the total energy. Beyond the octupole moment contribution there are various terms of opposite signs which will partially cancel.[244] This argument justifies the approximation in this case as well.

Another important source of error in the theoretical calculations is the experimental value of the ionic cavity size in water. The calculations are quite sensitive to the choice of these values. They were determined in Chapter 2 from the average solute-water distances derived from experimental results (diffraction and EXAFS) given in the literature.[193,168,82] The literature values generally vary over a reasonably large range. Although the average value can be determined accurately, some systematic error in the measurements due to the finite concentration of the solutions or other effects is possible. The experimental radii were supported by *ab initio* calculations which largely agreed with the experimental values. But more accurate estimates of these values may explain some of the error in the model. This is particularly true for the noble gas atoms where the radii were based on only a few molecular dynamics simulations.

One issue with the model is that the Tang-Toennies functions and its parameters (b and R_s) are not rigorously derived for use in this case. It is reasonable to think that equally plausible arguments could be made for other choices of the key parameters, and indeed this has been done for the cavity size parameter.[13,240] The final justification for the use of these functions and parameters though is the good agreement with experiment. However, this

does mean that there is a small degree of implicit empirical parametrization in the model.

There may also be additional contributions which this model neglects such as a repulsive wave function overlap energy, or a chemical ion-water interaction. These contributions are very hard to accurately calculate and the success of this model implies they are not important, or subsumed into other terms. In addition, in Chapter 4 we apply the model to calculate the temperature and pressure derivatives and compare with experimental solvation entropies and partial molar volumes with reasonable success. This provides additional support for the claim that the model includes all of the important contributions.

3.3.2 *Implications*

There are two important implications of this model. The first and most important is the importance of the dispersion interaction. The second is that it may be possible to ignore the structure and orientation of water molecules in calculating solvation energies.

3.3.2.1 *Dispersion Interaction*

Figure 3.4 clearly shows that for the anions as well as the silver and copper cations the dispersion contribution to the solvation energy is very significant. One third of the iodide ion solvation energy comes from the dispersion energy. In addition, and I believe crucially, the dispersion interaction is not simply a quantitative correction, but plays a role in a qualitative description of the solvation energies. The use of a different cavity size definition for cations and anions in previous models can be attributed to inaccurate modelling due to the neglect of the dispersion interaction. The larger solvation energy of an anion, compared with a cation of the same size, is due to the anion's larger dispersion energy. In addition, the dispersion energy explains the observation that the solvation energy of the silver(I) and copper(I) ions is significantly larger than expected based on the Born model and their

size. The most common explanation of the discrepancy between the solvation energy of similarly sized cations and anions is based on the different orientation of the water molecules.[110] This explanation cannot explain the unusually large solvation energies of copper(I) and silver(I). They are monovalent cations, the orientation of water molecules around them should not be very different than around a similarly sized alkali cation. This model provides a simple and consistent explanation. It is due to the fact that they have much larger polarisabilities than similarly sized alkali cations, and hence they have a much larger dispersion contribution to the solvation energy.

This result implies that we will profit from further attention focused on improving the description of dispersion energies. This task is already well under way. The continuum approach is clearly suited to this challenge due to its ability to take into account complex many body interactions through experimentally determined dielectric properties. One possibility is to combine continuum model calculations of the dispersion interaction with explicit solvent calculations of the electrostatic interaction. This would be particularly useful in the case of *ab initio* explicit solvent simulations using DFT, which give notoriously inaccurate dispersion energies.[92]

3.3.2.2 *Explicit Water*

The success of this model has some hopeful implications. The first is that it may be possible to build successful models of Specific Ion Effects using continuum solvent models that have predictive and explanatory power. Here a relatively simple continuum model reproduces cation, anion and neutral atom solvation energies. This means that it may be possible to neglect many contributions that are often cited as being the cause of ion specific effect such as specific chemical interactions with water or specific orientational structures, cage-like or otherwise, that the water molecules form. Indeed, the fact that the solvation energies show such a simple regular relationship with ion size already implies this fact. The consistency and completeness of the model is supported by the fact that the cation and anion discrepancy

disappears once the proper proton solvation energy is chosen and dispersion and cavity contributions are taken into account.

Explaining the discrepancy between cation and anion solvation is an important step in understanding Specific Ion Effects. This discrepancy is often used as a justification of the need for explicit water models.[186,110,157] But this work implies that it is due to the dispersion interaction, as the solvation energy has been modelled in exactly the same way for both types of ions, and the dispersion energy is the only contribution which does not solely scale with the size of the solute. This suggests the continuum model should be successful in other applications. This statement is supported by Chapter 6 and Chapter 7 of this thesis, where a successful continuum solvent treatment of surface tensions and activity/osmotic coefficients is outlined.

To a certain degree however, the model developed here is still consistent with the claim that explicit water structure and orientation are important. These effects may play a role in the R_S parameter and hence the size of the cavity. This is particularly the case for the silver (I) and copper (I) ions where there is a 0.1 Å deviation from $R_S = R_I + 1.38$ Å. The determination of this R_S parameter may also depend on explicit water simulation if the *ab initio* calculations or experimental estimates are not sufficiently accurate. However, the model can be generalized to calculate ion-ion and ion-surface interactions in water. For these problems the model has a significant computational advantage as it is these calculations that can require significant computational time at an explicit solvent level.

3.3.3 *Further Applications*

This solvation energy calculation can serve as a starting point for improving models of more complex phenomena. For instance, the size of the cavity, the magnitude of the cavity formation energy and the ion-solvent dispersion interaction are all important in determining the free energy change as an ion approaches a surface. These free energies determine the distribution profile of ions at the surface and hence the surface tensions and surface forces of

electrolyte systems, which are central problems in physical chemistry. This problem is addressed in Chapter 6.

3.3.3.1 *Other Properties*

The model can also, in principle, be applied to ion-mineral or ion-protein interactions, determining ion distribution profiles and hence explaining a wide range of experimental phenomena. Similarly, in Chapter 7 this model is applied to the calculation of ion–ion interactions in water and hence osmotic/activity coefficients. Lund et al.[157] have shown that the law of matching water affinity can largely be explained by the change in ionic solvation energy as two ions approach. Hence, an accurate continuum model of the solvation energy is essential to improve our understanding of ionic osmotic and activity coefficients. In addition, it should be possible to generalize the model to non-aqueous solvents, as a further test and to explore the role of water.[208]

3.4 CONCLUSION

I have presented a model which reproduces the solvation free energies of eleven monovalent spherical ions and four noble gas atoms with good accuracy using a continuum solvent model with no fitted parameters. The three key contributions are the electrostatic, dispersion (with multipoles) and cavity formation terms. This model shows that the discrepancy between anion and cation solvation energy which was previously attributed to solvent orientation effects can instead be explained by the larger dispersion interaction of the much more polarisable halide ions. This same explanation also explains the unusually large solvation energy of the copper(I) and silver(I) ions, which can not be explained by differing water orientations. This result underscores the important role dispersion interactions play in Specific Ion Effects, showing that specific water structure and chemical interactions can be neglected. In the following chapters I shall build on this model in order to understand more complex Specific Ion Effects.

4

PARTIAL MOLAR VOLUMES AND ENTROPIES

This chapter is reproduced with minor changes and with permission from Ref. 68: T. T. Duignan, D. F. Parsons, and B. W. Ninham. A Continuum Solvent Model of the Partial Molar Volumes and Entropies of Ionic Solvation. J. Phys. Chem. B, 118:3122–3132, 2014. Copyright 2014 American Chemical Society.

4.1 INTRODUCTION

The model presented in Chapter 3 is, I believe, an important step forward in our understanding of electrolyte solutions. Before I move on to generalize the model and apply it to ion–surface and ion–ion interactions, it is desirable to test its physical validity by comparison with simpler properties that are more directly related to the solvation free energy. In particular, as the criteria in Section 3.1.4 states, the partial molar volumes and entropies (enthalpies) of solvation, which correspond to the temperature and pressure derivatives of the solvation free energy respectively.

In this chapter I will show that a simple extension of the continuum solvent model, applied to the same group of ions, allows the determination of entropies of solvation and partial molar volumes that are consistent with experiment. I will argue that the extended model still meets all of the criteria laid out in Section 3.1.4 and hence can be considered a satisfactory model of ionic solvation.

Some important advances in understanding these properties have been made previously using both continuum[73,145] and explicit solvent models.[107,21]

4.2 THEORY

We proceed from the Gibbs solvation energy contributions given in Chapter 3.

4.2.1 *Entropies*

The entropies of solvation are given by:

$$S = -\left(\frac{\partial G}{\partial T}\right)_P \tag{4.1}$$

We can therefore simply take the derivative of the expressions given in Chapter 2 and 3 to determine the entropy. For the Born contribution this gives:

$$S_{Born} = \frac{q^2}{8\pi\epsilon_o}\left(\frac{1}{R_{cav}\epsilon_r^2}\frac{\partial\epsilon_r}{\partial T} - \left(1-\frac{1}{\epsilon_r}\right)\frac{1}{R_{cav}^2}\frac{\partial R_{cav}}{\partial T}\right) \tag{4.2}$$

These can be split this into two contributions: the first term is due to the temperature dependence of the dielectric constant, which I refer to as S_{Born1}:

$$S_{Born1} = \frac{q^2}{8\pi\epsilon_o}\left(\frac{1}{R_{cav}\epsilon_r^2}\frac{\partial\epsilon_r}{\partial T}\right) \tag{4.3}$$

and the second term is due to the temperature dependence of the cavity size, which I refer to as S_{Born2}:

$$S_{Born2} = -\frac{q^2}{8\pi\epsilon_o}\left(1-\frac{1}{\epsilon_r}\right)\frac{1}{R_{cav}^2}\frac{\partial R_{cav}}{\partial T} \tag{4.4}$$

For the dispersion contributions a similar procedure can be performed. I define:

$$f(\epsilon(i\xi_n)) = \frac{\epsilon(i\xi_n)-1}{2\epsilon(i\xi_n)+1} \tag{4.5}$$

The dispersion interaction depends on temperature directly and implicitly through the dielectric function. This dependence gives rise to the following entropy associated with the the dipole dispersion interaction(Eq. 2.14):

$$
\begin{aligned}
&S_{\text{Disp1D}} = f_6\left(bR_S\right)\frac{6k_BT}{R_{cav}^3}\sum_{n=0}^{\infty}\left(1-\frac{1}{2}\delta_{n0}\right)\times \\
&\Bigg[\left(\alpha\left(i\xi_n\right)/T+\frac{2\pi k_B n}{\hbar}\left(\frac{\partial}{\partial\xi_n}\left(\alpha\left(i\xi_n\right)\right)\right)\right)f\left(\epsilon\left(i\xi_n\right)\right) \\
&+\left(\frac{\partial f(\epsilon\left(i\xi_n\right))}{\partial\epsilon\left(i\xi_n\right)}\frac{2\pi k_B n}{\hbar}\left(\frac{\partial}{\partial\xi_n}\epsilon\left(i\xi_n\right)\right)+\frac{\partial f(\epsilon\left(i\xi_n\right))}{\partial\epsilon\left(i\xi_n\right)}\frac{\partial\epsilon\left(i\xi_n\right)}{\partial T}\right)\alpha\left(i\xi_n\right)\Bigg]
\end{aligned}
\tag{4.6}
$$

where

$$
\frac{\partial f(\epsilon\left(i\xi_n\right))}{\partial\epsilon\left(i\xi_n\right)} = \frac{3}{\left(2\epsilon(i\xi_n)+1\right)^2} \tag{4.7}
$$

Here we have made use of the chain rule:

$$
\frac{\partial f(\epsilon\left(i\xi_n\right))}{\partial T} = \frac{\partial f(\epsilon\left(i\xi_n\right))}{\partial\epsilon\left(i\xi_n\right)}\frac{\partial\epsilon\left(i\xi_n\right)}{\partial\xi_n}\frac{\partial\xi_n}{\partial T}+\frac{\partial f(\epsilon\left(i\xi_n\right))}{\partial\epsilon\left(i\xi_n\right)}\frac{\partial\epsilon\left(i\xi_n\right)}{\partial T} \tag{4.8}
$$

The complexity of this expression is mainly due to the temperature dependence of the Matsubara frequencies ($\xi_n = 2\pi k_B T n/\hbar$) as well as the dielectric function, i.e., $\epsilon(T, \xi_n(T))$ is a function of T and $\xi_n(T)$. For frequencies with $n > 0$, the temperature dependence of the dielectric function has not been directly measured. Following Ref. 59, I can approximate this dependence by using the Clausius-Mossotti relation:

$$
\frac{4\pi}{3}\alpha(i\xi_n)\rho(T) = \frac{\epsilon\left(i\xi_n, T\right)-1}{\epsilon\left(i\xi_n, T\right)+2} \tag{4.9}
$$

where $\rho(T)$ is the number density of water as a function of temperature. Because the calculation is at the Matsubara frequencies there is no contribution from dipole orientation. And I can assume that $\alpha(i\xi_n)$ is the molecular polarisability of water and is therefore independent of temperature.[59] I then

take the temperature derivative of both sides and substitute the Clausius-Mossotti relation in to eliminate $\alpha(i\xi_n)$, arriving at the expression:

$$\frac{\partial \epsilon\left(i\xi_n\right)}{\partial T} = \left(\epsilon\left(i\xi_n, T\right) - 1\right)\left(\epsilon\left(i\xi_n, T\right) + 2\right)\frac{\partial \rho(T)}{\partial T}\frac{1}{3\rho(T)} \tag{4.10}$$

This can then be substituted into Eq. 4.6.

We can also determine the contribution to the entropy from the temperature dependence of the cavity size in the dipole dispersion solvation energy:

$$S_{Disp2D} = 3\frac{G_D}{R_{cav}}\frac{\partial R_{cav}}{\partial T} \tag{4.11}$$

A third contribution comes from the temperature derivative of the R_S parameter:

$$S_{Disp3D} = \left(\sum_{k=0}^{6}\left(k - bR_S\right)\frac{b^k}{k!}R_S^{(k-1)}\exp^{-bR_S}\right)\frac{\partial R_S}{\partial T}G_D/f_6(bR_S) \tag{4.12}$$

The value of $\partial R_S/\partial T$ is not necessarily the same as $\partial R_{cav}/\partial T$. The expressions for the quadrupole and octupole moments are straightforward generalizations of these equations. I provide these expressions in Appendix B, they are added to give: $S_{Disp1} = S_{Disp1D} + S_{Disp1Q} + S_{Disp1O}$.

I make the reasonable assumption that the solute polarisabilities and the Born-Mayer b parameters do not have any temperature dependence as these properties are determined from *ab initio* calculations at 0 K. For the cavity formation energy we have:

$$S_{Cav1} = -\frac{\partial \sigma_{ion}}{\partial T}4\pi R_S^2 \tag{4.13}$$

There is no R_{cav} dependence in the cavity energy, so the final contribution is:

$$S_{Cav3} = -2\sigma_{ion}4\pi R_S\frac{\partial R_S}{\partial T} \tag{4.14}$$

4.2.1.1 *Physical Interpretation*

Although it is straightforward to perform calculations with these expressions it is important to keep in mind the physical origin of these terms. That is, after all, one of the central benefits of a continuum solvent approach, which we should seek to preserve.

The physical cause of the entropy change can be determined from the origin of the temperature dependence. The S_{Born1} term arises from the decrease in the dielectric constant of water as a function of temperature. This in turn is caused by the decrease in the orientational polarisability of water at higher temperatures and a decrease in the density of water at higher temperatures. I can therefore interpret this term as an entropic loss due to the average orientational restriction of the water surrounding the ion.

The first three contributions to S_{Disp1D}, shown in Eq. 4.6, arise from the direct temperature dependence of the quantum mechanical expression itself and are difficult to interpret intuitively. These contributions cancel to a large degree and leave the fourth contribution to make up between 60% to 80% of the total dispersion entropy. This contribution is the temperature derivative of the dielectric function itself and arises from the change in density of water. I can therefore interpret this term as arising predominantly from the entropy cost of the density increase of water, caused by the dispersion interaction pulling the water in.

The term S_{Cav1} also has a clear physical interpretation. At higher temperature the cavity energy decreases as the energy cost of forming a surface falls. This is because the hydrogen bonded structure of water becomes weaker as temperature increases. It is therefore clear that this term arises due to the entropy gained by breaking the hydrogen bonded structure and allowing the water molecules to rotate more freely.

The interpretation of the S_{Born2} and S_{Disp2} is less straightforward. As temperature increases R_{cav} increases.[73] This leads to a reduction in the magnitude of the Born and dispersion interaction energy, i.e., they become less negative. The interpretation is that at higher temperatures the water molecules

bind less readily to the ion, and therefore the energy is reduced in magnitude. This implies that these contributions capture the entropic cost of binding the water molecules immediately surrounding the ionic solute. I do not consider S_{Disp3} and S_{Cav3} in the discussion here for reasons addressed below.

4.2.2 *Partial Molar Volumes*

The calculation of the contribution to the Partial Molar Volumes from the electrostatic, dispersion and cavity contributions proceeds in much the same way as for the entropy calculation, except now the relevant thermodynamic relationship is:

$$V = \left(\frac{\partial G}{\partial P}\right)_T \tag{4.15}$$

So the contributions from the Born model are

$$V_{Born1} = -\frac{q^2}{8\pi\epsilon_o}\left(\frac{1}{R_{cav}\epsilon_r^2}\frac{\partial \epsilon_r}{\partial P}\right) \tag{4.16}$$

and

$$V_{Born2} = \frac{q^2}{8\pi\epsilon_o}\left(1-\frac{1}{\epsilon_r}\right)\frac{1}{R_{cav}^2}\frac{\partial R_{cav}}{\partial P} \tag{4.17}$$

The expression for the dispersion contribution to the partial molar volumes is:

$$\begin{aligned} V_{Disp1D} = &-\left(1-\sum_{k=0}^{6}\frac{(bR_S)^k}{k!}\exp^{-bR_S}\right) \\ &\times \frac{6k_BT}{R_{cav}^3}\sum_{m=0}^{\infty}\left(1-\frac{1}{2}\delta_{m0}\right)\alpha(i\xi_m)\frac{\partial f(\epsilon(i\xi_n))}{\partial \epsilon(i\xi_n)}\frac{\partial \epsilon(i\xi_n)}{\partial P} \end{aligned} \tag{4.18}$$

It is significantly simpler than for the entropy, as the Matsubara frequencies are not a function of the pressure. For frequencies with $n > 0$ we can determine the pressure dependence of the dielectric function with the same approximation[59] used to determine the temperature dependence.

Just as for the entropy I have additional contributions from the pressure dependence of R_{cav} and R_S:

$$V_{Disp2D} = -3\frac{G_D}{R_{cav}}\frac{\partial R_{cav}}{\partial P} \tag{4.19}$$

$$V_{Disp3D} = -\left(\sum_{k=0}^{6}(k - bR_S)\,\frac{b^k}{k!}R_S^{(k-1)}\exp^{-bR_S}\right)\frac{\partial R_S}{\partial P}G_D/f_6(R_S) \tag{4.20}$$

Again, this derivation can be straightforwardly generalized to arrive at the quadrupole and octupole moment contributions. There are also terms from the cavity surface tension and the R_S parameter. These are:

$$V_{Cav1} = \frac{\partial \sigma_{ion}}{\partial P}4\pi R_S^2 \tag{4.21}$$

$$V_{Cav3} = 2\sigma_{ion}4\pi R_S\frac{\partial R_S}{\partial P} \tag{4.22}$$

There is also a simple contribution to the solvation free energy that I neglected in the solvation energy model, as it is very small. It is the thermodynamic work (PV_{Cav}) done to create a cavity for an ion to occupy.[110] Although this gives a negligible free energy contribution, it will make up a significant proportion of the partial molar volumes, and is the most obvious first order contribution:

$$V_{Cav4} = V_{Cav} \tag{4.23}$$

The dielectric boundary gives a reasonable partitioning of space into two regions, one occupied by the water, the other by the ion. Hence I assume $V_{Cav} = (4/3)\pi R_{cav}^3$, as this should give a reasonable estimate of the volume change upon cavity formation.

4.2.2.1 *Physical Interpretation*

The increase in the dielectric constant of water as a function of pressure gives rise to the V_{Born1} and V_{Disp1} terms. The clear physical interpretation of this is that the ion-water interaction pulls the water molecules in, increasing the density of the water surrounding the ion and lowering the volume of the solution.

V_{Born2} and V_{Disp2} are again more complex cases. They arise from variation in R_{cav} as a function of pressure, i.e., from variations in the energy associated with the tightly held water molecules surrounding the ion. They can therefore be considered as contributions to the decrease in volume due the tight binding of a layer of water molecules around the ion.

V_{Cav4} is obviously the direct contribution from the size of the ion, and V_{Cav1}, V_{Cav3} and V_{Disp3} are not included in this discussion, again for reasons outlined below.

4.2.3 *Parameters*

4.2.3.1 *Size parameters*

The size parameters I use have been determined from independent experiment and *ab initio* calculations in Chapter 2 and are given in Table 2.1

4.2.3.2 *Temperature derivatives*

All of the properties used are taken at 298.15 K and 1 bar. The temperature derivative of the static dielectric function is a well determined property, I use a value[76] of $\frac{\partial \epsilon_r}{\partial T} = -0.359\ K^{-1}$.

As discussed in Chapter 2 the model developed by Fawcett,[73,74] uses the Mean Spherical Approximation (MSA) to derive an expression for the solvation free energy of a spherical ion. By comparison of this expression with the Born equation (Eq. 3.1), an expression for the cavity size can be determined: $R_{cav} = R_I + \delta_S$, where $\delta_S = 0.54$ Å and is the same as the R_{add} parameter used in Chapter 2.

To a good approximation, this relationship is consistent with the expression I use for the cavity radius ($R_{cav} = R_S - R_{adj}$), since $R_S \approx R_I + 1.38\text{Å}$.[163] The δ_S parameter is given as a function of the radius of a water molecule and the dielectric constant of water. This means that it is straight forward to determine the temperature dependence of this parameter from the temperature dependence of the dielectric function, this gives: $\frac{\partial \delta_S}{\partial T} = 5 \times 10^{-14}$ m K^{-1}. I assume that the intrinsic size is independent of temperature and this therefore gives $\frac{\partial R_{cav}}{\partial T} = 5 \times 10^{-14}$ m K^{-1}. I therefore adopt this value for this calculation. As mentioned above, the temperature dependence of the high frequency dielectric function can be given approximately in terms of the temperature dependence of the density of water. The density of water as a function of temperature is given in the CRC Handbook of Physics and Chemistry.[150] This gives a value of $\frac{1}{\rho}\frac{\partial \rho}{\partial T} = -2.04 \times 10^{-3}$ K^{-1} The temperature derivative of the surface tension of the bulk air-water interface[110] is -0.927 J mol^{-1} $Å^2$ K^{-1}. I use this value for the cavity formation entropy of the ionic solutes for the same reasons outlined in Chapter 3, namely that the surface of the water surrounding an ion will have the broken hydrogen bonds characteristic of the larger bulk air water interface.

However, around small neutral cavities it is well established[44,12] that the curvature allows for the maintenance of the hydrogen bonded network and hence a lowering of the effective surface tension as well as a change in sign of the entropy of cavity formation. This means that it is no longer appropriate to estimate the entropy of cavity formation with the temperature derivative of the surface tension of the bulk air water interface. The accurate calculation of the cavity formation entropy of these small noble gas atoms is difficult, and may require an explicit solvent model.

There is experimental[221] and theoretical[196] evidence that the R_S parameter for a water molecule in the bulk does not vary substantially as a function of temperature. R_S in this case is the distance to the peak in the oxygen-oxygen radial distribution function ($g_{OO}(r)$). This implies that $\frac{\partial R_S}{\partial T} = 0$ and so the S_{Disp3} and S_{Cav3} contributions can safely be neglected. This is consistent with the relations $R_{cav} = R_S - R_{adj}$, if I assume that $\frac{\partial R_{adj}}{\partial T} = -\frac{\partial \delta_S}{\partial T}$. This is reasonable

because $R_{adj} + \delta_S$ should be independent of temperature as it gives the intrinsic radius of a water molecule (1.38 Å). In addition, I have calculated this contribution assuming $\frac{\partial R_S}{\partial T} = \frac{\partial R_{cav}}{\partial T}$, and the resulting terms S_{Disp3} and S_{Cav3} are approximately equal but with opposite sign, resulting in negligible dependence on this contribution in any case.

4.2.3.3 *Pressure derivatives*

The pressure derivative of the bulk static dielectric constant[110] is $\frac{\partial \epsilon_r}{\partial P} = 37.4 \times 10^{-9}$ Pa $^{-1}$. I can determine the pressure derivative of the cavity size ($\partial R_{cav}/\partial P$) in the same way as I have for the temperature derivative, using the equations of Ref. 73 to obtain a value of -5.21×10^{-21} m Pa^{-1}. V_{Cav3} and V_{Disp3} are neglected for the same reason as S_{Cav3} and S_{Disp3}, i.e., by assuming $\frac{\partial R_S}{\partial P} = 0$.

The determination of $\frac{\partial \sigma_{ion}}{\partial P}$ to calculate V_{Cav1} is problematic. The pressure dependence of the macroscopic surface tension is very difficult to determine, as it depends on which gas is used to increase the pressure.[266] Approximate methods of determining this value indirectly[266] result in values for the partial molar volume that are far too large to be physical. (p. 59 of Ref. 110) There is a similar problem for the V_{Disp1} contribution. This contribution can be determined from Eq. 4.18 and the known isothermal compressibility of bulk water:[234]

$$\beta_T = \frac{\partial \rho(P)}{\partial P} / \rho(P) = 45.99 \times 10^{-11} \text{ Pa}^{-1} \tag{4.24}$$

This calculation again gives values that are implausibly large, but of opposite sign to the cavity contribution. I attribute the origin of these problems to a difference in response to changes in pressure between bulk water and water in the hydration shell surrounding an ion. This is consistent with observations that water in the presence of ions has a density consistent with a much high pressure.[174] As a result, an increase in the external pressure may have a much smaller effect on the density of water around an ion than it does on the density of bulk water. This is an electrostriction effect, with

the ion hydration environment becoming saturated with respect to water density. Hence, using the compressibility of bulk water overestimates this contribution significantly.

This effect could be properly understood with an electrostriction model, introducing a dependence of the local dielectric function, and its derivatives, on the local water density. However, the complexity of a full electrostriction model can be reduced by simply expressing this interpretation with the assumption that the pressure dependence of the hydration environment is small, i.e., $\partial\rho/\partial P \approx 0$ and $\frac{\partial \sigma_{ion}}{\partial P} \approx 0$. Consequently the V_{Cav1} and V_{Disp1} contributions become negligible. The validity of this assumption is aided by the fact that these two terms have opposite signs and may approximately cancel each other, as occurs for the cavity and dispersion contributions to the solvation energies.

4.2.4 *Experimental Values*

I use the experimental values of the enthalpy and free energy of Tissandier et al.[256] to determine the experimental solvation entropies for the alkali halides. A correction between standard states of 34 J $mol^{-1}K^{-1}$ needs to be applied to these values before they can be compared with experiment.[110] This choice of values is most consistent with the values with which I have compared the free energy model. However, I note an ongoing debate in the literature[110] regarding the correct splitting of the solvation entropies of salts into the individual cationic and anionic contributions.

The value for the difference in entropy between cesium and rubidium from Ref. 110 is used to determine a consistent value for the entropy of solvation of the cesium ion. Similarly, in order to determine the entropy of solvation for copper(I) and silver(I), the values for the differences between copper(I) and lithium, and silver(I) and sodium ions are taken from Marcus's data.[166] The entropies of solvation of the noble gas atoms are taken from Ref. 26 and Ref. 280.

For the partial molar volumes of the alkali halides I use the data of Hünenberger and Reif.[110] Again the values for the difference between copper(I) and lithium, and silver(I) and sodium from Marcus's data[165] were used to determine the partial molar volumes for copper(I) and silver(I).

4.3 RESULTS

4.3.1 *Entropies*

The components of the entropy of solvation for the ions are given in Table 4.1. The straightforward estimate of the theoretical values is referred to as $S_{Theory1}$ and given by: $S_{Theory1} = S_{Born1} + S_{Disp1} + S_{Cav1} + S_{Born2} + S_{Disp2}$. These are compared with experiment in Table 4.2 and Figure 4.1, they show a reasonable agreement for the larger cations; potassium through to cesium. Iodide is also in good agreement, in particular the peculiar positive entropy of iodide is reproduced. There is, however, a degree of apparent quantitative error. This error is significant for bromide and chloride but becomes much worse for the smaller ions; lithium and sodium are significantly too negative, and the highly polarisable copper(I), silver(I) and fluoride ions even more so. The experimental trend of increasing entropy with size is not followed for these ions.

We can understand the failure of the model for these small ions by considering the physical contributions discussed in the theoretical section. From Table 4.1 it is clear that the problem for the smaller ions originates predominantly from the strong S_{Born2} and S_{Disp2} contributions. These terms I argue correspond to the entropy of tightly binding the first layer of water molecules surrounding the ion. This model predicts that these terms are proportional to the strength of the binding of the water. However, physically this is only true for weakly bound systems. In these cases the stronger the binding of the water to the ions the more restricted the water molecules are, and the larger the entropic cost. However, once the binding energy becomes large enough, the water molecules become effectively fixed in position and are

Table 4.1: Contributions to the entropy of solvation of small monovalent ions in units of J $mol^{-1}K^{-1}$

Atom/Ion	S_{Born1}	S_{Born2}	S_{Cav1}	S_{Disp1}	S_{Disp2}
Li^+	−33.3	−230.4	49.4	−1.1	−9.3
Na^+	−26.9	−150.4	64.3	−3.4	−24.1
K^+	−20.9	−90.2	90.7	−7.3	−42.2
Rb^+	−19.6	−79.3	99.3	−9.5	−54.4
Cs^+	−17.9	−66.5	112.7	−11.1	−60.8
Cu^+	−28.8	−172.5	59.0	−16.5	−116.9
Ag^+	−25.9	−139.1	67.7	−17.8	−137.1
F^-	−22.1	−101.3	83.7	−13.4	−123.0
Cl^-	−17.2	−61.6	119.3	−11.8	−82.9
Br^-	−16.2	−54.4	130.7	−12.0	−79.9
I^-	−14.5	−43.7	154.3	−10.8	−64.2

Table 4.2: Comparison of theoretical and experimental entropies of solvation of small monovalent ions in units of J $mol^{-1}K^{-1}$

Atom/Ion	S_{Exp} [a]	$S_{Theory1}$ [b]	$S_{Theory2}$ [c]
Li^+	−134.5	−224.7	−93.0
Na^+	−101.1	−140.6	−74.0
K^+	−61.9	−69.9	−45.4
Rb^+	−53.3	−63.4	−37.7
Cs^+	−46.6	−43.6	−24.2
Cu^+	−135.5	−316.2	−94.3
Ag^+	−107.1	−252.3	−84.0
F^-	−85.4	−176.2	−59.8
Cl^-	−19.2	−54.2	−17.7
Br^-	−4.9	−31.8	−5.4
I^-	8.1	21.1	21.1

[a] From Ref. 256 with 34 J $mol^{-1}K^{-1}$ correction.[110] [b] $S_{Theory1} = S_{Born1} + S_{Disp1} + S_{Cav1} + S_{Born2} + S_{Disp2}$
[c] $S_{Theory2} = S_{Born1} + S_{Disp1} + S_{Cav1} + S_{Bind}$

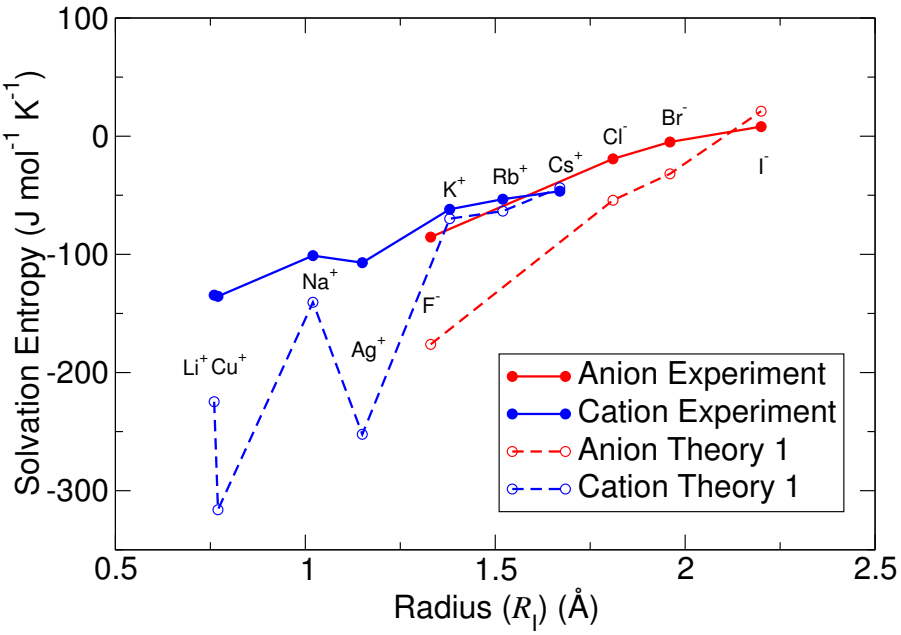

Figure 4.1: Comparison of the experimental and straightforward theoretical solvation entropies (S_{Theory1}) for the monovalent ions as a function of their inherent radius.

rigidly structured around the ions. As a result any increase in binding energy will not increase the entropy. I believe this is what is occurring here, and the continuum solvent model neglects it.

We can see this effect at work in Figure 4.2, where I have plotted the error in the straightforward theoretical estimates ($S_{\text{Exp}} - S_{\text{Theory1}}$) as a function of $S_{\text{Born2}} + S_{\text{Disp2}}$. It is clear that this contribution is relatively accurately modelled for the larger ions where the error is close to zero, but as $S_{\text{Born2}} + S_{\text{Disp2}}$ increases in magnitude the error increases proportionally. This proportional relationship is effectively due to dielectric saturation, i.e., at larger binding energies the response of the solvent begins to behave nonlinearly. This saturation has two elements, firstly a saturation of the orientation of the water molecules. Secondly, there is a saturation of the density of water molecules around the ion, i.e., a maximum density is reached. To account for this effect rigorously would require the inclusion of dielectric saturation effects in the solvation model, increasing the complexity of the model. The reason this problem is much more severe for the entropies than for the free energies is

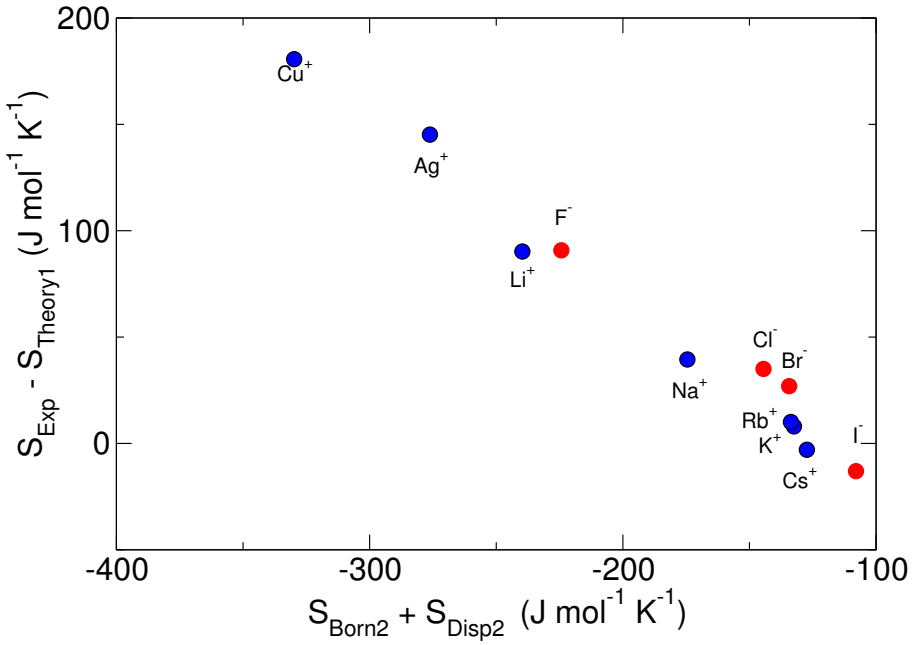

Figure 4.2: The error in the straightforward theoretical calculation as a function of the size of the $S_{Born2} + S_{Disp2}$ contribution.

likely due to entropy-enthalpy compensation, i.e., the model overestimates the entropy cost of binding the water molecules, but there is a cancelling contribution from an overestimate in the enthalpy of binding, again due to the neglect of dielectric saturation. Another way of stating the problem is that the drastic assumption of a constant temperature dependence of R_{cav}, has broken down for the small ions. This is consistent with the dielectric saturation interpretation, as R_{cav} depends on the dielectric constant, through the δ_S parameter.[73]

In order to correct for this problem I note that it appears that for the larger ions, iodide and cesium for instance, this issue has disappeared. That implies that the entropy cost of binding a layer of water molecules tightly is correctly estimated for these ions. I therefore take the value of $S_{Born2} + S_{Disp2}$ for the largest ion, iodide:

$$S_{Bind} = S_{Born2}(I^-) + S_{Disp2}(I^-) \tag{4.25}$$

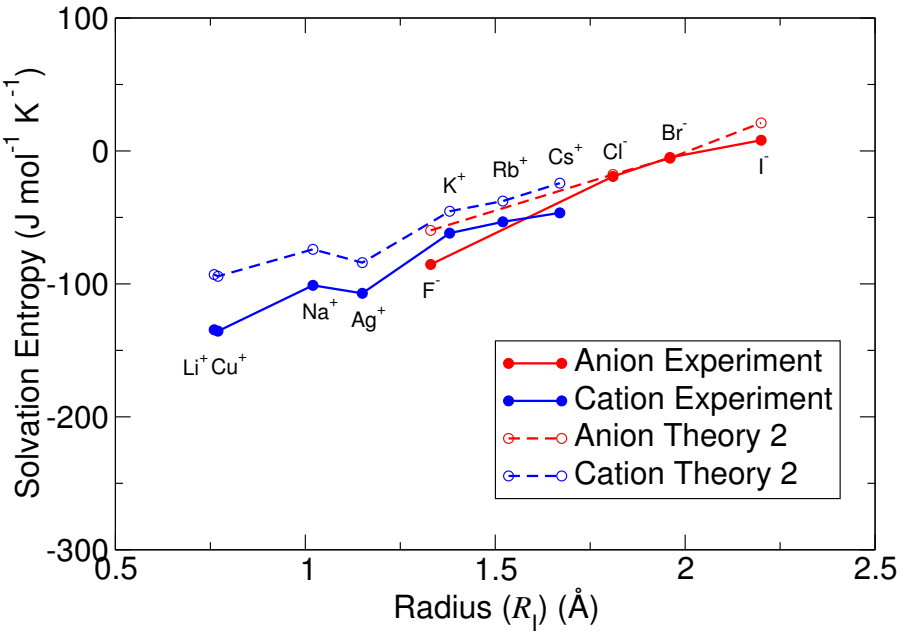

Figure 4.3: Comparison of the experimental and corrected theoretical solvation entropies for the monovalent ions as a function of their inherent radius.

I assume that the $S_{Born2} + S_{Disp2}$ contribution is fixed at S_{Bind} for all of the smaller ions, i.e., I assume that this value is the maximum possible entropy of binding, which will be roughly the same for all of the ions studied. This corrected theoretical estimate is then: $S_{Theory2} = S_{Born1} + S_{Disp1} + S_{Cav1} + S_{Bind}$, which is compared with experiment in Figure 4.3 and Table 4.2. Much better agreement with the experimental values is now observed. The experimental values are reproduced qualitatively and with reasonable quantitative accuracy, the values for the smaller cations are now only slightly overestimated. This is probably due to the fact that this entropic cost of binding water does increase gradually as the ions get smaller, just much more slowly than the unmodified dielectric model predicts. In other words, the dielectric medium is not completely saturated.

We can also calculate the dispersion contribution to the entropy of solvation for the noble gas atoms using the expressions derived above. It is not clear if any simple calculation is possible for the entropy of cavity formation for the noble gas elements. However, Irudayam and Henchman[111]

Table 4.3: Contributions to the solvation entropy of noble gas elements compared to experiment in units of J $mol^{-1}K^{-1}$

Atom	S_{Disp}	S_{Cav1} [a]	S_{The} [b]	S_{Exp} [c]
He	−5.9	–	–	−33.8
Ne	−10.5	−23.2	−33.7	−42.3
Ar	−23.0	−26.5	−49.5	−61.5
Kr	−26.0	−32.1	−58.1	−68.2

[a] Water entropy loss with SPC/E water model from Ref. 111
[b] $S_{The} = S_{Disp}+S_{Cav1}$ [c] From Ref. 26 and Ref. 280.

have calculated the entropy loss of the water molecules upon the solvation of the noble gas elements. When they combine these numbers with their calculated entropy change of the solute the net entropies are much too small compared with experiment. They attribute this to the neglect of temperature dependence in the Lennard-Jones interaction potentials. If I combine the loss of entropy of the water molecules calculated in Ref. 111 using the SPC/E model, but with the dispersion entropy loss calculated here instead, the resulting entropies are much closer to agreement with the experimental results as shown in Table 4.3, and the trend of increasing entropy loss with size is also captured.

4.3.2 *Partial Molar Volumes*

Further evidence for the procedure of treating $S_{Born2} + S_{Disp2}$ as saturated at a fixed value can be found in the calculation of the partial molar volumes. Table 4.4 shows the contributions to the partial molar volumes for the group of ions studied. Table 4.5 and Figure 4.4 compare these results with experiment where: $V_{Theory1} = V_{Born1} + V_{Born2} + V_{Cav4} + V_{Disp2}$. The agreement again is promising, in particular the values for iodide and the larger cations, potassium through to cesium, are reproduced satisfactorily, as is the shift to negative partial molar volumes for the smaller ions. Significantly, the errors in $V_{Theory1}$ are strikingly similar to the errors in $S_{Theory1}$. The smaller ions are quite significantly too negative, particularly the strongly polarisable fluoride,

Table 4.4: Contributions to the partial molar volumes of small monovalent ions in units of $cm^3\ mol^{-1}$

Atom/Ion	V_{Born1}	V_{Born2}	V_{Cav4}	V_{Disp2}
Li^+	−3.5	−24.0	4.6	−1.0
Na^+	−2.8	−15.7	8.7	−2.5
K^+	−2.2	−9.4	18.7	−4.4
Rb^+	−2.0	−8.3	22.7	−5.7
Cs^+	−1.9	−6.9	29.5	−6.3
Cu^+	−3.0	−18.0	7.1	−16.4
Ag^+	−2.7	−14.5	9.8	−14.3
F^-	−2.3	−10.6	15.7	−12.8
Cl^-	−1.8	−6.4	33.2	−8.6
Br^-	−1.7	−5.7	39.9	−8.3
I^-	−1.5	−4.6	55.4	−6.7

copper(I) and silver(I) ions. The errors are larger for the entropies, which can be attributed to the smaller significance of the pressure dependence of the electrostatic and dispersion contributions shown in in Table 4.4.

Because of the same pattern in the errors I can attribute the breakdown in the model to the same physical cause: The model does not account for the saturation of the dielectric medium at very large interaction strengths, and so overestimates the contraction of the solvent. More specifically, the density of the water layer immediately surrounding the ions has reached a limit, this is due to a maximum density that water can not easily exceed. This limit is reached for iodide and the larger cations, and from then on the density of the hydration shell does not increase in magnitude significantly. My continuum model neglects this effect and so overestimates the total contraction. This argument suggests that the same correction should work. I define $V_{Bind} = V_{Born2}(I^-) + V_{Disp2}(I^-)$ and $V_{Theory2} = V_{Born1} + V_{Cav4} + V_{Bind}$. This is compared with the experimental values in Figure 4.5 and Table 4.5, which show good agreement. This provides evidence that the description of the physical process is sound.

I do not apply this model to the partial molar volumes of the noble gas elements. This is because the only novel contribution is the V_{Disp2} term, which is negligibly small due to the relatively large R_{cav} values of the noble gas

Table 4.5: Comparison of theoretical and experimental partial molar volumes of small monovalent ions in units of $cm^3\ mol^{-1}$

Atom/Ion	V_{Exp} [a]	$V_{Theory1}$ [b]	$V_{Theory2}$ [c]
Li^+	−5.2	−23.9	−10.1
Na^+	−5.9	−12.3	−5.4
K^+	4.3	2.7	5.3
Rb^+	9.7	6.7	9.4
Cs^+	16.9	14.4	16.4
Cu^+	−12.4	−30.3	−7.2
Ag^+	−5.4	−21.7	−4.2
F^-	2.7	−10.0	2.2
Cl^-	22.2	16.3	20.1
Br^-	29.2	24.2	27.0
I^-	40.8	42.6	42.6

[a] From Ref. 110 and Ref. 165
[b] $V_{Theory1} = V_{Born1} + V_{Born2} + V_{Cav4} + V_{Disp2}$
[c] $V_{Theory2} = V_{Born1} + V_{Cav4} + V_{Bind}$

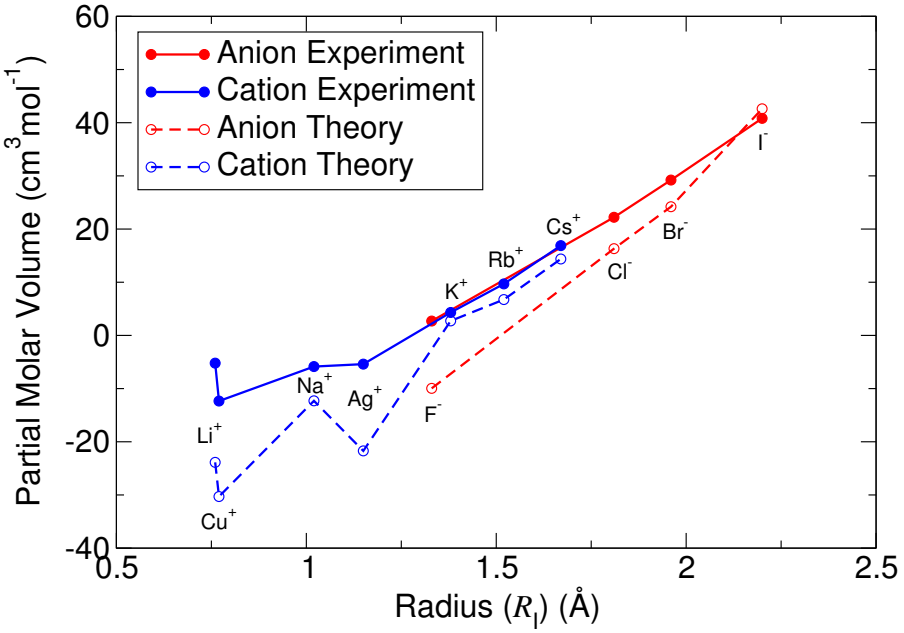

Figure 4.4: A comparison of the experimental and straightforward theoretical values for the partial molar volumes of the monatomic ions as a function of their inherent radius.

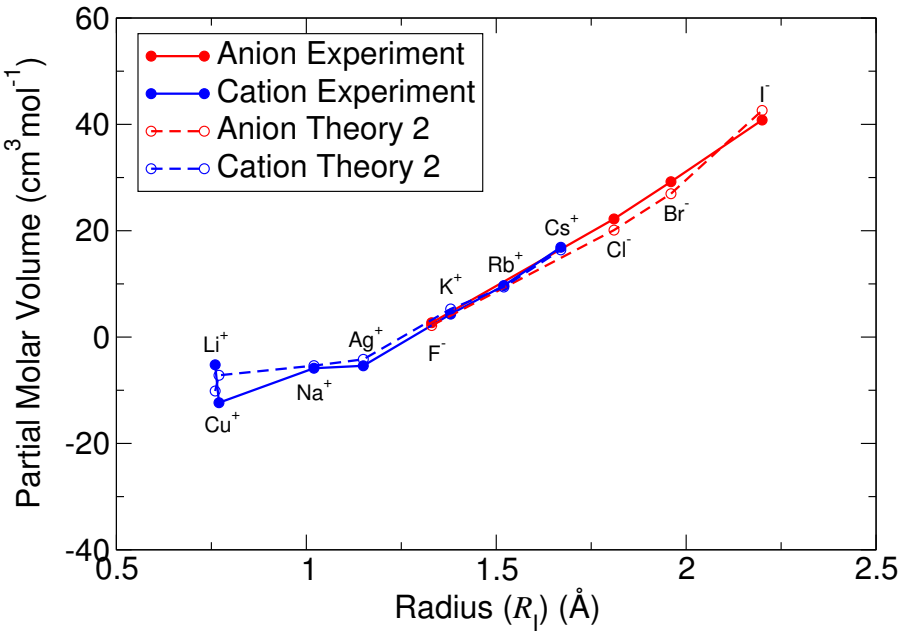

Figure 4.5: A comparison of the experimental and corrected theoretical values for the partial molar volumes of the monatomic ions as a function of their inherent radius.

elements. It is therefore possible to adequately reproduce the partial molar volumes of the noble gas elements considering only contributions from their size.[145] For noble gas atoms, this contribution is qualitatively different than for ions, due to their very different effect on the structure of the surrounding water.

4.4 DISCUSSION AND CONCLUSION

4.4.0.1 *Entropy of cavity formation*

The fact that the model reproduces at least qualitatively the solvation entropies of noble gas atoms and ions confirms an important observation from previous chapters: The properties of the small hydrophobic cavities that noble gas atoms form are qualitatively different to the cavities that ions form. More specifically, for small neutral cavities the entropy of formation is negative and becomes more negative with cavity size. This is not the case for

ionic solutes; The formation of cavities occupied by ions is better characterized by a larger positive entropy that scales with surface area, similar to the formation of a bulk air water interface.

There is a sensible physical explanation for this. Namely, for small neutral cavities the water molecules can still form a hydrogen bonded network around the strongly curved surfaces. This hydrogen bonded network has low entropy, so accounting for the entropy loss. However, for ions, the hydrogen bonded network is broken by the ion's charge. Hence the water structure around the ion resembles the bulk-air water interface and there is a large positive entropy change caused by breaking and disordering this network. This effect becomes larger with the size of the ion as more of the water's structure is disturbed. This is consistent with the common notion that large ions such as iodide are chaotropes. This effect can be seen from the temperature derivative of the surface tension as a function of cavity size.[12]

This conclusion has important implications. For instance, it has been hypothesized[148,64] that the cavity formation energy explains the excess of large ions at the air-water interface observed in experiment and simulation.[210] However, if the cavity formation energy of small neutral molecules is used to estimate the cavity formation energy of ions, then the magnitude of this force will be strongly underestimated and its entropy will have the wrong sign. I discuss this further in Chapter 6.

4.4.1 *Criteria Comparison*

I believe that the model outlined in Chapter 3 meets each of the criteria outlined in Section 3.1.4 (with reproduction of entropies and partial molar volumes—the last criterion—demonstrated in this Chapter). It reproduces quantitatively the solvation energies of the ions. The model includes charge hydration asymmetry, which, in the model, arises from the previously neglected dispersion contribution. Dispersion and cavity terms added to the electrostatic Born term are clearly separate and important contributions to the solvation energy. They are calculated at the same level of approximation

as the Born model and are therefore additive and not ad hoc. All of the parameters have clear physical interpretation and good external physical justification.

If the uncorrected models are used for the free energy derivatives, then there are no ad hoc corrections, all of the contributions come from a simple temperature or pressure derivative of the free energy with the parameters determined from external physical experiment or *ab initio* calculation. There is no reason to believe there will be overlap between the contributions as they all have clear separate physical origin. The model calculates entropies (enthalpies) of solvation, partial molar volumes and free energies. Hence it meets the criteria for a satisfactory model outlined above.

It is true that there is substantial quantitative error in the entropies and partial molar volumes for the smaller ions. However, the model still reproduces key qualitative properties such as the shift to positive entropy of solvation for iodide, and the negative partial molar volumes of the small cations. In addition, I have established the physical origin of the error in the model, and developed a very simple and physically motivated means of correcting for it that does not depend on any fitted parameters. I therefore believe that this does not constitute an ad hoc correction and makes the model significantly more satisfactory.

4.4.2 *Implicit Solvent Models*

These results provide evidence that the continuum solvation free energy model from which these entropies are derived is physically correct. This is quite remarkable considering the drastic level of approximation associated with a continuum solvent model. The assumption of a continuous medium explicitly neglects the position and orientation of the water molecules. Yet the model is capable of reproducing the entropies of solvation, a property whose key physical origin is a change in the number of ways the water molecules can be positioned and oriented. In addition to this the model was developed primarily with the solvation free energies as a target prop-

erty, and is not specifically tailored to reproduce these additional properties. This seems to be a nontrivial achievement, as supported by the observation that classical molecular dynamic simulations can not reproduce both single ion solvation free energies and entropies with the same parameter combinations.[107]

A common criticism of continuum solvent models is that they may be accurate for large systems where the solvent behaviour can be averaged over many water molecules. But when the solutes are of similar size to the water molecules it will break down. This is an important and rigorously true claim, as the mathematics of the dielectric response makes clear.[114] However, it is important to clarify at what length scale this breakdown occurs and how severe it is. Hence, we must build accurate continuum models that are rigorously true in the case of large molecules, and then extend these models down to smaller molecules observing where and in what way the break down occurs. The possibility that the approximation fortuitously works outside of its rigorous range of validity must be investigated, as it would be unfortunate if these simple and intuitive models were not discovered.

I have shown that in this case the breakdown is not too severe for the ions studied. The model works accurately for the largest ions with no corrections. Entropy-enthalpy cancellation leads to good estimates of the solvation energy for all ions. The breakdown in entropies and partial molar volumes observed for the smallest ions can be corrected in a very simple and intuitive way to account for the problem of dielectric saturation. The experimental entropies and partial molar volumes can then be reproduced all the way down to the smallest ions with an impressive degree of success.

The obvious caveats involved in the modelling of experimental properties of which the authors have prior knowledge are applicable here. In particular, there is some inherent discretion involved in the choices made when building these models, and in this case prior knowledge of the experimental data has had some influence on these choices. The most important examples of this are the use of the Tang-Toennies damping functions, the use of the surface tension of the bulk air-water interface, the dielectric satu-

ration correction, and the neglect of the V_{Cav1} and V_{Disp1} contributions as well as additional possible correction terms such as electrostriction.[183] These choices would not have been included unless comparison with experiment demanded it. It is very difficult to prevent this problem while preserving the simplicity of the model. I can however, mitigate it by ensuring any parameters have good physical justification and by widening the range of experimental comparison. Hopefully future tests shall validate the model further. For instance, generalizing the model to non-aqueous solvents will be an important test, and should provide insight into Hofmeister phenomena.[208]

As this model meets the criteria of a satisfactory continuum model of ionic solvation I believe it can serve as the basis of models of more complex Specific Ion Effects using the continuum solvent model. This area of research is already a well developed field. For instance, surface tensions,[30,148,64] and ion-ion interactions[157,227] are well studied with the use of continuum solvent models. These models are used because, unlike explicit solvent models, they allow for quick and simple calculations that provide clear and direct insight into the underlying physical origin of observed phenomena. However, they often still rely on somewhat limited ionic solvation models, which can make quantitative agreement with experiment difficult without the use of adjusted parameters.

I believe significantly improved continuum solvent models of these phenomena are possible by building them firmly on the foundations of a satisfactory model of ionic solvation energies such as the one outlined here. Doing so can remove the need for adjustable parameters to reproduce experiment and provide a unified picture of the interactions that dominate these properties. This is the aim of Chapter 6 and 7, where I generalize this model by applying it to surface tensions and activity/osmotic coefficients.

5

AB INITIO DISPERSION INTERACTIONS

This chapter is reproduced with minor changes from Ref. 69:
T. T. Duignan, D. F. Parsons, and B. W. Ninham. Collins's Rule, Hofmeister Effects and Ionic Dispersion Interactions. Chem. Phys. Lett., 608:55–59, 2014.

5.1 INTRODUCTION

A large body of previous work[187,153,206] has appeared to confirm the role of dispersion interactions in determining the properties of electrolytes. Some examples are the work determining the the ionic distribution profiles at the air-water interface,[30,33] and at mineral and protein surfaces.[31,34,204,27,35] These interactions however, have been insufficiently quantified. One issue was the incorrect use of static polarisabilities instead of the correct dynamic polarisabilities at imaginary frequencies.[205] Another was an inadequate treatment of ion size effects.[202]

There is still not a consensus on the importance of these dispersion interaction in the literature however. Some authors argue that dispersion interactions are negligible,[185] others simply ignore them,[148] and others believe they can be captured implicitly by small adjustments to the models parameters.[230].

In Chapter 2 I presented a more sophisticated semi-empirical continuum solvent model of ionic dispersion interactions with no fitted parameters. The model allows the inference of some important conclusions on the role of dispersion interactions in Specific Ion Effects. Prior to this, dispersion solvation energies of ions had only been calculated in Ref. 29. The model presented in this thesis constitutes a significant improvement in our understanding of these energies.

In this chapter I provide independent support for these and additional conclusions, by performing *ab initio* calculations of ion-water and ion-ion dispersion interactions. Accurate calculations of these energies are possible with the use of Symmetry Adapted Perturbation Theory with Density Functional Theory (DFT-SAPT).[104] This theory performs quantum mechanical calculations on the specified monomers at the DFT level and combines this with a SAPT calculation. The SAPT calculation takes the key properties of the monomers and inputs them into a perturbation expansion of the energy, which has had the correct permutational symmetry of the wavefunction imposed on it. This provides an estimate of the total interaction energy of the monomers. Crucially this energy is divided into various physical contributions, this enables us to look at the role of dispersion interactions explicitly.

These calculations demonstrate that, although dispersion interactions are only one piece of a complex balance of forces, they are necessary to achieve quantitative agreement with experiment and more importantly play a crucial role in the qualitative explanation of some outstanding puzzles that occur with Specific Ion Effects. Namely: the variation in solvation energy among ions of the same size, the small repulsion of iodide from the air-water interface, and the affinity of large ions for each other in water.

5.2 METHODS

I performed DFT-SAPT calculations on ion-water dimers for nine alkali halide ions and the copper(I) and silver(I) cations. These calculations output a value for the $E^{(2)}_{\text{disp}} + E^{(2)}_{\text{exch-disp}}$ contribution defined in Ref. 117, which I take to be the total dispersion interaction, labeling it E_{Disp}. To convert the ion-water dimer dispersion interaction energies into an estimate of the dispersion contribution to the solvation energy I use the coordination numbers of the ions as an estimate of the number of contact interactions the ion has with the water molecules. I then assume it is adequate to multiply the dimer energies by the coordination number of the hydrated ion.

Realistically there will be a many body correction to this energy due to the fact that the dispersion interaction is not pair-wise additive. This correction would likely reduce the magnitude of the energy by approximately 10%.[63] On the other hand, I have neglected the dispersion interactions with water molecules outside the hydration layer, this will lead to the calculation underestimating the magnitude of the dispersion solvation energy and these two effects will compensate each other to some degree.

The coordination numbers for the alkali halide ions from Ref. 288 are used, where the SWM4-NDP water model is used to give coordination numbers in 'excellent agreement with experiment.'[288] For silver(I) and copper(I), I estimate their coordination number with the average coordination number of the alkali halides (6.7) to determine a consistent value. Obviously, there is substantial uncertainty associated with this choice due to the significant variation in these values (4.0 – 9.7), unfortunately an improved consistent determination is not currently available.

Calculations of the DFT-SAPT dispersion energy of ions with a cluster of six water molecules were also performed at a smaller basis set size. The resulting values were very similar in size to six times the dimer energy. This confirms or at least supports the validity of this procedure.

5.3 COMPUTATIONAL DETAILS

DFT-SAPT calculations[104] using the PBE0 functional[4] with the asymptotic correction[105] were performed on ion-water and ion-ion dimers using the MOLPRO 2012.1 software package.[279,278] The ion-water separation is given by the R_S parameter determined from experimental measurements and given in Chapter 2 (Table 2.1). The geometries of the water molecules were taken from the structure optimizations of ion-water clusters also performed in Chapter 2. I used the aug-cc-pVQZ[128,284,285] basis sets for fluoride, chloride, bromide and water, aug-cc-pVQZ-PP for iodide,[212] copper(I) and silver(I),[211] and def2-QZVPPD[271] basis sets for the alkali cations. For rubidium, cesium and iodide the corresponding effective core potentials were also used.[143,213]

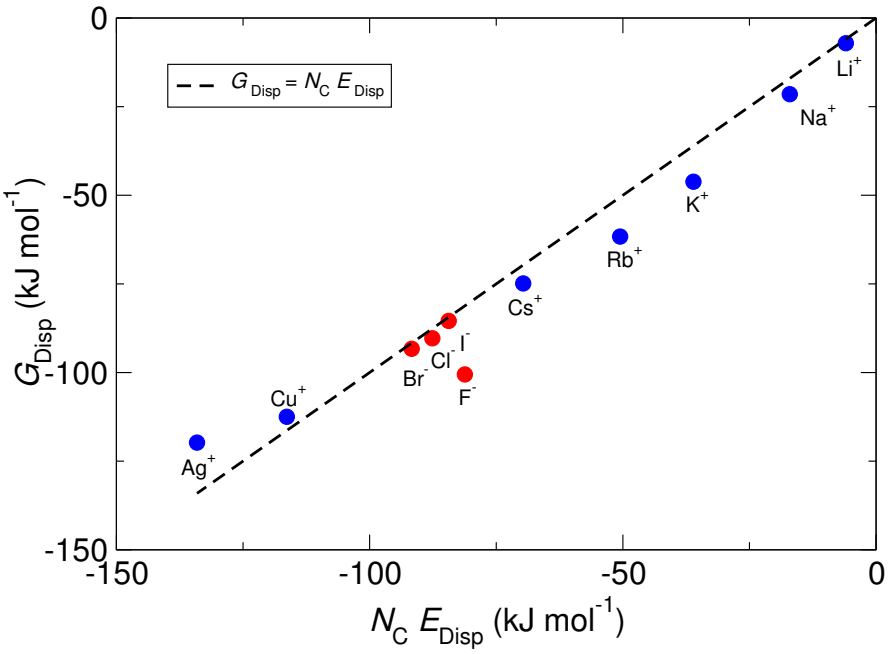

Figure 5.1: The dispersion interaction energy of the ion-water dimer from DFT-SAPT calculations multiplied by the coordination number ($N_C E_{Disp}$) agrees reasonably well with the dispersion contribution to the solvation energy of the ion in water (G_{Disp}) calculated with continuum theory in Chapter 2.

The DFT-SAPT calculations on ion water clusters with 6 water molecules were performed with the equivalent, but smaller double zeta basis sets. For the ion-ion dimer calculations I use the def2-QZVPPD[271,143,212] basis sets for all ions for simplicity and consistency. I determined the separation of the ion dimers from their crystal radii, as these values give a good estimate of the separation of the ions in water.[122] DFT-SAPT has been used previously on ion-ion and ion-water dimers with basis sets of this size or smaller with good accuracy.[173,10]

5.4 RESULTS AND DISCUSSION

5.4.1 *Ion-Water Interactions*

Figure 5.1 and Table 5.1 shows that the dispersion energies calculated with DFT-SAPT agree well with the dispersion solvation energy from Chapter 2.

Table 5.1: The dispersion solvation energy of some monovalent ions, G_{Disp} comes from the continuum solvent model presented in Chapter 2, N_c are the coordination numbers from Ref.[288], E_{Disp} are the contact dispersion energies from DFT-SAPT, $N_c E_{Disp}$ gives the present estimate.

Ion	G_{Disp}	N_c	E_{Disp}	$N_c E_{Disp}$
Li^+	−7.1	4.0	−1.5	−6.0
Na^+	−21.5	5.6	−3.0	−17.0
K^+	−46.2	6.9	−5.2	−36.1
Rb^+	−61.6	8.1	−6.2	−50.5
Cs^+	−74.9	9.7	−7.2	−69.7
Cu^+	−112.5	6.7	−17.4	−116.4
Ag^+	−119.8	6.7	−20.0	−134.1
F^-	−100.5	5.5	−14.8	−81.2
Cl^-	−90.3	6.5	−13.5	−87.6
Br^-	−93.3	6.8	−13.5	−91.7
I^-	−85.4	7.1	−11.9	−84.4

This agreement is quite impressive considering the substantial uncertainty associated with the coordination numbers and with the various approximations used. More specifically, all of the key qualitative behaviours observed in the previous method are reproduced with the new one. I review these important observations.

The first is the significant size of the dispersion energies. For instance, the dispersion solvation energy makes up 34% of the total solvation energy of iodide. The large size of this interaction is the result of two effects. Firstly, the ion-water separation is very small, and the dispersion interaction is very sensitive to this distance. Secondly, the anions have a particularly large polarisability caused by their extra electron. This enhanced polarisability effect is stronger for smaller anions, this therefore explains the counter intuitive ordering seen in Figure 5.1, where iodide has the smallest G_{Disp}. For fluoride there is a discrepancy between the quantum mechanical estimate and the continuum model due to its abnormally low coordination number of 5.5. Table 5.1 however shows that its dimer energy has the expected behaviour. Iodide's polarisability is still larger than the smaller anion's, but this is counteracted by iodide's much larger size, resulting in a net reduction of the dispersion interaction. Interestingly, bromide and chloride are reversed in

both estimates, with bromide having a more negative dispersion energy than chloride. This puzzling result indicates the non-trivial nature of dispersion interactions of anions.

The second and most important conclusion is that the variation in solvation energy of similarly sized ions is explained by the dispersion interaction, i.e., the puzzle as to why ions of similar size have quite different solvation energies. This is due to the difference in their polarisabilities and hence dispersion solvation energies. This is true for the cation-anion difference, i.e., the difference between potassium and fluoride. But it is also true for cation pairs such as silver and sodium, and copper and lithium, which have the same size but significantly different solvation energies.

The observation that negative ions are significantly more favourably solvated than positive ones of the same size is referred to as Charge Hydration Asymmetry (CHA). This effect has previously been attributed to the electrostatically asymmetric nature of the water molecule.[109] Although there is no evidence to conclusively disprove this mechanism, I would point out that the evidence in its favor tends to rely heavily on highly model dependent[184] classical simulation. In particular it relies primarily on the SPC/E water model which does have a significant CHA.[109,184] These simulations predict the difference to be roughly 200 kJ mol^{-1}.[109] When compared with Tissandier's experimental values,[256] this is too large to be physical. The experimental difference is roughly 50 kJ mol^{-1}, similar in size to the difference in dispersion energy. This could be due to the limitations of the water models used in the simulation. In particular, the lack of repulsive potentials centred on the hydrogen atoms.[109] In addition to this, recently Remsing et al.[231] have used *ab initio* molecular dynamics to show that TIP5P is much better than SPC/E at reproducing the surface potentials of water interfaces. The surface potential is strongly related to the symmetry properties of water and the CHA of TIP5P is less than a quarter the size of the CHA of SPC/E.[184] Additionally, some models with realistic multipole moments for water predict a negligible contribution from this effect.[184] This indicates that the CHA may be much smaller than originally thought. And it is far from clear how important this

contribution is. By contrast, the dispersion interaction alone appears capable of providing an adequate explanation of this variation.

I have presented two independent means of calculating the dispersion contribution to the solvation energies, the parameters of both models are not fitted to reproduce experiment but are derived from independent theoretical or experimental methods and have good physical justification. One approach uses a macroscopic, semi-empirical model of the water, treating it as a continuum. The other uses a microscopic model based on *ab initio* calculations. The consilience of these two methods allows us to conclude with confidence that this contribution to the solvation energy is being correctly modelled. Consequently, the observations regarding the role of these energies in the solvation of ions have strong support.

5.4.2 *Ion-Ion Interactions*

We now turn our attention to the role of dispersion interactions in the affinity of ions for each other in water. This question is significant because an understanding of pH, protein stability, ligand binding, surfactant behaviour, and surface forces all depend on the specificity of interaction of ions and ionic groups in water.[187]

A characterization that best sums up the affinity of ions for each other in water is that of Collins. His 'law of matching water affinity' states: 'oppositely charged ions in free solution form inner sphere ion pairs spontaneously only when they have equal water affinities.'[53] The statement has been useful for two reasons. Firstly, it gives a rule of thumb which allows the prediction of many properties[136,177] in a wide range of circumstances. Secondly, it provides a physical mechanism which explains some very puzzling experimental properties.[53]

Collins originally drew on the heats of solution of the salt crystal in the form of the 'Volcano Plot' of Morris[181] and on the solubilities of the salts as evidence of this rule.[52] However, appeal to these properties is somewhat problematic due to the fact that the heats of solution measure the enthalpy

change of dissolving the salt *at infinite dilution*, and so contain no information about the attraction of ion pairs for each other in water. In addition, the solubilities result from a balance between the chemical potential of the ion in the crystal and in solution at very high concentration. Their direct relevance to the interpretation of direct paired ion-ion affinities in water seems unclear.

The electrolyte properties that most clearly exhibit the 'law of matching water affinity' are the osmotic or equivalently the activity coefficients.[136] It has been shown that the activity or osmotic coefficient of a solution with a low concentration of weakly interacting solute, can be given in terms of an integral over the solvent averaged solute-solute interaction.[175] The situation is more complex for electrolytes due to the long range nature of the Coulomb interaction, but the basic principle remains: The activity coefficients give a measure of the strength of the ion-ion interactions, after averaging out the effects of the solvent. Conveniently these coefficients can be captured up to reasonably high concentrations and with decent accuracy using only one parameter, the B coefficients, determined by Bromley.[37] Bromley adjusted the value of this parameter empirically for each salt, so that when it is used in combination with a set of analytical equations it reproduces the activity and osmotic coefficients of that salt. The equations include a separate term that accounts for the effect of the non-ion specific long range electrostatic interaction. All of the ion-specificity in the ion-ion interaction is captured by a second term which depends on this parameter and arises from the ion-specific short range interaction. It is an analog of the second virial coefficient in the case of a non-ideal gas. The lower B is the smaller the osmotic and activity coefficients of the salts are and the more attractive the ion-ion interaction is. This topic is discussed in more detail in Chapter 7.

In Figure 5.2 I plot Bromley's empirical B values against the difference in cation and anion solvation energies determined by Tissandier et al.[256] These provide I believe the best estimates of the intrinsic solvation energies of ions,[110,43] as argued in Chapter 3, and hence are the best measure of the ion's affinity for water. The figure displays the same behaviour as the

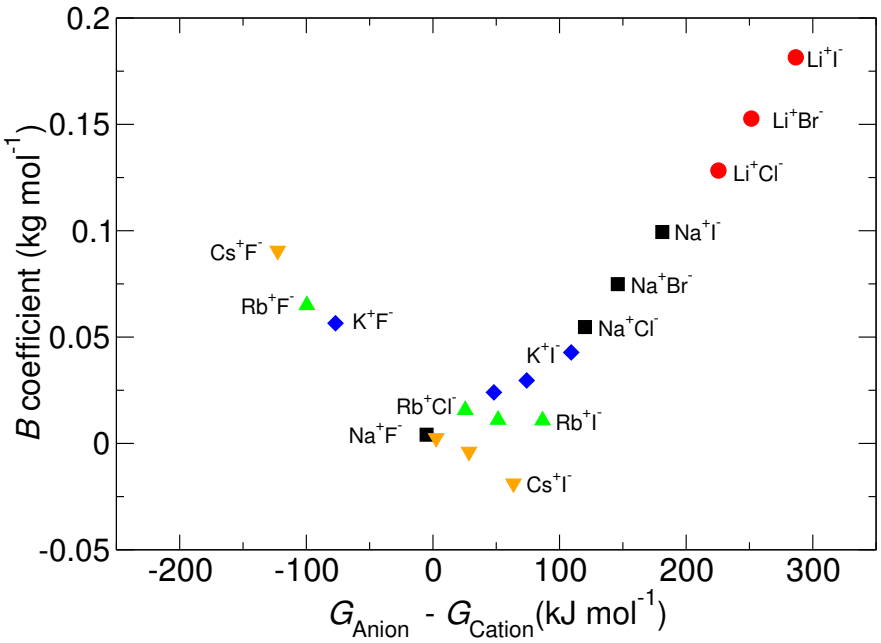

Figure 5.2: Bromley's Experimentally determined B coefficients[37] as a function of the difference in anion and cation solvation energies. B empirically represents the ion-ion interactions that determine activity and osmotic coefficients. Collins's 'law of matching water affinity' is seen in this 'inverted volcano plot.'

Volcano Plot, but with less random variation and a clearer physical interpretation.

The explanation and prediction of these osmotic coefficients remains one of the most challenging problems in physical chemistry. Many attempts to resolve this problem have met with limited success.[137]

A useful semi-quantitative model of this effect is that of Lund et al.[157] The fundamental physical mechanism is quite similar to the qualitative argument laid out by Collins, but with the essential additional insight of the 'shadowing effect'. This asserts that a large ion must remove a large amount of strongly held water from the surface of a small ion, so making this interaction particularly unfavorable.

While this idea captures some of the features sought, there remain significant puzzles regarding the strength of ion-ion affinity in water. In particular the ions most attracted to each other (with the lowest B coefficient) are not those of matching size as predicted by Lund et al., but those of matching

solvation energy. For instance, if it were matching size that mattered potassium fluoride should have lower activity/osmotic coefficients than sodium fluoride.

In addition, in the case of the large-large ion interaction Collins's explanation is that water-water interactions are more favorable than large ion-water interactions, and hence the formation of large ion contact pairs is favored to allow for more water-water bonds.[52] However, this is inconsistent with the fact that large ions still have significant negative solvation energies, indicating that the ion-water bonds are favored over water-water bonds. In addition the 'shadowing mechanism' will particularly enhance this energy loss for large ion pairs. In light of these facts, it is surprising that Figure 5.2 shows that large ion pairs (cesium and iodide) are even more strongly attracted to each other in water than small ion pairs are (sodium and fluoride).

What seems to be missing is some substantial direct ion-ion interaction between large ions which explains their affinity for each other. A plausible candidate for this mechanism is the dispersion interaction. This is generally larger for large ions due to their higher polarisability. Again, we can estimate this energy by performing DFT-SAPT calculations on ion-ion dimers in vacuum and extracting the dispersion contribution (E_{Disp}). The results of this calculation are shown in Figure 5.3. The first observation is that the size of these interactions very clearly establishes that they will play a significant role in determining ion-ion affinity. The energy minima of ionic interactions in water are typically only a few k_BT,[122] similar or smaller than the dispersion interaction energies calculated here. A caveat is that there will be a partially compensating loss in the ion-water dispersion interaction, which will somewhat mitigate this effect. A second observation is the significant variation of this energy among the cations ranging from $-4\ k_BT$ for the cesium salts to an almost negligible value for the lithium salts. This shows that this contribution is highly ion specific and most likely explains a substantial amount of variation among the ions. In particular, larger cations are more strongly attracted to anions than smaller cations. With the exception of the fluoride salts, this trend is consistent with experiment, as seen in Figure 5.2.

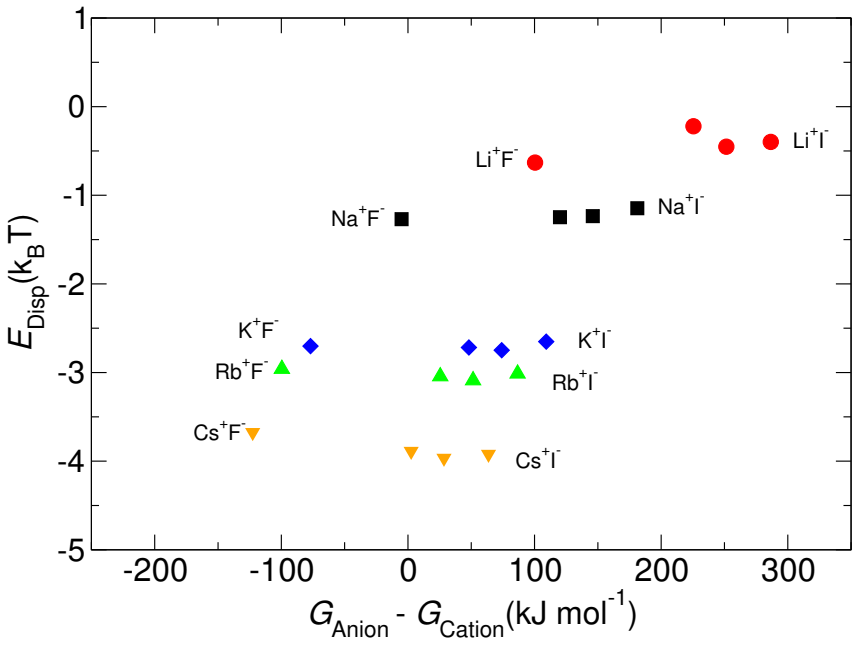

Figure 5.3: The dispersion interaction energy of the cation-anion dimer at contact calculated with DFT-SAPT as a function of the difference in the solvation energy of the cation and anion .

A more sophisticated calculation which includes the contribution from the loss of ion-water dispersion interaction is presented in Chapter 7. The resulting energies become repulsive, as expected due to the loss of two ion-water interactions for the gain of one ion-ion interaction. However, the variation among different ions remains roughly the same size.

In Chapter 7 I describe several additional contributions to the ion-ion affinity, including the 'shadowing' mechanism laid out by Lund et al. There clearly must be additional contributions for the anions, where the strength of the ion-ion dispersion interaction is relatively insensitive to the anion. This is similar to the ion-water dispersion interactions, which are also insensitive to the anion as discussed in Chapter 2.

The notion that dispersion interactions are important for ion solvation phenomena does not necessarily conflict with explicit solvent simulations. These calculations show that many important properties of electrolytes depend sensitively on the Lennard-Jones parameters. These parameters are intended to incorporate the effect of the dispersion interaction directly through the $-1/r^6$

term. However, its combination with the repulsive term and its fitted nature makes it difficult to quantify its importance.

5.5 CONCLUSIONS

From this work it is evident that dispersion forces, missing from many conventional analyses, cannot be ignored and play a major part in ion specificity. Both in terms of a quantitative correction to reach agreement with experiment, as well as a qualitative role in explaining several puzzling properties of electrolyte solutions.

These interactions, when combined with simple electrostatic, and dispersion terms give a satisfactory explanation of ionic solvation energies. In addition, a generalization of this model to ions at the air–water interface has been successfully developed and is outlined in Chapter 6. A development of a full model of ion–ion interactions in solution which also builds on the continuum solvation model is outlined in Chapter 7. It reaffirms the crucial role of the dispersion interaction in the attraction of large ions for each other.

6

ION INTERACTIONS WITH THE AIR-WATER INTERFACE

This chapter is reproduced with minor changes and with permission from Ref. 70: T. T. Duignan, D. F. Parsons, and B. W. Ninham. Ion Interactions with the Air–Water Interface Using a Continuum Solvent Model. J. Phys. Chem. B, 118:8700–8710, 2014. Copyright2014 American Chemical Society.

6.1 INTRODUCTION

Explaining and predicting the distribution of ions at the air–water interface has been a central problem in physical chemistry for nearly a century. This problem has been the subject of particularly intense focus over the last decade. Several recent review articles[210,120,186,257,2,170,88,147] provide a comprehensive account of the powerful new theoretical and experimental techniques that have been applied to solve it. These articles also provide a compelling justification for the intense focus on the problem. The justification firstly highlights the direct implications of this problem for atmospheric chemistry and bubble properties. Secondly, it points out that this problem corresponds to one of the most fundamental Specific Ion or Hofmeister effects.[190,187,153] Hence solving it is a necessary step in understanding these effects, which play a universal and vital role in biochemistry.

Early in this century polarisable molecular dynamics (MD) simulations[118,119] were used to predict an excess of large anions at the air–water interface. This significant success has been somewhat countered with the realization that these models may not be able to account for the experimentally observed surface excess of anions determined from surface tension data.[112,65] These increments appear to be somewhat more accurately reproduced by non–polarisable MD simulations.[257] This model dependence of explicit sol-

vent approaches has inspired attempts at *ab initio* MD approaches.[14] These approaches are promising but limited by extremely high computational demands.

Even if quantitative and predictive explicit solvent models of these properties had been developed, in many respects a continuum solvent model would still be desirable. This is because these models have low computational demands, in principle can easily be scaled up to explain more complex problems and can provide direct physical insight.

As discussed in Chapter 1, the only way to resolve the question of how accurate continuum solvent models are, is to build the best models we can and then test them. So far these continuum solvent approaches have shown promising results, in some respects performing on par with explicit solvent approaches.[257] However, the use of fitted parameters in both approaches limits the validity of such comparisons.

Many attempts have been made to build a continuum model capable of describing surface tensions of ions at the air-water interface.[195,125,80,138,33,161,148,247] A recent one is the model of Levin et al.[148] This model has rightly received significant attention, due to its ability to reproduce the surface tension of several electrolytes reasonably well, as well as its consistency with *ab initio* MD calculations of the iodide interaction potential with the air–water interface.[257] This model is an important and significant step forward in understanding this subtle problem. Its key physical insight is that there is a contribution from the release of the cavity formation energy, which drives the adsorption of large ions to the air–water interface.

Wang et al.[269] have recently presented an improved expression for the electrostatic energy of an ion crossing the interface. It distributes the ionic charge over a spherical shell, instead of using a point charge model. This allows for an analytic and continuous expression on both sides of the interface. It also seems to provide a larger and hence more realistic repulsion of kosmotropic ions from the interface. However, agreement with experimental surface tensions, which were not calculated in that work, may require additional repulsion.

One key potential improvement upon these two approaches is to take into account the change in shape of the interface as it overlaps with the ionic cavity. This has been neglected due to the extreme difficulty of developing analytical expressions with such low symmetry. In this chapter I use an alternative, numerical approach to solving the electrostatic problem. This allows for the shape change of the interface to be included, and also provides a more sophisticated quantum mechanical treatment of the ion.

I believe that there are many additional improvements that can be made to simple continuum solvent models of ions at the air–water interface. The end goal is to build a model that meets the criteria laid out in Section 1.3.1. This means firstly we should have a model that can reproduce several different experimental properties. This means following the approach used by Kunz et al.,[138] where a successful model of a separate property is generalised and applied to the new problem. For this I use the quantitatively accurate and, I claim, qualitatively satisfactory model of solvation energies developed in Chapter 3. Secondly, all of the important interactions must be included and the ions should be treated on a quantum mechanical basis. Thirdly, any parameters that are necessary such as the size and polarisability of the ions are determined independently by quantum mechanical calculation or direct experiment. Luckily almost all of the parameters we need have already been determined for the solvation model in Chapter 2 and 3. This means this third condition is relatively straight forward to meet.

In order to meet the second criteria we need to include all of the important contributions to the interactions. Several important contributions have been outlined before, but they have not been combined into a single model. Here we provide a list of all of the important contributions that need to be included:

- An electrostatic calculation that takes into account the change in shape of the interface as it overlaps with the ion's cavity.
- The loss of ion water dispersion interaction or equivalently the dispersion repulsion of the ion from the air–water interface.[33,66]

- The change in the cavity formation energy.[148]
- The contribution from the surface potential of the air–water interface.[23]
- The decrease in the air–water surface area on ionic adsorption.[198]
- Higher order induced multipoles, which could play an important role in stabilizing large ions at the interface.[286]
- Direct numerical calculation to determine the repulsion of kosmotropic ions from the interface, rather than using the hard sphere model with adjusted radii.

Including all of these contributions allows us to build a quantitative continuum solvent model of the ion–interaction with the air–water interface that meets the criteria laid out in Section 1.3.1. The model agrees with the consensus regarding the adsorption of iodide to the air–water interface. It also agrees quantitatively with experimentally determined surface tension increments. Because of its simplicity, the model also provides direct physical insight into the contributions that drive ionic behaviour.

This model therefore constitutes a significant step forward in our understanding of these properties and serves as a very promising candidate for the prediction and explanation of more complex and important ion–surface interactions.

6.2 THEORY

The total interaction potential of the ion with the air–water interface is given by:

$$G(z) = G_{COSMO}(z) + G_{image}(z) + \Delta G_{cav}(z) + \Delta G_{int}(z) + \Delta G_{disp}(z) + G_{SP}(z) \tag{6.1}$$

Where z is the distance of the ion from the air-water interface. Each of these terms describes a separate physical contribution to the interaction energy and will be described in the following sections.

6.2.1 *Electrostatics (COSMO)*

An important contribution to the interaction energy of an ion with the air–water interface is the loss of the ion–water electrostatic interaction. This is equivalent to a reduction in magnitude of the Born solvation energy, or a loss of interaction of the ionic charge with the induced polarisation of the water. At large separations this term is given analytically by the image charge repulsion.[195] However, at small separations the ion cavity overlaps with the surface, resulting in a highly asymmetric shape, illustrated in Figure 6.1. This asymmetry prevents exact analytical expressions for the required solution to Poisson's equation. In addition to this, the asymmetric solvation environment may create a non–negligible electric field, inducing a static polarisation of the ion. This induction effect has been posited as a key driver of the observed stabilization of large anions at the air–water interface.[120]

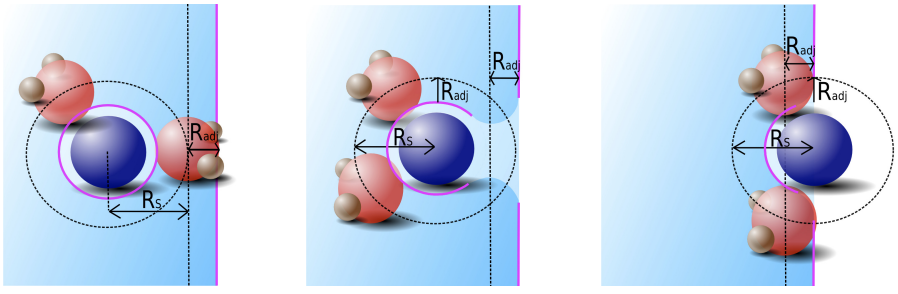

(a) (b) (c)

Figure 6.1: Depiction of the changes in the cavity as an ion crosses the air-water interface. The parameters are defined in Chapter 2. The pink line highlights the solvent accessible surface area.

A numerical solution is possible using the Conductor–like Screening Model (COSMO).[132,131] This method calculates the wave function of a solute using a given level of quantum mechanical theory, it includes the dielectric response of the solvent by modelling it approximately as a conductor and then including a correction to account for its deviation from this behaviour.

It outputs the total energy of the system. For an ion in a spherical cavity in bulk water, the dielectric response is spherically symmetric, thus there is no additional electric field created in the cavity and the ion's wave function does not change. As a result a COSMO calculation on this system outputs the Born energy associated with the supplied cavity size.

We can generalize this calculation to the case of an ion at the air–water interface by representing the interface with a second very large empty cavity which overlaps with the ion's cavity. This calculation can be implemented in TURBOMOLE.[1,5] See below for the calculation details. It calculates the change in the Born energy of the system incorporating the changing, anisotropic shape of the cavity as the ion reaches the interface. The calculation determines the value of the dipole induced on the ion, which allows us to examine the importance of the induction component of the interaction. The quantum mechanical treatment of the ion also means that higher order induced multipoles on the ion are included directly. Yagasaki et al.[286] argues that these multipoles make an important contribution to the energy of the ion at the air–water interface. This calculation has relatively low computational demand and is straightforward to apply and generalize. I refer to the energy resulting from this calculation as G_{COSMO}. The model works by calculating the induced charge on the surface of the cavity that is accessible to the solvent. This region is highlighted by the pink line in Figure 6.1. The induced surface charge is then scaled to correct for the non–conducting nature of the solvent.

6.2.1.1 *Induction Contribution*

The COSMO calculation can be divided into two parts. The first is the energy of desolvating the ion. This can be thought of as the loss of the Born solvation energy. The second is the interaction energy of the induced dipole on the ion with the solvent. It would be useful to know the energy associated with the induced dipole as its significance is currently under debate.[186]

I assume that the ion is linearly polarisable, i.e:

$$\boldsymbol{\mu} = \alpha \mathbf{E} \tag{6.2}$$

Then from the dipole moment and the polarisability of the ion, which can be calculated at the same level of theory, I can calculate the electric field at the centre of the ion. I can then calculate the energy of the induced dipole from the expression:[113]

$$G_{\mu} = -\frac{\alpha E^2}{2} \tag{6.3}$$

An alternative means of deriving this energy can be inferred by comparing the energy of an induced dipole in an electric field (Eq. 6.3) with the energy of a fixed dipole in an electric field:[113]

$$G_{\mu Fix} = -\alpha E^2 \tag{6.4}$$

The difference between these two dipole energies is due to the energy cost of inducing the dipole in the molecule (G_{pol}), which is therefore $G_{pol} = G_{\mu} - G_{\mu Fix} = -G_{\mu}$. The energy cost of inducing the dipole moment on the ion can be determined from the COSMO calculation. This is because COSMO firstly provides a calculation of the dielectric energy, which is the energy associated with the polarisation of the dielectric medium. Secondly it provides a value of the total energy, which is the dielectric energy plus the change in energy due to the distortion of the wavefunction of the molecule. Hence the difference between the dielectric energy and the total energy gives the energy cost of polarising the solute particle (G_{pol}). The negative of this difference thus gives G_{μ}. If only the dipole moment is significant these two calculations should agree. I can therefore write:

$$G_{COSMO} = G_{\mu} + \Delta G_{Born} \tag{6.5}$$

6.2.2 *Image Charge*

Because COSMO approximates the water as a conductor, the electrostatic image repulsion force at large separations is not included. This is because the electric field inside a conductor is zero. As a result the ion effectively does not interact with the air–water interface until it begins to overlap with it. This is physically inaccurate as there will be some longer range image charge repulsion of the ion from the interface:

$$G_{\text{Wagner}}(z, \rho = 0) = \frac{1}{4\pi\epsilon_o\epsilon_r}\frac{e^2}{4z} \tag{6.6}$$

However, it is actually useful that the calculation does not include this contribution. This is because this simple form for the image charge interaction must be incorrect at finite concentration, as it implies a surface excess of minus infinity.[195]

A more accurate, although by no means exact expression, was proposed by Wagner.[195] It incorporates Debye–Hückel damping of the charge of the ion due to the presence of a double layer of counterions at non zero concentration. This damping significantly reduces the electrostatic repulsion.

$$G_{\text{Wagner}}(z, \rho) = \frac{1}{4\pi\epsilon_o\epsilon_z}\frac{e^2}{4r}\exp^{-2\kappa z} \tag{6.7}$$

where κ is the inverse of the Debye Length: $\kappa = \sqrt{\rho}/3.04$ for 1:1 electrolytes in Å^{-1}, where ρ is in Molar (M).

This expression is problematic, not least because it assumes the ion has a full sphere of counterions around it, which is not possible if the ion is very close to the surface. However, at low concentration it serves as a reasonable first order estimate of this contribution. In addition, the main interest in this Chapter is explaining the ion–specific trends of the ions, together with the interaction of anions at the interface. This interaction is not very dependent on the salt and therefore should not play too significant a role in the ion–specific trends. This contribution will be accurate at large separations from the surface at low concentrations. I therefore add it to the other contributions

outlined below. However, it is only used in the region where the cavity does not overlap with the interface, which is where the conductor approximation leads to its neglect. The final expression is therefore

$$G_{image}(z,\rho) = \begin{cases} \frac{1}{4\pi\epsilon_o\epsilon_z}\frac{e^2}{4r}\exp^{-2\kappa z} & z > Rs + R_{adj} \\ 0 & z \leq Rs + R_{adj} \end{cases} \tag{6.8}$$

Following Chapter 2, R_S is defined as the distance from the centre of the ion to the centre of the water molecules in the first hydration layer. R_{adj} is the distance from the surface of the dielectric medium to the centre of the nearest water molecule. It is determined to be 0.84 Å. These values are provided in Table 2.1 and justified in Chapter 2. The reason this value was chosen for the cut off distance is clear from Figure 6.1.

6.2.3 *Cavity Energy Contribution*

In Chapter 3 I argued that the cavity formation energy of the ion could be modelled using the bulk surface tension of the air–water interface multiplied by the surface area of the cavity. We can calculate how this surface area of the ion cavity changes as the ion crosses the air–water interface by using the equation for the area of a spherical cap.

An important point about the height of this spherical cap is that it is not simply the distance that a sphere of radius R_S extends beyond the dielectric boundary. Instead it is in fact larger than this by 0.84 Å (R_{adj}). This is shown in Figure 6.1c and arises because the centre of the water molecules can only approach to within 0.84 Å of the interface. As a result, the ion–water surface area for an ion at $z = 0$ is not simply half the total surface area but smaller than this. The exact expression is:

$$\Delta A_{cav}(z) = \begin{cases} -2\pi R_S\left(R_S - z + R_{adj}\right) & z < Rs + R_{adj} \\ 0 & z \geq Rs + R_{adj} \end{cases} \tag{6.9}$$

This value for the area is consistent with the solvent accessible surface area, a property commonly used in continuum solvation models.[55]

In addition to this contribution an important and often neglected effect, is the reduction in the surface area of the air–water interface when an ion adsorbs.[198] We can calculate this surface area change straightforwardly, from the expression for the area of the base of the same spherical cap.

$$\Delta A_{int}(z) = \begin{cases} -\pi\left(R_S^2 - \left(z - R_{adj}\right)^2\right) & z < Rs + R_{adj} \\ 0 & z \geq Rs + R_{adj} \end{cases} \tag{6.10}$$

Multiplying both of these area changes by the surface tension of bulk water gives the cavity energy and air–water interface contributions to the interaction of the ion at the air–water interface:

$$\Delta G_{cav}(z) = \sigma \Delta A_{cav}(z) \tag{6.11}$$

and

$$\Delta G_{int}(z) = \sigma \Delta A_{int}(z) \tag{6.12}$$

where σ is the surface tension of the bulk air–water interface. ($\sigma = 0.178\ k_B T\ Å^{-2}$) These two terms are quite similar in size. (See Figure 6.3)

6.2.4 *Dispersion Contribution*

It is reasonable to assume that the dispersion energy is dominated by the interaction with the solvent molecules in the first water layer around a solute, due to its short range ($1/r^6$). I can therefore approximate the dispersion energy as being proportional to the number of water molecules in the first solvation layer around the solute. This number should be proportional to the solvent accessible surface area. This surface area decreases as the ion

crosses the air–water interface, and I therefore model the loss of ion–water dispersion interaction energy with:

$$\Delta G_{disp}(z) = (G_D + G_Q + G_O)\,\frac{\Delta A_{cav}(z)}{\left(4\pi R_S^2\right)} \tag{6.13}$$

Here $(G_D + G_Q + G_O)$ is the sum of the dipole, quadrupole and octupole moment contributions to the dispersion solvation energy in bulk solution. The values of this quantity for the ions considered in this Chapter are given in Chapter 2.

This expression replaces the B/z^3 term used to model the ion–surface dispersion interaction in previous work.[33] The B/z^3 expression is an asymptotic form true at large separations and analogous to the electrostatic image charge repulsion. But at the small separations of interest here, where the ion's cavity overlaps with the interface, its accuracy is questionable.

6.2.5 *Surface Potential*

It is likely that the asymmetry of the air–water interface creates a net electrostatic potential or surface potential, which will drive cations and anions towards or away from the interface depending on its sign.[23] There is substantial debate concerning the magnitude and even the sign of this contribution. Hünenberger and Reif[110] argue that the best value is +0.13 V, which is determined from the average of the values in the literature. I assume that for an ion at $z = 0$ half of this potential is felt and that the change scales with the surface area of the ion. Hence:

$$G_{SP}(z) = eq\phi\,\frac{\Delta A_{cav}(z)}{2\Delta A_{cav}(0)} \tag{6.14}$$

where $\phi = 0.13$V and q is the valency of the ion. This provides a weak driving force for cations towards the interface and anions away from the interface, which is consistent with *ab initio* simulations.[15]

6.2.6 *Additional Contributions*

I believe that the contributions described above provide a comprehensive account of the interaction of an ion at the air–water interface. The majority of explanations in the literature point to a combination of these interactions as explaining the observed distributions. Of course there have been alternative contributions proposed, the suppression of capillary waves for instance. This has been put forward as an explanation for the puzzling negative entropy change on adsorption of an ion.[198] I provide an alternative interpretation of this negative entropy, discussed below. I believe that the success of the model without this and other contributions indicates that they do not play a substantial role. Some fortuitous cancelling of errors is possible however. In particular, non ion–specific contributions may play a role in shifting the behaviour of all of the ions in one direction or another. But it appears the factors controlling the Specific Ion Effects in the surface behaviour are accounted for in this model.

6.2.7 *Calculation Details*

The TURBOMOLE package (v6.4)[1,5] was used with an implementation of COSMO.[132,131] Here I have used the aug–cc–pVQZ[128,284,281,274] basis sets for fluoride, chloride and bromide, aug–cc–pVQZ–PP was used for iodide.[212,101] The def2–QZVPP[271,102] basis sets were used for the alkali cations. In combination with the associated effective core potentials.[143,213] These are the same basis sets as those used in Chapter 2 for the determination of the ionic sizes in water. The calculations were performed both at the Hartree–Fock level using the DSCF program[97] and at the MP2 level using the RIMP2 program.[272,273,9] The polarisability of iodide was computed using the ESCF program at the same level of theory. Two cavities are input into the calculation, one of arbitrarily large size with a dummy atom at its centre. The second with an experimentally determined cavity size with the ion at its

centre at a distance z from the surface of the larger cavity. The NPPA and NSPA parameters define the number of basis points and segments per atom on the surface of the cavities.[132] They were increased to 12962 and 7292 respectively, in order to maintain a satisfactory density of sites on the surface of the large cavity. The dummy atom was placed in a cavity with a radius of 30 Å. The calculations were also performed at 50 Å and with smaller NPPA and NSPA values in order to confirm the convergence of the calculation to an effective flat air–water interface. The RSOLV parameter in COSMO was set to 0.84 Å, because it is equivalent to the R_{adj} parameter I have used here, i.e., they give the distance from the surface of the cavity to the centre of the solvent molecules. The epsilon parameter was set to 116.95 to reproduce the correct 1/78.3 damping of the long range coulomb interaction.

Some other important options are the charge overlap correction, which corrects for the charge that lies outside the solvent accessible surface, and the closed cavity, which involves adding extra points to the set of points that makes up the solvent accessible surface area to fill in the seams between atoms. Numerical problems arise in the calculation if the charge overlap correction is included or if the closed cavity option is used. I believe these are associated with the very large cavity size for which these options are not appropriate. I therefore perform the calculation without the overlapping charge correction and with an open rather than closed cavity.

For the cavity sizes of the ions I input the values of R_{cav} given in Table 6.1 and determined in Chapter 2. The solvation model has a mean unsigned error of 12 kJ mol^{-1} (3%). This error will lead to some corresponding error in the ion–interactions with the air–water interface, due to the fact that the total solvation energy is not correctly modelled. In order to remove this effect, I adjust R_{cav} to the nearest 0.01 Å to minimize the error in the solvation model. This is because the largest source of error in the model are the R_{cav} values. The solvation energies are quite sensitive to these values and they are difficult to determine accurately. This process reduces the mean unsigned error in the solvation model to 1 kJ mol^{-1}, which should allow for improved agreement with ion–water interaction potentials. I refer to these values as

Table 6.1: Values of the cavity sizes of the ions in water. R_{cav} is taken from Table 2.1. R_{cavA} is determined by adjustment that minimize the deviation from experimental bulk solvation energies.

Ion	R_{cav}(Å)	R_{cavA}(Å)
Li^+	1.22	1.24
Na^+	1.51	1.55
K^+	1.95	1.94
Rb^+	2.08	2.11
Cs^+	2.27	2.31
F^-	1.84	1.84
Cl^-	2.36	2.41
Br^-	2.51	2.59
I^-	2.80	2.83

R_{cavA}, listing them in Table 6.1. Adjusting R_{cav} also effects R_S through the relations $R_S = R_{cav} + R_{adj}$. Hence, the Born, dispersion and cavity contributions to the solvation energy are all altered by this adjustment. The COSMO and additional terms were calculated using both sets of cavity sizes in order to compare with experiment.

6.2.8 *Comparisons*

6.2.8.1 *Surface Tensions*

If we wish to determine the surface tension of an electrolyte solution we begin with the the Gibbs adsorption isotherm:

$$\Gamma = \frac{-a\beta}{N_A}\left(\frac{d\gamma}{da}\right)_T \tag{6.15}$$

where $\beta = 1/(k_B T)$, a is the activity of the solute and Γ is the surface excess, defined by:

$$\Gamma = \sum_i \int_0^\infty dz\,(\rho_i(z) - \rho_i(\infty)) + \int_{-\infty}^0 dz\rho_i(z) \tag{6.16}$$

where ρ is the concentration of the solute. At moderate concentrations where ion–ion correlations can be neglected the Poisson Boltzmann equation can be used to give the distribution profiles of an ionic species near a surface:

$$\rho_i(z) = \rho_i(\infty) \exp\left[-\beta \left(U_{i\text{-surf}}(z) + q_i \phi(z)\right)\right] \tag{6.17}$$

where

$$-\epsilon_r \epsilon_o \frac{d^2\phi(z)}{dz^2} = \sum_i q_i \rho_i(z) \tag{6.18}$$

There is substantial experimental uncertainty associated with the surface tensions of electrolyte solutions. For many common electrolyte solutions the data is consistent with a linear dependence of the surface tension on the concentration,[103] i.e., $(d\gamma/d\rho)_T = k$. This relationship often holds up to concentrations of several Molar. At low concentration the Gibbs adsorption isotherm can be written as:

$$\Gamma = \frac{-\rho\beta}{N_A}\left(\frac{d\gamma}{d\rho}\right)_T \tag{6.19}$$

Fitting the experimental data to Eq. 6.15 or Eq. 6.19, over a concentration range of 0.1M to 1M to a good approximation gives constant values of $\Gamma/\rho(\infty)$ within experimental error.[207,65] The theoretical problem therefore amounts to calculating a single $\Gamma/\rho(\infty)$ value for each electrolyte. The exponential term in Eq. 6.8 that damps the image charge repulsion is an approximate attempt to take into account the effect of ion–ion correlation on the electrostatic interaction of the ion. At high concentrations this expression becomes less accurate and in principle the Poisson–Boltzmann approach should be replaced by a more sophisticated one such as an integral equation approach.[129] The calculation also can not be performed at infinite dilution, firstly as the image charge repulsion leads to a surface excess of $-\infty$.[195] Secondly, experimental measurements of the surface tension at very low concentration show very puzzling properties,[209] such as the Jones–Ray decrease in surface tension as a function of concentration. I make no attempt to re-

produce or explain this effect here. It may arise from effects neglected in the model such as dissolved gas[187] or specific adsorption of hydroxide to the interface.[125]

The surface tension measurements are comparatively more reliable between 0.05 M to 1 M[170]. I therefore solve the Poisson–Boltzmann equation to calculate the surface excess at 0.05 M and 0.1 M, i.e., the lowest possible concentration consistent with experiment. This is in the range of experimental measurement, where ion correlation will be least important and Eq. 6.8 will be the least inaccurate.

Marcus[169] provides a review of the surface tension measurements in the literature, including the average values with standard deviations up to 2010. In order to avoid selectively comparing with the most favorable experiment it is best to compare with these averages. Ref. 169 also provides a best estimate of the surface tensions, using the assumption that the true values are additive. I compare with these values for reasons given below.

6.2.8.2 *Anionic adsorption*

Another key point of comparison of this calculation is with the *ab initio* calculation of the interaction of iodide with the air–water interface presented by Baer and Mundy.[14] This calculation is only approximate due to the extreme computational demands of this level of theory, but serves as an important check on the size of the adsorption energy minimum of iodide at the interface.

6.3 RESULTS

Figure 6.2 presents the interaction energy of the alkali halide ions as they approach the air–water interface calculated using the method outlined above. I emphasize that no fitting parameters have been used to artificially adjust these potentials, all of the features observed result straightforwardly from the calculation. The only aspect of the model that is deliberately fitted to reproduce experimental properties are the cavity sizes which have been ad-

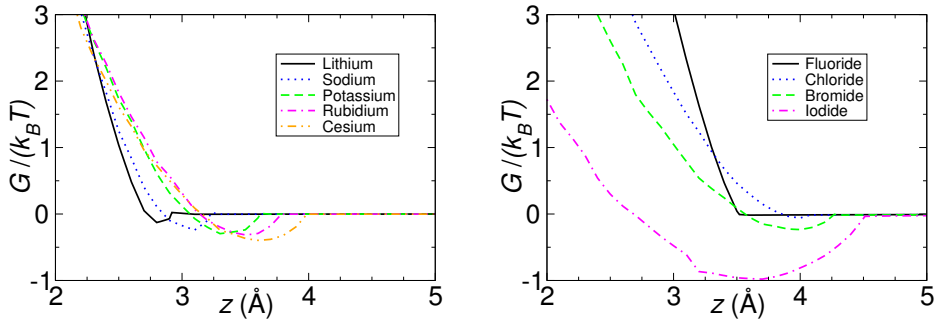

(a) Alkali cations (b) Halide Anions

Figure 6.2: Free energy change as the alkali halide ions approach the air-water interface. R_{cavA} is used for the ionic cavity size. The image repulsion is not included as it is concentration dependent and not ion-specific.

justed to reproduce the solvation energies, i.e., they are adjusted to R_{cavA}. This approach is similar to the adjustment of Lennard–Jones parameters in classical MD simulation. However, it is more physically reasonable as there is only one parameter per ion and it is adjusted within a tight range of plausible values.

The calculations were performed at both the MP2 level and at the Hartree Fock levels. There was a negligible difference between the two calculations, indicating that electron correlation is not significant, with the obvious exception of the dispersion interaction which is calculated separately.

The most studied of these interactions is that of the iodide ion. I find that the interaction has a potential well at z = 3.7 Å, with an energy minimum of -0.98 $k_B T$. A potential well of this size is consistent with the classical non–polarisable MD simulations with thermodynamically optimized parameters.[106] The model is also consistent with *ab initio* simulations of the iodide ion near the air–water interface,[14] where the largest negative energies of interaction are approximately -1 $k_B T$. It is not consistent with classical polarisable MD simulations where the adsorption energy is significantly larger.[119] However, these simulations disagree with experimental surface tension increments,[257] and it is possible that overpolarisation of the ions is occurring.[235]

The position of the well does appear to conflict with the *ab initio* simulations[14] and the continuum model of Ref. 148, where it is close to 1 Å and 0 Å

respectively. The disagreement with Ref. 14, may partly be due to subtleties in the definition of the distance to the interface.[250] The difference with Ref. 148 may be because that model neglects the change in the shape of the air–water interface as the ion crosses it. This shape change effectively removes some water from the surface of the ion, causing a significant electrostatic repulsion.

In addition to this, if we consider the extremely large solvation energy of ions, the notion that they are favorably adsorbed at $z \approx 0$ is, on the surface of it, an implausible proposition. At this position there are approximately half as many water molecules for the ion to interact with. I believe it is more plausible that there is a small region further in to the bulk water where longer range weak attractive interactions briefly outweigh the massive but shorter range repulsive contributions. This view is consistent with this calculation. This means I believe that iodide adsorbs in a manner consistent with Figure 6.1b, rather than Figure 6.1c.

The calculations are also consistent with experimental measurements[210,48] that indicate a surface enhancement of large anions at the interface. This means that they must have some negative adsorption energy. The position and size of this minium is not clearly determined by experiment due to the ambiguity in the probing range of the methods.

Figure 6.3 and Table 6.2 provide a breakdown of the contributions to the interaction energy of the ions with the air–water interface. This provides an explanation of the mechanisms driving adsorption to the interface.

The dipole moment of iodide at the contact minimum is 0.2 D and increases to 1.4 D at $z = 0$. This is consistent with the *ab initio* MD simulations.[14,186] These show that the dipole induced on iodide in the surface region is between 0.25 D to 1.4 D larger than it is in bulk. Of course the simulations also show a non–vanishing dipole moment in the bulk. This is in conflict with the continuum solvation model, where the spherical solvation environment does not allow for an induced dipole. This effect, to the degree that it is important, may be implicitly included in the Born model.

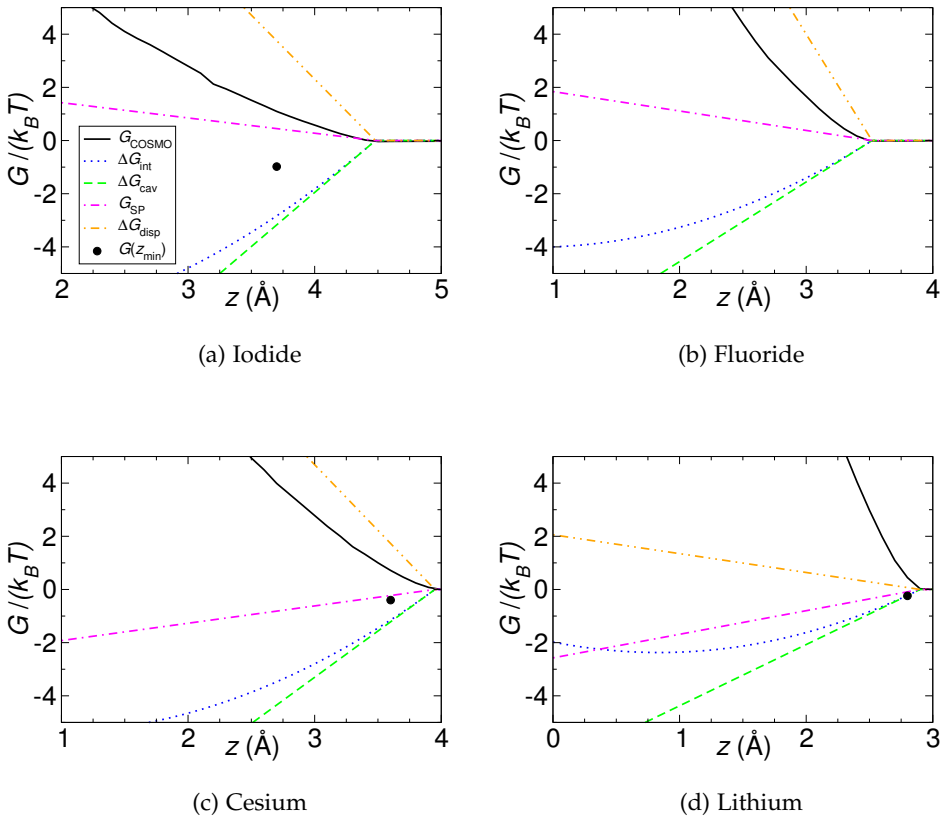

(a) Iodide

(b) Fluoride

(c) Cesium

(d) Lithium

Figure 6.3: Contributions to the interaction free energy of some ions at the air-water interface. Calculated with R_{cavA}. • gives the position of the contact minimum.

Iodide appears to be the only ion that approaches close enough to the interface for a substantial dipole moment to develop. The static polarisation or induction energy (G_μ) calculated using the polarisability of iodide is: $-0.05\ k_BT$ at z_{min} which increases in magnitude to $-2.73\ k_BT$ at $z = 0$. The second method of estimating G_μ, based on the energy cost of polarising the ion, gives: $-0.05\ k_BT$ at z_{min} which increases to $-2.74\ k_BT$ at $z = 0$. The fact that the two methods give almost identical results implies that only the induced dipole on the ion is significant and that higher order induced static multipole moments can be neglected. The small magnitude of the induced dipole explains why the MP2 level of theory does not improve the results. MP2 improves the description of the polarisability of the ion, but this effect is so small that the improvement is insignificant. Figure 6.4 shows the relative importance of the two contributions to G_{COSMO}: The induction en-

Table 6.2: z_{min} gives the position of the contact minimum, G is the free energy depth of the contact minimum. The other columns give contributions to the energy at that minimum. F^- is omitted as it has no contact minimum. All energies are given in units of k_BT.

Ion	z_{min}	$G(z_{min})$	ΔG_{Born}	ΔG_{cav}	ΔG_{int}	ΔG_{disp}	G_{SP}	G_μ
Li^+	2.8	−0.13	0.45	−0.28	−0.27	0.08	−0.11	0.00
Na^+	3.1	−0.24	0.33	−0.35	−0.34	0.22	−0.10	0.00
K^+	3.3	−0.30	0.76	−0.99	−0.94	1.11	−0.23	0.00
Rb^+	3.5	−0.31	0.56	−0.96	−0.91	1.19	−0.20	0.00
Cs^+	3.6	−0.40	0.73	−1.37	−1.29	1.80	−0.25	−0.01
Cl^-	4.0	−0.06	0.05	−0.33	−0.32	0.48	0.06	0.00
Br^-	4.0	−0.23	0.27	−1.04	−0.99	1.36	0.16	0.00
I^-	3.7	−0.98	1.15	−3.32	−2.96	3.74	0.46	−0.05

ergy makes a non–negligible contribution but is overwhelmed by the Born contributions.

6.3.1 *Surface Tensions*

Some important observations can be made based on a solution to the the Poisson–Boltzmann equation using these interaction potentials. Firstly at 0.1 M the electrostatic potential created is a few millivolts, i.e., it is small compared to thermal energy, and the exponential terms in Eq. 6.17 can be linearized and substituted it into Eq. 6.16 resulting in:

$$\begin{aligned}\Gamma/\rho_i(\infty) = &\int_0^\infty dz \left(e^{-G_{cat}(z)} - 1 + e^{-G_{an}(z)} - 1\right) \\ &- \beta e \int_0^\infty dz\, \phi(z) \left(e^{-G_{cat}(z)} - e^{-G_{an}(z)}\right)\end{aligned} \tag{6.20}$$

For the potentials I have calculated, the second term in this expression is much smaller than experimental error. Qualitatively this is because $\beta\phi e$ is typically ≈ 0.1 and because the cationic and anionic interaction potentials are not too dissimilar in size. This results in the difference in the exponential terms being approximately an order of magnitude smaller than the exponential terms themselves. These two orders of magnitude make the second

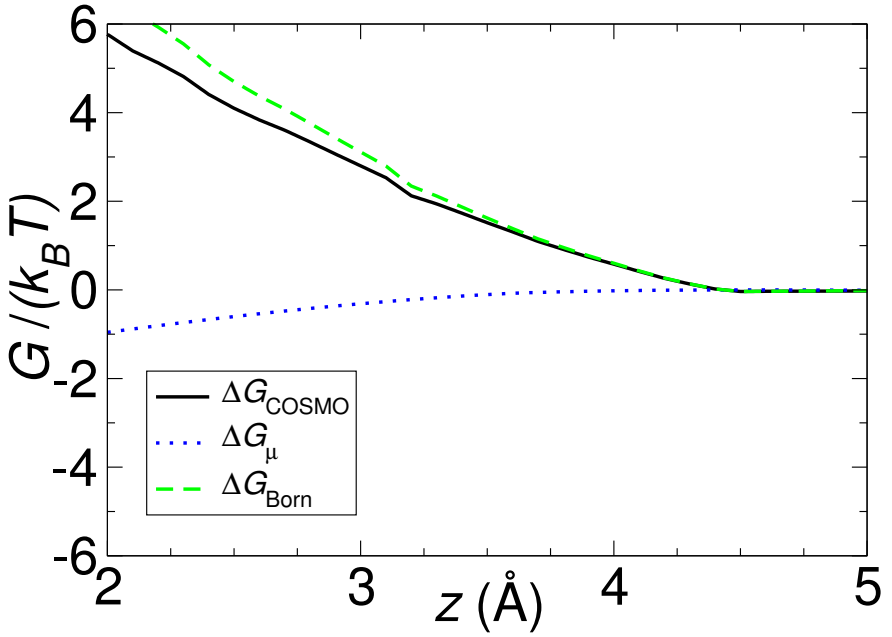

Figure 6.4: The Born and induced dipole contribution (G_{μ}) to the interaction energy calculated with COSMO

term a few percent of the first term. To a good approximation therefore the surface excess can be written as

$$\Gamma/\rho_i(\infty) \approx \int_0^{\infty} dz \left(e^{-G_{cat}(z)} + e^{-G_{an}(z)} - 2 \right) \tag{6.21}$$

The most important observation based on this expression is that there is no coupling between the cations and anions. This expression combined with Eq. 6.19 therefore implies that the surface tension increments should be additive. Mathematically this means that at 0.1 M the general version of the following condition should be true: $(d\gamma_{NaF}/dc) - (d\gamma_{KF}/dc) = (d\gamma_{NaCl}/dc) - (d\gamma_{KCl}/dc)$ This condition is not met by experimental surface tensions.[169] Because we have a good theoretical justification of additivity at low concentrations, it is reasonable to assume this lack of additivity is due to experimental error from contamination or due to Eq. 6.19 being inaccurate over the experimental range covered. This means that it is not possible to achieve good agreement with the average experimental values using a Poisson–Boltzmann approach. Marcus[169] has addressed this problem, establishing a set of val-

ues for the surface increments that are additive and as close to the experimental measurements as possible, including an associated uncertainty of 0.2×10^{-6} N m^2 mol^{-1}. The resulting values are linearly related[170] to those determined by Pegram and Record.[207]

From Marcus's values I can calculate Γ and compare with the theoretically determined values. The results of this calculation are presented in Figure 6.5 and Table 6.3. As the values are now additive in principle there are only 9 independent values. However, as with the solvation energies, splitting the experimental values measured for salts into an absolute cation and anion contribution is a difficult problem. I avoid having to make any assumptions regarding this problem by comparing with the surface tension increments of the 12 alkali halide salts that have had their surface tensions measured.

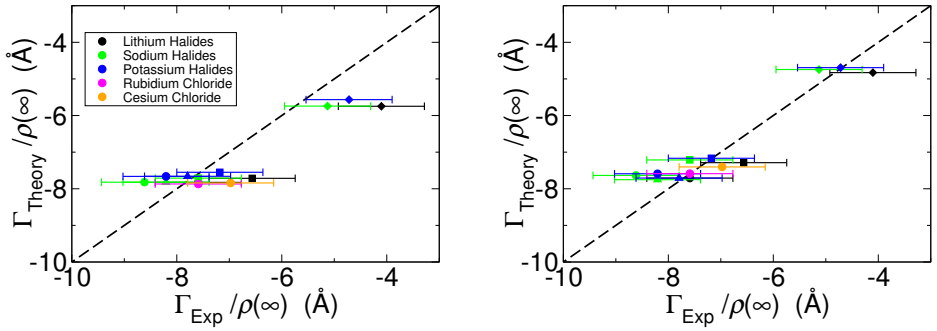

(a) 0.05 M with unadjusted cavity radii (R_{cav}) (b) 0.05 M with cavity sizes adjusted to R_{cavA}

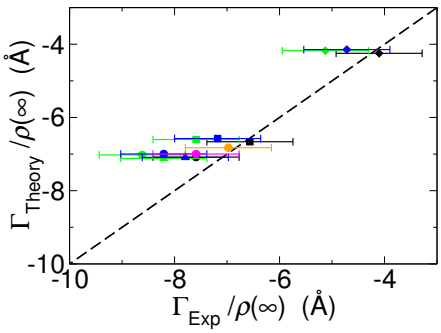

(c) 0.1 M with cavity sizes adjusted to R_{cavA}

Figure 6.5: A comparison of experimental surface excess compared with theoretical calculations. Colors indicate the cation: Lithium: Black, Sodium: green, Potassium: blue, Rubidium: magenta, and Cesium: orange. Anions are marked with a symbol: Fluoride: ▲, Chloride: ●, Bromide: ■, Iodide: ◆. R_{cavA}, used in (b) and (c), is the cavity size adjusted to best reproduce bulk solvation energies.

Table 6.3: A comparison of experimental surface excess compared with theoretical calculations at 0.05 M with cavity sizes adjusted to R_{cavA}

Electrolyte	$\Gamma_{theory}/\rho(\infty)$(Å)	$\Gamma_{exp}/\rho(\infty)$(Å) ± 0.8Å
LiCl	−7.69	−7.6
LiBr	−7.26	−6.6
LiI	−4.81	−4.1
NaF	−7.74	−8.2
NaCl	−7.61	−8.6
NaBr	−7.18	−7.6
NaI	−4.72	−5.1
KF	−7.71	−7.8
KCl	−7.58	−8.2
KBr	−7.15	−7.2
KI	−4.69	−4.7
RbCl	−7.57	−7.6
CsCl	−7.38	−7.0

These figures show that the calculation reproduces the surface tension increments well. The agreement in Figure 6.5b is as good as can be expected considering the substantial experimental uncertainty. By comparison with Figure 6.5a we can see that if the cavity radii are not adjusted to reproduce experimental bulk solvation energies exactly, the agreement with experiment is less satisfactory although still reasonable. The concentration of 0.05 M gives the best agreement. Once the concentration increases beyond 0.1 M (Figure 6.5c), significant deviations begin to occur. I attribute this to the expression for the image charge repulsion (Eq. 6.8) breaking down. The presence of the surface significantly limits the double layer that can build up around the ions. This effect is neglected by Eq. 6.8. Hence the damping of this interaction is overestimated at higher concentrations and the surface excess is underestimated. More sophisticated treatment of the image charge repulsion should show a linear dependence on concentration as observed experimentally. However at 0.05 M this approximation is not too severe and it is reasonable that experimental and theoretical calculations agree.

An additional point is that the model reproduces the ion–specificity well, which is the key question of interest for a range of applications, as the exact description of the profiles of ions near the air–water interface at moder-

ate concentrations, even in the primitive model is a non–trivial problem,[130] which I shall not address here.

An additional point can be made with regards to the position of the minimum. If a minimum of size $\approx -1 k_B T$, is located at $z \approx 0$, as some models suggests, it is very difficult to reach agreement with experimental surface tension values. Levin et al.[148] achieve this only by having an adsorption energy for iodide close to 0 and by comparing with experimental values well below the experimental average.[169] This implies that a potential well occurring at a distance of $z \approx 3.5$Å from the Gibbs dividing surface is more consistent with surface tensions then one at $z \approx 0$.

6.4 DISCUSSION

6.4.1 *Dispersion Contribution*

It is clear from Figure 6.5 that the surface tension increments of electrolytes decrease with the size of the halide ions. This has caused problems with simple models which attempt to explain ion specific surface tension increments purely on the basis of the dispersion interaction.

Intuitively, if dispersion interactions are the origin of the ion-specificity of surface tensions, it would be expected that the larger ions, because of their larger polarisability would have stronger dispersion interactions with the air-water interface. As this interaction is repulsive, these larger ions would be more strongly repelled. In this way surface tension increments would be expected to increase with halide ion size. If the polarisabilities of anions are fitted to reproduce surface tensions they have to decrease with size.[30] This is unphysical.[136] The simplest explanation, which is that dispersion forces can be neglected, is clearly incorrect.[251,30] The model presented here provides a satisfactory explanation.

In the solvation model used here the dispersion solvation energy of fluoride is larger than for iodide. This means that fluoride has a larger dispersion repulsion from the air–water interface than iodide, which is consistent with

the experimental surface tension measurements. This counter–intuitive result is due to the fact that it is not polarisability alone which determines the dispersion interaction energy, but rather polarisability and size. This obviously does not mean that the dispersion energy can explain electrolyte surface tensions alone as all of the contributions outlined above play a role.

The model of Levin et al.[148,64] can almost reproduce electrolyte surface tensions while neglecting the significant dispersion repulsion of ions from a surface. How can we reconcile this with this model where the dispersion contribution cancels out a significant part of the cavity energy? The answer is that the model of Levin et al. uses the hard sphere solute model to calculate the cavity formation energy, which I have argued significantly underestimates the actual ionic cavity formation energy. In addition, it uses the Born cavity size. This cavity size represents the region where the polarisation of the water molecules is insignificant. This is different from the region where the centres of the water molecules cannot penetrate, which is the definition used in a hard sphere solute model. The resulting underestimation of the cavity size provides a plausible explanation of why the model can neglect the repulsive dispersion contribution and still achieve reasonable results.

6.4.2 *Mechanism of Iodide Adsorption*

Figure 6.3 provides physical insight into the adsorption of large ions. We can see that there is a cancellation of several large effects at the contact minimum. It is therefore unreasonable to point to a single contribution as the explanation for the minimum in the interaction potential. The primary attractive contribution is the decrease in water interfacial area, both at the ion–water and air–water interfaces. In particular these two effects are roughly equal. Hence the attraction is double what it would be if only the ionic cavity formation energy was included. This mechanism is in essence what is commonly referred to as a hydrophobic attraction. Secondly, on comparing iodide to fluoride we can see that the dispersion repulsion from the interface is actually lower in magnitude for iodide compared with fluoride. This is firstly because fluoride

has a stronger total dispersion interaction with the water, as seen in Chapter 2, and secondly because fluoride interacts with fewer water molecules, i.e., it has a smaller hydration number.[288] (This arises from its smaller surface area in this model.) As a result it experiences a sharper repulsion than iodide does. The last contributor is the small slope in the G_{COSMO} contribution for iodide. This can be attributed to three effects, the first two are the same as for the dispersion interaction. Namely the smaller magnitude of the total Born solvation energy and secondly the larger hydration number of iodide. The third contribution is the induced dipole moment interaction. But the small size of the induction energy for iodide shown in Table 6.2 and Figure 6.4 indicates that this contribution is not qualitatively important in explaining iodide's potential well at contact. This is consistent with the observation that non–polarisable MD simulations reproduce a negative adsorption energy of iodide at the air–water interface[106] even though the ion has no static polarisation response. It is also consistent with polarisable MD simulations of Caleman et al.[42], where the authors conclude that the induced dipole on the anion does not contribute to its stabilization at the interface. That is to say, it is consistent with the observation that the dominant driver of adsorption to the air–water interface is the release of cavity and interfacial surface energy as well as the small solvation energy of iodide.

The partitioning of the energies determined here is qualitatively similar to the partitioning determined by Arslanargin and Beck[11] from non–polarisable MD simulations, particularly the cavity and dispersion energies. However, the electrostatic contribution is significantly different. The differences could be due to physical inaccuracies in one of the approaches, or could arise from different methods of partitioning the energy. The final potentials are also similar, although the adsorption well determined by the MD calculation is significantly smaller.

6.4.3 *Surface Potential*

To a certain degree the surface potential makes a less significant contribution to the salt surface tensions then might be expected. This is because it drives cations in one direction and anions in the other. This means that minor errors in the surface potential will not substantially affect the predicted surface tension values. This is fortuitous as there is substantial uncertainty regarding the correct value for this property.

However, because of the non–linear nature of the Boltzmann distribution, substantial deviations will occur if the surface potential is shifted by a large amount. For instance, if a negative surface potential of ≈ -0.5 V is used, rather than +0.13 V, then the model's predictions diverge significantly from experimental surface tensions. Beck[23,219] argues that a surface potential of ≈ -0.5 V is correct. It is clear however, that this value should not be combined with the model used here. To make sense of a surface potential of ≈ -0.5 V, it is necessary to assume that Marcus's values[167] for the ionic solvation energies give the correct intrinsic solvation energies. This is inconsistent with the underlying solvation model used here, which predicts that the Cluster Pair Approximation[127] gives the intrinsic values. I am of the opinion that the CPA (applied to small clusters) gives the intrinsic values and have justified this view in Chapter 3. However, there is significant debate in the literature regarding this issue. It is certainly possible that Marcus's values are the true intrinsic values combined with a surface potential of ≈ -0.5 V. If this is the case the underlying solvation model would be wrong, or at least incomplete, and its agreement with experiment would be a coincidence. However, the resulting real solvation energies that include the surface potential are quite similar. Because it is the real solvation energies that are important in determining ion–surface interactions, the success of this model may be consistent with either case.

6.4.4 *Specific Ion Effects*

An important observation is that there is significant error associated with the experimental values. This severely limits the rigorousness of the test that can be applied to the surface tensions. For instance, the average experimental values show that sodium and chloride have the highest surface tension increments of the alkali and halide ions respectively.[169] This fact is not reflected in the results of this model, where the surface tension increments are highest for lithium and fluoride. This is not necessarily in contradiction with experiment because these trends are within experimental error. I therefore cannot conclude that the trends are physically real.

However, these calculations do provide some insight into this phenomena, namely the question of why the ion specificity is so weak that it cannot be adequately resolved with experiment, other than for the iodide ion. The explanation is clear from Figure 6.3 where we see that as the ion size increases, several effects come into play. Firstly, the distance at which the removal of the ion's first water layer commences takes place further from the interface. i.e., iodide starts losing its solvation shell well before fluoride does. If this energy cost were independent of the ion this would result in a larger repulsion from the air–water interface and hence a more negative surface excess for larger ions. In reality however, this energy loss changes with ion size. For both cations and anions the electrostatic (G_{COSMO}) and cavity terms (ΔG_{cav}) become respectively less repulsive and more attractive as the ion's size increases. On the other hand for cations the dispersion energy (ΔG_{disp}) becomes more repulsive with increasing ion size. This means that as the cation size increases two contributions increase repulsion and two contributions decrease repulsion. These effects approximately cancel and the overall repulsion from the interface is fairly constant for cations, consistent with the fact that the difference in their surface tension increment cannot be clearly resolved experimentally. Anions behave similarly, except that their dispersion repulsion decreases with ion size. This changes the balance and results in a significant decrease in the overall repulsion as anion size increases. This

explains why the surface tension trends are more significant for anions and is consistent with the more general observation[136] that anions tend to have a more significant ion–specific effect than cations.

6.4.5 *Entropic Contribution*

Levin et al.[148] use a cavity formation energy of ions that is the same as for neutral solutes and argue that this energy drives the adsorption of large ions to the air–water interface. It has been shown that this cavity formation energy of small neutral solutes is primarily an entropic cost.[12] Their model therefore implies that the entropic component of the force at the air–water interface should be attractive, but this is in conflict with experiment and simulation.[198,42] The Born and dispersion contributions to the solvation energy have negative entropies and should therefore both be entropically attractive to the interface. The induced dipole moment may give rise to an entropic cost, but the entropic repulsion is observed in non–polarisable MD simulation where there is no inducible dipole, excluding this mechanism as an explanation. It is possible that this entropic repulsion arises from a contribution from the change in water–water entropy. This could be neglected while still achieving agreement with free energies, as it is exactly cancelled by a change in water–water enthalpy.[289,24]

In contrast, I have argued in Chapter 3 and Chapter 4 that it is not appropriate to use the same cavity formation free energy for ions and for small neutral solutes. This is because the cavity energy of a small neutral solute arises from the ability of water to form a hydrogen bonded structure around the cavity.[44] It is therefore small and dominated by a negative entropic component. This structure will be broken by the ion's charge which reorients the water molecules. Hence, this form of the cavity formation energy is not appropriate for ions. The formation energy of a cavity occupied by an ion will be more accurately characterized by the bulk air–water interfacial surface tension.

The free energy of forming a bulk air–water interface is entropically favored, i.e., the entropy of surface formation is positive. This model is therefore consistent with the entropic repulsion of ions from the air–water interface, because in this model the change in surface area of the system is the key driver of ionic adsorption to the interface. This may be because the temperature dependence of the surface tension includes the full contribution from water–water interactions.

6.4.6 *Implications*

This calculation has important implications. Firstly, due to is simplicity and low computational demand it should be generalizable to more complex and important situations. The interaction of an ion with the air–water interface serves as a kind of simplest case or prototypical system [198] for more complex ion–surface interactions. For instance, the ionic interactions with mineral surfaces is a source of large uncertainty in the prediction of surface forces. Even more importantly the direct interaction of ions with protein surfaces is believed to be a key determinant of the Specific Ion Effects of protein precipitation. [292] Understanding this fundamental and long standing problem is a necessary prerequisite to building models of a vast range of biological phenomena on the basis of physical chemistry.

I emphasize here that no parameters have been deliberately fitted to reproduce surface tensions. A small quantitative improvement is made by adjusting to reproduce the solvation energies of the ions exactly, but these are a separate physical quantity and this adjustment does not substantially alter the qualitative conclusions. In order to meet agreement with experimental surface tensions a concentration of 0.05 M was chosen. This is justified by the fact that at 0.1M and above non–trivial ion–ion correlations begin to become important and the simple form for the image charge repulsion is known to break down. Even so this contribution is only weakly ion–specific and so the trends are still preserved at higher concentrations, offset by a constant from the experimental values.

All of the choices made for the form of the interaction potentials are simple and well justified, any parameters used have independent physical justification. I believe this gives the model a strong degree of support as it is not victim to the usual criticism of continuum solvent models that they are equations fitted to reproduce whatever data they are applied to. This has been achieved by basing the model on a satisfactory model of the bulk solvation energy of ions, which is the most fundamental property in the determination of ionic interactions in water.

6.5 CONCLUSION

In summary, I have reproduced the experimentally measured surface tension increments of the alkali halide salts by generalizing my solvation model in order to calculate the free energy of an ion as it approaches the air–water interface. The potential of iodide is consistent with *ab initio* MD simulation and experimental observations of an enhancement of iodide at the interface, although the position of the adsorption maximum does occur further into the bulk water than in comparable models. The dominant attractive contribution to this enhancement is clearly identified as the reduction in surface area of the system and the importance of the dispersion interaction in determining the ion–specific trends is established. In particular, I have shown that iodide has a weaker dispersion repulsion from the interface than fluoride. This is due to iodide's smaller total dispersion solvation energy and is more consistent with experimental surface tensions.

7

ION-ION INTERACTIONS

This chapter is reproduced with minor changes from Ref. 71:
T. T. Duignan, D. F. Parsons, and B. W. Ninham. A Continuum Solvent Model of Ion–Ion Interactions in Water. Phys. Chem. Chem. Phys., 16:22014-22027, 2014–Reproduced by permission of the PCCP Owner Societies.

7.1 INTRODUCTION

Ion–ion interactions in water are central to understanding a vast range of biological and industrial processes that involve electrolytes.[187,153] As discussed in Chapter 5, the most direct expression of ion–ion interactions in water are the osmotic and activity coefficients of electrolyte solutions. Activity/osmotic coefficients are a key to derived properties such as the pH, buffer capacity, osmotic pressure, chemical equilibria, specific heats, colloid interactions and many more. A parameter-free theory that predicts ion specific activities is therefore the goal. Specifically, what is required is a theory that minimises computation and is easily used by non–experts.

We can develop a model of these properties by building on the solvation model outlined in Chapter 3 and the ion–surface interaction model outlined in Chapter 6. Ion–ion interactions serve as a third example of these 'simple' properties. With a model of all three of these properties we will have a firm foundation on which to attempt to build predictive quantitative models of more complex systems that exhibit Specific Ion effects.

In a hierarchy of theoretical approaches we recall that the simplest so called 'primitive' model of these properties is the Debye–Hückel theory.[60,233] It includes only the mean field ion–ion electrostatic interaction and a continuum solvent. A bulk liquid dielectric constant mediates (electrostatic) ion

interactions. For real electrolytes, at very low concentrations the osmotic or activity coefficients depend only on the ionic valencies, and this model reproduces them well. At moderate concentrations, ion–specific short–range interactions become important. These are very difficult to model accurately, due to changes in ion–water interactions with separation and direct non–electrostatic interactions of the ions.

The next development from a practical viewpoint is to add extra (empirical) terms and parameters to the expressions derived from the Debye–Hückel model, in attempts to capture these short–range ion specific interactions. As discussed in Chapter 5, two benchmark examples of this approach are those of Pitzer[216] and Bromley.[37] Bromley's formulation is particularly useful as it shows that the activity and osmotic coefficients of salts at a single temperature can be reproduced with reasonable accuracy up to moderate concentrations with only one parameter per salt. This parameter is analogous to a second virial coefficient, or B coefficient, in the case of a non–ideal gas. This dramatically simplifies the problem from a theoretical perspective, as the task is reduced to predicting only these parameters, which have a clear physical interpretation, rather than having to reproduce the non–trivial concentration dependence of these properties. Important physically based extensions of the Debye–Hückel approach have also been developed,[199] as well as generalizations to asymmetric and mixed electrolytes.[134]

Numerous alternative approaches to modelling these properties have been considered. Some examples are HNC,[226] NRTL,[46,45,249] MSA,[154,246,123] TPCP,[151,87] eCOSMO–SAC,[270] Monte Carlo or classical Molecular Dynamics (MD) simulation,[144,122] hybrid implicit/explicit solvent approaches,[268,179] and *ab initio* MD approaches.[214,267,217,158] This incomplete list provides an indication of the variety of approaches taken to solve the problem.

None of them have proven satisfactory. This is due to their complexity and, apart from *ab initio* approaches, a strong dependence on fitting parameters. These parameters are often adjusted for each salt. This limits their usefulness and obscures physical insight. The state of affairs is well captured by Kunz and Neueder in 2010, in the introductory chapter to Ref. 137, where

they state: 'there is not a single published work in which a prediction of these values can be found.' Further, 'Today, it seems that the most physical model is one of the oldest: the Friedman–Gurney (FG) model' developed by Ramanathan and Friedman[226] in 1971. This model uses sophisticated HNC calculations to treat the statistical mechanics, but still relies on 'Gurney potentials' (discussed in Section 1.4.2,) which rely on parameters adjusted for each salt. Improvements in the physical basis of models as well as their predictive and explanatory power are therefore crucially needed.

The bringing to bear of simulation to treat the position and orientation of water molecules explicitly does not appear to have moved us much closer to a predictive understanding of these interactions. Although these models can reproduce qualitative features of these interactions,[75] it appears that ion–ion interaction potential parameters and combining rules must be adjusted for each salt separately to reproduce these properties quantitatively.[84,83] In principle, this is not very different to relying on fitted Gurney potentials. It may be that only *ab initio* simulations[217] will be capable of providing a model that does not rely on fitting. But their extreme computational demands make such a program very difficult to implement.

There is an alternative approach. This is to look for interesting correlations in the data, and interpret these using qualitative arguments or simplified models. Collins's[52] very useful 'law of matching water affinity' exemplifies this approach. As discussed in Chapter 5, he argues that ions with similar water affinity, that is, similar ion-water interaction strength, are more strongly attracted to each other, and indeed this pattern is observed in osmotic or activity coefficients.[136] This point was shown in Figure 5.2, but can be seen more clearly in Figure 7.1, where the osmotic coefficients of several salts are plotted as a function of concentration. As I will show below, lower osmotic coefficients indicate a stronger solvent averaged ion-ion attraction. Intuitively, this is because stronger ion-ion attraction reduces the pressure the ions exert on the container walls. Figure 7.1 shows that when the cation and anion of a salt are similar in size, then it has a lower osmotic coefficients. The size of an ion also correlates roughly with its interaction strength

with water. Hence, like–prefers–like is consistent with the 'law of matching water affinity.' This is a key observation on which it is necessary to remark further. Collins provides a qualitative argument to justify this law. And as discussed earlier, Lund et al.[157] have provided a simple continuum solvent model of ion–ion interactions, which qualitatively reproduces the like–like affinity of ions. The insights are real enough. But they fall short of the ultimate goal. This is to provide a model that can reproduce quantitatively the activity/osmotic coefficients of all salts without parameters fitted for each. Only then can we have confidence that the model has captured accurately the actual physical mechanisms that would allow a foundation for prediction and application to more complex systems. The calculation of the direct ion–

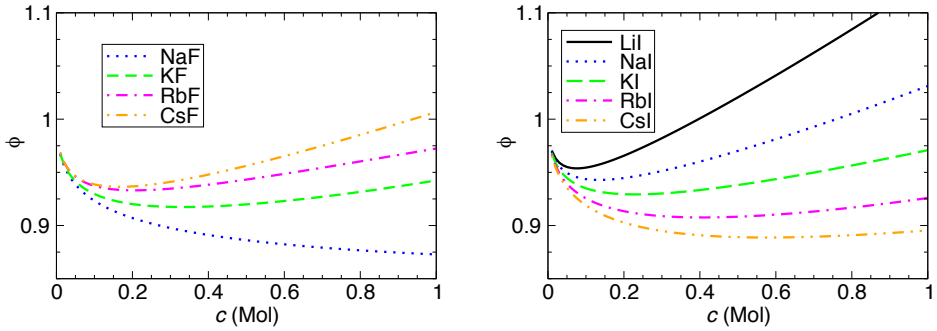

(a) Fluoride salts

(b) Iodide salts

Figure 7.1: The osmotic coefficients of the fluoride and iodide salts exhibit the like prefers like behaviour. Ions of similar size have the lowest osmotic coefficient and hence the strongest attraction.

ion interactions in vacuum is a relatively straightforward task using modern quantum chemistry software. The fundamental difficulty in predicting these interactions in water is ionic hydration, i.e., the interaction of the ions with the water molecules around them and how this interaction changes as the two ions come together. The basic problem therefore amounts to calculating how the solvation energy of the two ions changes as they come together. The model of solvation energies, outlined in Chapter 3, can be generalized to the case of two ions in close proximity to each other.

This is exactly the approach I have used in Chapter 6 for the ion-surface interaction. Those results were encouraging and invite extension to other

properties of electrolyte solution. The end goal is to build a model that meets the criteria outlined in Section 1.3.1. By generalising a model of solvation energies we can build a model that meets all three criteria. If it works, the assumptions of the model will be reinforced and there will be less need for fitting parameters. As discussed in Chapter 1, Kunz et al.[138] used this approach. A model for osmotic coefficients was fitted to determine the dispersion interaction contributions by adjusting the polarisabilities and ionic sizes. These ion–specific interactions are missing from conventional approaches. It was then generalized to determine ion–surface interactions. Although the model had limited success due to some neglected contributions, the general approach is still suggestive.

7.2 THEORY

Similar to the approach applied in Chapter 6, the solvent averaged free energy of interaction of two ions is taken to be given by the expression:

$$G(d) = G_{COSMO}(d) + \Delta G_{cav}(d) + \Delta G_{disp}(d) \tag{7.1}$$

where d is the separation between the two ions.

Each of these three terms is a generalization of one of the three terms in the solvation model. $G_{COSMO}(d)$ corresponds to the change in the electrostatic Born solvation energy plus the direct ion–ion interaction. $\Delta G_{cav}(d)$ and $\Delta G_{disp}(d)$ give the change in the cavity formation energy and the ion–water dispersion interaction energy of the two ions as the approach each other. Each of these terms is described in more detail in the following sections. The cavity and van der Waals (dispersion) interactions are missing from standard treatments in which the first term would be an electrostatic interaction with a hard core cut–off.

This interaction energy will be used to determine experimental activity and osmotic coefficients. I discuss this in the Experimental Values section below.

7.2.1 *Direct Electrostatic Contributions*

As two ions come together they experience a direct electrostatic interaction. At large separations (several water molecules) this is given to a good approximation by Coulomb's law with the static dielectric constant of water used.

$$G_{\text{Coulomb}} = \frac{e^2}{4\pi\epsilon_o\epsilon_w d} \tag{7.2}$$

The dielectric constant of water has its bulk static value. At large separations and at infinite dilution the Coulomb term is the only contribution to the interaction. It is used in the derivation of the original Debye–Hückel model, which is the origin of the non–ion specific term in the Pitzer and Bromley equations.

However, at short–range this expression is inaccurate. This is because it assumes that the ions are point charges embedded in the dielectric medium. It is often asserted that at small separations, i.e., where r is of the order of the size of a molecule, the continuum solvent approximation will break down and explicit solvent or more sophisticated treatments will be necessary. Although on the face of it this seems like a reasonable statement, it is worth testing by building the best possible continuum models we can, and looking at their degree of accuracy. There are several potential improvements of the simple continuum solvent model that can still be made. In the context of the electrostatic interaction this means including the change in geometry,[228] magnitude[144] or isotropy[189] of the dielectric medium as the two ions come together.

More specifically, as the two ions approach there will eventually come a point where the separation is so small that a water molecule can no longer fit between them. There will be some substantial cost to removing this water from the surfaces of the ions. But there will be a corresponding increase in attraction of oppositely charged ions, due to the decrease in the effective dielectric constant of the medium between them. These effects arise because

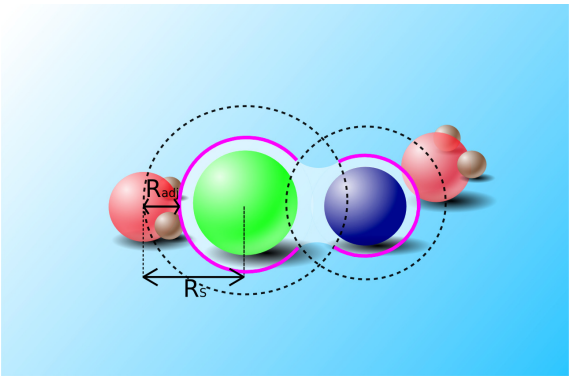

Figure 7.2: Depiction of the COSMO calculation of the ion–ion interaction. The pink line shows the surface of the cavity where the surface charges are located.

the ions occupy finite sized cavities in the water where the relative dielectric constant is 1. To take care of this problem we need the solution of Poisson's equation with the complex boundary condition created by the two overlapping spherical cavities.

We can use a numerical approach to model this situation approximately with the Conductor Like Screening Model (COSMO).[132,131] This model treats the solutes on a quantum mechanical basis. The water is approximated as a conductor, and the interface between the cavity occupied by the solutes and the background medium is determined from the Solvent Accessible Surface Area (SASA). The electric field of the solutes induces a surface charge on this interface. The calculation proceeds until self–consistency is reached. This calculation is depicted in Figure 7.2. The advantages of this approach are: firstly, it includes the repulsion due to the loss of electrostatic ion–water interactions upon the removal of water from the first hydration layer. Secondly, it includes the reduced damping of direct ion–ion interaction, due to the removal of water. Thirdly, it provides an accurate calculation of the direct ion–ion interaction as both solutes are treated at a quantum mechanical level. This quantum mechanical treatment does mean that the COSMO calculation includes the direct ion–ion dispersion interaction and Pauli repulsion of the two ions. Hence, it is not purely an electrostatic calculation.

This calculation can be thought of as the direct ion–ion interaction plus the change in Born energy of the two ions as they come together. This is consistent with the fact that the COSMO calculation of the two ions at infinite

separation gives the Born solvation energy of the two ions. The calculation details are provided below. If the cavities do not overlap, the COSMO calculation reproduces the normal Coulomb interaction. The methodology is in principle the same as the one presented by Rashin[228] and Pratt et al.,[223] except that I have applied a more sophisticated quantum treatment of the ion.

7.2.2 *Cavity Energy*

The next contribution to the ion–ion interaction arises from a change in the shape of the ionic cavities as the two cavities overlap. As the ions come together some water in their hydration shells will be removed and will move back into bulk. There will be some energy gain associated with this due to the fact that there is an energy cost of forming the cavity in water that the ion occupies, which is now released. This has been put forward by Collins[52] as a key mechanism driving the experimentally observed affinity of large ions for each other. In Chapter 5, it was identified as a key driver of anionic adsorption to the air water interface.[148,70] This can be thought of as a hydrophobic attraction, although it may not have the usual entropic character.

In the solvation model the energy of forming the cavity of the ion is calculated by multiplying the surface area of the cavity by the surface tension of the bulk air–water interface. This is different to the cavity formation energy of small neutral solutes, which is smaller and entropically dominated. The reason for this difference is that water molecules can form a hydrogen bonded network around a neutral molecule.[44] This is not applicable to ions, which will reorient nearby water molecules and break this structure.

The use of bulk interfacial tension can obviously be disputed. However it did lead to reasonable results in previous chapters.

I therefore use the same bulk interface surface tension to calculate the cavity contribution to the ion–ion interaction energy. For instance, for solutes i and j in contact, we have:

$$\Delta G_{cav} = \sigma_{ion}\big(\Delta A_i(d) + \Delta A_j(d)\big) \tag{7.3}$$

where $\sigma_{ion} = 0.178\ k_B T\ \text{Å}^{-2}$. $\Delta A_i(d)$ is the change in surface area of ion i due to the presence of ion j as a function of separation, and vice versa for $\Delta A_j(d)$. The change in area is straightforwardly determined by the area of the spherical cap that is removed when the two ions overlap.[282]

$$\Delta A_i(d) = \begin{cases} -\pi R_{S,i}\left(R_{S,i} + R_{S,j} - d\right)\left(1 + \frac{R_{S,j} - R_{S,i}}{d}\right) & d < R_{S,i} + R_{S,j} \\ 0 & d \geq R_{S,i} + R_{S,j} \end{cases} \tag{7.4}$$

$R_{S,i}$ is the R_S parameter of ion i, defined as the distance to the peak in the solute–oxygen radial distribution function. Similarly, we have:

$$\Delta A_j(d) = \begin{cases} -\pi R_{S,j}\left(R_{S,j} + R_{S,i} - d\right)\left(1 + \frac{R_{S,i} - R_{S,j}}{d}\right) & d < R_{S,j} + R_{S,i} \\ 0 & d \geq R_{S,j} + R_{S,i} \end{cases} \tag{7.5}$$

7.2.3 *Dispersion*

7.2.3.1 *Ion–Water Dispersion*

The next important contribution is the change in the ion–water dispersion interaction. The simplest approximation to this energy is to assume that it decreases in proportion to the change in the surface area. This is the approximation I have used in Chapter 6 for the case of the ion interaction with the air–water interface. However, this will not work in this situation as the water molecules are not being removed completely from the ion as they are in the case of an ion at the air–water interface, but simply displaced to a distance slightly further away. The accurate computation of this energy would require the calculation of the Green's function with the boundary condition

given by the overlapping cavity. This is equivalent to solving Poisson's equation for these rather complicated geometrical configurations. This task is underway, but significant difficulties remain. We can use an intermediate approximation. I assume that the dispersion solvation energy is approximately pairwise additive, with a C_{2n}/r^{2n} behaviour. $n = 3$ for the dipolar dispersion energy, $n = 4$ for the quadrupole term and $n = 5$ for the octupole term. In other words, I assume:

$$G_D = \int d^3\mathbf{r}'\rho(\mathbf{r}')\frac{C_6}{|\mathbf{r}' - \mathbf{r}_i|^6} \tag{7.6}$$

$$G_Q = \int d^3\mathbf{r}'\rho(\mathbf{r}')\frac{C_8}{|\mathbf{r}' - \mathbf{r}_i|^8} \tag{7.7}$$

$$G_O = \int d^3\mathbf{r}'\rho(\mathbf{r}')\frac{C_{10}}{|\mathbf{r}' - \mathbf{r}_i|^{10}} \tag{7.8}$$

Where the G_D, G_Q and G_O are the same as defined in Chapter 2. For the water density ($\rho(\mathbf{r}')$) I use a function that is ρ_w outside the cavity and 0 inside it. This function is dependent on the distance between the two ions, as well as the size of the cavities etc. I therefore write it as $\rho(\mathbf{r}', d)$.

I can then write the change in dispersion interaction as a function of separation:

$$\Delta G_D(d) = \left(\frac{\int d^3\mathbf{r}'\rho(\mathbf{r}', d)\frac{C_6}{|\mathbf{r}'-\mathbf{r}_i|^6}}{\int d^3\mathbf{r}'\rho(\mathbf{r}', \infty)\frac{C_6}{|\mathbf{r}'-\mathbf{r}_i|^6}} - 1 \right) G_D \tag{7.9}$$

$$\Delta G_Q(d) = \left(\frac{\int d^3\mathbf{r}'\rho(\mathbf{r}', d)\frac{C_8}{|\mathbf{r}'-\mathbf{r}_i|^8}}{\int d^3\mathbf{r}'\rho(\mathbf{r}', \infty)\frac{C_8}{|\mathbf{r}'-\mathbf{r}_i|^8}} - 1 \right) G_Q \tag{7.10}$$

$$\Delta G_O(d) = \left(\frac{\int d^3\mathbf{r}' \rho(\mathbf{r}', d) \frac{C_{10}}{|\mathbf{r}' - \mathbf{r}_i|^{10}}}{\int d^3\mathbf{r}' \rho(\mathbf{r}', \infty) \frac{C_{10}}{|\mathbf{r}' - \mathbf{r}_i|^{10}}} - 1 \right) G_O \tag{7.11}$$

The density of water and the dispersion constants cancel out, and these expressions can be calculated analytically using toroidal coordinates. This calculation is presented in the Appendix C.

This allows a calculation of the change in ion–water dispersion interaction at contact. I then assume that this interaction scales with the change in surface area of the ions. There are several reasons for this: Firstly, for ease of computation, which would otherwise require the use of bispherical coordinates at larger separations. Secondly, because the cavity formation and dispersion energy should have similar distance dependence as both arise from the removal of water. Thirdly, for consistency with the previously developed model of ion–surface interactions where this approximation worked well. The expression is therefore given by:

$$\begin{aligned} \Delta G_{disp}(d) = &\Big(\Delta G_{D,i}(d_c) + \Delta G_{Q,i}(d_c) + \Delta G_{O,i}(d_c) \Big) \frac{\Delta A_i(d)}{\Delta A_i(d_c)} \\ &+ \Big(\Delta G_{D,j}(d_c) + \Delta G_{Q,j}(d_c) + \Delta G_{O,j}(d_c) \Big) \frac{\Delta A_j(d)}{\Delta A_j(d_c)} \end{aligned} \tag{7.12}$$

Where d_c gives the separation of the ions in contact. For this I use the sum of the crystal radii of the ions, given in Table 2.1. This is approximately the position of the minimum in the ion–ion interaction potential.

7.2.3.2 *Ion–Ion Dispersion*

In Chapter 5 I suggested that the direct ion–ion dispersion interaction plays a significant role in the affinity of large ions for each other in water. This contribution can be included in the COSMO calculation by using an MP2 level of theory. Hence, it does not need to be calculated separately, i.e., the term $G_{COSMO}(d)$ includes both the electrostatic and ion–ion dispersion interactions. We can probe the importance of this interaction by comparing calculations at the MP2 level and the Hartree–Fock level. The difference is likely

to be predominantly due to the dispersion interaction, as the dispersion interaction arises entirely from the electronic correlation effects included in the MP2 level but not at the Hartree–Fock level. This is clear from the interaction of noble gas atoms where the difference between these two levels of theories is very close to analytical calculations of the dispersion interaction. This calculation does neglect the many body correction to this interaction due to the presence of the surrounding water molecules, that may be on the order of 10%.[63] Including this contribution would again require the Green's function with the given boundary conditions.

7.2.4 *Experimental Values*

The most rigorous approach to compare the interaction potentials with experiment would be to use the solvent averaged ion–ion interactions to calculate the activity/osmotic coefficients accurately at all concentrations using relatively sophisticated statistical mechanics such as HNC calculations[226] or simulations.[268] These calculations are prone to numerical difficulties, and are sensitive to small perturbations in the interaction potential.[122] I adopt a simpler approach.

I start with the osmotic and activity coefficients of a solute that only interacts only via short–range interactions with other solutes at low concentrations. The osmotic coefficient is given by:[25,175]

$$\phi(c) = 1 + Bc \tag{7.13}$$

and the activity coefficients by:

$$\ln \gamma(c) = 2Bc \tag{7.14}$$

where B is the second virial coefficient:

$$B = -2\pi \int_0^\infty dr r^2 \left(e^{-\beta G(r)} - 1 \right) \tag{7.15}$$

Here $G(r)$ is the free energy of interaction of two solutes as a function of separation. I use the variable r instead of d for clarity. The situation is significantly more complicated for ions because they undergo long–range electrostatic interactions, and so these expressions are invalid. However, this long–range electrostatic interaction depends only on the valency of the ions. It is well established[122] that ion–specificity, for ions of the same valence, is primarily attributable to the short–range interactions. If we assume that these two effects make additive contributions, a significant assumption but one worth testing, then the osmotic coefficients can be written as:

$$\phi_{ij}(c) = 1 + f_\phi(c) + B_{ij}c \tag{7.16}$$

and the activity coefficient as

$$\ln \gamma_{ij}(c) = f_\gamma(c) + 2B_{ij}c \tag{7.17}$$

Where $f_\phi(c)$ and $f_\gamma(c)$ depend only on the valency of the ions and are attributable to the long–range electrostatic Coulomb interaction, while the ion–specificity is captured by the B_{ij} parameter.

Indeed, this expected behaviour seems to be roughly correct. The Specific Interaction Theory (SIT)[36] shows that these values can be reasonably well captured over a range of concentrations using only one parameter (B_{ij}) per salt. In SIT the Debye–Hückel expression is used to calculate the Coulomb term's contribution:

$$f_\gamma(c) = \frac{A\sqrt{c}}{1 + 1.5\sqrt{c}} \tag{7.18}$$

This simple formulation of the ion–specific variation is consistent with Figure 7.1, where the osmotic coefficients do not cross, but simply spread out as concentration increases. More exactly, the difference between the osmotic coefficients of two different salts as a function of concentration is approximately a straight line though the origin, which supports this formulation.[95] The activity coefficients behave similarly.

This provides a much simpler and more direct means of testing theoretically calculated potentials, and bypasses the need to perform complex concentration dependent calculations. We can take the solvent averaged ion–ion potentials, subtract the long–range Coulomb interaction and then substitute this potential into Eq. 7.15. In principle, the resulting values should approximately agree with the B_{ij} parameters derived from experiment. Although this procedure is approximate the error is likely to be less than that associated with a continuum solvent approximation and more sophisticated calculations should be possible once a satisfactory model is discovered. Reproducing the B_{ij} parameters is practically equivalent to reproducing the osmotic and activity coefficients over a large concentration range and with reasonable accuracy. The simplest model[199] for the B_{ij} parameter is to assume a hard sphere potential, in which case Eq. 7.15 reduces to: $\frac{2}{3}\pi a^3$, where a is the size of the ions. However, this model is unsatisfactory as the ion sizes must be adjusted to unphysical values, and are not additive, that is, the size depends on the counterion.

SIT is very similar to the Pitzer and Bromley formulations with some exceptions. Firstly, some empirical adjustments are made to the parameters of the $f(c)$ term to improve agreement. Secondly, in Bromley's model the B_{ij} parameter has a weak concentration dependence. Thirdly, in the Pitzer formulation there are some additional higher order salt specific parameters. These differences are not so important as they only improve agreement by a few per cent, or extend the concentration range. Hence, for our purposes the three approaches are equivalent and we can compare with the B_{ij} parameters from any approach to reach similar conclusions.

I will compare the model predictions with the parameters determined by Bromley, since this formulation requires only a single parameter per salt, achieves agreement over a wide concentration range and the values have been tabulated for a large number of ions. The conclusions are very similar if we compare with the $\beta^{(0)}$ parameters of Pitzer's model,[216] or the ϵ_0 parameters of SIT.[36] In addition, technically I should compare with B_{ij} coefficients adjusted to reproduce experimental activity coefficients that have

been adjusted to the McMillan–Mayer system as well as adjustment to molarity for the concentration units.[81,199,245] This difficulty arises because experiments are typically performed under constant pressure (Gibbs free energy), within the Lewis–Randall system. Whereas the theoretical values are calculated using the McMillan–Mayer system (constant solvent chemical potential). This more rigorous approach requires a thermodynamics conversion and has been completed. It does not alter the conclusions of the work significantly; I therefore neglect it for simplicity.

Evidence indicates that the cation–cation and anion–anion short–range interactions are not too important at low to moderate concentrations as Coulomb repulsion prevents them from approaching close enough to each other. Hence, I assume that it is a reasonable approximation in calculating the B_{ij} parameter to use only the cation–anion interactions.[122]

7.2.4.1 *Collins's Rules*

I will refer to the B coefficients determined by Bromley as B_{Brom}. As discussed in Chapter 5 these B_{Brom} parameters show an intriguing regularity when plotted as a function of difference in the solvation energy of the ions. This was presented in Figure 5.2 and is reproduced below in Figure 7.5 for ease of comparison with the theoretical values. Although the trend appears inverted, the values are consistent with the classic 'Volcano behaviour.'[52] Hence they reflect Collins's 'Law of Matching Water Affinity.' Ions with similar solvation energies have the lowest B_{Brom} coefficients and hence have the lowest osmotic and activity coefficients and are most strongly attracted to each other. Reproducing these B_{Brom} coefficients should therefore also mean this useful and puzzling correlation has been explained.

7.2.5 *Calculation Details*

The calculation details are very similar to those used in Chapter 6. I used the TURBOMOLE package (v6.4)[1,5] with COSMO[132,131] implemented. The def2–QZVPP[275,271,98,102] basis sets, and associated ECPs[143,212] were used for

all nine alkali and halide ions. I did not use def2-QZVPPD due to implementation constraints of RIMP2, and because there is some evidence diffuse basis sets do not work well with a continuum solvent model.[152]

The calculations were performed both at the Hartree–Fock level using the DSCF program[97] and at the MP2 level using the RIMP2 program.[272,273,9] There is some evidence that the MP2 level of theory may overestimate dispersion interactions somewhat, compared with the more accurate CCSD(T) level.[90] For a more quantitatively exact approach it would be preferable to use this higher level. There are implementation problems with this approach however and the error is likely substantially less than that associated with the continuum approximation.

Exactly as in Chapter 6 I ran the calculations using both R_{cav} and R_{cavA} for the ionic cavity radius. R_{cavA} is the cavity radius adjusted to minimize the error in in bulk solvation energies. These values for all of the ions are given in Table 6.1. In chapter 6 this procedure improved experimental agreement slightly, as expected.

Again COSMO's RSOLV parameter was set to 0.84 Å. This is equivalent to the R_{adj} parameter I have used in the solvation model. An open cavity was constructed for simplicity and consistency with Chapter 6. The outlying charge correction was included although the ROUTF parameter had to be reduced to 0.3, due to numerical error with the default value. The epsilon parameter was set to 116.95 to reproduce the correct 1/78.3 damping of the Coulomb interaction. The ion–specific short–range interaction has a negligible dependence on this parameter.

7.3 RESULTS AND DISCUSSION

7.3.1 *Interactions*

The interaction potentials calculated using the above method are shown in Figure 7.3. The most obvious and concerning observation is that the attrac-

tion between two ions is too large to be physical. The potential wells should be of the order of a few k_BT. Here they can exceed $-20k_BT$.

Nonetheless there are two encouraging features of these potentials. Firstly, and most clearly evident for small ions, there is an oscillatory character to the interaction potentials. This character is consistent with simulation and is occasionally used as justification for the necessity of explicit solvent approaches. This calculation shows that it is possible to predict an oscillatory potential solely on the basis of a continuum approach. This was originally pointed out by Rashin.[228] Indeed, if the Hartree-Fock level of theory is used with the same cavity sizes chosen by Rashin in the COSMO calculation, the calculated potentials are consistent with the ones in Ref. 228. The contributions to these potentials are discussed below, and Figure 7.6 shows that it is the COSMO contribution that drives this oscillation. It arises from the lost ion–water electrostatic interaction as the solvent is removed from the surface of the ion. This results in a repulsion when the ionic cavities first overlap. This repulsion is then overcome by the large electrostatic attraction, which is no longer damped by intervening solvent molecules. However, the oscillatory character is not observed for the larger ions. This is presumably another symptom of whatever is causing the large over–attraction in the potentials. Indeed, by reducing the cavity size arbitrarily I can prevent the over–attraction and a qualitatively correct oscillatory interaction emerges. I should point out that the attractive surface area term, which is analogous to a hydrophobic attraction, should have an oscillatory character as well. It arises from the changing environment from one containing bulk water molecules to a vacuum as the two ions come together. It is clear from simulation of neutral molecule interactions in water, and could be partially included in the model with a more sophisticated definition of the change in surface area.[248] Also only one peak in the oscillation is present as the removal of discrete second and third water layers is not modelled.

The second promising feature of these potentials is that they appear to be consistent with Collins's 'law of matching water affinity', i.e., like–prefers–like. For instance, Figure 7.3a shows the interactions of the lithium ion. We

see that as the anion increases in size the interaction becomes more repulsive. Whereas for cesium's interactions (Figure 7.3b), as the anion increases in size, the potential well widens but the depth remains relatively constant. This will be countered to some extent by the additional repulsion from the larger ion sizes.

This Hofmeister series reversal with activities has been noted previously,[136] and is clear from Figure 7.5a. This Hofmeister cation reversal is is also apparent between iodide and fluoride salts. This is consistent with Collins's law, and Figure 7.6 below provides physical insight into its cause.

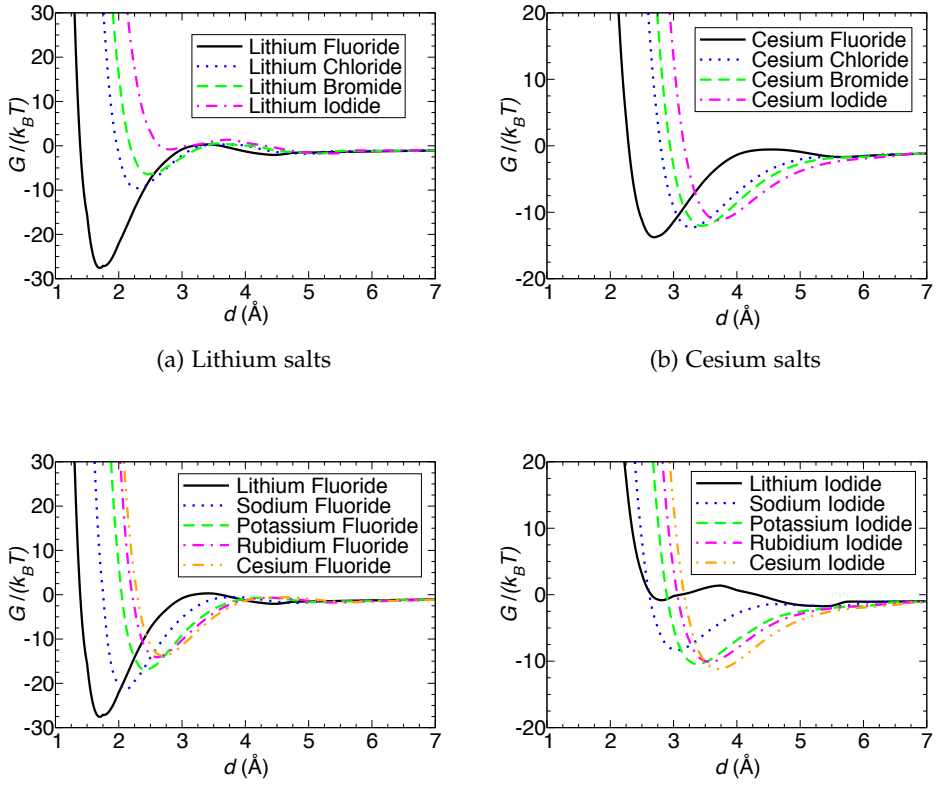

(a) Lithium salts

(b) Cesium salts

(c) Fluoride salts

(d) Iodide salts

Figure 7.3: Ion–ion interaction potentials. Calculated using R_{cavA}.

7.3.2 *Experimental Comparison*

It is useful to have a quantitative comparison of the theoretical ion–ion affinity with experiment. It is clear that I cannot use these potentials to directly

calculate B coefficients. (Eq. 7.15) The exponential term combined with potentials that are much larger than thermal energy means there will be huge variation in these calculated B values, in clear disagreement with experiment. The simplest and most straightforward fix to this problem is to normalize the potentials to reduce them to a size on the order of thermal energy. If I divide all of the potentials by a single factor (λ) and then calculate the B coefficients, I achieve much better results. That is:

$$B_{Theory} = -2\pi k \int_0^\infty dr r^2 \left(\exp^{-\beta G(r)/\lambda} - 1 \right) \tag{7.19}$$

where

$$G(r) = \left(G_{COSMO}(r) + \frac{e^2}{4\pi\epsilon_w r} + \Delta G_{cav}(r) + \Delta G_{disp}(r) \right) \tag{7.20}$$

and where $k = 2/\ln(10)$ is a conversion factor which allows B_{Theory} to be compared directly with B_{Brom}. If Ångstroms are used in the calculation then an additional factor of $N_A \rho_w \times 10^{-30}$ is needed to convert to kg mol^{-1}.

The theoretical values calculated with Eq. 7.19 have a good linear correlation with the experimental Bromley B coefficients, as shown in Figure 7.4. If $\lambda = 6.9$ then $R^2 = 0.95$. This value is insensitive to the choice of lambda, with the correlation staying above $R^2 = 0.9$ for $\lambda = 4.3 \rightarrow 22$. This level of agreement cannot be explained by chance and the physics must be correctly captured to some degree. With $\lambda = 6.9$ the resulting linear correlation has a slope of 1. The resulting B coefficients thus calculated are shown in Figure 7.5b. It is clear that the behaviours seen in Figure 7.5a are reproduced, although with some error. The largest affinity of sodium fluoride and cesium iodide is reproduced. The upturn for the fluoride salts is also reproduced, as is the linear trend for the smaller alkali cations. As shown in Figure 7.4, with the unadjusted cavity radii the correlation is significantly worse ($R^2 = 0.84$).

As the correlation has a slope of 1 only a constant needs to be added to the theoretical values in order to predict the experimental values. This constant is 0.13 if R_{cavA} are used. It is essentially an additional fitted parameter. It is non–ion–specific and accounts for the deviation of Bromley's B coefficient

from the ones defined here. There could be several causes of this deviation. One could be that there is a contribution from the like charge interaction, which I neglect. Alternatively, it could arise from the fairly artificial process of applying the damping parameter λ. It could also be an issue arising from the splitting of the Coulomb and short–range interaction into additive contributions. Calculating the real potentials from those calculated here is likely a more complex task. The key point is that this parameter is not salt specific and so the model should be able to provide improved predictability and explanatory power, over existing models that often depend on salt specific parameters.

Reproducing the ion–specific trends in the activity coefficients has been a long–standing and central goal of physical chemistry for nearly a century. During this time there has been limited success in reproducing these trends without the use of parameters fitted to each salt. Here I reproduce the trend with good accuracy for all nineteen soluble alkali halide salts. Two parameters reproducing 19 values with such a good correlation is strong evidence that the Specific Ion Effects have been correctly modelled. I emphasize that apart from the damping parameter and the offset constant, there has been no deliberate adjustment of parameters to reproduce desired properties of the interaction potentials. They are determined from a straightforward generalization of the solvation model.

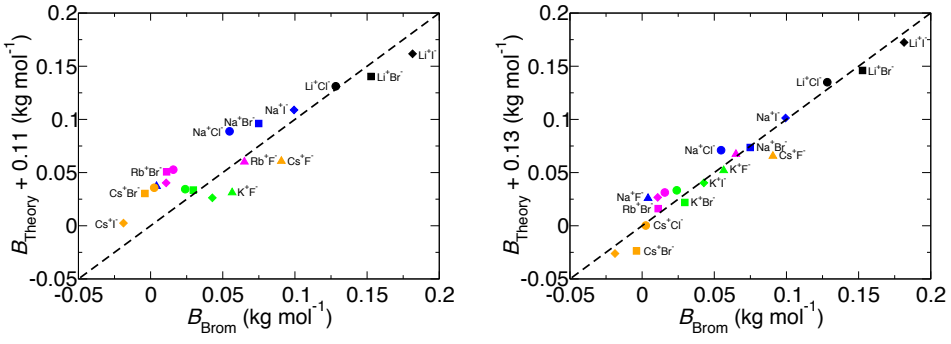

(a) With R_{cav} (b) With R_{cavA}

Figure 7.4: Comparison of the theoretical B coefficients with Bromley's values.

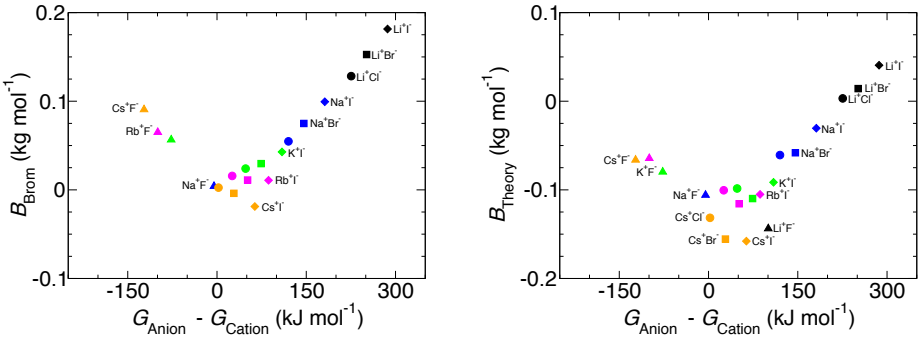

(a) Experimental Bromley B coefficients. (Same as Figure 5.2)

(b) Theoretical B coefficients.

Figure 7.5: Theoretical and experimental B coefficients vs. the difference in the solvation energy of the ions. Colours indicate the cation: Lithium: Black, Sodium: blue, Potassium: green, Rubidium: magenta and Cesium: orange. Anions are marked with a symbol: Fluoride: ▲, Chloride: ●, Bromide: ■, Iodide: ◆. R_{cavA} is used, this is the cavity size adjusted to best reproduce bulk solvation energies.

7.3.3 *Possible Causes of Over–Attraction*

Although the good correlation seen in the theoretical comparison (Figure 7.4) is compelling, I need to answer the question of how the potentials could be so strongly over–attractive. This over–attraction of ion pairs has been observed previously.[223,155] To a lesser degree, it also occurs in continuum solvent models applied to more complex protein systems,[89,85] as well as in non–polarisable explicit solvent simulations of ion–pairing.[75,218] These studies put forward various physical explanations of this effect and introduce empirical corrections to account for it.

One straightforward explanation is that there is some missing repulsive contribution. For instance, as the two ions come together their electric fields will partially cancel. This may result in a reduced attraction with the surrounding water molecules, which then relax away from the ions. This would effectively cause an increase in the R_{cav} parameters. The corresponding energetic cost could substantially cancel the large attractive potentials calculated here.[222] This explanation however conflicts with classical molecular dynamics simulation and quantum mechanical geometry optimizations of hydrated

ion dimer pairs. These calculations show that the water molecules stay at roughly the same distance away from the ions as they come together.

Alternatively, entropic effects associated with the discrete water molecules may be important. It is plausible that the simple continuum solvent approach cannot account for these effects. For instance, an ordered profile of water molecules will form around an ion. This may lead to an entropic repulsion as that profile is disturbed. This is in essence the mechanism identified in Ref. 171. Similarly, it appears that there is a substantially enhanced solvent ordering around ion pairs.[75] Again this would provide an entropic repulsion which may be neglected by the continuum approach. Additional possibilities are a loss of electronic ion–water interactions,[217] bridging water molecule effects,[290] or an underestimate of the dielectric screening at short–range. This underestimate could arise from the fact that the continuum model neglects the enhanced density of water molecules in the hydration layer around ions. These explanations apply only to ion-pairs. This is important because the same approach appears to work well without any damping when applied to ion-surface interactions and to single ion solvation energies.

However, an issue with these explanations is that if there is some missing repulsive contribution of the size of $\approx 10 k_B T$, presumably it would play an important role in determining the ion–specificity. How can the correct Specific Ion Effect be reproduced with such a large missing contribution? One plausible answer lies in the notion of entropy–enthalpy compensation. It is known that ion–ion interactions are the result of the cancelling of an entropic attraction and enthalpic repulsion.[17] It is possible that the entropic component has been overestimated, and hence the potentials are too attractive. This is consistent with the fact seen in Chapter 4, that the underlying solvation model calculates entropies of solvation that are too negative if not corrected to account for dielectric saturation effects. This amplification of the entropy changes may lead to the over attraction, and the damping of these potentials to bring them into line with the expected size can therefore simply be interpreted as a means of artificially imposing entropy–enthalpy cancella-

tion, and hence is all that is required to achieve quantitative agreement with experiment.

7.3.4 *Mechanism of Collins's law*

Having established a plausible candidate for the cause of the over–attraction, I can investigate the contributions to the ion–ion interactions in order to determine a physical explanation of the like–prefers–like behaviour. I assume that the relative balance of contributions will be the same in the true interaction as they are in the overly attractive ones calculated here. If this were not the case, it is difficult to see how the correct Specific Ion Effect could be so well reproduced. These contributions are shown in Figure 7.6, where the interactions of representative large–large, small–small, small–large and large–small pairs are presented. I omit lithium fluoride, as it is insoluble.

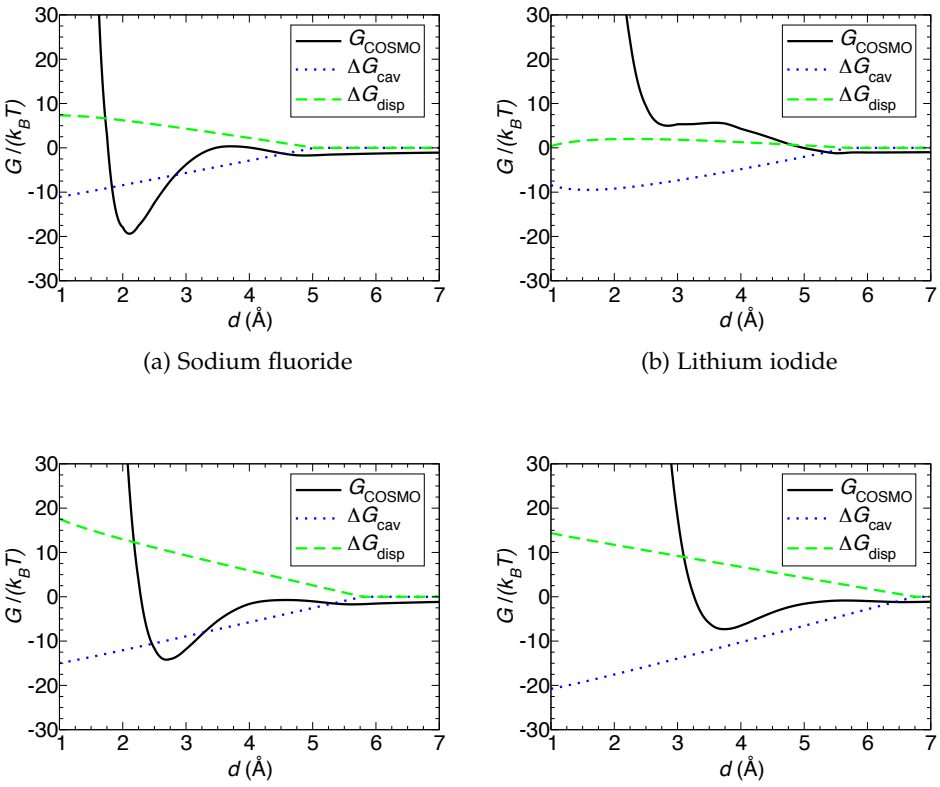

(a) Sodium fluoride

(b) Lithium iodide

(c) Cesium fluoride

(d) Cesium iodide

Figure 7.6: Contributions to the ion–ion interaction potentials, for some representative ion pairs. Calculated using R_{cavA}.

7.3.4.1 *COSMO Contribution*

The G_{COSMO} term includes contributions from the ion–ion dispersion interaction and Pauli repulsion as well as the ionic electrostatic interaction. I can identify several important behaviours of this contribution. For small pairs, there is a substantial cost to removing the tightly bound water resulting in a repulsion at larger separations. A large attraction, likely from direct electrostatics, cancels this effect at short–range, and results in a narrow and deep potential well at contact. As one of the ions gets larger, two effects come into play; the water is less tightly bound to the large ion and hence easier to remove. But this is overwhelmed by a weaker direct ion–ion attraction as well as the 'shadowing mechanism' laid out by Lund et al.,[157] where the large ion removes additional water from the surface of the small ion. This is included implicitly in the COSMO calculation. As a result there is a strong repulsion of large–small ion pairs at small separations. For two large ions the contact minimum is significantly smaller than for two small ions. This is because the direct electrostatic attraction is substantially weaker for two large ions, although the larger dispersion attraction will somewhat obscure this decrease. However, there is also much less, if any, repulsion at larger separations. This corresponds with the fact that the energy cost of removing water molecules from the surface of large ions is low. The result is that the net interaction is similar to small-small ion pairs. An important corollary is that ion–ion interactions cannot be characterized solely by the depth of the potential well at contact.

7.3.4.2 *Non–Electrostatic Ion–Water Contributions*

We can see that the cavity and dispersion contributions approximately cancel each other. This is similar to the behaviour of the total solvation energies. However, they do still play an important role in determining the puzzling ion–specific trends. Firstly, the sum of these two contributions is attractive for sodium fluoride and repulsive for cesium fluoride. This can be attributed in part to the significant increase in cation–water dispersion interaction with

cation size. Figure 7.7a presents the calculation of B coefficients without these contributions. From this figure it is clear that the increase in repulsion with cation size is necessary to reproduce the reversed trend of the fluoride salt series compared with the other anions. This reversed trend can be seen in Figure 7.5a.

For cesium salts as the anion increases in size the repulsive ion–water dispersion contribution decreases and the cavity attraction increases. This increased attraction with increasing anion size is necessary to reproduce the reversal in the cesium salt trend compared with the other cations. Again, as seen in Figure 7.7a. For cesium iodide the cavity attraction outweighs the repulsive dispersion contribution. This is important in explaining the fact that large–large ion pairs have a similar affinity to small–small ion pairs. In essence, this corresponds to the hydrophobic type mechanism of large–large ion attraction outlined by Collins.

7.3.4.3 *Ion–Ion Dispersion*

Next I probe the importance of the direct ion–ion dispersion interaction by performing the calculation at the Hartree–Fock level, where this contribution is neglected unlike at the MP2 level used previously. It is true that other contributions such as the static polarisation interaction may be altered by this change in level of theory. However, the change in the dispersion interaction is likely to dominate, due to the fact that the static electronic effects are damped by the large dielectric response of the water.

This calculation at Hartree–Fock level is presented in Figure 7.7b. By comparison with Figure 7.5 it is immediately clear that the Hartree–Fock level gives far inferior results to the MP2 level of theory used above. In addition, the observed deviation is exactly what one would expect if the ion–ion dispersion contribution were neglected. Although counter–intuitive I have previously shown in Chapter 2 and Chapter 5 that the anionic dispersion interaction is relatively constant with size. On the other hand, the cationic dispersion interaction increases substantially with ion size. We see that it is the larger cations that have their B coefficients substantially overestimated.

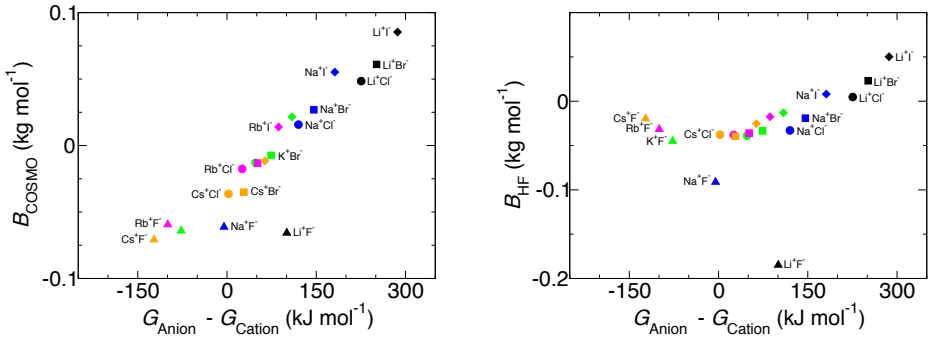

(a) COSMO only (b) Hartree–Fock

Figure 7.7: The theoretical B coefficients vs. the difference in the solvation energy of the ions. (a) Only the COSMO contribution is used, i.e, with $\Delta G_{cav} = \Delta G_{disp} = 0$. (b) The Hartree–Fock level of theory is used instead of MP2 for the COSMO contribution. R_{cavA} is used in both cases.

Indeed the difference between Figure 7.7b and Figure 7.5b, correlates with Figure 5.3, where DFT–SAPT calculations were performed on ions in vacuum to calculate the strength of their dispersion interaction. This provides strong evidence that the affinity of large ions for each other as constituted in Collins's law is critically dependent on their large direct dispersion interaction.

7.3.4.4 *Polarisation Interaction*

As the ions approach each other their electric fields will induce a dipole on their partner and result in a net attractive interaction. It is in principle possible to probe the magnitude of this contribution based on the quantum mechanical calculations. However, this extension is beyond the scope of this thesis.

7.4 CONCLUSION

In summary, I have generalized the model of ionic solvation energies in order to calculate the free energy of a pair of ions as a function of separation. The calculation includes the essential contributions to these interactions. The cavity sizes were adjusted to match solvation energies, but otherwise there was no deliberate adjustment of ion–specific parameters to achieve agree-

ment. Only two global parameters are necessary to calculate the B coefficients. One is used to normalize the potentials which leads to good direct linear correlation with the experimental B coefficients. A second offset constant is also required. Enthalpy–entropy compensation is hypothesized as the justification for this normalization. This means that the most direct example of Collins's 'law of matching water affinity' has been quantitatively reproduced and the driving contributions of this law identified, including the importance of the dispersion interaction.

This work therefore represents, I hope, a significant advance in our understanding of this frustrating and long unsolved problem of physical chemistry. Its resolution serves as a necessary step towards developing a quantitative and predictive understanding of the interaction of solutes in water.

8

CONCLUSIONS

8.1 SUMMARY

Here I provide a summary of the important advances, results and conculsions of the work outlined in this thesis. In Chapter 2 (Ref. 66) I presented a model of the dispersion contribution to the solvation energy of monatomic ions and noble gas atoms. The model uses the same approximations as the Born theory of electrostatic solvation, although damping functions did have to be included to account for the short–range wavefunction overlap. The parameters for the model were determined from *ab initio* calculation and independent experiment. Intriguingly, for the anions the dispersion solvation energy decreased slightly in magnitude as the ions increased in size. For the noble gas atoms, the magnitude of the dispersion solvation energy increased linearly with the atomic radii. Finally, for the cations it increased superlinearly with the exception of copper(I) and silver(I). These ions likely behave unusually due to their inner shell electrons resulting in large polarisabilities. The dispersion energy made up a non–negligible proportion of the solvation energy for all but the smallest alkali cations.

In Chapter 3 (Ref. 67) I combined this energy with the Born electrostatic solvation energy and a simple calculation of the cavity formation energy. The resulting values agreed well with experimental solvation energies for 11 ions and 4 noble gas atoms without any explicitly fitted parameters. In particular, the difference in solvation energy of ions of similar sizes was reproduced and shown to be attributable to the large difference in their polarisabilities leading to a large difference in dispersion solvation energies.

In Chapter 4 (Ref. 68) I showed that the temperature and pressure derivatives of these free energies did a reasonable job of reproducing the solva-

tion entropies and partial molar volumes of the larger ions. For the smaller ions the calculated values were significantly too negative. I showed that a simple method of correcting for dielectric saturation that did not involve fitted parameters brought the values of both of these properties into reasonable experimental agreement for the smaller ions. For the noble gas atoms simulation was required to estimate the entropic contribution to the cavity formation energy, but the resulting experimental agreement did show an improvement on previous estimates.

In Chapter 5 (Ref. 69) I used Density Functional Theory with Symmetry Adapted Perturbation Theory in order to obtain direct *ab initio* estimates of the dispersion interaction energies of ion–ion and ion–water dimers. When the ion–water dimer energies were multiplied by the coordination number of the ions the resulting values were consistent with the continuum calculation of the dispersion solvation energies. The ion–ion dispersion interactions illustrated that dispersion interactions play an important role in the well known observation that large ions are strongly attracted to each other in water.

In Chapter 6 (Ref. 70) I used COSMO and surface area arguments to generalise the solvation model of Chapter 3 to calculate the solvation energy of an ion as it approaches the air–water interface. No explicitly fitted parameters were used. The resulting free energies reproduced the experimentally observed enhancement of iodide at the air–water interface. These free energies reproduced experimental surface tension increments when they were inserted into the Poisson-Boltzmann equation. The surface area changes were shown to be a key component in stabilizing the large ions at the interface and the induced dipole moment was shown to be negligible at the position of the contact minimum.

Finally in Chapter 7 (Ref. 71) the solvation model was again generalised using *ab initio* COSMO calculations and surface area arguments to calculate the free energy of an ion–ion dimer as a function of separation. The resulting energies were significantly too negative. However, by introducing

a parameter to normalize them to a reasonable size, the 'law of matching water affinity' could be quantitatively reproduced.

8.2 IMPLICATIONS

8.2.1 *Continuum Solvent Modelling*

There are many important implications of this work. The first and most important point is that this thesis provides significant evidence that it is possible to build predictive and quantitatively accurate models of electrolyte solutions that treat water as a continuous medium. This is a counter–intuitive and controversial observation. Currently the large majority of research in this area is focussed on building explicit solvent simulations and extracting information from them in order to provide an understanding of electrolyte solutions. The results of this thesis suggest that perhaps some of this effort could be redirected to simpler continuum solvent models.

This conclusion in turn has important and hopeful implications. This is because of the computational advantage of these models. For the simple properties considered in this paper explicit solvent treatments are feasible. But if we attempt to scale up models of these simple systems and apply them to systems of direct practical importance, the computational demands rapidly increase. As a result the continuum solvent treatment becomes hugely advantageous, even essential, for many applications. For example, modelling protein–protein interactions,[176] drug–protein interactions[86] and nanoparticle interactions[159] is far easier with a continuum solvent approach.

It is for this very reason that continuum solvent models are widely applied with significant success to problems at this larger scale. We can use a successful model of ionic solvation energies as a foundation to improve these types of models and develop tools that are practical and useful in application to larger scale problems.

One caveat is that the success of these models in reproducing solvation energies and related properties obviously does not mean that all properties

are reproducible with this approach. Dynamics of water molecules in the ionic hydration shells will obviously need at least several explicitly treated water molecules. In addition, there may be effects of explicit water structure that are important and need to be incorporated with parameters adjusted to reproduce experimental quantities. For example, this could be the reason for the damping parameter used in the ion–ion interaction model. Further investigation into it is therefore required in order to determine precisely why it is necessary. This does not render these models useless however, as they can still provide significant physical insight as well as quantitatively accurate predictions as long as the parameters meet the criteria outlined in the introduction.

8.2.2 *Dispersion and Cavity Interactions*

A second important implication of this work is that the dispersion and cavity interactions play a crucial role in Specific Ion Effects, and these effects cannot be understood on the basis of simple electrostatic interactions. The dispersion and cavity terms provide both a quantitative correction, necessary to reach experimental agreement, as well as a qualitatively important contribution. For instance, these interactions can explains several puzzles regarding the experimental properties of these solutions. In particular, we can see that the so called Charge Hydration Asymmetry effect may not be a property of the electrostatic asymmetry of a water molecule but rather the result of the dispersion interaction of ions with the surrounding water. In addition, the affinity of large ions for each other in water is partially a result of their large dispersion interaction and an attractive cavity contribution. This necessarily implies that a more sophisticated treatment of these interactions is necessary in many models of Specific Ion Effects. For instance, adjusting C_6 coefficients to reproduce bulk properties, as is commonly done in classical molecular dynamics simulation, is in my opinion, inadequate. These interactions are too important to be swept into in a single catch all fitted parameter that needs to correct for all of the limitations of the model. Instead they need

to be calculated *ab initio*, including higher order multipole contributions (C_8 and C_{10} terms) and many body corrections. Similarly, we need to improve our understanding of the cavity contribution for ionic solutes on the basis of *ab initio* calculation.

8.2.3 *Combining Contributions*

A third and final implication of this work is that it is clear that electrolyte properties such as surface tensions and osmotic coefficients result from a delicate balance of many opposing contributions. To achieve agreement with experiment we therefore need to include *all* of them. Several of the important advances presented in this thesis have actually been separately presented before. For instance, Rashin[228] showed the importance of including the cavity shape in the dielectric that the ion occupies. Levin et al.[148] showed that cavity formation energies are important in stabilizing large anions at the interface. Ninham and co–workers showed the importance of dispersion interactions in determining solvation energies[29] and the profiles of ions at interfaces.[190] Lund et al.[157] showed the importance of the change in solvation energy in explaining ion–ion affinity. However, none of these approaches provided satisfactory comparison with experiment on their own. In this thesis we have incorporated all of these important contributions, improved the treatment of them where necessary, and showed that when combined they could together lead to a satisfactory and comprehensive explanation and understanding of the Specific Ion effects of these crucially important electrolyte properties.

8.3 FUTURE WORK

Future work building on this thesis can be categorised into two general directions. One is connecting the model to more fundamental physical models, i.e., models that incorporate explicit solvent. In particular, it would be desir-

able to use *ab initio* molecular dynamics approaches, which are beginning to be applied to these problems, in order to test the key conclusions of the model. For instance, Quasi-Chemical Theory[22] provides a rigorous statistical mechanical method for partitioning the contributions to solvation energies. These methods when combined with *ab initio* approaches such as dispersion corrected DFT have the potential, I believe, to provide a rigorous and complete understanding of the solvation of simple ions. This understanding would be hugely useful in testing and improving the model. Currently as discussed in Chapter 3 there is no agreement on the correct experimental values to compare with. This is a huge problem that severely limits progress in understanding these properties. Additionally, there are more specific improvements to be made to the model. The first one is to understand what has caused the overattraction of the ion–ion potentials seen in Chapter 7 and how to correct for it more rigorously. The second improvement is to determine whether the position of the minimum in the ionic interaction with the the air–water interface is correct and why it disagrees with simulation. Thirdly, it is important to combine these calculations with more sophisticated treatments of ion–ion correlation (such as HNC) so they can be applied to understand electrolyte solutions at higher concentration.

The second direction of future work is in the opposite direction: to generalize the model in order to apply it to systems of more direct practical importance. So far the model has only been applied to monatomic and monovalent solutes dissolved in water. However, there is no reason in principle that the model cannot be generalised and applied to more complex solvents and solutes. Although it is likely that additional complications will arise and it is not guaranteed that it will be successful. For example, the model can potentially be applied to non–aqueous solvents, polar molecules, multivalent ions and anisotropic ions. In fact promising initial results have been observed in applying the model to the hydronium and hydroxide ions. It should also be applied to mixed electrolytes and to calculate the temperature dependence of key properties. These generalisations will serve both as a crucial test of the model and help develop it into a useful tool for industrial applications,

where mixed electrolytes and temperature dependence effects are very important. For instance, we know that water behaves dramatically differently at temperatures close to its boiling point.

These are important tasks that will make the model useful for many chemical engineering applications in industry and for understanding biological systems. In addition to this, although it needs to be tested, I postulate that the approach used to calculate the ionic energy at the air–water interface can be used to calculate the interaction of ions with oil and mineral interfaces. Similarly, the model of ion–ion interactions can be used to calculate the interaction of ions with the charged headgroups on interfaces. These generalisations will allow us to predict the distribution of ions between larger particles in water, which in turn will allow us to build an improved understanding of a wide range of crucial experimental systems. For example, understanding the Hofmeister series reversal on hydrophobic and hydrophilic surfaces is an important problem,[241] as is the prediction of surface forces between minerals, the stability of colloidal systems and the self assembly of nanoparticles in solution, which are all strongly affected by the distribution of ions between them. Similarly, these distributions are at the heart of understanding the effect of ions on the interaction between proteins in water and hence their stability.[177,156] This is the classic Hofmeister effect and is an exciting and natural direction in which to apply this promising model of the properties of electrolyte solutions.

Part II

APPENDIX

A

DERIVATION OF THE DISPERSION SOLVATION ENERGY EXPRESSIONS

A.1 SCATTERING GREEN'S FUNCTION FOR A SPHERICAL CAVITY

The Green's function for a spherical cavity in a dielectric medium required for Chapter 2, i.e., Eq. 2.1, Eq. 2.2 and Eq. 2.3, is given by:[149]

$$\begin{aligned} G_{ij}^{(1)}(\mathbf{r},\mathbf{r}',i\xi) = &-\frac{\xi}{4\pi c}\sum_{n=1}^{\infty}\sum_{m=0}^{n}(2-\delta_{m0})\frac{2n+1}{n(n+1)}\frac{(n-m)!}{(n+m)!} \\ &\left[C_n^M \sum_{p=-1,1}(M_{nm,p})_i(\mathbf{r})\,(M_{nm,p})_j(\mathbf{r}') + \right. \\ &\left. C_n^N \sum_{p=-1,1}(N_{nm,p})_i(\mathbf{r})\,(N_{nm,p})_j(\mathbf{r}')\right] \end{aligned} \tag{A.1}$$

where

$$\begin{aligned} \mathbf{M}_{nm,\pm1}(\mathbf{r}) = &\mp\frac{m}{\sin(\theta)} j_n(k_0 r)\, P_n^m(\cos\theta) \times \begin{matrix}\sin\\\cos\end{matrix}(m\phi)\boldsymbol{e}_\theta \\ &- j_n(k_0 r)\frac{dP_n^m(\cos\theta)}{d\theta} \times \begin{matrix}\cos\\\sin\end{matrix}(m\phi)\boldsymbol{e}_\phi \end{aligned} \tag{A.2}$$

$$\begin{aligned} \mathbf{N}_{nm,\pm1}(\mathbf{r}) = &n(n+1)\frac{j_n(k_0 r)}{k_0 r} P_n^m(\cos\theta) \times \begin{matrix}\cos\\\sin\end{matrix}(m\phi)\boldsymbol{e}_r \\ &+ \frac{1}{k_0 r}\frac{d\,[r j_n(k_0 r)]}{dr}\left[\frac{dP_n^m(\cos\theta)}{d\theta} \times \begin{matrix}\cos\\\sin\end{matrix}(m\phi)\boldsymbol{e}_\theta \right. \\ &\left. \mp\frac{m}{\sin(\theta)} P_n^m(\cos\theta)\begin{matrix}\sin\\\cos\end{matrix}(m\phi)\boldsymbol{e}_\phi\right] \end{aligned} \tag{A.3}$$

where $k_0 = \omega/c = i\xi/c$. The coefficients are given by:

$$C_n^M = \frac{[z_0 h_n^{(1)}(z_0)]' h_n^{(1)}(z_1) - [z_1 h_n^{(1)}(z_1)]' h_n^{(1)}(z_0)}{j_n(z_0)\,[z_1 h_n^{(1)}(z_1)]' - [z_0 j_n(z_0)]' h_n^{(1)}(z_1)} \tag{A.4}$$

and

$$C_n^N = \frac{[z_1 h_n^{(1)}(z_1)]' h_n^{(1)}(z_0) - \epsilon(\omega)[z_0 h_n^{(1)}(z_0)]' h_n^{(1)}(z_1)}{\epsilon(\omega)[z_0 j_n(z_0)]' h_n^{(1)}(z_1) - j_n(z_0)[z_1 h_n^{(1)}(z_1)]'} \tag{A.5}$$

where $z_1 = k_0\sqrt{\epsilon(\omega)}R$ and $z_0 = Rk_0$. To determine these expression I used the fact that $\mu_1 = \mu_2$, $k_2 = k_0$ and $k1 = k_0\sqrt{\epsilon(\omega)}$. $\epsilon(\omega)$ is the dielectric response of water.

The following definition is useful:

$$A_n(R, i\xi) \equiv \frac{\epsilon(i\xi) - 1}{\left(1 + \frac{n+1}{n}\epsilon(i\xi)\right)} \frac{1}{R^{2n+1}} \tag{A.6}$$

It allows us to derive a simplified expression for the Green's function by taking the nonretarded case, i.e., taking the limit: $\frac{\xi}{c} \to 0$. The following expressions result from taking this limit.

$$\frac{\xi^3}{c^3} C_n^N \frac{j_n(k_0 r)}{k_0 r} \frac{j_n(k_0 r')}{k_0 r'} \to \frac{1}{(2n+1)} A_n(R, i\xi)\, r^{(n-1)} r'^{(n-1)} \tag{A.7}$$

$$\frac{\xi^3}{c^3} C_n^N \frac{j_n(k_0 r)}{k_0 r} \frac{d[r' j_n(k_0 r')]}{dr'} \frac{1}{k_0 r'} \to \frac{(n+1)}{(2n+1)} A_n(R, i\xi)\, r^{(n-1)} r'^{(n-1)} \tag{A.8}$$

$$\frac{\xi^3}{c^3} C_n^N \frac{d[r j_n(k_0 r)]}{dr} \frac{1}{k_0 r} \frac{d[r' j_n(k_0 r')]}{dr'} \frac{1}{k_0 r'} \to \frac{(n+1)^2}{(2n+1)} A_n(R, i\xi)\, r^{(n-1)} r'^{(n-1)} \tag{A.9}$$

All the C_n^M terms are 0 so the Green's function reduces to.

$$\begin{aligned} \frac{\xi^2}{c^2} G_{rr}^{(1)}(\mathbf{r}, \mathbf{r}', i\xi) = &-\frac{1}{4\pi} \sum_{n=1}^{\infty} \sum_{m=0}^{n} (2 - \delta_{m0}) \\ &\times \sum_{p=-1,1} n(n+1) \frac{(n-m)!}{(n+m)!} P_n^m(\cos\theta) \times \begin{matrix}\cos \\ \sin\end{matrix}(m\phi) \\ &\times P_n^m(\cos\theta') \times \begin{matrix}\cos \\ \sin\end{matrix}(m\phi') A_n(R, i\xi)\, r^{(n-1)} r'^{(n-1)} \end{aligned} \tag{A.10}$$

$$\frac{\xi^2}{c^2}G^{(1)}_{\theta\theta}(\mathbf{r},\mathbf{r}',i\xi) = -\frac{1}{4\pi}\sum_{n=1}^{\infty}\sum_{m=0}^{n}(2-\delta_{m0}) \times \sum_{p=-1,1}\frac{n+1}{n}\frac{(n-m)!}{(n+m)!}\frac{dP_n^m(\cos\theta)}{d\theta}\times{}^{\cos}_{\sin}(m\phi) \times \frac{dP_n^m(\cos\theta')}{d\theta'}\times{}^{\cos}_{\sin}(m\phi')A_n(R,i\xi)\,r^{(n-1)}r'^{(n-1)} \tag{A.11}$$

$$\frac{\xi^2}{c^2}G^{(1)}_{\phi\phi}(\mathbf{r},\mathbf{r}',i\xi) = -\frac{1}{4\pi}\sum_{n=1}^{\infty}\sum_{m=0}^{n}(2-\delta_{m0}) \times \sum_{p=-1,1}\frac{n+1}{n}\frac{(n-m)!}{(n+m)!}\frac{m}{\sin(\theta)}P_n^m(\cos\theta)^{\sin}_{\cos}(m\phi) \times \frac{m}{\sin(\theta')}P_n^m(\cos\theta')^{\sin}_{\cos}(m\phi')A_n(R,i\xi)\,r^{(n-1)}r'^{(n-1)} \tag{A.12}$$

$$\frac{\xi^2}{c^2}G^{(1)}_{r\phi}(\mathbf{r},\mathbf{r}',i\xi) = -\frac{1}{4\pi}\sum_{n=1}^{\infty}\sum_{m=0}^{n}(2-\delta_{m0}) \times \sum_{p=-1,1}(n+1)\frac{(n-m)!}{(n+m)!}P_n^m(\cos\theta)\times{}^{\cos}_{\sin}(m\phi) \times \frac{\mp m}{\sin(\theta')}P_n^m(\cos\theta')^{\sin}_{\cos}(m\phi')A_n(R,i\xi)\,r^{(n-1)}r'^{(n-1)} \tag{A.13}$$

$$\frac{\xi^2}{c^2}G^{(1)}_{r\theta}(\mathbf{r},\mathbf{r}',i\xi) = -\frac{1}{4\pi}\sum_{n=1}^{\infty}\sum_{m=0}^{n}(2-\delta_{m0}) \times \sum_{p=-1,1}(n+1)\frac{(n-m)!}{(n+m)!}P_n^m(\cos\theta)\times{}^{\cos}_{\sin}(m\phi) \times \frac{dP_n^m(\cos\theta')}{d\theta'}\times{}^{\cos}_{\sin}(m\phi')A_n(R,i\xi)\,r^{(n-1)}r'^{(n-1)} \tag{A.14}$$

$$\frac{\xi^2}{c^2}G^{(1)}_{\phi\theta}(\mathbf{r},\mathbf{r}',i\xi) = -\frac{1}{4\pi}\sum_{n=1}^{\infty}\sum_{m=0}^{n}(2-\delta_{m0}) \times \sum_{p=-1,1}\frac{n+1}{n}\frac{(n-m)!}{(n+m)!}\frac{\mp m}{\sin(\theta)}P_n^m(\cos\theta)^{\sin}_{\cos}(m\phi) \times \frac{dP_n^m(\cos\theta')}{d\theta'}\times{}^{\cos}_{\sin}(m\phi')A_n(R,i\xi)\,r^{(n-1)}r'^{(n-1)} \tag{A.15}$$

where the primes swap if the order of the indices switch. $p = 1$ means the top option is chosen and $p = -1$ the bottom.

For these purposes we can take both the coordinates at the origin. ($\theta = \phi = r = \theta' = \phi' = r' = 0$) It is essential to be mindful of the range of θ ($0 < \theta < \pi$) in this calculation. Only the diagonal terms contribute and because of the r^{n-1} term, only the $n = 1$ term survives. The result is:

$$\frac{\xi^2}{c^2} G^{(1)}_{rr}(0,0,i\xi) = \frac{\xi^2}{c^2} G^{(1)}_{\theta\theta}(0,0,i\xi) = \frac{\xi^2}{c^2} G^{(1)}_{\phi\phi}(0,0,i\xi) = -\frac{A_1(R,i\xi)}{2\pi} \quad \text{(A.16)}$$

In order to calculate quadrupole interactions the derivative of these functions are required. We calculate their derivative and then take the limit $\theta = \phi = r = \theta' = \phi' = r' = 0$.

A.2 POLARISABILITY

Next we need to establish the correct expression for the polarizability. From Kaplan's Intermolecular Interactions[124] we have the generalised polarisability of an isotropic atom. It is a scalar quantity, given by.

$$\alpha_l(i\omega) = \frac{2e^2}{\hbar} \sum_{n=1} \frac{\omega_{n0} \left|\langle n \left| Q^0_l \right| 0 \rangle\right|^2}{\omega^2_{n0} + \omega^2} \quad \text{(A.17)}$$

where

$$Q^m_l = \sum_{i=1}^{N} \left(\frac{4\pi}{2l+1}\right)^{\frac{1}{2}} r^l_i Y^m_l(\Omega_i) \quad \text{(A.18)}$$

The factor of $e^2/\hbar$ does not appear in the atomic units expression in Kaplan. The transformation can be performed by substituting conversion factors for all of the parameters from au to SI. The polarisabilities calculated using ADF in Chapter 2 and determined from Ref. 99, Ref. 100 and Ref. 178 are consistent with this definition. We can reduce the dipole term to:

$$\alpha_1(i\omega) = \frac{2e^2}{\hbar} \sum_{n=1} \frac{\omega_{n0} \left|\langle n \left| z \right| 0 \rangle\right|^2}{\omega^2_{n0} + \omega^2} \quad \text{(A.19)}$$

where we have used $Q_1^0 = z$. We want to compare this expression to ensure that it is consistent with the one used by Scheel and Buhmann in Ref. 239:

$$\boldsymbol{\alpha}^{(2)}(i\omega) = \frac{2}{\hbar}\sum_{n=1}\frac{\omega_{n0}\mathbf{d}_{0n}\otimes\mathbf{d}_{n0}}{\omega_{n0}^2+\omega^2} \tag{A.20}$$

where $\mathbf{d}_{0n} = \left|\left\langle n\left|e\vec{r}\right|0\right\rangle\right|$. This is the rank 2 tensor, as indicated by the superscript 2, which also indicates it is the dipole polarisability. It can be reduced to the isotropic case through multiplication by the rank 2 averaging tensor, which is: (Eq. (81) of Ref. 58)

$$I_{ij}^{\alpha\beta} = \frac{1}{3}\delta_{ij}\delta_{\alpha\beta} \tag{A.21}$$

Applying this to Eq. A.20 gives:

$$I_{ij}^{\alpha\beta}\alpha_{\alpha\beta}^{(2)}(i\omega) = \frac{2e^2}{3\hbar}\sum_{n=1}\frac{\omega_{n0}\left|\mathbf{d}_{0n}\right|^2}{\omega_{n0}^2+\omega^2} = \alpha_1(i\omega)\,\mathbf{I} \tag{A.22}$$

where we have used the fact that:

$$\left|\mathbf{d}_{0n}\right|^2 = \left|\langle n|z|0\rangle\right|^2 + \left|\langle n|y|0\rangle\right|^2 + \left|\langle n|x|0\rangle\right|^2 = 3\left|\langle n|z|0\rangle\right|^2 \tag{A.23}$$

This shows the two definitions are the same.

The next step is the quadrupole interactions. Using the Kaplan definition we have

$$\alpha_2(i\omega) = \frac{2e^2}{\hbar}\sum_{n=1}\frac{\omega_{n0}\left|\left\langle n\left|z^2-\frac{x^2}{2}-\frac{y^2}{2}\right|0\right\rangle\right|^2}{\omega_{n0}^2+\omega^2} \tag{A.24}$$

From Ref. 57 (Eq. (16)) we have:

$$\boldsymbol{\alpha}^{(4)}(i\omega) = \frac{e^2}{2\hbar}\sum_{n=1}\frac{\omega_{n0}\left\langle n\left|\vec{r}\otimes\vec{r}\right|0\right\rangle\otimes\left\langle 0\left|\vec{r}\otimes\vec{r}\right|n\right\rangle}{\omega_{n0}^2+\omega^2} \tag{A.25}$$

so

$$\alpha_{\alpha\beta\mu\nu}^{(4)}(i\omega) = \frac{e^2}{2\hbar}\sum_{n=1}\frac{\omega_{n0}\left\langle n\left|x_\alpha x_\beta\right|0\right\rangle\left\langle 0\left|x_\mu x_\nu\right|n\right\rangle}{\omega_{n0}^2+\omega^2} \tag{A.26}$$

For isotropic molecules the resulting tensor must be of the form[232]

$$\alpha\delta_{ij}\delta_{kl} + \beta\delta_{ik}\delta_{jl} + \beta\delta_{il}\delta_{jk} \tag{A.27}$$

where the second two terms must be equal due to the properties of the polarisability. We can take out a factor and write it as.

$$\begin{aligned}\alpha^{(4)}_{\alpha\beta\mu\nu}(i\omega) =& \frac{e^2}{2\hbar}\sum_{n=1}\frac{\omega_{n0}\left|\langle n|x^2|0\rangle\right|^2}{\omega_{n0}^2+\omega^2} \\ &\times\left(\gamma\delta_{\alpha\beta}\delta_{\mu\nu}+\frac{(1-\gamma)}{2}\left(\delta_{\alpha\mu}\delta_{\beta\nu}+\delta_{\alpha\nu}\delta_{\beta\mu}\right)\right)\end{aligned} \tag{A.28}$$

where

$$\gamma = \frac{C_Q}{C_Q+2} \tag{A.29}$$

and

$$C_Q = \sum_{n=1}\frac{\omega_{n0}\langle n|xx|0\rangle\langle 0|yy|n\rangle}{\omega_{n0}^2+\omega^2}\Bigg/\sum_{n=1}\frac{\omega_{n0}\langle n|xy|0\rangle\langle 0|xy|n\rangle}{\omega_{n0}^2+\omega^2} \tag{A.30}$$

We can then write

$$\alpha_2(i\omega) = \frac{e^2}{\hbar}\sum_{n=1}\frac{\omega_{n0}\left|\langle n|x^2|0\rangle\right|^2}{\omega_{n0}^2+\omega^2}(3-3\gamma) \tag{A.31}$$

so

$$\alpha^{(4)}_{\alpha\beta\mu\nu}(i\omega) = \frac{\alpha_2(i\omega)}{(6-6\gamma)}\left(\gamma\delta_{\alpha\beta}\delta_{\mu\nu}+\frac{(1-\gamma)}{2}\left(\delta_{\alpha\mu}\delta_{\beta\nu}+\delta_{\alpha\nu}\delta_{\beta\mu}\right)\right) \tag{A.32}$$

We can perform the same procedure with the octupole polarisability to determine the form of an isotropic atom. We get

$$\begin{aligned}\alpha^{(6)}_{ijklmn} =& \frac{e^2}{18\hbar}\sum_{n=1}\frac{\omega_{n0}\left|\langle n|x^3|0\rangle\right|^2}{\omega_{n0}^2+\omega^2}\Bigg(\mu\left(\delta_{il}\delta_{jm}\delta_{kn}+\delta_{il}\delta_{jn}\delta_{km}\right.\\ &\left.+\delta_{im}\delta_{jl}\delta_{kn}+\delta_{im}\delta_{jn}\delta_{kl}+\delta_{in}\delta_{jl}\delta_{km}+\delta_{in}\delta_{jm}\delta_{kl}\right)\\ &+\frac{1-6\mu}{9}\left(\delta_{ij}\delta_{kl}\delta_{mn}+\delta_{ij}\delta_{kn}\delta_{ml}+\delta_{ij}\delta_{km}\delta_{ln}+\delta_{ik}\delta_{jl}\delta_{mn}\right.\\ &\left.+\delta_{ik}\delta_{jm}\delta_{ln}+\delta_{ik}\delta_{jn}\delta_{ml}+\delta_{il}\delta_{jk}\delta_{mn}+\delta_{im}\delta_{jk}\delta_{ln}+\delta_{in}\delta_{jk}\delta_{ml}\right)\Bigg)\end{aligned} \tag{A.33}$$

where

$$\mu = \frac{C_O}{6C_O+9} \tag{A.34}$$

where

$$C_O = \frac{e^2}{18\hbar}\sum_{n=1}\frac{\omega_{n0}\langle n|xyz|0\rangle\langle 0|xyz|n\rangle}{\omega_{n0}^2+\omega^2}\Bigg/\frac{e^2}{18\hbar}\sum_{n=1}\frac{\omega_{n0}\langle n|xxy|0\rangle\langle 0|yzz|n\rangle}{\omega_{n0}^2+\omega^2} \tag{A.35}$$

Using this expression we can write Eq.A.17 for the octupole case as:

$$\begin{aligned}\alpha_3(\omega) &= \frac{2e^2}{\hbar}\sum_{n=1}\frac{\omega_{n0}\left|\left\langle n\left|z^3-\frac{3zx^2}{2}-\frac{3zy^2}{2}\right|0\right\rangle\right|^2}{\omega_{n0}^2+\omega^2}\\ &= \frac{30\mu e^2}{\hbar}\sum_{n=1}\frac{\omega_{n0}\left|\langle n|x^3|0\rangle\right|^2}{\omega_{n0}^2+\omega^2}\end{aligned} \tag{A.36}$$

so

$$\begin{aligned}\alpha^{(6)}_{ijklmn} =& \frac{\alpha_3(\omega)}{540\mu}\times\Bigg(\mu\left(\delta_{il}\delta_{jm}\delta_{kn}+\delta_{il}\delta_{jn}\delta_{km}\right.\\ &\left.+\delta_{im}\delta_{jl}\delta_{kn}+\delta_{im}\delta_{jn}\delta_{kl}+\delta_{in}\delta_{jl}\delta_{km}+\delta_{in}\delta_{jm}\delta_{kl}\right)\\ &+\frac{1-6\mu}{9}\left(\delta_{ij}\delta_{kl}\delta_{mn}+\delta_{ij}\delta_{kn}\delta_{ml}+\delta_{ij}\delta_{km}\delta_{ln}+\delta_{ik}\delta_{jl}\delta_{mn}\right.\\ &\left.+\delta_{ik}\delta_{jm}\delta_{ln}+\delta_{ik}\delta_{jn}\delta_{ml}+\delta_{il}\delta_{jk}\delta_{mn}+\delta_{im}\delta_{jk}\delta_{ln}+\delta_{in}\delta_{jk}\delta_{ml}\right)\Bigg)\end{aligned} \tag{A.37}$$

A.3 ENERGIES

Before proceeding we need the definitions of the tensor product and the Frobenius inner product. The formal definitions can be found in appropriate mathematics text book.[232] We provide the appropriate examples here. For the tensor product:

$$\left[\overrightarrow{\nabla} \otimes \mathbf{G}^{(1)}(\mathbf{r},\mathbf{r}',i\xi_n) \otimes \overleftarrow{\nabla}'\right]_{ijkl} = \partial_i \partial'_l G^{(1)}_{jk}(\mathbf{r},\mathbf{r}',i\xi_n) \tag{A.38}$$

and for the Frobenius inner product:

$$\boldsymbol{\alpha}^{(2)}(i\xi_n) \bullet \mathbf{G}^{(1)}(\mathbf{r}_A,\mathbf{r}_A,i\xi_n) = \sum_{i=1}^{i=3}\sum_{j=1}^{j=3} \alpha_{ij} G^{(1)}_{ij}(\mathbf{r},\mathbf{r}',i\xi_n) \tag{A.39}$$

A.3.1 *Dipole*

We now use these expressions in order to calculate the Casimir–Polder interaction energy of an ion in a cavity formed in water. This will give the dispersion interaction contribution to the solvation energy of a spherical ion in water. The calculation is straightforward using Eq. A.16 and Eq. 2.1, resulting in the expression:

$$\begin{aligned} U_D(0) &= -6k_B T \sum_{m=0}^{\infty}{}' \left(1-\frac{1}{2}\delta_{m0}\right) \alpha(i\xi_m) A_1(R,i\xi_m) \\ &= -\frac{6k_B T}{R^3} \sum_{m=0}^{\infty}{}' \left(1-\frac{1}{2}\delta_{m0}\right) \alpha(i\xi_m) \frac{\epsilon(i\xi_m)-1}{2\epsilon(i\xi_m)+1} \end{aligned} \tag{A.40}$$

This is the Eq. 2.5 given in Chapter 2.

By comparing the Green's function for a point dipole outside a dielectric sphere with a point dipole inside a cavity we can see the two cases are identical except that the two functions h^1_n and j_n have been swapped.[41] The properties of these functions are not used throughout the rest of the derivation so we may use exactly the same final expression with these two functions swapped. This allows a derivation for the full retarded interaction

energy of a dielectric medium with a polarisable atom inside a spherical cavity:

$$U(\mathbf{r}) = -\frac{k_B T}{c^3} \sum_{m=0}^{\infty} \left(1 - \frac{1}{2}\delta_{m0}\right) \left(\xi_m^3 \alpha(i\xi_m) \sum_{n=1}^{\infty} (2n+1) \left\{ C_{n,m}^{M} \left[j_n(k_{0,m} r) \right]^2 + n(n+1) C_{n,m}^{N} \left[\frac{j_n(k_{0,m} r)}{k_{0,m} r} \right]^2 + C_{n,m}^{N} \left[\frac{1}{k_{0,m} r} \frac{d\left[r j_n(k_{0,m} r) \right]}{dr} \right]^2 \right\} \right) \tag{A.41}$$

where $\xi_m = 2\pi k_B T m/\hbar$ and $k_{0,m} = i\xi_m/c$. The important case is for a molecule at the origin in which case taking the limit $r \to 0$ the expression becomes

$$U(0) = -2k_B T \sum_{m=0}^{\infty} \left(1 - \frac{1}{2}\delta_{m0}\right) \frac{\xi_m^3}{c^3} \alpha(i\xi_n) C_{1,m}^{N} \tag{A.42}$$

This can be evaluated numerically by using the expression for $C_{1,m}^{N}$. If we take the nonretarded limit this reduces to the correct expression A.40. It also allows us to check the importance of retardation in the case of the Casimir–Polder interaction. As expected by inference from the atom-atom interaction this effect is negligible.

A.3.2 *Quadrupole*

The next step is the inclusion of the quadrupole energy. Eq. 2.2 can be written explicitly as

$$U_Q(\mathbf{r}_A) = \left| \frac{4\pi k_B T}{c^2} \sum_{n=0}^{\infty} \left(1 - \frac{1}{2}\delta_{n0}\right) \xi_n^2 \alpha_{ijkl}^{(4)}(i\xi_n) \partial_i \partial'_l G_{jk}^{(1)}(\mathbf{r}, \mathbf{r}', i\xi_n) \right|_{\mathbf{r},\mathbf{r}' \to \mathbf{r}_A} \tag{A.43}$$

Next we substitute in the expression for the quadrupole polarisability. We get

$$U_Q(\mathbf{r}_A) = \left| \frac{4\pi k_B T}{c^2} \sum_{n=0}^{\infty} \left(1 - \frac{1}{2}\delta_{n0}\right) \xi_n^2 \frac{\alpha_2(i\xi_n)}{(6-6\gamma)} \left(\gamma \partial_i \partial'_j G^{(1)}_{ij}(\mathbf{r},\mathbf{r}',i\xi_n) + \frac{1-\gamma}{2}\left(\partial_i \partial'_j G^{(1)}_{ji}(\mathbf{r},\mathbf{r}',i\xi_n) + \partial_i \partial'_i G^{(1)}_{jj}(\mathbf{r},\mathbf{r}',i\xi_n)\right)\right)\right|_{\mathbf{r},\mathbf{r}'\to\mathbf{r}_A} \tag{A.44}$$

To evaluate this expression for the solvation energy we need to use the derivatives of the Green's function of a spherical cavity and then take the limit at the origin. It can be shown that $\partial_i \partial'_j G^{(1)}_{ij}(\mathbf{r},\mathbf{r}',i\xi_n) = 0$. So the gamma is cancelled out. The two terms inside brackets actually come out identically. Hence we need

$$\begin{aligned} &\lim_{\mathbf{r}',\mathbf{r}\to 0,\frac{\xi}{c}\to 0} \frac{\xi^2}{c^2}\Bigg(\gamma \partial_i \partial'_j G^{(1)}_{ij}(\mathbf{r},\mathbf{r}',i\xi_n) + \\ &\qquad \frac{1-\gamma}{2}\left(\partial_i \partial'_j G^{(1)}_{ji}(\mathbf{r},\mathbf{r}',i\xi_n) + \partial_i \partial'_i G^{(1)}_{jj}(\mathbf{r},\mathbf{r}',i\xi_n)\right)\Bigg) \\ &= -\frac{1}{4\pi}\sum_{n=1}^{\infty}\sum_{m=0}^{n}(2-\delta_{m0})\frac{n+1}{n}\frac{(n-m)!}{(n+m)!}A_n(R,i\xi)\frac{1-\gamma}{2}\times \\ &\quad 2\delta_{n2}(6\delta_{m0}+36\delta_{m1}+144\delta_{m2}) \\ &= -\frac{1}{4\pi}45(1-\gamma)A_2(R,i\xi_n) \end{aligned} \tag{A.45}$$

Hence for the quadrupole solvation energy we have:

$$\begin{aligned} U_Q(0) &= -\frac{45k_BT}{2\times 6}\sum_{n=0}^{\infty}\left(1-\frac{1}{2}\delta_{n0}\right)\alpha_2(i\xi_n)A_2(R,i\xi_n) \\ &= -\frac{15k_BT}{2R^5}\sum_{n=0}^{\infty}\left(1-\frac{1}{2}\delta_{n0}\right)\alpha_2(i\xi_n)\frac{\epsilon(i\xi_n)-1}{\frac{3}{2}\epsilon(i\xi_n)+1} \end{aligned} \tag{A.46}$$

Here we have used the definition of the partial derivatives in spherical coordinates as well as the definition of the transformation matrix to spherical coordinates. These are[277]

$$T = \begin{bmatrix} \sin(\theta)\cos(\phi) & \cos(\theta)\cos(\phi) & -\sin(\phi) \\ \sin(\theta)\sin(\phi) & \cos(\theta)\sin(\phi) & \cos(\phi) \\ \cos(\theta) & -\sin(\theta) & 0 \end{bmatrix} \tag{A.47}$$

where $\mathbf{G}^{(c)} = \mathbf{T}\mathbf{G}^{(s)}\mathbf{T}'^{T}$

$$\frac{\partial}{\partial x} = \cos(\phi)\sin(\theta)\frac{\partial}{\partial r} - \frac{\sin(\phi)}{r\sin(\theta)}\frac{\partial}{\partial \phi} + \frac{\cos(\phi)\cos(\theta)}{r}\frac{\partial}{\partial \theta} \tag{A.48}$$

$$\frac{\partial}{\partial y} = \sin(\phi)\sin(\theta)\frac{\partial}{\partial r} + \frac{\cos(\phi)}{r\sin(\theta)}\frac{\partial}{\partial \phi} + \frac{\sin(\phi)\cos(\theta)}{r}\frac{\partial}{\partial \theta} \tag{A.49}$$

$$\frac{\partial}{\partial z} = \cos(\theta)\frac{\partial}{\partial r} - \frac{\sin(\theta)}{r}\frac{\partial}{\partial \theta} \tag{A.50}$$

A.3.3 *Octupole*

For the octupole we proceed with Eq. 2.2 (Given originally in Ref. 58) which gives the octupole contribution. It expands out to:

$$\begin{aligned} U_O(\mathbf{r}_A) = \Bigg| \frac{4\pi k_B T}{540\mu c^2} \sum_{n=0}^{\infty} \left(1 - \frac{1}{2}\delta_{n0}\right) \xi_n^2 \alpha_3(i\xi_n) \times \\ \Big(6\mu \partial_i \partial_i' \partial_j' \partial_j G_{kk}^{(1)}(\mathbf{r}, \mathbf{r}', i\xi_n) \\ + 9\frac{1-6\mu}{9} \partial_i \partial_i \partial_j' \partial_j' G_{kk}^{(1)}(\mathbf{r}, \mathbf{r}', i\xi_n)\Big)\Big|_{\mathbf{r},\mathbf{r}' \to \mathbf{r}_A} \end{aligned} \tag{A.51}$$

It turns out that the second term in the brackets comes out to zero. So we need

$$\begin{aligned} \lim_{\mathbf{r},\mathbf{r}' \to 0, \frac{\xi}{c} \to 0} \frac{\xi^2}{c^2} \left(6\mu \partial_i \partial_i' \partial_j' \partial_j G_{kk}^{(1)}(\mathbf{r}, \mathbf{r}', i\xi_n) + 9\frac{1-6\mu}{9} \partial_i \partial_i \partial_j' \partial_j' G_{kk}^{(1)}(\mathbf{r}, \mathbf{r}', i\xi_n)\right) \\ = -\frac{1}{4\pi} \sum_{n=1}^{\infty} \sum_{m=0}^{n} (2 - \delta_{m0}) \frac{n+1}{n} \frac{(n-m)!}{(n+m)!} A_n(R, i\xi) \times \\ 6\mu\delta_{n3} \left(90\delta_{m0} + 1080\delta_{m1} + 10800\delta_{m2} + 64800\delta_{m3}\right) \\ = -\frac{6\mu \times 840}{4\pi} A_3(R, i\xi) \end{aligned} \tag{A.52}$$

Hence for the octupole solvation energy we have:

$$\begin{aligned} U_O(0) &= -\frac{6\mu \times 840 k_B T}{540\mu} \sum_{n=0}^{\infty} \left(1 - \frac{1}{2}\delta_{n0}\right) \alpha_3(i\xi_n) A_3(R, i\xi_n) \\ &= -\frac{28 k_B T}{3R^7} \sum_{n=0}^{\infty} \left(1 - \frac{1}{2}\delta_{n0}\right) \alpha_3(i\xi_n) \frac{\epsilon(i\xi_n) - 1}{\frac{4}{3}\epsilon(i\xi_n) + 1} \end{aligned} \tag{A.53}$$

The cancellation of the γ and μ terms is likely due to the trace of the Green's function being zero in free space.

A.4 ANISOTROPIC MOLECULES

For anisotropic molecules we can take the spherical average and calculate an isotropic polarisability tensor:

$$\alpha_l^{iso}(i\omega) = \frac{1}{2l+1} \sum_{m=-l}^{m=+l} \frac{2e^2}{\hbar} \sum_{n=1} \frac{\omega_{n0} \left|\langle n \left| Q_l^m \right| 0 \rangle\right|^2}{\omega_{n0}^2 + \omega^2} \tag{A.54}$$

We can then use this expression in the above equations for the dispersion solvation energy.

This expression can be derived by replacing the spherical harmonics with the version for the spherical harmonic in a rotated reference frame[182]:

$$Y_l^m(\theta, \phi) \rightarrow \sum_{\mu=-l}^{\mu=+l} Y_l^\mu(\theta, \phi) D_{\mu,m}^l(\alpha, \beta, \gamma) \tag{A.55}$$

where $D_{\mu,m}^l(\alpha, \beta, \gamma)$ are the elements of the Wigner-D matrices, and α, β, and γ are the Euler angles of the coordinate transformation. And then averaging over all orientations with:

$$\frac{1}{8\pi} \int_0^{2\pi} \int_0^{\pi} \int_0^{2\pi} \sin(\beta) d\alpha d\beta d\gamma \tag{A.56}$$

B

QUADRUPOLE AND OCTUPOLE CONTRIBUTIONS TO ENTROPY AND PARTIAL MOLAR VOLUMES OF SOLVATION

The contributions to the entropy and partial molar volumes from the quadrupole and octupole moments of the dispersion solvation energy (Eq. 2.15 and Eq. 2.16) are given here:

$$\begin{aligned} S_{Disp1Q} =& f_{10}(bR_S)\frac{15k_BT}{2R_{cav}^5}\sum_{n=0}^{\infty}\left(1-\frac{1}{2}\delta_{n0}\right)\times \\ &\left[\left(\alpha_2(i\xi_n)/T+\frac{2\pi k_B n}{\hbar}\left(\frac{\partial}{\partial\xi_n}(\alpha_2(i\xi_n))\right)\right)f_2(\epsilon(i\xi_n))\right. \\ &+\left(\frac{\partial f_2(\epsilon(i\xi_n))}{\partial\epsilon(i\xi_n)}\frac{2\pi k_B n}{\hbar}\left(\frac{\partial}{\partial\xi_n}\epsilon(i\xi_n)\right)+\right. \\ &\left.\left.\frac{\partial f_2(\epsilon(i\xi_n))}{\partial\epsilon(i\xi_n)}\frac{\partial\epsilon(i\xi_n)}{\partial T}\right)\alpha_2(i\xi_n)\right] \end{aligned} \tag{B.1}$$

and

$$\begin{aligned} S_{Disp1O} =& f_{14}(bR_S)\frac{28k_BT}{3R_{cav}^7}\sum_{n=0}^{\infty}\left(1-\frac{1}{2}\delta_{n0}\right)\times \\ &\left[\left(\alpha_3(i\xi_n)/T+\frac{2\pi k_B n}{\hbar}\left(\frac{\partial}{\partial\xi_n}(\alpha_3(i\xi_n))\right)\right)f_3(\epsilon(i\xi_n))\right. \\ &+\left(\frac{\partial f_3(\epsilon(i\xi_n))}{\partial\epsilon(i\xi_n)}\frac{2\pi k_B n}{\hbar}\left(\frac{\partial}{\partial\xi_n}\epsilon(i\xi_n)\right)\right. \\ &\left.\left.+\frac{\partial f_3(\epsilon(i\xi_n))}{\partial\epsilon(i\xi_n)}\frac{\partial\epsilon(i\xi_n)}{\partial T}\right)\alpha_3(i\xi_n)\right] \end{aligned} \tag{B.2}$$

where

$$f_2(\epsilon(i\xi_n)) = \frac{\epsilon(i\xi_n)-1}{\frac{3}{2}\epsilon(i\xi_n)+1} \tag{B.3}$$

and

$$f_3\left(\epsilon\left(i\xi_n\right)\right) = \frac{\epsilon\left(i\xi_n\right) - 1}{\frac{4}{3}\epsilon\left(i\xi_n\right) + 1} \tag{B.4}$$

The derivatives of these expressions are given by

$$\frac{\partial f_2(\epsilon\left(i\xi_n\right))}{\partial \epsilon\left(i\xi_n\right)} = \frac{5/2}{(\frac{3}{2}\epsilon\left(i\xi_n\right) + 1)^2} \tag{B.5}$$

and

$$\frac{\partial f_3(\epsilon\left(i\xi_n\right))}{\partial \epsilon\left(i\xi_n\right)} = \frac{7/3}{(\frac{4}{3}\epsilon\left(i\xi_n\right) + 1)^2} \tag{B.6}$$

We also have:

$$S_{Disp2Q} = 5\frac{G_Q}{R_{cav}}\frac{\partial R_{cav}}{\partial T} \tag{B.7}$$

$$S_{Disp2O} = 7\frac{G_O}{R_{cav}}\frac{\partial R_{cav}}{\partial T} \tag{B.8}$$

where $S_{Disp2} = S_{Disp2D} + S_{Disp2Q} + S_{Disp2O}$. As well as:

$$S_{Disp3Q} = \left(\sum_{k=0}^{10}\left(k - bR_S\right)\frac{b^k}{k!}R_S^{(k-1)}\exp^{-bR_S}\right)\frac{\partial R_S}{\partial T}G_Q/f_{10}(bR_S) \tag{B.9}$$

$$S_{Disp3O} = \left(\sum_{k=0}^{14}\left(k - bR_S\right)\frac{b^k}{k!}R_S^{(k-1)}\exp^{-bR_S}\right)\frac{\partial R_S}{\partial T}G_O/f_{14}(bR_S) \tag{B.10}$$

where $S_{Disp3} = S_{Disp3D} + S_{Disp3Q} + S_{Disp3O}$.

The expressions for the partial molar volumes are straightforwardly determined in the same manner. For instance, we have:

$$\begin{aligned} V_{Disp1Q} = &-\left(1 - \sum_{k=0}^{10}\frac{\left(bR_S\right)^k}{k!}\exp^{-bR_S}\right) \\ &\times \frac{15k_BT}{2R_{cav}^5}\sum_{m=0}^{\infty}\left(1 - \frac{1}{2}\delta_{m0}\right)\alpha_2\left(i\xi_m\right)\frac{\partial f_2(\epsilon\left(i\xi_n\right))}{\partial \epsilon\left(i\xi_n\right)}\frac{\partial \epsilon\left(i\xi_n\right)}{\partial P} \end{aligned} \tag{B.11}$$

and

$$V_{\mathrm{Disp1O}} = -\left(1 - \sum_{k=0}^{14} \frac{(bR_S)^k}{k!} \exp^{-bR_S}\right) \times \frac{28 k_B T}{3 R_{cav}^7} \sum_{m=0}^{\infty} \left(1 - \frac{1}{2}\delta_{m0}\right) \alpha_3(i\xi_m) \frac{\partial f_3(\epsilon(i\xi_n))}{\partial \epsilon(i\xi_n)} \frac{\partial \epsilon(i\xi_n)}{\partial P} \tag{B.12}$$

In addition to this, V_{Disp2Q}, V_{Disp2O}, V_{Disp3Q}, V_{Disp3O} are identical to the respective entropy contributions except with the temperature derivative replaced by a pressure derivative.

C

TOROIDAL COORDINATES

In order to perform the integrals in Eqs. 7.9–7.11 we used toroidal coordinates as given in Ref. 20:

$$x = \frac{R_0\sqrt{1-\xi^2}\cos(\phi)}{1-\xi\cos(\eta)} \tag{C.1}$$

$$y = \frac{R_0\sqrt{1-\xi^2}\sin(\phi)}{1-\xi\cos(\eta)} \tag{C.2}$$

$$z = \frac{R_0\xi\sin(\eta)}{1-\xi\cos(\eta)} \tag{C.3}$$

Where $0 < \eta < 2\pi, 0 < \phi < 2\pi, 0 < \xi < 1$

Surfaces of constant η give spherical bowls with a centre on the z axis. They are cut off in the xy plane with at a circle of radius R_0. If $\eta_c < \pi$ the sphere is above the xy plane((+)ve z) and taking the surface with $\eta_n = \eta_c + \pi$ gives the rest of the circle below the xy plane. We can easily create the surface of two overlapping spherical cavities in this coordinates system. Given the radii of the two cavities ($R_{cav,i}$ and $R_{cav,j}$) and the separation (d) between their centres, we can give the z coordinates of the centre of the two spheres:

$$c_i = \frac{d^2 - R_{cav,j}^2 + R_{cav,i}^2}{2d} \tag{C.4}$$

$$c_j = \frac{-d^2 + R_{cav,i}^2 - R_{cav,j}^2}{2d} \tag{C.5}$$

The values of constant η which give the surfaces are:

$$\eta_i = \arccos\left(\frac{c_i}{R_{cav,i}}\right) \tag{C.6}$$

$$\eta_j = \arccos\left(\frac{c_j}{R_{cav,j}}\right) + \pi \tag{C.7}$$

Also $R_0 = R_{cav,i}\sin(\eta_i) = R_{cav,j}\sin(\eta_j)$. The positions of the centres can be written in toroidal coordinates as $\xi_{c,i} = \xi_{c,j} = 1, \phi_{c,i} = \phi_{c,j} = 0$, and $\eta_{c,i} = 2\arctan(\frac{R_0}{c_i})$ and $\eta_{c,j} = 2\arctan(\frac{R_0}{c_j}) + 2\pi$ For ion i we can then rewrite the two integrals in each of Eqs. 7.9–7.11 as

$$\frac{\left[\int_0^{\eta_i} + \int_{\eta_j}^{2\pi}\right]\int_0^1\int_0^{2\pi} d\phi d\xi d\eta (J_t) U(\xi,\eta)}{4\pi\int_{R_{cav,i}}^{\infty} dr r^2 U(r)} \tag{C.8}$$

Where $U(r) = 1/r^{2n}$. From the transformation equations above we also have:

$$\begin{aligned} &U(\xi,\eta) = \\ &1/(x(\xi,\eta) + y(\xi,\eta)^2 + (z(\xi,\eta) - z(\xi_{c,i},\eta_{c,i}))^2)^n \end{aligned} \tag{C.9}$$

n is 3 for dipolar, 4 for quadrupole and 6 for octupole. The Jacobian is

$$(J_t) = \frac{R_0^3\xi}{(1-\xi\cos(\eta))^3} \tag{C.10}$$

This integral can be solved analytically, and for the dipole operator we arrive at:

$$\begin{aligned} \frac{\pi}{6R_0^3}(\cos(\eta-\eta_{c,i})-2)\cot\left(\frac{\eta-\eta_{c,i}}{2}\right)\csc\left(\frac{\eta-\eta_{c,i}}{2}\right)^2 \\ \times\sin\left(\frac{\eta_{c,i}}{2}\right)^6\Bigg]_{\eta=\eta_j}^{\eta=\eta_i} \end{aligned} \tag{C.11}$$

with similar although significantly longer expressions for the quadrupole and octupole moments. This is straightforwardly generalized for the second

ion by replacing $z(\xi_{c,i}, \eta_{c,i})$ with $z(\xi_{c,j}, \eta_{c,j})$ in Eq. C.9 and $R_{cav,i}$ with $R_{cav,j}$ in the denominator of Eq. C.8.

BIBLIOGRAPHY

[1] Turbomole V6.4 2012. A Development of University of Karlsruhe and Forschungszentrum Karlsruhe GmbH; available from http://www.turbomole.com.

[2] B. Abel. Hydrated Interfacial Ions and Electrons. *Annu. Rev. Phys. Chem.*, 64:533–552, 2013. doi: 10.1146/annurev-physchem-040412-110038.

[3] M. H. Abraham and J. Liszi. Calculations on Ionic Solvation. *J. Chem. Soc., Faraday Trans. 1*, 74:1604–1614, 1978. doi: 10.1039/F19787401604.

[4] C. Adamo and V. Barone. Toward Reliable Density Functional Methods Without Adjustable Parameters: The PBEo Model. *J. Chem. Phys.*, 110:6158–6170, 1999. doi: 10.1063/1.478522.

[5] R. Ahlrichs, M. Bär, M. Häser, H. Horn, and C. Kölmel. Electronic Structure Calculations on Workstation Computers: The Program System Turbomole. *Chem. Phys. Lett.*, 162:165–169, 1989. doi: 10.1016/0009-2614(89)85118-8.

[6] C. Amovilli. Calculation of the Dispersion Energy Contribution to the Solvation Free Energy. *Chem. Phys. Lett.*, 229:244–249, 1994. doi: 10.1016/0009-2614(94)01044-7.

[7] C. Amovilli and F. M. Floris. A Study of Dispersion Forces with Quantum Monte Carlo: Towards a Continuum Model for Solvation. *J. Phys. Chem. A*, 2014. doi: 10.1021/jp510072n.

[8] C. Amovilli and B. Mennucci. Self-Consistent-Field Calculation of Pauli Repulsion and Dispersion Contributions to the Solvation Free Energy in the Polarizable Continuum Model. *J. Phys. Chem. B*, 101:1051–1057, 1997. doi: 10.1021/jp9621991.

[9] J. G. Ángyán. Choosing Between Alternative MP2 Algorithms in the Self-Consistent Reaction Field Theory of Solvent Effects. *Chem. Phys. Lett.*, 241:51–56, 1995. doi: 10.1016/0009-2614(95)00602-Z.

[10] F. Archambault, C. Chipot, I. Soteras, F. J. Luque, K. Schulten, and F. Dehez. Polarizable Intermolecular Potentials for Water and Benzene Interacting with Halide and Metal Ions. *J. Chem. Theory Comput.*, 5: 3022–3031, 2009. doi: 10.1021/ct9004189.

[11] A. Arslanargin and T. L. Beck. Free Energy Partitioning Analysis of the Driving Forces that Determine Ion Density Profiles near the Water Liquid-Vapor Interface. *J. Chem. Phys.*, 136:104503, 2012. doi: 10.1063/1.3689749.

[12] H. S. Ashbaugh, D. Asthagiri, L. R. Pratt, and S. B. Rempe. Hydration of Krypton and Consideration of Clathrate Models of Hydrophobic Effects from the Perspective of Quasi-Chemical Theory. *Biophys. Chem.*, 105:323–338, 2003. doi: 10.1016/S0301-4622.

[13] C. S. Babu and C. Lim. Incorporating Nonlinear Solvent Response in Continuum Dielectric Models Using a Two-Sphere Description of the Born Radius. *J. Phys. Chem. A*, 105:5030–5036, 2001. doi: 10.1021/jp0044633.

[14] M. D. Baer and C. J. Mundy. Toward an Understanding of the Specific Ion Effect Using Density Functional Theory. *J. Phys. Chem. Lett.*, 2: 1088–1093, 2011. doi: 10.1021/jz200333b.

[15] M. D. Baer, A. C. Stern, Y. Levin, D. J. Tobias, and C. J. Mundy. Electrochemical Surface Potential Due to Classical Point Charge Models Drives Anion Adsorption to the Air-Water Interface. *J. Phys. Chem. Lett.*, 3:1565–1570, 2012. doi: 10.1021/jz300302t.

[16] P. Ball and J. Hallsworth. Water Structure and Chaotropicity: Their Uses, Abuses and Implications for Biology. *Phys. Chem. Chem. Phys.*, 2015. doi: 10.1039/c4cp04564e.

[17] A. J. Ballard and C. Dellago. Toward the Mechanism of Ionic Dissociation in Water. *J. Phys. Chem. B*, 116:13490–13497, 2012. doi: 10.1021/jp309300b.

[18] J. P. Bardhan, P. Jungwirth, and L. Makowski. Affine-Response Model of Molecular Solvation of Ions: Accurate Predictions of Asymmetric Charging Free Energies. *J. Chem. Phys.*, 137:124101, 2012. doi: 10.1063/1.4752735.

[19] M. V. Basilevsky and D. F. Parsons. Nonlocal Continuum Solvation Model with Exponential Susceptibility Kernels. *J. Chem. Phys.*, 108:9107–9113, 1998. doi: 10.1063/1.476357.

[20] J. W. Bates. On Toroidal Green's Functions. *J. Math. Phys.*, 38:3679–3691, 1997. doi: 10.1063/1.532061.

[21] T. L. Beck. A Local Entropic Signature of Specific Ion Hydration. *J. Phys. Chem. B*, 115:9776–9781, 2011. doi: 10.1021/jp204883h.

[22] T. L. Beck. Hydration Free Energies by Energetic Partitioning of the Potential Distribution Theorem. *J. Stat. Phys.*, 145:335–354, 2011. doi: 10.1007/s10955-011-0298-4.

[23] T. L. Beck. The Influence of Water Interfacial Potentials on Ion Hydration in Bulk Water and Near Interfaces. *Chem. Phys. Lett.*, 561-562:1–13, 2013. doi: 10.1016/j.cplett.2013.01.008.

[24] D. Ben-Amotz, F. O. Raineri, and G. Stell. Solvation Thermodynamics: Theory and Applications. *J. Phys. Chem. B*, 109:6866–6878, 2005. doi: 10.1021/jp045090z.

[25] A. Ben-Naim. *Hydrophobic Interactions*. Plenum Press, 1980.

[26] A. Ben-Naim and Y. Marcus. Solvation Thermodynamics of Non Ionic Solutes. *J. Chem. Phys.*, 81:2016–2027, 1984. doi: 10.1063/1.447824.

[27] J. M. Borah, S. Mahiuddin, N. Sarma, D. F. Parsons, and B. W. Ninham. Specific Ion Effects on Adsorption at the Solid/Electrolyte Interface: A

Probe into the Concentration Limit. *Langmuir*, 27:8710–8717, 2011. doi: 10.1021/la2006277.

[28] V. M. Born. Volumen und Hydratationswärme der ionen. *Z. Phys.*, 1: 45–48, 1919. doi: 10.1007/BF01881023.

[29] M. Boström and B. W. Ninham. Contributions from Dispersion and Born Self-Free Energies to the Solvation Energies of Salt Solutions. *J. Phys. Chem. B*, 108:12593–12595, 2004. doi: 10.1021/jp048517a.

[30] M. Boström, D. R. M. Williams, and B. W. Ninham. Surface Tension of Electrolytes: Specific Ion Effects Explained by Dispersion Forces. *Langmuir*, 17:4475–4478, 2001. doi: 10.1021/la0102298.

[31] M. Boström, D. R. M. Williams, and B. W. Ninham. Influence of Hofmeister Effects on Surface pH and Binding of Peptides to Membranes. *Langmuir*, 18:8609–8615, 2002. doi: 10.1021/la020299u.

[32] M. Boström, V. S. J. Craig, R. Albion, D. R. M. Williams, and B. W. Ninham. Hofmeister Effects in pH Measurements: Role of Added Salt and Co-Ions. *J. Phys. Chem. B*, 107:2875–2878, 2003. doi: 10.1021/jp026804d.

[33] M. Boström, W. Kunz, and B. W. Ninham. Hofmeister Effects in Surface Tension of Aqueous Electrolyte Solution. *Langmuir*, 21:2619–2623, 2005. doi: 10.1021/la047437v.

[34] M. Boström, V. Deniz, G. V. Franks, and B. W. Ninham. Extended DLVO Theory: Electrostatic and Non-Electrostatic Forces in Oxide Suspensions. *Adv. Colloid Interface Sci.*, 123-126:5–15, 2006. doi: 10.1016/j.cis.2006.05.001.

[35] M. Boström, D. F. Parsons, A. Salis, B. W. Ninham, and M. Monduzzi. Possible Origin of the Inverse and Direct Hofmeister Series for Lysozyme at Low and High Salt Concentrations. *Langmuir*, 27: 9504–9511, 2011. doi: 10.1021/la202023r.

[36] C. Bretti, C. Foti, N. Porcino, and S. Sammartano. SIT Parameters for 1:1 Electrolytes and Correlation with Pitzer Coefficients. *J. Solution Chem.*, 35:1401–1415, 2006. doi: 10.1007/s10953-006-9068-3.

[37] L. A. Bromley. Thermodynamic Properties of Strong Electrolytes in Aqueous Solutions. *AIChE J.*, 19:313–320, 1973. doi: 10.1002/aic.690190216.

[38] A. D. Buckingham. A Theory of Ion-Solvent Interaction. *Discuss. Faraday Soc.*, 24:151–157, 1957. doi: 10.1039/DF9572400151.

[39] S. Y. Buhmann and S. Scheel. Thermal Casimir versus Casimir-Polder Forces: Equilibrium and Nonequilibrium Forces. *Phys. Rev. Lett.*, 100: 253201, 2008. doi: 10.1103/PhysRevLett.100.253201.

[40] S. Y. Buhmann and D.-G. Welsch. Dispersion Forces in Macroscopic Quantum Electrodynamics. *Prog. Quantum Electron.*, 31:51–130, 2007. doi: 10.1016/j.pquantelec.2007.03.001.

[41] S. Y. Buhmann, H. T. Dung, and D.-G. Welsch. The Van der Waals Energy of Atomic Systems Near Absorbing and Dispersing Bodies. *J. Opt. B: Quantum Semiclassical Opt.*, 6:S127–S135, 2004. doi: 10.1088/1464-4266/6/3/020.

[42] C. Caleman, J. S. Hub, P. J. van Maaren, and D. van der Spoel. Atomistic Simulation of Ion Solvation in Water Explains Surface Preference of Halides. *Proc. Natl. Acad. Sci. U. S. A.*, 108:6838–6842, 2011. doi: 10.1073/pnas.1017903108.

[43] D. M. Camaioni and C. A. Schwerdtfeger. Comment on "Accurate Experimental Values for the Free Energies of Hydration of H^+, OH^-, and H_3O^+". *J. Phys. Chem. A*, 109:10795–10797, 2005. doi: 10.1021/jp054088k.

[44] D. Chandler. Interfaces and the Driving Force of Hydrophobic Assembly. *Nature*, 437:640–647, 2005. doi: 10.1038/nature04162.

[45] C.-C. Chen and Y. Song. Generalized Electrolyte-NRTL Model for Mixed-Solvent Electrolyte Systems. *AIChE J.*, 50:1928–1941, 2004. doi: 10.1002/aic.10151.

[46] C.-C. Chen, H. I. Britt, J. F. Boston, and L. B. Evans. Local Composition Model for Excess Gibbs Energy of Electrolyte Systems. *AlChe*, 28:588–596, 1982. doi: 10.1002/aic.690280410.

[47] J. Chen, C. L. Brooks, and J. Khandogin. Recent Advances in Implicit Solvent-Based Methods for Biomolecular Simulations. *Curr. Opin. Struct. Biol.*, 18:140–148, 2008. doi: 10.1016/j.sbi.2008.01.003.

[48] J. Cheng, C. D. Vecitis, M. R. Hoffmann, and A. J. Colussi. Experimental Anion Affinities for the Air/Water Interface. *J. Phys. Chem. B*, 110: 25598–25602, 2006. doi: 10.1021/jp066197k.

[49] D. P. Chong, E. van Lenthe, S. van Gisbergen, and E. J. Baerends. Even-Tempered Slater-Type Orbitals Revisited: From Hydrogen to Krypton. *J. Comput. Chem.*, 25:1030–1036, 2004. doi: 10.1002/jcc.20030.

[50] H. Coker. Empirical Free-Ion Polarizabilities of the Alkali Metal, Alkaline Earth Metal, and Halide Ions. *J. Phys. Chem.*, 80:2078–2084, 1976. doi: 10.1021/j100560a006.

[51] H. Coker. Polarizability Changes on Ion Hydration. *J. Phys. Chem.*, 80: 2084–2091, 1976. doi: 10.1021/j100560a007.

[52] K. D. Collins. Charge Density-Dependent Strength of Hydration and Biological Structure. *Biophys. J.*, 72:65–76, 1997. doi: 10.1016/S0006-3495(97)78647-8.

[53] K. D. Collins. Ions from the Hofmeister Series and Osmolytes: Effects on Proteins in Solution and in the Crystallization Process. *Methods*, 34: 300–311, 2004. doi: 10.1016/j.ymeth.2004.03.021.

[54] V. S. J. Craig, B. W. Ninham, and R. M. Pashley. Effect of Electrolytes on Bubble Coalescence. *Nature*, 364:317–319, 1993. doi: 10.1038/364317a0.

[55] C. J. Cramer and D. G. Truhlar. Implicit Solvation Models: Equilibria, Structure, Spectra, and Dynamics. *Chem. Rev.*, 99:2161–2200, 1999. doi: 10.1021/cr960149m.

[56] C. J. Cramer and D. G. Truhlar. A Universal Approach to Solvation Modeling. *Acc. Chem. Res.*, 41:760–768, 2008. doi: 10.1021/ar800019z.

[57] J. Crosse, S. A. Ellingsen, K. Clements, S. Y. Buhmann, and S. Scheel. Thermal Casimir-Polder shifts in Rydberg atoms near metallic surfaces. *Phys. Rev. A*, 82:010901, 2010. doi: 10.1103/PhysRevA.82.010901.

[58] J. A. Crosse and S. Scheel. Atomic Multipole Eelaxation Eates Near Surfaces. *Phys. Rev. A*, 79:062902, 2009. doi: 10.1103/PhysRevA.79.062902.

[59] R. Dagastine, D. Prieve, and L. White. The Dielectric Function for Water and Its Application to Van der Waals Forces. *J. Colloid Interface Sci.*, 231:351–358, 2000. doi: 10.1006/jcis.2000.7164.

[60] P. Debye and E. Hückel. Zur Theorie der Elektrolyte. I. Gefrierpunktserniedrigung und Verwandte Erscheinungen [The Theory of Electrolytes. I. Lowering of Freezing Point and Related Phenomena]. *Phys. Z.*, 24:185–206, 1923.

[61] R. A. DiStasio, V. V. Gobre, and A. Tkatchenko. Many-Body Van der Waals Interactions in Molecules and Condensed Matter. *J. Phys.: Condens. Matter*, 26:213202, 2014. doi: 10.1088/0953-8984/26/21/213202.

[62] J. F. Dobson and T. Gould. Calculation of Dispersion Energies. *J. Phys.: Condens. Matter*, 24:073201, 2012. doi: 10.1088/0953-8984/24/7/073201.

[63] A. G. Donchev. Many-Body Effects of Dispersion Interaction. *J. Chem. Phys.*, 125:074713, 2006. doi: 10.1063/1.2337283.

[64] A. P. dos Santos, A. Diehl, and Y. Levin. Surface Tensions, Surface Potentials, and the Hofmeister Series of Electrolyte Solutions. *Langmuir*, 26:10778–10783, 2010. doi: 10.1021/la100604k.

[65] D. J. V. A. dos Santos, F. Müller-Plathe, and V. C. Weiss. Consistency of Ion Adsorption and Excess Surface Tension in Molecular Dynamics Simulations of Aqueous Salt Solutions. *J. Phys. Chem. C*, 112:19431–19442, 2008. doi: 10.1021/jp804811u.

[66] T. T. Duignan, D. F. Parsons, and B. W. Ninham. A Continuum Solvent Model of the Multipolar Dispersion Solvation Energy. *J. Phys. Chem. B*, 117:9412–9420, 2013. doi: 10.1021/jp403595x.

[67] T. T. Duignan, D. F. Parsons, and B. W. Ninham. A Continuum Model of Solvation Energies Including Electrostatic, Dispersion, and Cavity Contributions. *J. Phys. Chem. B*, 117:9421–9429, 2013. doi: 10.1021/jp403596c.

[68] T. T. Duignan, D. F. Parsons, and B. W. Ninham. A Continuum Solvent Model of the Partial Molar Volumes and Entropies of Ionic Solvation. *J. Phys. Chem. B*, 118:3122–3132, 2014. doi: 10.1021/jp410956m.

[69] T. T. Duignan, D. F. Parsons, and B. W. Ninham. Collins's Rule, Hofmeister Effects and Ionic Dispersion Interactions. *Chem. Phys. Lett.*, 608:55–59, 2014. doi: 10.1016/j.cplett.2014.05.056.

[70] T. T. Duignan, D. F. Parsons, and B. W. Ninham. Ion Interactions with the Air-Water Interface using a Continuum Solvent Model. *J. Phys. Chem. B*, 118:8700–8710, 2014. doi: dx.doi.org/10.1021/jp502887e.

[71] T. T. Duignan, D. F. Parsons, and B. W. Ninham. A Continuum Solvent Model of Ion–Ion Interactions in Water. *Phys. Chem. Chem. Phys.*, 16:22014–22027, 2014. doi: 10.1039/c4cp02822h.

[72] T. T. Duignan, D. F. Parsons, and B. W. Ninham. Modelling Water as a Continuum Solvent to Understand Ion–Specific Effects. In B. W. Ninham and P. Lo Nostro, editors, *Aqua Incognita: Why Ice Floats on Water and Galileo 400 Years On*, pages 443–455. Connor Court Publishers, 2014.

[73] W. R. Fawcett. Thermodynamic Parameters for the Solvation of Monatomic Ions in Water. *J. Phys. Chem. B*, 103:11181–11185, 1999. doi: 10.1021/jp991802n.

[74] W. R. Fawcett. *Liquids, Solutions, and Interfaces: From Classical Macroscopic Descriptions to Modern Microscopic Details*. Oxford University Press Inc., 2004.

[75] C. J. Fennell, A. Bizjak, V. Vlachy, and K. A. Dill. Ion Pairing in Molecular Simulations of Aqueous Alkali Halide Solutions. *J. Phys. Chem. B*, 113:6782–6791, 2009. doi: 10.1021/jp809782z.

[76] D. P. Fernández, A. R. H. Goodwin, E. W. Lemmon, J. M. H. Levelt Sengers, and R. C. Williams. A Formulation for the Static Permittivity of Water and Steam at Temperatures from 238 K to 873 K at Pressures up to 1200 MPa, Including Derivatives and Debye-Hückel Coefficients. *J. Phys. Chem. Ref. Data*, 26:1125–1166, 1997. doi: 10.1063/1.555997.

[77] R. P. Feynman. *Surely You're Joking Mr. Feynman*. W. W. Norton, 1985.

[78] A. Filipponi, D. T. Bowron, C. Lobban, and J. L. Finney. Structural Determination of the Hydrophobic Hydration Shell of Kr. *Phys. Rev. Lett.*, 79:1293–1296, 1997. doi: 10.1103/PhysRevLett.79.1293.

[79] F. Franks. *Water: A Matrix of Life*. The Royal Society of Chemistry, second edition, 2000.

[80] L. Frediani, R. Cammi, S. Corni, and J. Tomasi. A Polarizable Continuum Model for Molecules at Diffuse Interfaces. *J. Chem. Phys.*, 120: 3893–3907, 2004. doi: 10.1063/1.1643727.

[81] H. L. Friedman. Lewis-Randall to McMillan-Mayer Conversion for the Thermodynamic Excess Functions of Solutions. Part II. Excess Energy and Volume. *J. Solution Chem.*, 1:413–417, 1972. doi: 10.1007/BF00645605.

[82] J. L. Fulton, D. M. Pfund, S. L. Wallen, M. Newville, E. A. Stern, and Y. Ma. Rubidium Ion Hydration in Ambient and Supercritical Water. *J. Chem. Phys.*, 105:2161–2166, 1996. doi: 10.1063/1.472089.

[83] M. Fyta and R. R. Netz. Ionic Force Field Optimization Based on Single-Ion and Ion-Pair Solvation Properties: Going Beyond Standard Mixing Rules. *J. Chem. Phys.*, 136:124103, 2012. doi: 10.1063/1.3693330.

[84] M. Fyta, I. Kalcher, J. Dzubiella, L. Vrbka, and R. R. Netz. Ionic Force Field Optimization Based on Single-Ion and Ion-Pair Solvation Properties. *J. Chem. Phys.*, 132:024911, 2010. doi: 10.1063/1.3292575.

[85] E. Gallicchio, K. Paris, and R. M. Levy. The AGBNP2 Implicit Solvation Model. *J. Chem. Theory Comput.*, 5:2544–2564, 2009. doi: 10.1021/ct900234u.

[86] E. Gallicchio, N. Deng, P. He, L. Wickstrom, A. L. Perryman, D. N. Santiago, S. Forli, A. J. Olson, and R. M. Levy. Virtual Screening of Integrase Inhibitors by Large Scale Binding Free Energy Calculations: The SAMPL4 Challenge. *J. Comput.-Aided Mol. Des.*, 28:475–490, 2014. doi: 10.1007/s10822-014-9711-9.

[87] X. Ge, X. Wang, M. Zhang, and S. Seetharaman. Correlation and Prediction of Activity and Osmotic Coefficients of Aqueous Electrolytes at 298.15 K by the Modified TCPC Model. *J. Chem. Eng. Data*, 52:538–547, 2007. doi: 10.1021/je700446q.

[88] P. L. Geissler. Water Interfaces, Solvation, and Spectroscopy. *Annu. Rev. Phys. Chem.*, 64:317–337, 2013. doi: 10.1146/annurev-physchem-040412-110153.

[89] R. Geney, M. Layten, R. Gomperts, V. Hornak, and C. Simmerling. Investigation of Salt Bridge Stability in a Generalized Born Solvent Model. *J. Chem. Theory Comput.*, 2:115–127, 2006. doi: 10.1021/ct050183l.

[90] I. C. Gerber and J. G. Ángyán. London Dispersion Forces by Range-Separated Hybrid Density Functional with Second Order Perturbational Corrections: The Case of Rare Gas Complexes. *J. Chem. Phys.*, 126:044103, 2007. doi: 10.1063/1.2431644.

[91] E. Gouaux and R. MacKinnon. Principles of Selective Ion Transport in Channels and Pumps. *Science*, 310:1461–1465, 2005. doi: 10.1126/science.1113666.

[92] S. Grimme, J. Antony, T. Schwabe, and C. Mück-Lichtenfeld. Density Functional Theory with Dispersion Corrections for Supramolecular Structures, Aggregates, and Complexes of (Bio)Organic Molecules. *Org. Biomol. Chem.*, 5:741–758, 2007. doi: 10.1039/b615319b.

[93] S. Grimme, J. Antony, S. Ehrlich, and H. Krieg. A Consistent and Accurate *Ab Initio* Parametrization of Density Functional Dispersion Correction (DFT-D) for the 94 Elements H-Pu. *J. Chem. Phys.*, 132:154104, 2010. doi: 10.1063/1.3382344.

[94] C. F. Guerra, J. G. Snijders, G. te Velde, and E. J. Baerends. Towards an Order-N DFT Method. *Theor. Chem. Acc.*, 99:391–403, 1998. doi: 10.1007/s002149800m26.

[95] E. A. Guggenheim. *Applications of Statistical Mechanics*. Clarendon Press, 1966.

[96] E. Harder and B. Roux. On the Origin of the Electrostatic Potential Difference at a Liquid-Vacuum Interface. *J. Chem. Phys.*, 129:234706, 2008. doi: 10.1063/1.3027513.

[97] M. Häser and R. Ahlrichs. Improvements on the Direct SCF Method. *J. Comput. Chem.*, 10:104–111, 1989. doi: 10.1002/jcc.540100111.

[98] C. Hättig. Optimization of Auxiliary Basis Sets for RI-MP2 and RI-CC2 Calculations: Core-Valence and Quintuple-ζ Basis Sets for H to Ar and QZVPP Basis Sets for Li to Kr. *Phys. Chem. Chem. Phys.*, 7:59–66, 2005. doi: 10.1039/B415208E.

[99] C. Hättig and B. A. Hess. TDMP2 Calculation of Dynamic Multipole Polarizabilities and Dispersion Coefficients of the Noble Gases Ar, Kr, Xe, and Rn. *J. Phys. Chem.*, 100:6243–6248, 1996. doi: 10.1021/jp9528121.

[100] C. Hättig and B. A. Hess. TDMP2 Calculation of Dynamic Multipole Polarizabilities and Dispersion Coefficients for the Halogen Anions F-, Cl-, Br- and I-. *J. Chem. Phys.*, 108:3863–3870, 1998. doi: 10.1063/1.475789.

[101] C. Hättig, G. Schmitz, and J. Kossmann. Auxiliary Basis Sets for Density-Fitted Correlated Wavefunction Calculations: Weighted Core-Valence and ECP Basis Sets for Post-d Elements. *Phys. Chem. Chem. Phys.*, 14:6549–6555, 2012. doi: 10.1039/c2cp40400a.

[102] A. Hellweg, C. Hättig, S. Höfener, and W. Klopper. Optimized Accurate Auxiliary Basis Sets for RI-MP2 and RI-CC2 Calculations for the Atoms Rb to Rn. *Theor. Chem. Acc.*, 117:587–597, 2007. doi: 10.1007/s00214-007-0250-5.

[103] C. L. Henry, C. N. Dalton, L. Scruton, and V. S. J. Craig. Ion-Specific Coalescence of Bubbles in Mixed Electrolyte Solutions. *J. Phys. Chem. C*, 111:1015–1023, 2007. doi: 10.1021/jp066400b.

[104] A. Heßelmann and G. Jansen. The Helium Dimer Potential from a Combined Density Functional Theory and Symmetry-Adapted Perturbation Theory Approach using an Exact Exchange-Correlation Potential. *Phys. Chem. Chem. Phys.*, 5:5010–5014, 2003. doi: 10.1039/b310529f.

[105] A. Heßelmann and G. Jansen. Intermolecular Dispersion Energies from Time-Dependent Density Functional Theory. *Chem. Phys. Lett.*, 367:778–784, 2003. doi: 10.1016/S0009-2614(02)01796-7.

[106] D. Horinek, A. Herz, L. Vrbka, F. Sedlmeier, S. I. Mamatkulov, and R. R. Netz. Specific Ion Adsorption at the Air/Water Interface: The Role of Hydrophobic Solvation. *Chem. Phys. Lett.*, 479:173–183, 2009. doi: 10.1016/j.cplett.2009.07.077.

[107] D. Horinek, S. I. Mamatkulov, and R. R. Netz. Rational Design of Ion Force Fields Based on Thermodynamic Solvation Properties. *J. Chem. Phys.*, 130:124507, 2009. doi: 10.1063/1.3081142.

[108] D. M. Huang, P. L. Geissler, and D. Chandler. Scaling of Hydrophobic Solvation Free Energies. *J. Phys. Chem. B*, 105:6704–6709, 2001. doi: 10.1021/jp0104029.

[109] G. Hummer, L. R. Pratt, and A. E. García. Free Energy of Ionic Hydration. *J. Phys. Chem.*, 100:1206–1215, 1996. doi: 10.1021/jp951011v.

[110] P. Hünenberger and M. Reif. *Single-Ion Solvation: Experimental and Theoretical Approaches to Elusive Thermodynamic Quantities*. The Royal Society of Chemistry, 2011. doi: 10.1039/9781849732222.

[111] S. J. Irudayam and R. H. Henchman. Solvation Theory to Provide a Molecular Interpretation of the Hydrophobic Entropy Loss of Noble-Gas Hydration. *J. Phys.: Condens. Matter*, 22:284108, 2010. doi: 10.1088/0953-8984/22/28/284108.

[112] T. Ishiyama and A. Morita. Molecular Dynamics Study of Gas - Liquid Aqueous Sodium Halide Interfaces. I. Flexible and Polarizable Molecular Modeling and Interfacial Properties. *J. Phys. Chem. C*, 111:721–737, 2007. doi: 10.1021/jp065191s.

[113] J. N. Israelachvili. *Intermolecular and Surface Forces*. Academic Press, third edition, 2011.

[114] J. D. Jackson. *Classical Electrodynamics*. John Wiley & Sons, Inc., third edition, 1998.

[115] B. Jayaram, R. Fine, K. Sharp, and B. Honig. Free Energy Calculations of Ion Hydration: An Analysis of the Born Model in Terms of Microscopic Simulations. *J. Phys. Chem.*, 93:4320–4327, 1989. doi: 10.1021/j100347a081.

[116] P. J̈emmer, P. W. Fowler, M. Wilson, and P. A. Madden. Environmental Effects on Anion Polarizability: Variation with Lattice Parameter and

Coordination Number. *J. Phys. Chem. A*, 102:8377–8385, 1998. doi: 10.1021/jp982029j.

[117] B. Jeziorski, R. Moszynski, and K. Szalewicz. Perturbation Theory Approach to Intermolecular Potential Energy Surfaces of Van der Waals Complexes. *Chem. Rev.*, 94:1887–1930, 1994. doi: 10.1021/cr00031a008.

[118] P. Jungwirth and D. J. Tobias. Molecular Structure of Salt Solutions: A New View of the Interface with Implications for Heterogeneous Atmospheric Chemistry. *J. Phys. Chem. B*, 105:10468–10472, 2001. doi: 10.1021/jp012750g.

[119] P. Jungwirth and D. J. Tobias. Ions at the Air/Water Interface. *J. Phys. Chem. B*, 106:6361–6373, 2002. doi: 10.1021/jp020242g.

[120] P. Jungwirth and D. J. Tobias. Specific Ion Effects at the Air/Water Interface. *Chem. Rev.*, 106:1259–1281, 2006. doi: 10.1021/cr0403741.

[121] P. Jungwirth, D. J. Tobias, and J. Heyrovsky. Chloride Anion on Aqueous Clusters, at the Air-Water Interface, and in Liquid Water: Solvent Effects on Cl- Polarizability. *J. Phys. Chem. A*, 106:379–383, 2002. doi: 10.1021/jp012059d.

[122] I. Kalcher and J. Dzubiella. Structure-Thermodynamics Relation of Electrolyte Solutions. *J. Chem. Phys.*, 130:134507, 2009. doi: 10.1063/1.3097530.

[123] Y. V. Kalyuzhnyi, V. Vlachy, and K. A. Dill. Aqueous Alkali Halide Solutions: Can Osmotic Coefficients be Explained on the Basis of the Ionic Sizes Alone? *Phys. Chem. Chem. Phys.*, 12:6260–6266, 2010. doi: 10.1039/b924735a.

[124] I. G. Kaplan. *Intermolecular Interactions*. John Wiley & Sons Ltd, 2006.

[125] K. A. Karraker and C. J. Radke. Disjoining Pressures, Zeta potentials and Surface Tensions of Aqueous Non-Ionic Surfactant/Electrolyte Solutions: Theory and Comparison to Experiment. *Adv. Colloid Interface Sci.*, 96:231–264, 2002. doi: 10.1016/S0001-8686(01)00083-5.

[126] S. M. Kathmann, I.-F. W. Kuo, C. J. Mundy, and G. K. Schenter. Understanding the Surface Potential of Water. *J. Phys. Chem. B*, 115:4369–4677, 2011. doi: 10.1021/jp1116036.

[127] C. P. Kelly, C. J. Cramer, and D. G. Truhlar. Aqueous Solvation Free Energies of Ions and Ion-Water Clusters Based on an Accurate Value for the Absolute Aqueous Solvation Free Energy of the Proton. *J. Phys. Chem. B*, 110:16066–16081, 2006. doi: 10.1021/jp063552y.

[128] R. A. Kendall, T. H. Dunning, and R. J. Harrison. Electron Affinities of the First-Row Atoms Revisited. Systematic Basis Sets and Wave Functions. *J. Chem. Phys.*, 96:6796–6806, 1992. doi: 10.1063/1.462569.

[129] R. Kjellander. Intricate Coupling between Ion-Ion and Ion-Surface Correlations in Double Layers as Illustrated by Charge Inversion-Combined Effects of Strong Coulomb Correlations and Excluded Volume. *J. Phys.: Condens. Matter*, 21:424101, 2009. doi: 10.1088/0953-8984/21/42/424101.

[130] R. Kjellander and S. Marčelja. Inhomogeneous Coulomb Fluids with Image Interactions Between Planar Surfaces. I. *J. Chem. Phys.*, 82:2122–2135, 1985. doi: 10.1063/1.448350.

[131] A. Klamt. The COSMO and COSMO-RS Solvation Models. *Wiley Interdiscip. Rev.: Comput. Mol. Sci.*, 1:699–709, 2011. doi: 10.1002/wcms.56.

[132] A. Klamt and G. Schüürmann. COSMO: A New Approach to Dielectric Screening in Solvents with Explicit Expressions for the Screening Energy and its Gradient. *J. Chem. Soc. Perkin Trans. 2*, 5:799–805, 1993. doi: 10.1039/p29930000799.

[133] B. Klasczyk and V. Knecht. Kirkwood-Buff Derived Force Field for Alkali Chlorides in Simple Point Charge Water. *J. Chem. Phys.*, 132:024109, 2010. doi: 10.1063/1.3273903.

[134] M. A. Knackstedt and B. W. Ninham. Correlations and Thermodynamic Coefficients in Dilute Asymmetric Electrolyte Solutions. *J. Phys. Chem.*, 100:1330–1335, 1996. doi: 10.1021/jp951505s.

[135] P. Kollman. Free Energy Calculations: Applications to Chemical and Biochemical Phenomena. *Chem. Rev.*, 93:2395–2417, 1993. doi: 10.1021/cr00023a004.

[136] W. Kunz. Specific Ion Effects in Colloidal and Biological Systems. *Curr. Opin. Colloid Interface Sci.*, 15:34–39, 2010. doi: 10.1016/j.cocis.2009.11.008.

[137] W. Kunz. *Specific Ion Effects*. World Scientific, 2010.

[138] W. Kunz, L. Belloni, O. Bernard, and B. W. Ninham. Osmotic Coefficients and Surface Tensions of Aqueous Electrolyte Solutions: Role of Dispersion Forces. *J. Phys. Chem. B*, 108:2398–2404, 2004. doi: 10.1021/jp036113x.

[139] W. Kunz, J. Henle, and B. W. Ninham. 'Zur Lehre vod der Wirkung der Salze' (About the Science of the Effect of Salts): Franz Hofmeister's Historical Papers. *Curr. Opin. Colloid Interface Sci.*, 9:19–37, 2004. doi: 10.1016/j.cocis.2004.05.005.

[140] W. Kunz, P. Lo Nostro, and B. W. Ninham. The Present State of Affairs with Hofmeister Effects. *Curr. Opin. Colloid Interface Sci.*, 9:1–18, 2004. doi: 10.1016/j.cocis.2004.05.004.

[141] G. Lamoureux and B. Roux. Absolute Hydration Free Energy Scale for Alkali and Halide Ions Established from Simulations with a Polarizable Force Field. *J. Phys. Chem. B*, 110:3308–3322, 2006. doi: 10.1021/jp056043p.

[142] W. M. Latimer, K. S. Pitzer, and C. M. Slansky. The Free Energy of Hydration of Gaseous Ions, and the Absolute Potential of the Normal Calomel Electrode. *J. Chem. Phys.*, 7:108–111, 1939. doi: 10.1063/1.1750387.

[143] T. Leininger, A. Nicklass, W. Küchle, H. Stoll, M. Dolg, and A. Bergner. The Accuracy of the Pseudopotential Approximation: Non-Frozen-Core Effects for Spectroscopic Constants of Alkali Fluorides XF (X = K, Rb, Cs). *Chem. Phys. Lett.*, 255:274–280, 1996. doi: 10.1016/0009-2614(96)00382-X.

[144] P. J. Lenart, A. Jusufi, and A. Z. Panagiotopoulos. Effective Potentials for 1:1 Electrolyte Solutions Incorporating Dielectric Saturation and Repulsive Hydration. *J. Chem. Phys.*, 126:044509, 2007. doi: 10.1063/1.2431169.

[145] L. Lepori and P. Gianni. Partial Molar Volumes of Ionic and Nonionic Organic Solutes in Water: A Simple Additivity Scheme Based on the Intrinsic Volume Approach. *J. Solution Chem.*, 29:405–447, 2000. doi: 10.1023/A:1005150616038.

[146] K. Leung, S. B. Rempe, and O. A. von Lilienfeld. *Ab Initio* Molecular Dynamics Calculations of Ion Hydration Free Energies. *J. Chem. Phys.*, 130:204507, 2009. doi: 10.1063/1.3137054.

[147] Y. Levin and A. P. dos Santos. Ions at Hydrophobic Interfaces. *J. Phys.: Condens. Matter*, 26:203101, 2014. doi: 10.1088/0953-8984/26/20/203101.

[148] Y. Levin, A. P. dos Santos, and A. Diehl. Ions at the Air-Water Interface: An End to a Hundred-Year-Old Mystery? *Phys. Rev. Lett.*, 103:257802, 2009. doi: 10.1103/PhysRevLett.103.257802.

[149] L.-W. Li, P.-S. Kooi, M.-S. Leong, and T.-S. Yeo. Electromagnetic Dyadic Green's Function in Spherically Multilayered Media. *IEEE Trans. Microwave Theory Tech.*, 42:2302–2310, 1994. doi: 10.1109/22.339756.

[150] D. R. Lide, editor. *CRC Handbook of Chemistry and Physics, Internet Version*. Taylor and Francis, eighty sev edition, 2007.

[151] C.-L. Lin, L.-S. Lee, and H.-C. Tseng. Thermodynamic Behavior of Electrolyte Solutions Part I . Activity Coefficients and Osmotic Coef-

ficients of Binary Systems. *Fluid Phase Equilib.*, 90:57–79, 1993. doi: 10.1016/0378-3812(93)85004-6.

[152] J. Liu, C. P. Kelly, A. C. Goren, A. V. Marenich, C. J. Cramer, D. G. Truhlar, and C.-G. Zhan. Free Energies of Solvation with Surface, Volume, and Local Electrostatic Effects and Atomic Surface Tensions to Represent the First Solvation Shell. *J. Chem. Theory Comput.*, 6:1109–1117, 2010. doi: 10.1021/ct100025j.

[153] P. Lo Nostro and B. W. Ninham. Hofmeister Phenomena: An Update on Ion Specificity in Biology. *Chem. Rev.*, 112:2286–2322, 2012. doi: 10.1021/cr200271j.

[154] J.-F. Lu, Y.-X. Yu, and Y.-G. Li. Modification and Application of the Mean Spherical Approximation Method. *Fluid Phase Equilib.*, 85:81–100, 1993. doi: 10.1016/0378-3812(93)80006-9.

[155] M. Lukšič, C. J. Fennell, and K. A. Dill. Using Interpolation for Fast and Accurate Calculation of Ion-Ion Interactions. *J. Phys. Chem. B*, 118: 8017–8025, 2014. doi: 10.1021/jp501141j.

[156] M. Lund, L. Vrbka, and P. Jungwirth. Specific Ion Binding to Nonpolar Surface Patches of Proteins. *J. Am. Chem. Soc.*, 130:11582–11583, 2008. doi: 10.1021/ja803274p.

[157] M. Lund, B. Jagoda-Cwiklik, C. E. Woodward, R. Vácha, and P. Jungwirth. Dielectric Interpretation of Specificity of Ion Pairing in Water. *J. Phys. Chem. Lett.*, 1:300–303, 2010. doi: 10.1021/jz900151f.

[158] Y. Luo, W. Jiang, H. Yu, A. D. MacKerell, and B. Roux. Simulation Study of Ion Pairing in Concentrated Aqueous Salt Solutions with a Polarizable Force Field. *Faraday Discuss.*, 160:135–149, 2013. doi: 10.1039/c2fd20068f.

[159] W. Lv, W. He, X. Wang, Y. Niu, H. Cao, J. H. Dickerson, and Z. Wang. Understanding the Oriented-Attachment Growth of Nanocrystals

from an Energy Point of View: A Review. *Nanoscale*, 6:2531–2547, 2014. doi: 10.1039/c3nr04717b.

[160] J. Mahanty and B. W. Ninham. *Dispersion Forces*. Academic Press, 1976.

[161] M. Manciu and E. Ruckenstein. On the Interactions of Ions with the Air/Water Interface. *Langmuir*, 21:11312–11319, 2005. doi: 10.1021/la051979a.

[162] F. E. Manuel. *"Fragments from a Treatise on Revelation" in The Religion of Isaac Newton*. Clarendon Press, 1974.

[163] Y. Marcus. Ionic Radii in Aqueous Solutions. *Chem. Rev.*, 88:1475–1498, 1988. doi: 10.1021/cr00090a003.

[164] Y. Marcus. Thermodynamics of Solvation of Ions. Part 5. Gibbs Free Energy of Hydration at 298.15 K. *J. Chem. Soc., Faraday Trans.*, 87:2995–2999, 1991. doi: 10.1039/ft9918702995.

[165] Y. Marcus. Thermodynamics of Solvation of Ions: Part 6. The Standard Partial Molar Volumes of Aqueous Ions at 298.15 K. *J. Chem. Soc., Faraday Trans.*, 89:713–718, 1993. doi: 10.1039/FT9938900713.

[166] Y. Marcus. A Simple Empirical Model Describing the Thermodynamics of Hydration of Ions of Widely Varying Charges, Sizes, and Shapes. *Biophys. Chem.*, 51:111–127, 1994. doi: 10.1016/0301-4622(94)00051-4.

[167] Y. Marcus. *Ion Properties*. CRC Press, 1997.

[168] Y. Marcus. Effect of Ions on the Structure of Water: Structure Making and Breaking. *Chem. Rev.*, 109:1346–1370, 2009. doi: 10.1021/cr8003828.

[169] Y. Marcus. Surface Tension of Aqueous Electrolytes and Ions. *J. Chem. Eng. Data*, 55:3641–3644, 2010. doi: 10.1021/je1002175.

[170] Y. Marcus. Individual Ionic Surface Tension Increments in Aqueous Solutions. *Langmuir*, 29:2881–2888, 2013. doi: 10.1021/la3041659.

[171] S. Marčelja and N. Radić. Repulsion of Interfaces due to Boundary Water. *Chem. Phys. Lett.*, 42:129–130, 1976. doi: 10.1016/0009-2614(76)80567-2.

[172] D. Marx and J. Hutter. Ab Initio *Molecular Dynamics: Basic Theory and Advanced Methods*. Cambridge University Press, 2009.

[173] P. Matczak. Application of Symmetry-Adapted Perturbation Theory to Small Ionic Systems. *J. Phys. Chem. A*, 116:8731–8736, 2012. doi: 10.1021/jp302548u.

[174] S. McLain, S. Imberti, A. Soper, A. Botti, F. Bruni, and M. Ricci. Structure of 2 Molar NaOH in Aqueous Solution from Neutron Diffraction and Empirical Potential Structure Refinement. *Phys. Rev. B*, 74:094201, 2006. doi: 10.1103/PhysRevB.74.094201.

[175] W. G. Mcmillan and J. E. Mayer. The Statistical Thermodynamics of Multicomponent Systems. *J. Chem. Phys.*, 13:276–305, 1945. doi: 10.1063/1.1724036.

[176] L. Medda, B. Barse, F. Cugia, M. Boström, D. F. Parsons, B. W. Ninham, M. Monduzzi, and A. Salis. Hofmeister Challenges: Ion Binding and Charge of the BSA Protein as Explicit Examples. *Langmuir*, 28:16355–63, 2012. doi: 10.1021/la3035984.

[177] L. Medda, C. Carucci, D. F. Parsons, B. W. Ninham, M. Monduzzi, and A. Salis. Specific Cation Effects on Hemoglobin Aggregation below and at Physiological Salt Concentration. *Langmuir*, 29:15350–15358, 2013. doi: 10.1021/la404249n.

[178] J. Mitroy and M. Bromley. Semiempirical Calculation of Van der Waals Coefficients for Alkali-Metal and Alkaline-Earth-Metal Atoms. *Phys. Rev. A*, 68:052714, 2003. doi: 10.1103/PhysRevA.68.052714.

[179] J. J. Molina, J.-F. Dufrêche, M. Salanne, O. Bernard, and P. Turq. Primitive Models of Ions in Solution from Molecular Descriptions:

A Perturbation Approach. *J. Chem. Phys.*, 135:234509, 2011. doi: 10.1063/1.3668098.

[180] J. J. Molina, S. Lectez, S. Tazi, M. Salanne, J.-F. Dufrêche, J. Roques, E. Simoni, P. A. Madden, and P. Turq. Ions in Solutions: Determining their Polarizabilities from First-Principles. *J. Chem. Phys.*, 134:014511, 2011. doi: 10.1063/1.3518101.

[181] D. F. C. Morris. Ionic Radii and Enthalpies of Hydration of Ions. *Struct. Bond.*, 6:157–159, 1969. doi: 10.1007/BFb0119185.

[182] M. A. Morrison and G. A. Parker. A Guide to Rotations in Quantum Mechanics. *Aust. J. Phys.*, 40:465–497, 1987. doi: 10.1071/PH870465.

[183] H. S. Muddana, N. V. Sapra, A. T. Fenley, and M. K. Gilson. The Electrostatic Response of Water to Neutral Polar Solutes: Implications for Continuum Solvent Modeling. *J. Chem. Phys.*, 138:224504, 2013. doi: 10.1063/1.4808376.

[184] A. Mukhopadhyay, A. T. Fenley, I. S. Tolokh, and A. V. Onufriev. Charge Hydration Asymmetry: The Basic Principle and How to Use It to Test and Improve Water Models. *J. Phys. Chem. B*, 116:9776–9783, 2012. doi: 10.1021/jp305226j.

[185] R. Netz. Water and Ions at Interfaces. *Curr. Opin. Colloid Interface Sci.*, 9:192–197, 2004. doi: 10.1016/j.cocis.2004.06.007.

[186] R. R. Netz and D. Horinek. Progress in Modeling of Ion Effects at the Vapor/Water Interface. *Annu. Rev. Phys. Chem.*, 63:401–418, 2012. doi: 10.1146/annurev-physchem-032511-143813.

[187] B. W. Ninham and P. Lo Nostro. *Molecular Forces and Self Assembly*. Cambridge University Press, 2010.

[188] B. W. Ninham and P. Lo Nostro, editors. *Aqua Incognita: Why Ice Floats on Water and Galileo 400 Years On*. Connor Court Publishers, 2014.

[189] B. W. Ninham and R. A. Sammut. Refractive Index of Arrays of Spheres and Cylinders. *J. Theor. Biol.*, 56:125–149, 1976. doi: 10.1016/S0022-5193(76)80049-5.

[190] B. W. Ninham and V. Yaminsky. Ion Binding and Ion Specificity: The Hofmeister Effect and Onsager and Lifshitz Theories. *Langmuir*, 13: 2097–2108, 1997. doi: 10.1021/la960974y.

[191] B. W. Ninham, T. T. Duignan, and D. F. Parsons. Approaches to Hydration, Old and New: Insights through Hofmeister Effects. *Curr. Opin. Colloid Interface Sci.*, 16:612–617, 2011. doi: 10.1016/j.cocis.2011.04.006.

[192] S. Niu, M.-L. Tan, and T. Ichiye. The Large Quadrupole of Water Molecules. *J. Chem. Phys.*, 134:134501, 2011. doi: 10.1063/1.3569563.

[193] H. Ohtaki and T. Radnai. Structure and Dynamics of Hydrated Ions. *Chem. Rev.*, 93:1157–1204, 1993. doi: 10.1021/cr00019a014.

[194] A. W. Omta, M. F. Kropman, S. Woutersen, and H. J. Bakker. Negligible Effect of Ions on the Hydrogen-Bond Structure in Liquid Water. *Science*, 301:347–349, 2003. doi: 10.1126/science.1084801.

[195] L. Onsager and N. N. T. Samaras. The Surface Tension of Debye-Hückel Electrolytes. *J. Chem. Phys.*, 2:528–536, 1934. doi: 10.1063/1.1749522.

[196] J. Ortega, J. P. Lewis, and O. F. Sankey. First Principles Simulations of Fluid Water: The Radial Distribution Functions. *J. Chem. Phys.*, 106: 3696–3702, 1997. doi: 10.1063/1.474121.

[197] V. P. Osinga, S. J. A. van Gisbergen, J. G. Snijders, and E. J. Baerends. Density Functional Results for Isotropic and Anisotropic Multipole Polarizabilities and C_6, C_7, and C_8 Van der Waals Dispersion Coefficients for Molecules. *J. Chem. Phys.*, 106:5091–5101, 1997. doi: 10.1063/1.473555.

[198] D. E. Otten, P. R. Shaffer, P. L. Geissler, and R. J. Saykally. Elucidating the Mechanism of Selective Ion Adsorption to the Liquid Wa-

ter Surface. *Proc. Natl. Acad. Sci. U. S. A.*, 109:3190–3190, 2012. doi: 10.1073/pnas.1201349109.

[199] B. A. Pailthorpe, D. J. Mitchell, and B. W. Ninham. Ion-Solvent Interactions and the Activity Coefficients of Real Electrolyte Solutions. *J. Chem. Soc., Faraday Trans. 2*, 80:115–139, 1984. doi: 10.1039/f29848000115.

[200] V. A. Parsegian. *Van der Waals Forces*. Cambridge University Press, 2006.

[201] V. A. Parsegian and G. H. Weiss. Electrodynamic Interactions Between Curved Parallel Surfaces. *J. Chem. Phys.*, 60:5080–5085, 1974. doi: 10.1063/1.1681026.

[202] D. F. Parsons and B. W. Ninham. *Ab Initio* Molar Volumes and Gaussian Radii. *J. Phys. Chem. A*, 113:1141–1150, 2009. doi: 10.1021/jp802984b.

[203] D. F. Parsons and B. W. Ninham. Importance of Accurate Dynamic Polarizabilities for the Ionic Dispersion Interactions of Alkali Halides. *Langmuir*, 26:1816–1823, 2010. doi: 10.1021/la902533x.

[204] D. F. Parsons and B. W. Ninham. Surface Charge Reversal and Hydration Forces Explained by Ionic Dispersion Forces and Surface Hydration. *Colloids Surf., A*, 383:2–9, 2011. doi: 10.1016/j.colsurfa.2010.12.025.

[205] D. F. Parsons, V. Deniz, and B. W. Ninham. Nonelectrostatic Interactions Between Ions with Anisotropic *Ab Initio* Dynamic Polarisabilities. *Colloids Surf., A*, 343:57–63, 2009. doi: 10.1016/j.colsurfa.2009.01.029.

[206] D. F. Parsons, M. Boström, P. Lo Nostro, and B. W. Ninham. Hofmeister Effects: Interplay of Hydration, Nonelectrostatic Potentials, and Ion Size. *Phys. Chem. Chem. Phys.*, 13:12352–12367, 2011. doi: 10.1039/c1cp20538b.

[207] L. M. Pegram and M. T. Record. Hofmeister Salt Effects on Surface Tension Arise from Partitioning of Anions and Cations between Bulk

Water and the Air-Water Interface. *J. Phys. Chem. B*, 111:5411–5417, 2007. doi: 10.1021/jp070245z.

[208] N. Peruzzi, B. W. Ninham, P. Lo Nostro, and P. Baglioni. Hofmeister Phenomena in Nonaqueous Media: The Solubility of Electrolytes in Ethylene Carbonate. *J. Phys. Chem. B*, 116:14398–14405, 2012. doi: 10.1021/jp309157x.

[209] P. B. Petersen and R. J. Saykally. Adsorption of Ions to the Surface of Dilute Electrolyte Solutions: The Jones-Ray Effect Revisited. *J. Am. Chem. Soc.*, 127:15446–15452, 2005. doi: 10.1021/ja053224w.

[210] P. B. Petersen and R. J. Saykally. On the Nature of Ions at the Liquid Water Surface. *Annu. Rev. Phys. Chem.*, 57:333–364, 2006. doi: 10.1146/annurev.physchem.57.032905.104609.

[211] K. A. Peterson and C. Puzzarini. Systematically Convergent Basis Sets for Transition Metals. II. Pseudopotential-Based Correlation Consistent Basis Sets for the Group 11 (Cu, Ag, Au) and 12 (Zn, Cd, Hg) Elements. *Theor. Chem. Acc.*, 114:283–296, 2005. doi: 10.1007/s00214-005-0681-9.

[212] K. A. Peterson, D. Figgen, E. Goll, H. Stoll, and M. Dolg. Systematically Convergent Basis Sets with Relativistic Pseudopotentials. II. Small-Core Pseudopotentials and Correlation Consistent Basis Sets for the Post-d Group 16-18 Elements. *J. Chem. Phys.*, 119:11113–11123, 2003. doi: 10.1063/1.1622924.

[213] K. A. Peterson, B. C. Shepler, D. Figgen, and H. Stoll. On the Spectroscopic and Thermochemical Properties of ClO, BrO, IO, and Their Anions. *J. Phys. Chem. A*, 110:13877–13883, 2006. doi: 10.1021/jp065887l.

[214] L. Petit, R. Vuilleumier, P. Maldivi, and C. Adamo. *Ab Initio* Molecular Dynamics Study of a Highly Concentrated LiCl Aqueous Solution. *J. Chem. Theory Comput.*, 4:1040–1048, 2008. doi: 10.1021/ct800007v.

[215] R. A. Pierotti. A Scaled Particle Theory of Aqueous and Nonaqueous Solutions. *Chem. Rev.*, 76:717–726, 1976. doi: 10.1021/cr60304a002.

[216] K. S. Pitzer. Thermodynamics of Electrolytes. I. Theoretical Basis and General Equations. *J. Phys. Chem.*, 77:268–277, 1972. doi: 10.1021/j100621a026.

[217] E. Pluhařová, O. Marsalek, B. Schmidt, and P. Jungwirth. *Ab Initio* Molecular Dynamics Approach to a Quantitative Description of Ion Pairing in Water. *J. Phys. Chem. Lett.*, 4:4177–4181, 2013. doi: 10.1021/jz402177q.

[218] E. Pluhařová, P. E. Mason, and P. Jungwirth. Ion Pairing in Aqueous Lithium Salt Solutions with Monovalent and Divalent Counter-Anions. *J. Phys. Chem. A*, 117:11766–11773, 2013. doi: 10.1021/jp402532e.

[219] T. Pollard and T. L. Beck. Quasichemical Analysis of the Cluster-Pair Approximation for the Thermodynamics of Proton Hydration. *J. Chem. Phys.*, 140:224507, 2014. doi: 10.1063/1.4881602.

[220] A. Pomogaeva and D. M. Chipman. New Implicit Solvation Models for Dispersion and Exchange Energies. *J. Phys. Chem. A*, 117:5812–5820, 2013. doi: 10.1021/jp404624x.

[221] P. Postorino, M. A. Ricci, and A. K. Soper. Water Above its Boiling Point: Study of the Temperature and Density Dependence of the Partial Pair Correlation Functions. I. Neutron Diffraction Experiment. *J. Chem. Phys.*, 101:4123–4132, 1994. doi: 10.1063/1.467462.

[222] L. R. Pratt, G. Hummer, and A. E. García. Ion Pair Potentials-of-Mean-Force in Water. *Biophys. Chem.*, 51:147–165, 1994. doi: 10.1016/0301-4622(94)00057-3.

[223] L. R. Pratt, G. J. Tawa, G. Hummer, A. E. García, and S. A. Corcelli. Boundary Integral Methods for the Poisson Equation of Continuum Dielectric Solvation Models. *Int. J. Quantum Chem.*, 64:121–141, 1997. doi: 10.1002/(SICI)1097-461X(1997)64:1<121::AID-QUA12>3.0.CO;2-E.

[224] N. C. Pyper, C. G. Pike, and P. P. Edwards. The Polarizabilities of Species Present in Ionic Solutions. *Mol. Phys.*, 76:353–372, 1992. doi: 10.1080/00268979200101381.

[225] S. Rajamani, T. M. Truskett, and S. Garde. Hydrophobic Hydration from Small to Large Lengthscales: Understanding and Manipulating the Crossover. *Proc. Natl. Acad. Sci. U. S. A.*, 102:9475–9480, 2005. doi: 10.1073/pnas.0504089102.

[226] P. S. Ramanathan and H. L. Friedman. Study of a Refined Model for Aqueous 1-1 Electrolytes. *J. Chem. Phys.*, 54:1086–1099, 1971. doi: 10.1063/1.1674941.

[227] P. S. Ramanathan, C. V. Krishnan, and H. L. Friedman. Models Having the Thermodynamic Properties of Aqueous Solutions of Tetraalkylammonium Halides. *J. Solution Chem.*, 1:237–262, 1972. doi: 10.1007/BF00645104.

[228] A. A. Rashin. Electrostatics of Ion-Ion Interactions in Solution. *J. Phys. Chem.*, 93:4664–4669, 1989. doi: 10.1021/j100348a051.

[229] A. A. Rashin and B. Honig. Reevaluation of the Born Model of Ion Hydration. *J. Phys. Chem.*, 89:5588–5593, 1985. doi: 10.1021/j100272a006.

[230] M. M. Reif and P. H. Hünenberger. Computation of Methodology-Independent Single-Ion Solvation Properties from Molecular Simulations. IV. Optimized Lennard-Jones Interaction Parameter Sets for the Alkali and Halide Ions in Water. *J. Chem. Phys.*, 134:144104, 2011. doi: 10.1063/1.3567022.

[231] R. C. Remsing, M. D. Baer, G. K. Schenter, C. J. Mundy, and J. D. Weeks. The Role of Broken Symmetry in Solvation of a Spherical Cavity in Classical and Quantum Water Models. *J. Phys. Chem. Lett.*, 5:2767–2774, 2014. doi: 10.1021/jz501067w.

[232] K. F. Riley, M. P. Hobson, and S. J. Bence. *Mathematical Methods for Physics and Engineering*. Cambridge University Press, third edition, 2006.

[233] R. A. Robinson and R. H. Stokes. *Electrolyte Solutions*. Butterworth & Co., 1959.

[234] M. Rodnikova. A New Approach to the Mechanism of Solvophobic Interactions. *J. Mol. Liq.*, 136:211–213, 2007. doi: 10.1016/j.molliq.2007.08.003.

[235] D. M. Rogers and T. L. Beck. Quasichemical and Structural Analysis of Polarizable Anion Hydration. *J. Chem. Phys.*, 132:014505, 2010. doi: 10.1063/1.3280816.

[236] A. Salis and B. W. Ninham. Models and Mechanisms of Hofmeister Effects in Electrolyte Solutions, and Colloid and Protein Systems Revisited. *Chem. Soc. Rev.*, 43:7358–7377, 2014. doi: 10.1039/C4CS00144C.

[237] A. Sambale, S. Y. Buhmann, D.-G. Welsch, and M.-S. Tomaš. Local-Field Correction to One- and Two-Atom Van der Waals Interactions. *Phys. Rev. A*, 75:042109, 2007. doi: 10.1103/PhysRevA.75.042109.

[238] L. Sandberg and O. Edholm. Nonlinear Response Effects in Continuum Models of the Hydration of Ions. *J. Chem. Phys.*, 116:2936–2944, 2002. doi: 10.1063/1.1435566.

[239] S. Scheel and S. Y. Buhmann. Macroscopic Quantum Electrodynamics - Concepts and Applications. *Acta Phys. Slovaca*, 58:675–809, 2008. doi: 10.2478/v10155-010-0092-x.

[240] R. Schmid, A. M. Miaha, and V. N. Sapunovb. A New Table of the Thermodynamic Quantities of Ionic Hydration: Values and Some Applications (Enthalpy–Entropy Compensation and Born Radii). *Phys. Chem. Chem. Phys.*, 2:97–102, 2000. doi: 10.1039/A907160A.

[241] N. Schwierz, D. Horinek, and R. R. Netz. Anionic and Cationic Hofmeister Effects on Hydrophobic and Hydrophilic Surfaces. *Langmuir*, 29:2602–2614, 2013. doi: 10.1021/la303924e.

[242] SCM, Theoretical Chemistry, Vrije Universiteit, Amsterdam, The Netherlands. ADF2012.

[243] R. D. Shannon. Revised Effective Ionic Radii and Systematic Studies of Interatomic Distances in Halides and Chalcogenides. *Acta Cryst.*, A32: 751–767, 1976. doi: 10.1107/S0567739476001551.

[244] X. W. Sheng, P. Li, and K. T. Tang. A Combining Rule Calculation of the Ground State Van der Waals Potentials of the Mercury Rare-Gas Complexes. *J. Chem. Phys.*, 130:174310, 2009. doi: 10.1063/1.3126779.

[245] J.-P. Simonin. Study of Experimental-to-McMillan-Mayer Conversion of Thermodynamic Excess Functions. *J. Chem. Soc., Faraday Trans.*, 92: 3519–3523, 1996. doi: 10.1039/FT9969203519.

[246] J.-P. Simonin, O. Bernard, and L. Blum. Real Ionic Solutions in the Mean Spherical Approximation. 3. Osmotic and Activity Coefficients for Associating Electrolytes in the Primitive Model. *J. Phys. Chem. B*, 102:4411–4417, 1998. doi: 10.1021/jp9732423.

[247] R. I. Slavchov and J. K. Novev. Surface Tension of Concentrated Electrolyte Solutions. *J. Colloid Interface Sci.*, 387:234–243, 2012. doi: 10.1016/j.jcis.2012.07.020.

[248] E. Sobolewski, M. Makowski, C. Czaplewski, A. Liwo, S. Oldziej, and H. A. Scheraga. Potential of Mean Force of Hydrophobic Association: Dependence on Solute Size. *J. Phys. Chem. B*, 111:10765–10774, 2007. doi: 10.1021/jp070594t.

[249] Y. Song and C.-C. Chen. Symmetric Electrolyte Nonrandom Two-Liquid Activity Coefficient Model. *Ind. Eng. Chem. Res.*, 48:7788–7797, 2009. doi: 10.1021/ie9004578.

[250] A. C. Stern, M. D. Baer, C. J. Mundy, and D. J. Tobias. Thermodynamics of Iodide Adsorption at the Instantaneous Air-Water Interface. *J. Chem. Phys.*, 138:114709, 2013. doi: 10.1063/1.4794688.

[251] L. Sun, X. Li, T. Hede, Y. Tu, C. Leck, and H. Ågren. Molecular Dynamics Simulations of the Surface Tension and Structure of Salt Solutions and Clusters. *J. Phys. Chem. B*, 116:3198–3204, 2012. doi: 10.1021/jp209178s.

[252] K. T. Tang and J. P. Toennies. An Improved Simple Model for the Van der Waals Potential Based on Universal Damping Functions for the Dispersion Coefficients. *J. Chem. Phys.*, 80:3726–3741, 1984. doi: 10.1063/1.447150.

[253] K. T. Tang and J. P. Toennies. The Van der Waals Potentials between All the Rare Gas Atoms from He to Rn. *J. Chem. Phys.*, 118:4976–4983, 2003. doi: 10.1063/1.1543944.

[254] G. te Velde, F. M. Bickelhaupt, E. J. Baerends, C. Fonseca Guerra, S. J. A. van Gisbergen, J. G. Snijders, and T. Ziegler. Chemistry with ADF. *J. Comput. Chem.*, 22:931–967, 2001. doi: 10.1002/jcc.1056.

[255] K. H. Thompson and C. Orvig. Boon and Bane of Metal Ions in Medicine. *Science*, 300:936–939, 2003. doi: 10.1126/science.1083004.

[256] M. D. Tissandier, K. A. Cowen, W. Y. Feng, E. Gundlach, M. H. Cohen, A. D. Earhart, J. V. Coe, and T. R. Tuttle. The Proton's Absolute Aqueous Enthalpy and Gibbs Free Energy of Solvation from Cluster-Ion Solvation Data. *J. Phys. Chem. A*, 102:7787–7794, 1998. doi: 10.1021/jp982638r.

[257] D. J. Tobias, A. C. Stern, M. D. Baer, Y. Levin, and C. J. Mundy. Simulation and Theory of Ions at Atmospherically Relevant Aqueous Liquid-Air Interfaces. *Annu. Rev. Phys. Chem.*, 64:339–359, 2013. doi: 10.1146/annurev-physchem-040412-110049.

[258] J. Tomasi. Thirty Years of Continuum Solvation Chemistry: A Review, and Prospects for the Near Future. *Theor. Chem. Acc.*, 112:184–203, 2004. doi: 10.1007/s00214-004-0582-3.

[259] J. Tomasi and M. Persico. Molecular Interactions in Solution: An Overview of Methods Based on Continuous Distributions of the Solvent. *Chem. Rev.*, 94:2027–2094, 1994. doi: 10.1021/cr00031a013.

[260] J. Tomasi, B. Mennucci, and R. Cammi. Quantum Mechanical Continuum Solvation Models. *Chem. Rev.*, 105:2999–3093, 2005. doi: 10.1021/cr9904009.

[261] A. Tongraar and B. Michael Rode. The Hydration Structures of F^- and Cl^- Investigated by *Ab Initio* QM/MM Molecular Dynamics Simulations. *Phys. Chem. Chem. Phys.*, 5:357–362, 2003. doi: 10.1039/b209240a.

[262] M. E. Tuckerman. *Statistical Mechanics: Theory and Molecular Simulation*. Oxford University Press, 2010.

[263] S. J. A. van Gisbergen, J. G. Snijders, and E. J. Baerends. A Density Functional Theory Study of Frequency-Dependent Polarizabilities and Van der Waals Dispersion Coefficients for Polyatomic Molecules. *J. Chem. Phys.*, 103:9347–9354, 1995. doi: 10.1063/1.469994.

[264] R. van Leeuwen and E. J. Baerends. Exchange-Correlation Potential with Correct Asmptotic Behaviour. *Phys. Rev. A*, 49:2421–2431, 1994. doi: 10.1103/PhysRevA.49.2421.

[265] E. van Lenthe and E. J. Baerends. Optimized Slater-Type Basis Sets for the Elements 1-118. *J. Comput. Chem.*, 24:1142–1156, 2003. doi: 10.1002/jcc.10255.

[266] I. Vavruch. On the Evaluation of the Surface Tension-Pressure Coefficient for Pure Liquids. *J. Colloid Interface Sci.*, 169:249–250, 1995. doi: 10.1006/jcis.1995.1029.

[267] M. Vazdar, F. Uhlig, and P. Jungwirth. Like-Charge Ion Pairing in Water: An *Ab Initio* Molecular Dynamics Study of Aqueous Guanidinium Cations. *J. Phys. Chem. Lett.*, 3:2021–2024, 2012. doi: 10.1021/jz3007657.

[268] L. Vrbka, M. Lund, I. Kalcher, J. Dzubiella, R. R. Netz, and W. Kunz. Ion-Specific Thermodynamics of Multicomponent Electrolytes: A Hybrid HNC/MD Approach. *J. Chem. Phys.*, 131:154109, 2009. doi: 10.1063/1.3248218.

[269] R. Wang and Z.-G. Wang. Continuous Self-Energy of Ions at the Dielectric Interface. *Phys. Rev. Lett.*, 112:136101, 2014. doi: 10.1103/PhysRevLett.112.136101.

[270] S. Wang, Y. Song, and C.-C. Chen. Extension of COSMO-SAC Solvation Model for Electrolytes. *Ind. Eng. Chem. Res.*, 50:176–187, 2011. doi: 10.1021/ie100689g.

[271] F. Weigend and R. Ahlrichs. Balanced Basis Sets of Split Valence, Triple Zeta Valence and Quadruple Zeta Valence Quality for H to Rn: Design and Assessment of Accuracy. *Phys. Chem. Chem. Phys.*, 7:3297–3305, 2005. doi: 10.1039/b508541a.

[272] F. Weigend and M. Häser. RI-MP2: First Derivatives and Global Consistency. *Theor. Chem. Acc.*, 97:331–340, 1997. doi: 10.1007/s002140050269.

[273] F. Weigend, M. Häser, H. Patzelt, and R. Ahlrichs. RI-MP2: Optimized Auxiliary Basis Sets and Demonstration of Efficiency. *Chem. Phys. Lett.*, 294:143–152, 1998. doi: 10.1016/S0009-2614(98)00862-8.

[274] F. Weigend, A. Köhn, and C. Hättig. Efficient Use of the Correlation Consistent Basis Sets in Resolution of the Identity MP2 calculations. *J. Chem. Phys.*, 116:3175–3183, 2002. doi: 10.1063/1.1445115.

[275] F. Weigend, F. Furche, and R. Ahlrichs. Gaussian Basis Sets of Quadruple Zeta Valence Quality for Atoms H-Kr. *J. Chem. Phys.*, 119:12753–12762, 2003. doi: 10.1063/1.1627293.

[276] V. Weijo, B. Mennucci, and L. Frediani. Toward a General Formulation of Dispersion Effects for Solvation Continuum Models. *J. Chem. Theory Comput.*, 6:3358–3364, 2010. doi: 10.1021/ct1004565.

[277] E. W. Weisstein. Spherical Coordinates– http://mathworld.wolfram.com/SphericalCoordinates.html, 1999.

[278] H.-J. Werner, P. J. Knowles, G. Knizia, F. R. Manby, and M. Schütz. Molpro: A General-Purpose Quantum Chemistry Program Package. *Wiley Interdiscip. Rev.: Comput. Mol. Sci.*, 2:242–253, 2012. doi: 10.1002/wcms.82.

[279] H.-J. Werner, P. J. Knowles, G. Knizia, F. R. Manby, M. Schütz, and others. Molpro, version 2012.1, a package of *ab initio* programs, 2012. see http://www.molpro.net.

[280] E. Wilhelm, R. Battino, and R. J. Wilcock. Low-Pressure Solubility of Gases in Liquid Water. *Chem. Rev.*, 77:219–262, 1977. doi: 10.1021/cr60306a003.

[281] A. K. Wilson, D. E. Woon, K. A. Peterson, and T. H. Dunning. Gaussian Basis Sets for Use in Correlated Molecular Calculations. IX. The Atoms Gallium through Krypton. *J. Chem. Phys.*, 110:7667–7676, 1999. doi: 10.1063/1.478678.

[282] S. J. Wodak and J. Janin. Analytical Approximation to the Accessible Surface Area of Proteins. *Proc. Natl. Acad. Sci. U. S. A.*, 77:1736–1740, 1980. doi: 10.1073/pnas.77.4.1736.

[283] R. H. Wood. Thermodynamics of a Charged Hard Sphere in a Compressible Dielectric Fluid. A Modification of the Born Equation To Include the Compressibility of the Solvent. *J. Phys. Chem.*, 85:3944–3949, 1981. doi: 10.1021/j150625a047.

[284] D. E. Woon and T. H. Dunning. Gaussian Basis Sets for use in Correlated Molecular Calculations. III. The Atoms Aluminum through Argon. *J. Chem. Phys.*, 98:1358–1371, 1993. doi: 10.1063/1.464303.

[285] D. E. Woon and T. H. Dunning. Gaussian Basis Sets for use in Correlated Molecular Calculations. IV. Calculation of Static Electrical Response Properties. *J. Chem. Phys.*, 100:2975–2988, 1994. doi: 10.1063/1.466439.

[286] T. Yagasaki, S. Saito, and I. Ohmine. Effects of Nonadditive Interactions on Ion Solvation at the Water/Vapor Interface : A Molecular Dynamics Study. *J. Phys. Chem. A*, 114:12573–12584, 2010. doi: 10.1021/jp1084795.

[287] H. Yu, C. L. Mazzanti, T. W. Whitfield, R. E. Koeppe, O. S. Andersen, and B. Roux. A Combined Experimental and Theoretical Study of Ion Solvation in Liquid N-Methylacetamide. *J. Am. Chem. Soc.*, 132:10847–10856, 2010. doi: 10.1021/ja103270w.

[288] H. Yu, T. W. Whitfield, E. Harder, G. Lamoureux, I. Vorobyov, V. M. Anisimov, A. D. Mackerell, and B. Roux. Simulating Monovalent and Divalent Ions in Aqueous Solution Using a Drude Polarizable Force Field. *J. Chem. Theory Comput.*, 6:774–786, 2010. doi: 10.1021/ct900576a.

[289] H.-A. Yu and M. Karplus. A Thermodynamic Analysis of Solvation. *J. Chem. Phys.*, 89:2366–2379, 1988. doi: 10.1063/1.455080.

[290] Z. Yu, M. P. Jacobson, J. Josovitz, C. S. Rapp, and R. A. Friesner. First-Shell Solvation of Ion Pairs: Correction of Systematic Errors in Implicit Solvent Models. *J. Phys. Chem. B*, 108:6643–6654, 2004. doi: 10.1021/jp037821l.

[291] C.-G. Zhan and D. A. Dixon. Hydration of the Fluoride Anion: Structures and Absolute Hydration Free Energy from First-Principles Electronic Structure Calculations. *J. Phys. Chem. A*, 108:2020–2029, 2004. doi: 10.1021/jp0311512.

[292] Y. Zhang and P. S. Cremer. Interactions Between Macromolecules and Ions: The Hofmeister Series. *Curr. Opin. Chem. Biol.*, 10:658–663, 2006. doi: 10.1016/j.cbpa.2006.09.020.

[293] Y. Zhang and P. S. Cremer. Chemistry of Hofmeister Anions and Osmolytes. *Annu. Rev. Phys. Chem.*, 61:63–83, 2010. doi: 10.1146/annurev.physchem.59.032607.093635.

[294] Y. O. Zhang and Z. Xu. Atomic Radii of Noble Gas Elements in Condensed Phases. *Am. Mineral.*, 80:670–675, 1995.

COLOPHON

This document was typeset using the typographical look-and-feel `classicthesis` developed by André Miede. The style was inspired by Robert Bringhurst's seminal book on typography "*The Elements of Typographic Style*". `classicthesis` is available for both LaTeX and LyX:

http://code.google.com/p/classicthesis/

Final Version as of May 28, 2015 (`classicthesis` version 1).